THE UNIVERSITY OF MICHIGAN

INDUSTRY PROGRAM OF THE COLLEGE OF ENGINEERING

AN EXPERIMENTAL INVESTIGATION OF THE COMBINED EFFECTS OF PRESSURE, TEMPERATURE, AND SHEAR STRESS UPON VISCOSITY

John D. Novak

A dissertation submitted in partial fulfillment
of the requirements for the degree of
Doctor of Philosophy in
The University of Michigan

April, 1968

IP-820

ACKNOWLEDGMENTS

The author is most grateful to his thesis committee for their continuous interest, counsel, and cooperation throughout the period of this research. The understanding and assistance of the author's chairman, Professor Ward O. Winer, is particularly appreciated. The many discussions with Mr. W. A. Wright were very interesting and educational. The author is also indebted to him for his help in obtaining several of the experimental fluids.

The research reported herein was supported in part by the National Science Foundation (GP-2737) and by the donors of the Petroleum Research Fund, which is administered by the American Chemical Society (PRF #2468). Grant-in-aid assistance was also received from the Sun Oil Company, Dow Corning Corporation, Dow Chemical Company and the American Oil Company. These companies and the Rohm and Haas Company also donated the experimental fluids and the corresponding descriptive data.

Fellowship support from the Chrysler Corporation (1967-1968), an NDEA Title IV grant (1966-1967), and a Ford Fellowship in Mechanical Engineering (1966-1967) are greatly appreciated.

The author also wishes to thank Miss Ruth Howard for her assistance in typing this manuscript and especially Mr. Hossein Ehya for his able assistance in a wide variety of tasks.

Finally, this work would have been much more difficult had it not been for my understanding wife Juley who assisted me where ever possible.

TABLE OF CONTENTS

TABLE OF CONTENTS (Continued)

LIST OF TABLES

LIST OF FIGURES

LIST OF FIGURES (Continued)

LIST OF FIGURES (Continued)

LIST OF FIGURES (Continued)

CHAPTER I

INTRODUCTION

The viscosity of several well defined fluids was measured in a capillary-type viscometer. The fluids were subjected to pressures up to 80,000 psi, temperatures of 100, 210, and 300°F and shear stresses from 300 to 1.2×10^6 dynes/cm^2. The shear stress was varied via the pressure differential across the capillary which was independent of pressure level. Four interchangeable capillaries were employed to cover the shear stress range. The viscosity range examined was from 1.0 to 100,000 centipoise.

The behavior of ten fluids was observed including one (bis-2-ethyl hexyl sebacate) which had been previously examined and reported in the 1953 ASME Pressure-Viscosity Report.[10] Agreement within two percent was obtained between the present results and the ASME report. Data correlation and presentation techniques were also investigated in order to facilitate comprehension of the significant trends and interrelations among the fluids examined.

A. Need for this Research

There is a need for knowledge of the rheological behavior of liquid lubricants under the combined effects of high pressure and high shearing rates (or shear stress). Such information will not only contribute to the understanding of the physics of lubrication mechanisms but also act as a guide in the formulation of future lubricants. Many mechanisms of lubrication formerly thought to be in the category of "boundary" lubrication[1,2] (i.e. dependent on the chemical interaction of the

lubricant and the surface being lubricated) are, in light of recent analytical and experimental investigations, now thought to be of the elastohydrodynamic type[3,4,5,6] (i.e. dependent on the mechanical interaction of the physical properties of the lubricant and those of the solid being lubricated). Orcutt[7] in his studies in elastohydrodynamic lubrication and others (c.f. 8) recommend that the rheological models of the lubricant be modified to include effects of shear stress and time dependence. Existing work does not consider either of these effects because of the mathematical complexity involved and lack of realistic physical properties. Thus, a major problem associated with the work in the area of elastohydrodynamic lubrication is the lack of data on the behavior of the liquids when they are subjected to the combined effects of high pressure and high shear rate. This lack of realistic data arises because the viscosity-pressure relation has generally been investigated at low values of shear stress, and the viscosity-shear stress relation has only been investigated at pressures up to 15,000 psig.

The research described herein is an attempt to determine the combined effects of pressure, temperature and shear rate on lubricating fluids. A capillary viscometer has been employed and ten chemically well defined fluids investigated. Only time independent properties have been determined. It is recognized, however, that time dependent properties may be significant in high speed, highly loaded devices. Therefore some lubricants may behave differently in some applications than they did in this investigation.

This data should contribute to the understanding of the relative importance of the two modes of lubrication in highly loaded contacts such as gears, cam followers and rolling element bearings. A better understanding of the relative importance of boundary and elastohydrodynamic lubrication mechanisms is clearly of value in the formulation and use of lubricants because on the one hand the chemical properties of the lubricant are more important and therefore must be studied and enhanced, and on the other hand the physical properties are more important. A clear understanding of the two modes of lubrication is also of value in the mechanical design of lubricated mechanisms. The results of this research will also allow elastohydrodynamic lubrication theory to be advanced by extending the knowledge of the combined effects of pressure, temperature, and shear stress upon rheological properties. These effects can be considered in future rheological models. The existing models may also be improved by using more realistic data.

Previous investigators have examined the rheological properties of lubricants over wide temperature and pressure ranges at low shear rates. There is a need to include viscosity data over a wide shear stress range in order to obtain a better understanding of the lubricant behavior. The knowledge gained from data obtained over a wide range of these three variables could then be used to improve the behavior of lubricants by the addition of viscosity-index improvers to hydrocarbon lubricants or by changing the chemical composition of synthetic lubricants, i.e., silicone fluids could be altered by varying molecular structure.

B. Previous Research

1. Fluid Properties

The effect of pressure upon the viscosity of liquids has received much attention. The earliest investigation reported was dated in 1892.[9] The most extensive single investigation was that reported by the ASME in 1953.[10] This ASME viscosity-pressure report presents viscosity and density data for forty lubricating fluids of known composition at pressures to 150,000 psi and temperatures to 425°F.

Hersey[11] summarized the work reported in the literature prior to 1952 and more recently[12] has summarized the work conducted between 1952 and 1965. The maximum pressure in past investigations has ranged from as low as 2000 psi to as high as 425,000 psi by Bridgmen.[13] With few exceptions the research into the effect of high pressure on viscosity has been conducted with a falling-body type viscometer. The disadvantage of this type of instrument is that the fluid is subjected to very low shear stresses (approximately 250 dynes/cm^2 in 10) and therefore gives no indication of the effect of shear stress upon viscosity.

2. Experimental Equipment

One exception to the trend of low shear stresses has been the work of Philippoff[14] in which he employed a vibrating crystal viscometer in a pressure cell. This technique made possible the measurement of viscosity at discrete shear rates which are a function of the crystal geometry used. By employing a reduced variable approach the data could then be made applicable to a wide range of shear rates. Philippoff's maximum pressure was 15,000 psi which was limited in part by the fact

current instrumentation for vibrating crystal viscometers is limited to the measurement of viscosities below about 5 to 10 poise.

The National Aeronautics and Space Administration has published a bibliography on "Lubrication, Corrosion, and Wear,"[15] which contains abstracts of reports and journal articles published during the period January, 1962--March, 1965. This bibliography indicates that very few researchers have investigated effects of elevated pressure upon viscosity during that time. The only paper directly concerned with high pressure rheology of fluids is that by Bell[16] in which he reported an attempt to determine rheological behavior of a lubricant in the contact zone of rolling contact bodies. This was accomplished by rolling two contacting disks together with a small amount of sliding superimposed on a relatively high rolling velocity. This equipment does not readily produce viscosity data because the specimen is not uniformly stressed in the contact region (extreme pressure variation, for example). Therefore interpretation of the experimental results is necessary and it remains to be seen how well the results can be used to infer purely rheological properties of a fluid.

Two additional previous investigations deserve special mention because of their relation to this work. These are the works of Hersey and Snyder[17] in 1932 and that of Norton[18] et.al., in 1941. Both of these investigations also employed a capillary viscometer to determine the pressure-viscosity variations.

Hersey and Snyder[17] studied the flow of liquids in capillaries which exited to the atmosphere with inlet pressures up to 40,000 psi. This pressure was high enough to cause an appreciable change in the

viscosity of the test fluid. Thus, the viscosity could not be treated as uniform throughout the capillary. The results were put in the form of Poiseuille's law with a correction factor obtained by integration of the empirical viscosity-pressure relation for each fluid. If the form of the viscosity-pressure function was unknown, it was determined by differentiation of the flow rate versus inlet pressure curve. This method was less sensitive and less accurate but much more rapid than the rolling ball and falling weight methods previously used.

Norton[18] was the first to eliminate the problem of viscosity variation along the capillary at elevated pressures. His equipment had a maximum pressure level of 50,000 psi and eliminated the viscosity variation by using two capillaries in series. The first was a short test capillary with a Bourdon pressure gage at each end. The second capillary was a long flow resistance tube with atmospheric pressure at the exit. This technique enabled him to subject the test fluid to a high pressure level and still maintain a small pressure drop across the capillary. The results were presented as preliminary and the problems associated with the technique were not solved before his untimely death. The lack of repeatable accuracy of the Bourdon gages was the major problem in accurately measuring the pressure drop across the capillary.

C. Equipment Selection

The viscometers most frequently used to detect non-Newtonian behavior are the rotational and capillary types. Since many varieties of these are commercially available, a survey was made to determine if any available viscometers could be modified to obtain data over the desired ranges of temperature, pressure, and shear stress.

Two commercially available high pressure viscometers are described by Van Wazer.[19] The first has a maximum operating pressure of 2,000 psi, the second 30,000 psi. Since this research is concerned with much higher pressures, neither of these was acceptable. Van Wazer also describes several other types of viscometers. Some of them utilize a rolling ball, a rising bubble, or a vibrating reed to determine the viscosity. All of the commercially available viscometers have the same major limitation. That is, they do not operate at the desired high pressure levels. Since an existing viscometer could not be modified to obtain the desired range of variables, a viscometer was designed specifically for this research.

As previously mentioned, the viscometers most frequently used to detect non-Newtonian behavior are the rotational and capillary types. Therefore, the feasibility of using both types was investigated. The two most common rotational viscometers are the concentric cylinder, and the cone and plate types. One of the advantages of these viscometers is that it is not necessary to account for the elastic energy* stored in the fluid (if any exists), while this energy can be very significant in capillary viscometers. The major disadvantage of rotational viscometers for this research is the difficulty of accurately measuring torque through a high pressure seal. Another disadvantage is that temperature control of the test fluid is very difficult. For these reasons a capillary viscometer was designed. The details of this viscometer are presented in Chapter III.

---

* The elastic energy correction is discussed in Chapter II.

CHAPTER II

EXPERIMENTAL METHOD

The basic concepts of capillary viscometry are discussed in the first section of this chapter. The second section contains a discussion of the data reduction techniques used in this research.

A. Basic Concepts

The data necessary to determine the viscosity of a fluid in a capillary viscometer are the volumetric flow rate, pressure difference across the capillary, and the capillary geometry. Since viscosity is greatly affected by temperature and pressure, both of these must also be measured. The pressure difference and capillary geometry are used to determine the fluid shear stress at the capillary wall. The volumetric flow rate and capillary diameter are used to calculate the shear rate (i.e. velocity gradient), also at the capillary wall. The viscosity of the fluid at any set of conditions is the ratio of shear-stress to shear-rate. For a detailed justification of the standard techniques employed in capillary viscometry the reader is referred to Philippoff[20] and other standard references (cf. 19).

An analysis of the forces acting on the fluid shows that the shearing stress at the capillary wall is determined by the expression (cf. 21):

$$\tau_\omega = \frac{\Delta P_t}{4(L/D)} \qquad (1)$$

where ΔP_t is the total, or measured pressure differential across the capillary, L and D are the capillary length and diameter, respectively.

This shear stress is a mathematical reference quantity and is only correct for the special case of an infinite capillary where all of the mechanical energy supplied to the fluid, $\Delta P_t Q$, is dissipated in shearing the fluid "layers". In the general case for capillary viscometry, however, Philippoff[20] states that the energy balance for the capillary can be written as:

$$\Delta P_t Q = \Delta P_c Q + KE + EE \qquad (2)$$

or

$$\Delta P_t = \Delta P_c + KE/Q + EE/Q \qquad (3)$$

where ΔP_c is the pressure differential held in equilibrium inside the capillary, KE is the kinetic energy of the fluid leaving the capillary and EE is the elastic energy stored in the fluid. This last term, EE , also accounts for any geometrical end correction.

A fluid which discharges from a capillary may have an appreciable amount of kinetic energy. Thus, an error in the viscosity calculation will result unless this energy is reversibly recovered in a pressure rise or considered separately. For a parabolic velocity distribution (i.e. Newtonian fluid) the kinetic energy correction per unit volume, KEC , is expressed by:

$$KEC = KE/Q = \rho V^2/g \qquad (4)$$

where ρ is the fluid density and V is the average velocity.*

If a fluid acquires an elastic energy in steady flow, this energy is imparted to the liquid at the capillary entrance, carried

---

* For a uniform velocity profile, the kinetic energy is expressed by $KEC = (1/2)\,\rho V^2/g$.

through the capillary, and finally dissipated outside the capillary. In Philippoff's[20] discussion of the elastic energy he states that a measure of this energy per unit volume is the "normal stress", constant for each shear rate, which acts as a tension in the flow direction. He has shown (cf. 22) that the normal stress, P_n, is a product of the true shearing stress, τ_{cr}, and the recoverable shear, S_r.

$$EE/Q = P_n = \tau_{cr} S_r \tag{5}$$

Thus Equation (3) can be rearranged to give

$$\Delta P_t = \Delta P_c + KEC + P_n \tag{6}$$

Since any real capillary has a finite length, the entrance region in which the fluid velocity profile is developed must be considered. This region increases the active capillary length by $\delta L = nR$, where n is proportional to the Reynolds number and is called the "Couette Correction".* The true shearing stress at the capillary wall is then

$$\tau_{cr} = \frac{\Delta P_c}{4(L+\delta L)/D} = \frac{\Delta P_c}{4(L+nR)/D} \quad . \tag{7}$$

Substituting Equations (5) and (7) into Equation (6) results in

$$\Delta P_t - KEC = \tau_{cr} \left(\frac{4(L+nR)}{D} + S_r \right) . \tag{8}$$

Thus the true shear stress at the capillary wall is

$$\tau_{cr} = \frac{\Delta P_{corr}}{4(L/D)+EEC} \tag{9}$$

where

---

* The entrance region is discussed further in the next section of this chapter.

$$\Delta P_{corr} = \Delta P_t - KEC \ , \tag{10}$$

$$EEC = (2n + S_r) \ . \tag{11}$$

ΔP_{corr} is the corrected pressure differential across the capillary and EEC is the elastic energy correction.

The elastic energy stored in the fluid must be evaluated experimentally by obtaining constant shear rate data from capillaries with different length-to-diameter ratios. Philippoff[20] presents two techniques for evaluating EEC which are based on the fact the ΔP_{corr} is a linear function of the capillary length-to-diameter ratio for constant shear rate.

Equation (9) can be rearranged to give

$$\Delta P_{corr} = \tau_{cr} \left[4(L/D) + EEC\right] \ . \tag{12}$$

By letting ΔP_{corr} approach zero, one obtains

$$EEC = - 4(L/D) \tag{13}$$

This technique is presented in Figure 1(a) which shows that when the corrected pressure drop across the capillary is plotted against four times the length-to-diameter ratio, the intercept of the resulting straight line with the abscissa is equal to the negative of the elastic energy correction.

An equivalent method for evaluating the magnitude of the elastic energy correction utilizes the calculated shear stresses (including the kinetic energy correction) and the capillary diameter-to-length ratios (Figure 1(b)). The corrected shear stress, τ_{corr}, is

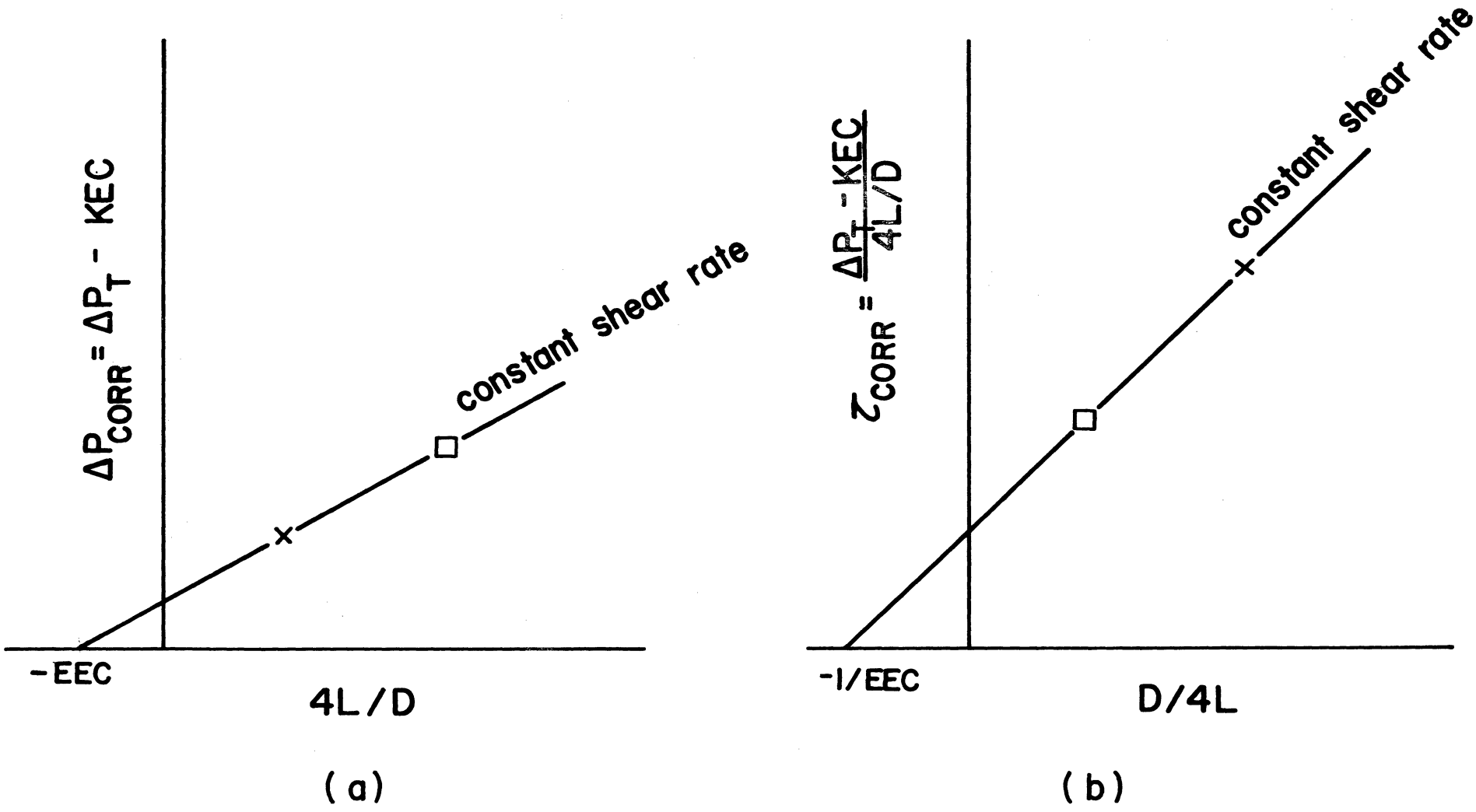

Figure 1. Elastic Energy Correction.

defined as:

$$\tau_{corr} \equiv \frac{P_{corr}}{4(L/D)} \tag{14}$$

Substituting Equation (12) into Equation (14) and simplifying, gives

$$\tau_{corr} = \tau_{cr}\left(1 + \frac{EEC}{4}(D/L)\right). \tag{15}$$

Equation (13) is again obtained by letting τ_{corr} approach zero. In this method, however, the intercept of the resulting straight line with the abscissa is equal to the negative of the reciprocal of the elastic energy correction (i.e. - 1/EEC). Thus a horizontal line is obtained when the fluid has negligible elastic energy whereas the previous method resulted in a line passing through the origin when the elastic energy is negligible.

This latter technique leads to an easy method of determining whether or not an elastic energy correction is negligible. It is negligible if, at a constant shear rate, the corrected shear stress is the same for all capillaries. In other words, the elastic energy is negligible if the uncorrected data are consistent between capillaries of different length-to-diameter ratios. The flow curves of each fluid readily indicate whether or not an elastic energy correction must be made. If data from different capillaries coincide, or "over-lap", the correction is unnecessary, i.e. elastic energy is negligible.

The above discussion is valid for all fluids because it is only based on force and energy balances and is independent of the fluid properties and fluid behavior. The technique used to evaluate the fluid shear rate (i.e. velocity gradient), however, is dependent upon the fluid

behavior. The technique assumes the fluid has a Newtonian behavior and then applies the Rabinwitsch[23] analysis* to determine the correct shear rate at the wall where this method indicates that the fluid has a non-Newtonian behavior.

Steady laminar flow of a Newtonian fluid through a circular tube produces a parabolic velocity profile (cf. 21). This is expressed by

$$v(r) = \frac{\Delta P\, R^2}{4\,\mu L}\left(1 - \left(\frac{r}{R}\right)^2\right) \tag{16}$$

where ΔP = pressure difference across tube (psi)

R = radius (inches)

L = length (inches)

μ = absolute viscosity (poise).

The velocity gradient at the wall is

$$\gamma_N = \left.\frac{dv}{dr}\right|_R = \frac{\Delta P}{2\mu}\,\frac{R}{L} \quad . \tag{17}$$

Integration of Equation (16) shows that the volumetric flow rate through the capillary is

$$Q = \frac{\Delta P\, R^4}{8\,\mu L} \quad (in^3/sec). \tag{18}$$

Thus from Equations (17) and (18), the shear rate at the capillary wall for Newtonian fluids is expressed by the relation

$$\gamma_N = \frac{32Q}{\pi D^3} = \frac{8V}{D} \quad (sec^{-1}) \tag{19}$$

where V is the average fluid velocity.

---

* This technique is often referred to by other names such as Mooney-Metzner or Weissenberg.

The shear stress and shear rate data obtained by using the above techniques, (Equations (9) and (19)), can then be used to determine whether or not the assumption of a Newtonian fluid in the shear rate calculation is valid. For Newtonian fluids, these data produce straight lines with a unit slope when plotted on log-log paper*. Similar curves for non-Newtonian fluids may be straight lines with a slope greater or less than one, (i.e. Power Law Fluids), or curved lines, (i.e. Psuedo-plastic Fluids).

The Rabinowitsch analysis is valid only for purely viscous fluids with time independent properties. Van Wazer[19] presents a complete discussion of this analysis and lists the following basic assumptions:

1. steady, laminar flow,
2. no radial or tangential velocity components,
3. no slippage at the wall,
4. negligible end effects,
5. incompressible fluid,
6. no external forces,
7. isothermal conditions prevail throughout,
8. viscosity does not change appreciably with the change in pressure down the tube, and
9. the shear rate is an arbitrary function of the shear stress.

This analysis shows that the true shear rate at the capillary wall is:

$$\gamma = \left(\frac{3+S}{4}\right) \gamma_N \qquad (20)$$

or

$$\gamma = \left(\frac{3+S}{4}\right) \frac{32Q}{D^3} \qquad (21)$$

where S is the slope of the γ_N versus shear-stress curve

---

* For a Newtonian fluid $\tau = \mu \gamma_N$

$$\log \tau = \log \mu + \log \gamma_N$$

plotted on log-log paper. As mentioned previously, this slope is unity for Newtonian fluids and thus the additional factor reduces to unity.

Of the assumptions listed by Van Wazer, only the following four need to be checked in this work: (a) time steady flow, (b) negligible entrance length, (c) negligible viscous heating, and (d) the absence of thixotropic or rheopectic fluid behavior.

B. Data Reduction Techniques

The raw data as described in Chapter III were transcribed into digital form and analyzed by a computer program which determined the pressures, kinetic energy, shear stress, shear rate, viscosity and additional quantities such as the Reynolds number and entrance length. The details of these calculations are presented in Appendix C as well as an explanation of the computer program. This computer program only evaluates one of the four assumptions listed by Van Wazer which needed to be checked, namely the magnitude of the entrance length. The validity of the other three assumptions was checked by other means.

The entrance length is that distance from the capillary entrance in which the fluid velocity profile is developed to some percentage (i.e. 95%) of the profile which would exist in an infinitely long capillary. This distance is expressed by the relation (cf. 20)

$$L_e = 0.029\ R_e\ D \qquad (22)$$

where R_e is the fluid Reynolds number and D is the capillary diameter (approximately 0.01 inch). In general the Reynolds number was not greater than 20 and always less than 750. Therefore, the entrance length

was a negligible fraction of the total capillary length. Note that this also insures that only laminar flow conditions (i.e. $R_e \leq 2000$) exist. The shape of the capillary ends were not well rounded, but the method of determining the capillary diameter included the appropriate end correction (cf. 20).

Time steady flow could be assured by observing the recording of the transducer signals because the fluid motion transient time* was at least one order of magnitude shorter than the slowest responding element in the recording system. Hence, if the data record indicated steady behavior over a time period large enough to obtain readings, the fluid motion was steady during that time.

The problem of viscous heating in capillary experiments has often lead to misleading results. Physically it cannot be avoided because the experiment is based on the visous dissipation of mechanical energy supplied to the system. The only question is whether or not the thermal energy is removed at a rate sufficient to keep the resulting decrease in viscosity negligible. The work of Gerrard et al.[24,25,26] was used to minimize heating effects. No correction was applied to the data for any possible heating effect.

The absence of thixotropic or rheopectic behavior is indicated by the agreement between data on the same fluid taken in capillaries of differing length-to-diameter ratios as long as there was no gelatin in the fluid. Gelatin results from the solidification of some constituents in the fluid at certain combinations of pressure and temperature. It was readily detected in the instrument because it caused the differential

---

* See Chapter III, Section B for calculations.

pressure signals to be delayed with respect to the displacement signal and resulted in an inability to repeat data successively under supposedly identical conditions. The temperature-pressure combinations at which gelatin was observed to begin agreed well with those at which "solidification" was reported in the ASME Viscosity-Pressure Report[10] for similar fluids. Although it may be possible, no attempt was made to systematically determine the rheological behavior of the fluids when a gel structure existed. The gelatin problem is discussed further in Chapter III.

C. Summary

The mathematical model used to reduce the raw experimental data was basically the Hagen-Poiseuille relation for flow in a tube. Modifications of this model were made when necessary to account for the kinetic energy, elastic energy, and/or non-Newtonian behavior of the test fluid. The viscosity was determined from the following expression:

$$\mu = \frac{K}{Q}\left(\frac{\Delta P_t - KEC}{4\ L/D + EEC}\right) \qquad (23)$$

where

μ = viscosity (poise)

K = constant

ΔP_t = measured pressure differential across the capillary (psi)

KEC = kinetic energy correction (psi)

Q = volumetric flow rate (in^3/sec)

L = capillary length (inches)

D = capillary diameter (inches)

EEC = elastic energy correction (in/in).

CHAPTER III

EXPERIMENTAL EQUIPMENT

A. Description

The experimental apparatus* used to measure the steady-state rheological behavior of liquids was a two-way high pressure capillary viscometer which has an upper pressure limit of 100,000 psi. The temperature of the test sample was controlled by a constant temperature bath which has a range of approximately -30 to 450°F.

A schematic drawing of the test apparatus is presented in Figure 2. The test fluid is in two reservoirs, R1 and R2 , the high pressure tubing, and the capillary section. The fluid in the test section is pressurized by pumping low pressure hydraulic fluid into cavity I and venting hydraulic fluid from cavity II. The high pressure is generated by an intensifier which has a 50 to 1 area ratio between piston P1 and the high pressure piston P2 . After the test fluid is pressurized, the moveable ram is locked in position by sealing both cavities I and II.

Flow through the capillary is caused by venting hydraulic fluid from cavity IV and pressurizing cavity III which results in the translating piston (pressure chamber) moving along the high pressure rams. The test fluid is then forced from reservoir R2 through the capillary into reservoir R1 . The motion can be reversed. The test section, the high pressure tubing, and the pressure transducers are attached to the translating piston, and, therefore, move with it.

---

* 4340 steel used for all components except as noted.

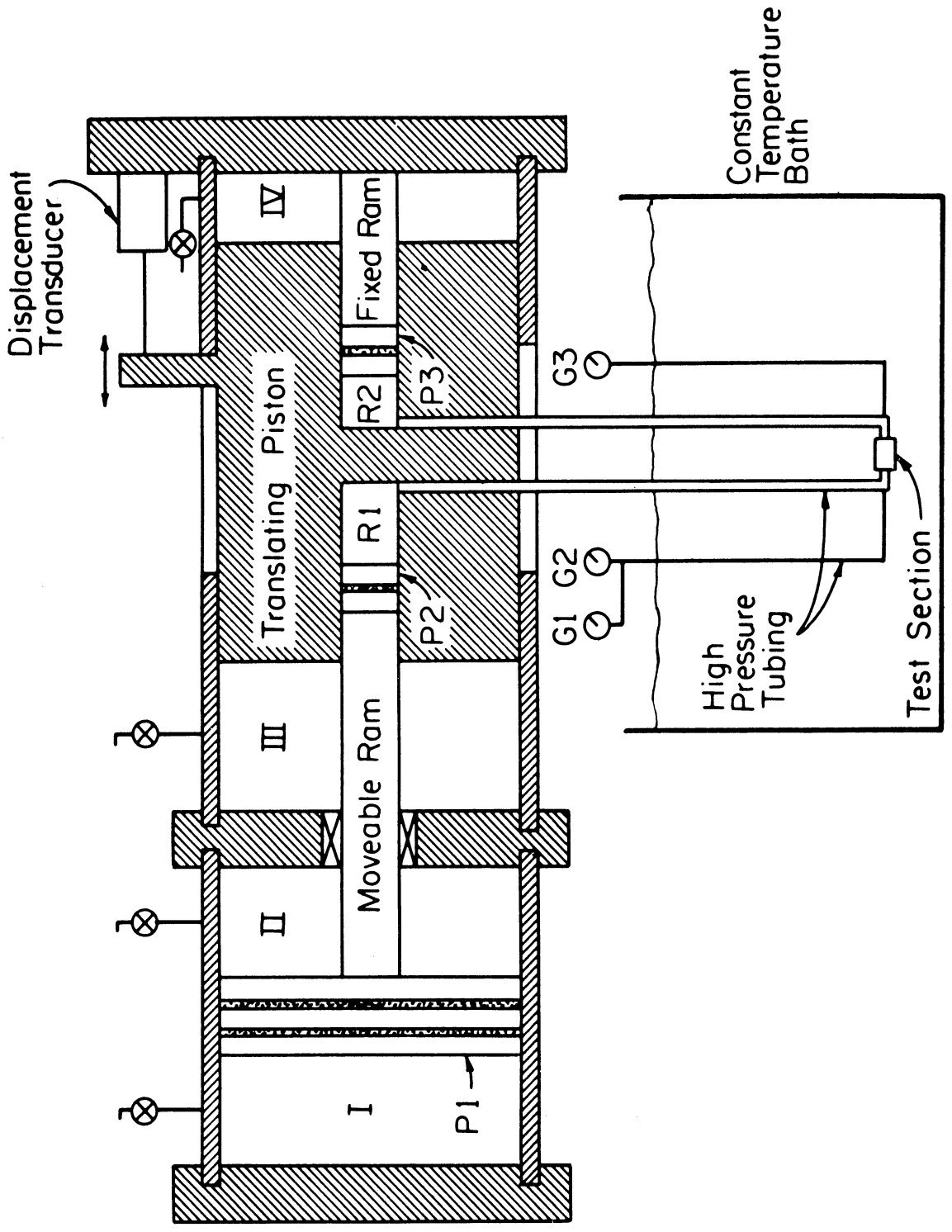

Figure 2. Schematic Drawing of Viscometer.

The moveable high pressure seals at P2 and P3 were Bridgman type seals with urethane washers and metal anti-extrusion backup rings. The pressure transducers were sealed with standard "O-rings". The remaining high pressure seals, in the standard 100,000 psi tubing, were metal-to-metal conical seals. Figure 3 is an exploded view of the high pressure moveable seals which shows the seal head (No. 1), the anti-extrusion rings (No.2), the polyurethane washer (No. 3), and the base of the seal (No. 4) which is actually the end of the moveable ram in reservoir R1 and the end of the fixed ram in reservoir R2 (Figure 2).

Figure 4 is a general view of the experimental apparatus which shows the high pressure viscometer, low pressure hydraulic system and the instrumentation cart as well as the constant temperature bath. Control of the low pressure hydraulic system is achieved by two manual pumps and a series of valves. The pump with the lower operating pressure (800 psi maximum, 1.08 in^3/stroke) is used primarily to control the translating piston motion. The major function of the other pump (3,000 psi maximum operating pressure, 0.28 in^3/stroke) is to pressurize the test fluid. One valve is positioned between the two pumps which allows both pumps to pressure the test fluid, move the translating piston, or to be isolated from each other. There are eight additional values in the hydraulic system, two for each cavity. Four of these are connected to the common pressurizing line, the other four are connected to the common return line.

The capillary section (Figure 5) consists of a fine-bore stainless steel capillary of 0.01 inch nominal inside diameter pressed into a 3-1/2 inch long nipple of standard 100,000 psi tubing.* Four capillaries

*Purchased from American Instrument Company, 1/4 inch O.D., 1/16 inch I.D., Chrome Molybdenum Alloy.

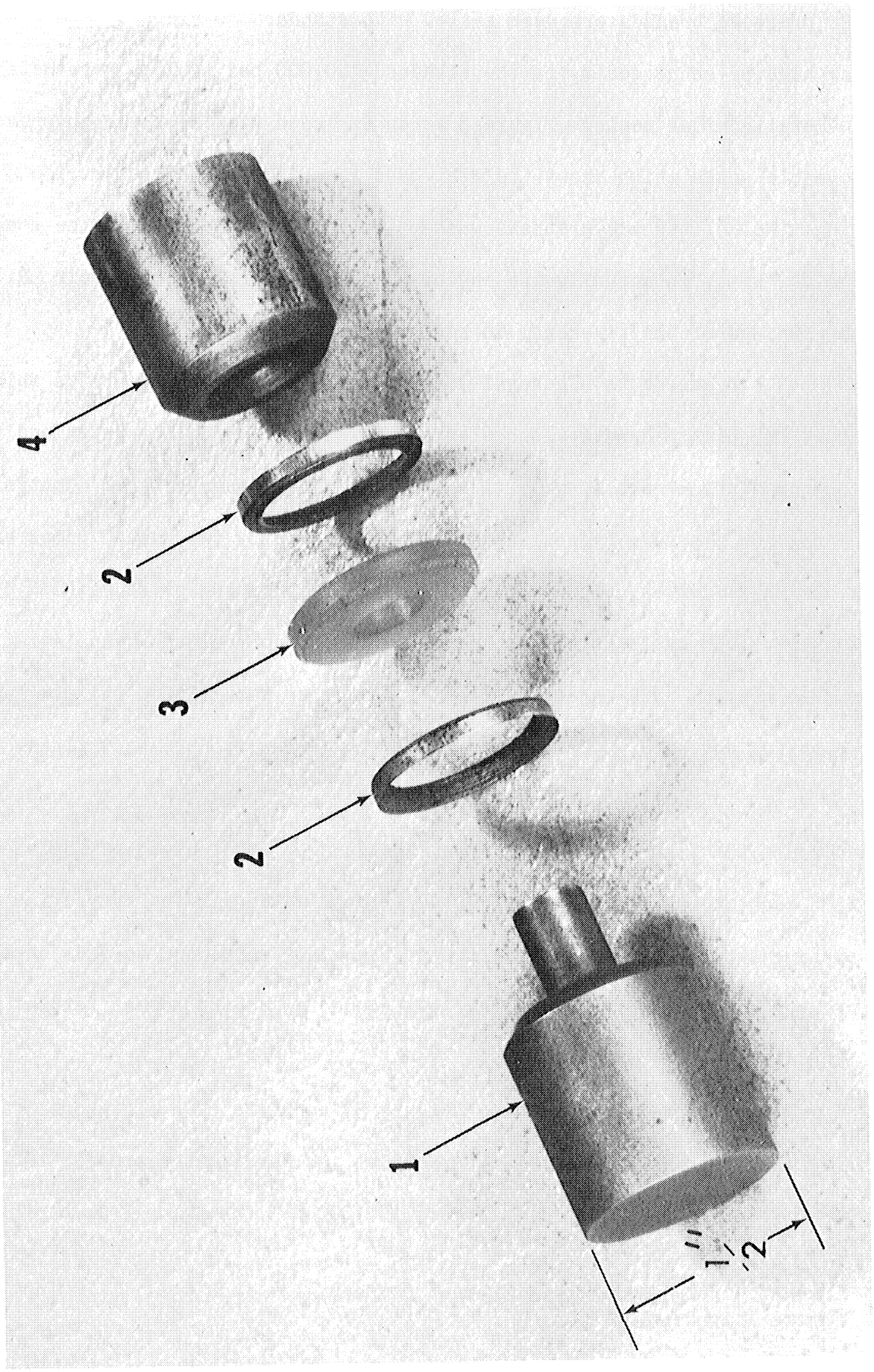

Figure 3. Exploded View of High Pressure Moveable Seal.

1. Viscometer Housing and Fluid Reservoirs
2. Constant Temperature Bath
3. Proportional Temperature Controller
4. Instrumentation Control Box
5. Oscillographic Recorder

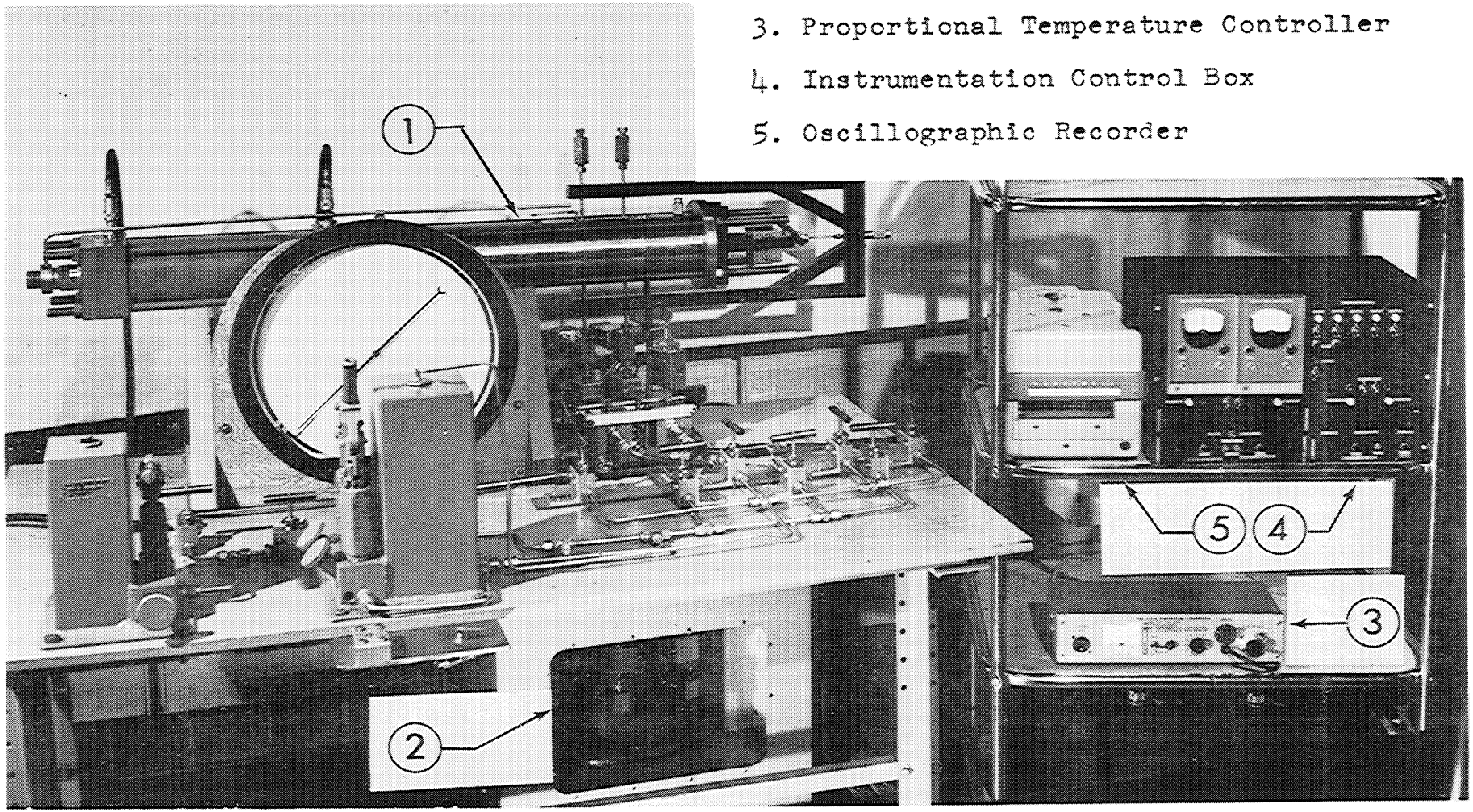

Figure 4. General View of Experimental Apparatus.

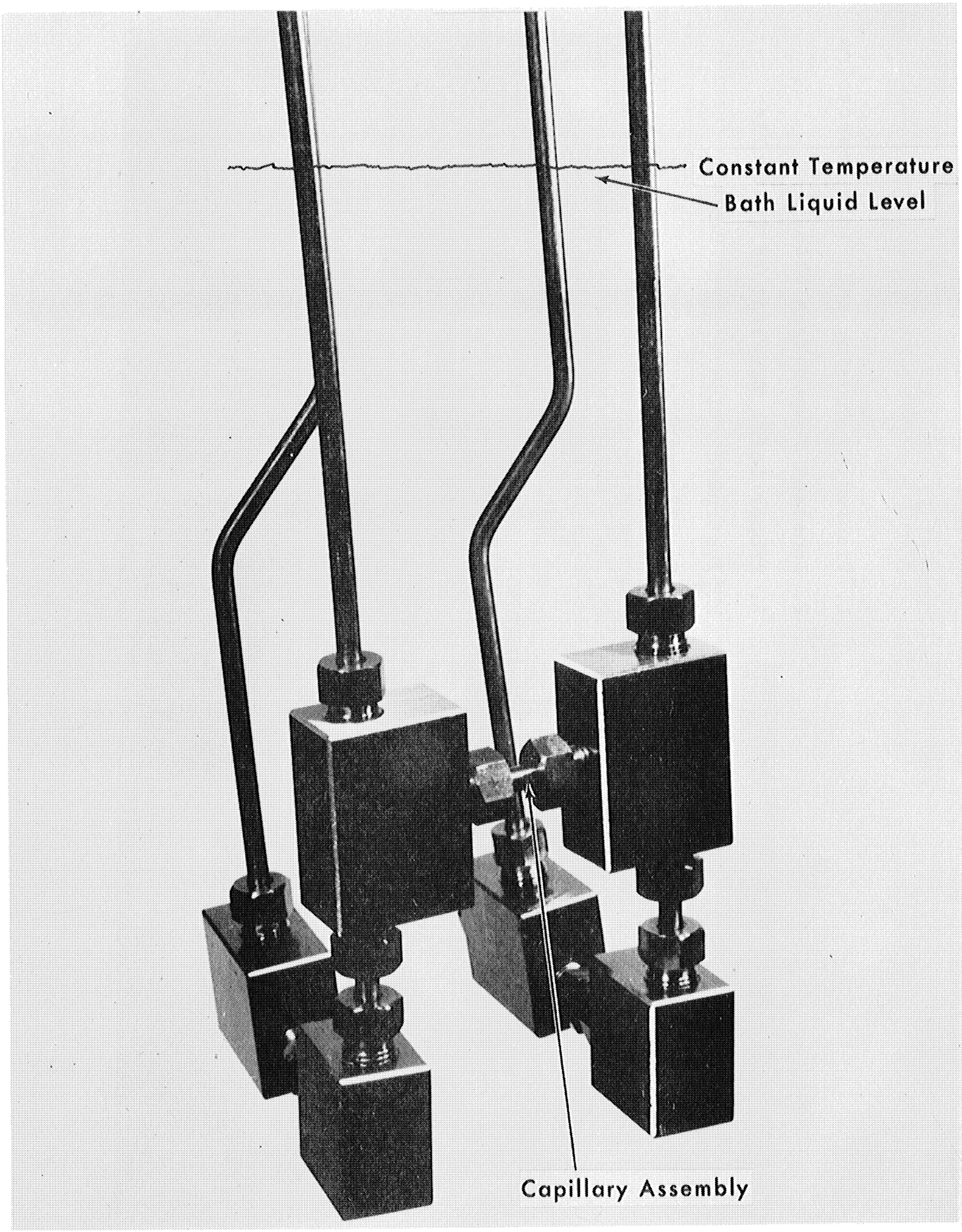

Figure 5. Capillary Test Section.

were available for this research which had length-to-diameter ratios of 11.6, 50.9, 100.2 and 280.0. The method used to determine the diameter of each capillary is discussed in Section C of this chapter.

In addition to the capillary diameter, the data required consisted of the fluid temperature and pressure, the volume flow rate, and the pressure drop across the capillary. The temperature of the bath, in which the capillary section and much of the high pressure tubing was immersed, was determined with the calibrated mercury-in-glass thermometer.* The bath temperature was controlled by a proportional temperature controller which could maintain a temperature variation of less than 0.1°F.

Three pressure transducers and a displacement transducer were used to obtain the remaining data. The signals from these four transducers were supplied to galvanometers in an ultraviolet oscillographic recorder and were recorded continuously as a function of time. A time base signal was also recorded. A typical recording trace is shown in Figure 6.

The volume flow rate was determined by measuring the displacement between the fixed high pressure ram and the translating piston (see Figure 2). This measurement was made with an inductance displacement transducer. Precautions were taken to keep the fluid which was in the high pressure tubing above the constant temperature bath from flowing into the capillary section. The permissible volume displaced was calculated and this calculation was confirmed by performing an experiment

---

* ASTM 64-F, 66-F, and 67-F thermometers were used.

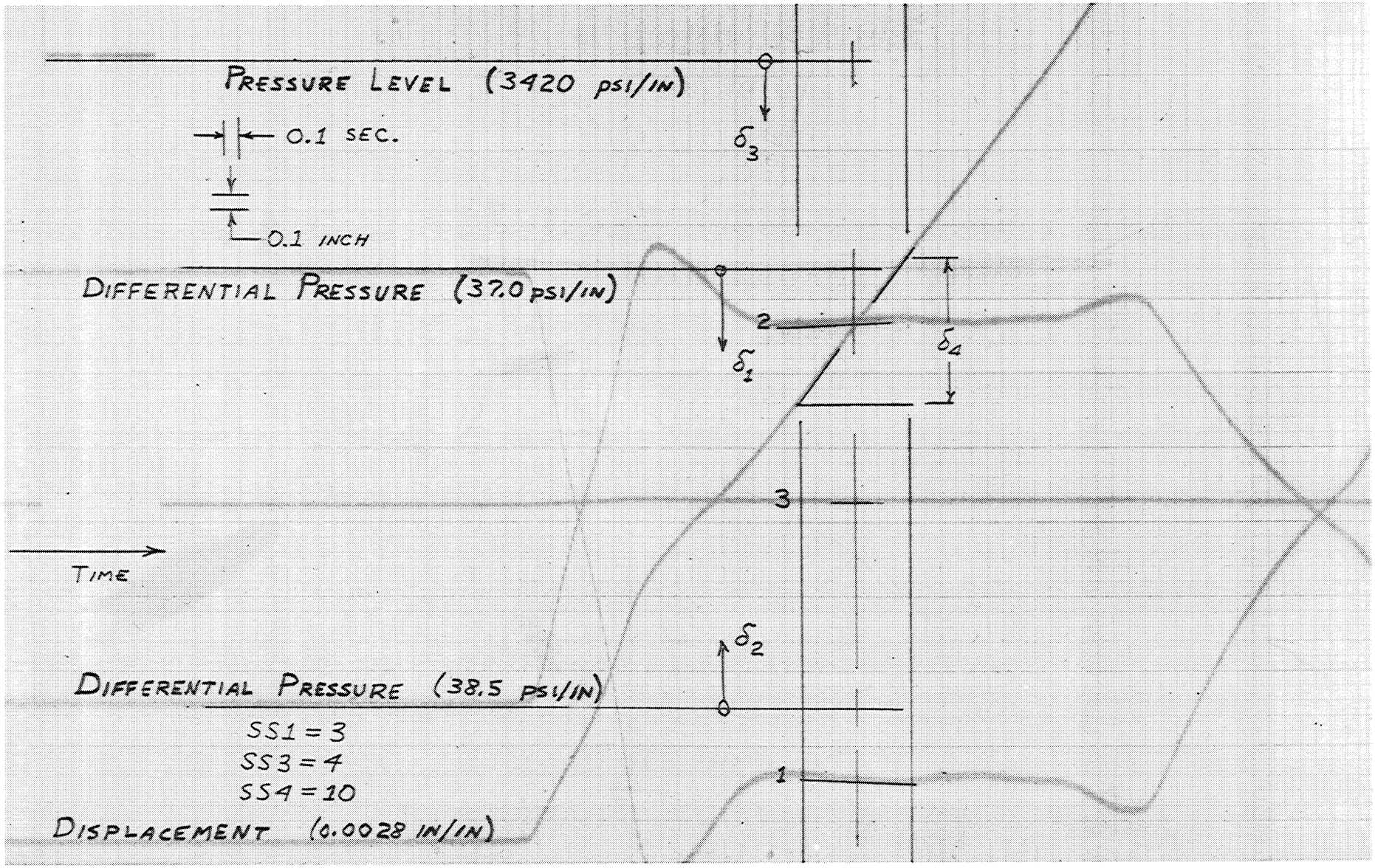

Figure 6. Typical Transducer Output

with thermocouples mounted in the test fluid at each end of the capillary. The maximum volume permissible was 0.037 in^3 which was more than required to obtain the necessary data.

Two displacement transducers* were available which enabled a wide range of displacement magnitudes to be measured. Table I contains data which show that the available transducer signal-to-displacement ratios (amplification) range from a minimum of 4.24 to a maximum of 2870. The sensitivity switch position refers to the five position rotary switch on the instrumentation control box. The first five positions are for the model 1000 transducer and the second five positions are for the model 050 transducer.

One of the important features of the instrumentation is that the fluid pressure and the differential pressure across the capillary are measured directly in the high pressure fluid and thus the influence of seal friction on these measurements is eliminated. The unique innovation of the system, however, is the differential pressure measurement. The instrumentation is capable of measuring small pressure fluctuations about the high pressure level with considerable accuracy (i.e. 1.0 psi variation about 10,000 psi is detectable).

The pressures (pressure level and pressure differential) were measured with three identical commercial strain gage pressure transducers,** two mounted at one end of the capillary and the third mounted at the other

---

* Model 7DCDT-050 and 7DCT-1000 manufacturered by the Sanborn Division of Hewlett-Packard Company.

** Norwood model 114 manufactured by the Advanced Technology Division of American-Standard.

TABLE I*

DISPLACEMENT TRANSDUCER SIGNAL SUMMARY

Sensitivity Switch Position (SS4)	Transducer Amplification (δ_4/d) (in^4/in)	Shear Rate Slope $\gamma/(\delta_4/t)$ $sec^{-1}/(in/sec)$.
1	119.1	1.68×10^4
2	4.24	4.72×10^5
3	6.41	3.12×10^5
4	18.55	1.08×10^5
5	74.8	2.67×10^4
6	2870.	7.2×10^2
7	26.6	7.51×10^4
8	40.9	4.89×10^4
9	113.1	1.53×10^4
10	722.	2.77×10^3

* Six-volt excitation. The first five positions of the sensitivity switch, SS4, are for the model 7DCDT1000 displacement transducer. The last five positions are for model 7DCDT050.

end. The pressure level of the test fluid was measured with pressure transducer G1 , (see Figure 2). The pressure differential across the capillary was measured with a pair of pressure transducers, G2 and G3 , which were placed at opposite ends of the capillary. At any pressure level, the electrical outputs of G2 and G3 were nulled through electrical balancing. Then, by amplifying the signals from these transducers through high gain dc amplifiers, small pressure fluctuations about the high pressure level were detected.

The maximum sensitivity of the differential pressure instrumentation is such that a galvanometer deflection of 0.11 inch was produced when the pressure in the dead weight gage was increased from 10,000 to 10,0001 psi. Thus the maximum sensitivity was 9.1 psi/inch. However, in order to increase the maximum measurable pressure differential the data were collected with lower amplifier gain settings (12.1-256 psi/inch). The following tables summarize the galvanometer output of the three pressure transducers. These tables show the sensitivity and range of each signal assuming six volt excitation for all transducers. The sensitivity of the differential pressure transducers can be increased or decreased by changing the gain of the appropriate amplifier. The ranges of the three pressure transducer signals were calculated assuming a maximum galvanometer deflection of five inches.

TABLE II

DIFFERENTIAL PRESSURE TRANSDUCER SIGNAL SUMMARY

Sensitivity Switch Position (SS1)	Transducer No. 1		Transducer No. 2	
	Galvanometer Signal			
	Sensitivity (psi/in.)	Range (±psi)	Sensitivity (psi/in.)	Range (±psi)
1	247.	1235.	256.	1280.
2	82.1	410.	84.7	423.
3	37.0	185.	38.5	192.
4	12.1	60.5	13.0	65.0

TABLE III

PRESSURE LEVEL TRANSDUCER SIGNAL SUMMARY

Sensitivity Switch Position (SS1)	Galvanometer Signal	
	slope (psi/in.)	Range (psi)
1	15300	0-77400*
2	9470	0-48000
3	6070	0-29500
4	3420	0-18000

* 100,000 psi can be measured by recording the output signal at any arbitrary pressure, then electrically nulling the output, and finally increasing the pressure. The correct galvanometer signal, δ_3 , is equal to the sum of the nulled signal and the recorded signal.

B. Experimental Limits

The two measurements which limit the range of experimental data are the shear stress and the flow rate. The minimum shear stress obtainable (approximately 300 dyn/cm^2) is limited by the largest capillary length-to-diameter ratio and the smallest measurable pressure differential across the capillary. The maximum shear stress obtainable (approximately 1.2 x 10^6 dyn/cm^2) is limited by the smallest capillary length-to-diameter ratio and the pressure difference at which the viscosity of the test fluid in the capillary cannot be considered uniform. These limits are represented by the vertical lines in Figure 7. The positions of the two constant shear rate lines in Figure 7 are determined by maximum and minimum flow rate. If the viscosity of the test fluid is greater than 200 cp, the minimum obtainable shear stress is limited by the smallest measurable flow rate (shear rate of 100 sec^{-1}). Similarly, if the viscosity is less than 150 cp, the maximum obtainable shear stress is limited by the maximum measurable flow rate (shear rate of 10^6 sec^{-1}).

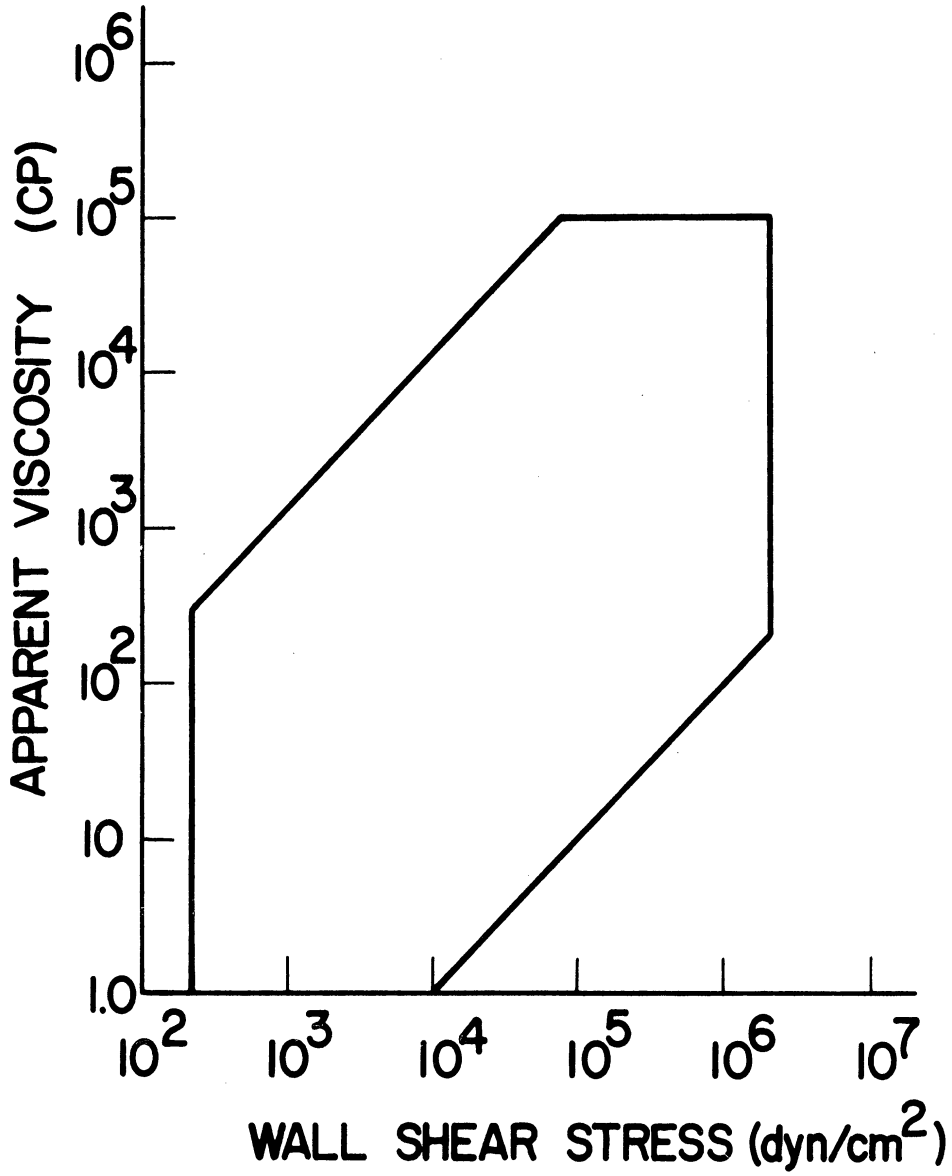

Figure 7. Approximate Experimental Limits.

The shear stress range (3×10^2 to 1.2×10^6 dyn/cm^2) is satisfactory and there is little to be gained by any extension less than an order of magnitude. There are only two possibilities for increasing the maximum shear stress. Namely, increase the maximum pressure differential across the capillary or decrease the capillary length-to-diameter ratio. The maximum pressure difference across the capillary (1000 psi) already causes a significant viscosity variation inside the capillary. Therefore increasing this variable by an order of magnitude is not permissible. The capillary length cannot be shortened much less than the existing 0.1 inch without causing fabrication problems. The 0.01 inch capillary diameter cannot be increased significantly without increasing the flow resistance of the high pressure tubing (I.D. = 0.06 inch) to an unacceptable magnitude. The minimum obtainable shear stress approaches the magnitude obtained in falling weight viscometers and thus the lower range does not need to be extended.

The minimum measurable flow rate is determined by the smallest displacement transducer signal which can be accurately measured. Thus any reduction in the flow rate measurement must be accompanied by an increase in the transducer signal. Amplification of the existing transducer signal is not practical because machinery induced vibration may result in an unacceptable noise level. Vibration isolation might solve this problem, however. A more sensitive displacement transducer may be helpful, but any such transducer should be able to measure large displacements as well as small ones. Thus a cantilevered beam, for example, would not be satisfactory even though it would have an increased sensitivity.

The most promising method for decreasing the measurable flow rate would be to increase the flow time. Thus satisfactory displacement signals could be obtained, even though the slopes of these signals would be decreased. This solution requires that the steady flow period be increased by increasing the duration of constant pressure in the low pressure hydraulic system.

The above limits are only imposed by the differential pressure transducers, the capillary geometry, and the displacement transducer. There are other factors, however, which may further reduce the experimental range. These include significant viscous heating, the low pressure hydraulic system characteristics, seal friction, the transient response of the test fluid, and gelation of the test fluid.

In Chapter II it was mentioned that the problem of viscous heating could not be avoided because the experiment is based on the viscous dissipation of mechanical energy to determine the viscosity of the fluid. This heating effect can be reduced, however, by employing short capillaries and low pressure drops to obtain the high shear rate data. In this investigation the pressure drop across the capillary was generally in the range of 100-200 psi and always less than 1000 psi. For a given capillary, shear rate, and shear stress, various fluids will exhibit differing viscous heating behavior depending on their thermal diffusivity, and viscosity-temperature characteristics. The thermal diffusivity does not vary greatly for the fluids examined, hence, the viscosity-temperature characteristics will have the most influence on viscous heating effects. The fluids with the greatest change of viscosity with temperature will be more likely to show the effects of viscous heating.

The best indication of the extent to which viscous heating was negligible is found in Figures 11, 13 and 25 where fluids which are expected to be Newtonian exhibit Newtonian behavior to shear stresses of 600,000 d/cm^2. Figure 25 shows the viscosity of the naphthenic base oil beginning to decrease at a shear stress of 220,000 d/cm^2, (shear rate of 45,000 sec^{-1}), or a shear-rate shear-stress product of 10^{10} ergs/sec cm^3 (1 kw/cm^3) at the wall. This fluid has the largest variation of viscosity with temperature of those examined. Thus it seems that the viscosity decrease is the result of viscous heating and not a pseudoplastic behavior of the fluid. Hence the data itself is an indication that viscous heating is negligible over the range of shear-rate shear-stress product up to 10^3 $watts/cm^3$.

The capillary geometry and the short time duration required to obtain data appear to be the reasons that viscous heating is not a problem below 10^3 $watts/cm^3$. This high rate of viscous dissipation only occurs for a few seconds at the capillary wall. Thus the volume of fluid actually subjected to this high rate of energy input is extremely small. The high thermal capacity of the capillary wall enables it to act as an effective heat sink during this short time period, thus justifying the assumption of an isothermal wall.

The low pressure hydraulic system characteristics also influence the range of experimental data because a constant flow rate of the hydraulic fluid is necessary to obtain steady flow through the capillary. This factor is only a problem when the viscosity of the test fluid is relatively low and thus only a very small hydraulic pressure is necessary to move the translating piston. Various methods such as applying weights to the pump handles and using the control valves as

flow restrictors were only partially successful in eliminating the relatively minor problem of unsteady flow through the capillary. The easiest solution to this problem is to use an experienced operator with a "gentle touch".

Friction between the high pressure seals and the translating piston can also reduce the experimental data range because of stick-slip behavior at low shear rates and pressures above 60,000 psi. This behavior increases the difficulty of obtaining steady flow through the capillary.

One additional factor which might have further restricted the range of useful data is the transient flow behavior of the test fluid. Bird[21] presents the solution to the problem of transient flow in a tube for a fluid initially at rest and subjected to a step pressure gradient. The solution shows that the time, t, required for the fluid to reach more than 92 percent of its final velocity is:

$$t = \frac{.5\,R^2}{\nu} \quad (\text{sec})$$

where R = tube radius,

ν = kinematic viscosity.

For the available capillaries, $R \approx 0.005$ inch.

Thus,

$$t = \frac{(.5)(5 \times 10^{-3}\ \text{in})^2}{1.55 \times 10^{-3}\ \left(\frac{\text{in}^2/\text{sec}}{\text{cs}}\right)\ \nu\ (\text{cs})} = \frac{8.07 \times 10^{-3}\ \text{sec}}{\nu}$$

where

$\nu_{min} \approx 1.0$ cs, and

$\nu_{max} \approx 10^5$ cs,

Therefore, $t_{max} = 8.07 \times 10^{-3}$ sec and

$t_{min} = 8.07 \times 10^{-8}$ sec.

The response time for the differential amplifiers is approximately 0.1 sec, therefore the transient behavior of the test fluid is negligible compared with either the amplifier response or the normal test runs of 0.4 second or greater.

As mentioned in Chapter II, gelation of the test fluid results from the solidification of some constituents in the fluid at certain combinations of pressure and low temperatures (usually below 0°F). For this research, gelation of the paraffinic and naphthenic based fluids occurred in the high pressure sections outside the constant temperature bath. The existence of this phenomena is readily observed because the differential pressure transducer signals lag the displacement transducer signal, thus making the results meaningless.

An unsuccessful attempt was made to prevent this gelation problem by heating the appropriate sections with electrical heaters. Other possible solutions were also considered but were not feasible for various reasons. Therefore it was concluded that the gelation problem could not be eliminated for certain fluids without major equipment modifications.

Another factor which might have further restricted the range of useful data, or required correction, was change in the capillary diameter at elevated temperature and/or pressure. This factor was

investigated analytically and the possible effect on the viscosity data was shown to be negligible.

C. Calibration

In this section the method used to determine the capillary diameter is discussed. The calibration methods for each of the four transducers are also explained. Typical calibration curves and a summary of the calibration data for each transducer are presented in Appendix B as well as a discussion of the accuracy of each transducer signal.

The diameter of each capillary was determined by passing a viscosity standard fluid* through the capillary and measuring the volumetric flow rate, the pressure drop, and the capillary length. These quantities were then substituted into the Hagen-Poiseuille equation to determine an "average" or "effective" diameter. This was performed separately from the high pressure system and employed relatively low pressure drops (i.e. 50 psi) across the capillary which exited to atmospheric pressure. Table IV contains the dimensions of the four capillaries available.

TABLE IV

CAPILLARY GEOMETRY

Capillary No.	Length (in.)	Diameter (in.)	Length-to-Diameter Ratio
1	0.109	0.00938	11.6
2	0.501	0.009834	50.9
3	1.007	0.01004	100.2
4	2.933	0.01048	280.0

*These fluids conform to the ASTM viscosity standard and were purchased from the Cannon Instrument Company.

The instrument (Figure 8) used for the calibration of the capillary diameters was also used to obtain the atmospheric high shear data. It consisted of a pressure source (bottled gaseous nitrogen), a pressure regulator, a ballast tank, a pressure gage, the fluid reservoir, the capillary section, a fluid collector, and a flow meter. The capillary inlet pressure, was measured with a calibrated 500 psi Heise bourdon gage. The capillary exit was connected to one end of a glass fluid collector. The other end of this collector was connected to a calibrated bubble meter. The bubble rise time was measured with an electronic timer which was triggered by pulses from a Wheatstone bridge circuit containing two light sensitive resistors. When the bubble passed between the light source and corresponding resistor, a signal pulse was generated which started or stopped the timer.

The temperature of the fluid in this system was controlled by placing the fluid reservoir, the capillary section and the fluid collector in a constant temperature bath. The temperature was measured with a calibrated mercury-in-glass thermometer (ASTM 64-F).

Calibration of the displacement transducers was very straight forward because the core of the displacement transducer was attached to a micrometer head mounted on the translating piston. Thus the calibration was obtained by recording micrometer displacement versus recorder galvanometer displacement. Table I (Chapter III, Section A) contains a summary of the amplification ratios available. The calibration curves are presented in Appendix B.

The manufacturer of the three strain gage pressure transducers supplied calibration data for each transducer up to 100,000 psi. Because

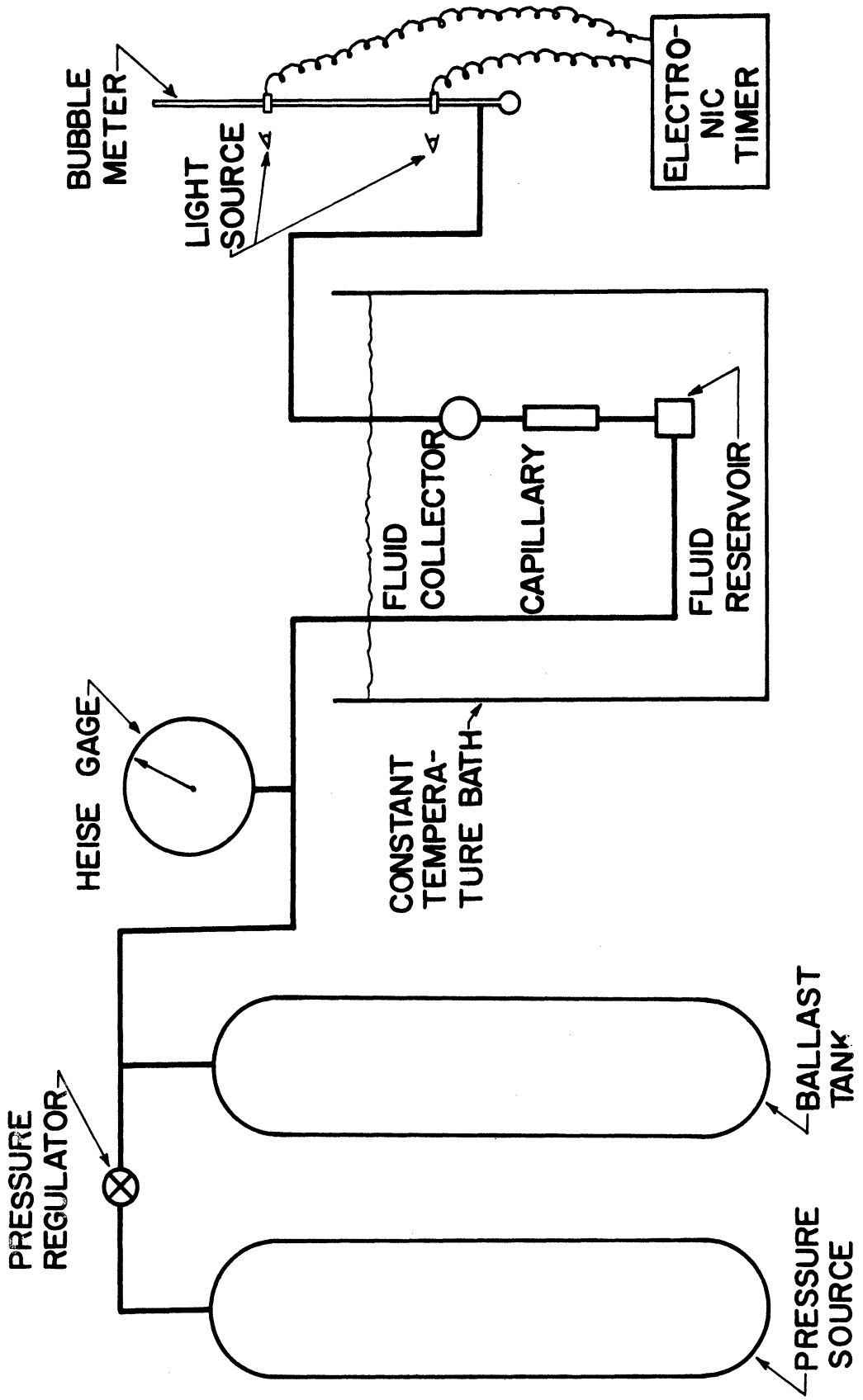

Figure 8. Schematic Drawing of Atmospheric Pressure Capillary Viscometer.

of the extreme amplification of the signal from the two gages used for the differential pressure measurement further calibration was made. This consisted of a calibration on a dead weight gage to 12,000 psi and of the measurement of viscosity in the system of a well defined fluid for which viscosity-pressure data had been reported. The dead weight gage calibration is discussed in the following paragraphs and the system verification procedure which compared measured data with reported data is discussed in the next section of this chapter.

The goals of the calibration procedure for the pressure transducers were (1) to check the accuracy of the manufacturer's data where possible, (2) to determine equivalent pressures for the calibration resistors, and (3) to demonstrate the feasibility of the method for determining the pressure difference across the capillary. The ideal equipment to calibrate these transducers would have been a dead weight gage capable of accurately producing small pressure variations about any pressure level between atmospheric pressure and 150,000 psi. The small pressure variations should have been between one and one hundred psi. Since there is no such dead weight gage in existence, it was necessary to use the equipment available at the University of Michigan. The dead weight gage which was available was a Ruska Model 2400. With certain corrections, this device is capable of accurately determining pressures to within ten parts per million at any pressure level below 12,140 psi. Without using any corrections, the accuracy is approximately 0.2 psi. The existing instrumentation could not detect pressure deviations of this latter magnitude and thus it was not necessary to use any corrections for the calibration data.

Since the available dead weight gage had an upper pressure limit of 12,140 psi, it was necessary to rely on the supplied calibration data above this limit. The Ruska equipment did allow a means of satisfying above mentioned goals for pressures below 12,140 psi. The equivalent pressures for the calibration resistors are summarized in Appendix B. The method for determining the pressure difference across the capillary is based on the assumption that the slopes (percent output versus pressure) of the calibration curves are constant between the calibration points supplied by the manufacturer. The accuracy of all experimental data therefore depends upon the accuracy of this assumption. Figure 9 shows that this assumption is verified at 10,000 and 12,000 psi.

Since it was not possible to obtain the desired calibration data above 12,000 psi, it was necessary to verify that the equipment worked properly for pressures greater than 12,000 psi. This was accomplished by comparing the measured low shear viscosity values of a chemically well-defined fluid with those published by the American Society of Mechanical Engineers.[10] This verification procedure is discussed in the next section.

D. Verification

As mentioned previously, it was necessary to verify that the accuracy of the experimental apparatus was satisfactory above 12,000 psi because calibration above this pressure level was impossible. This verification procedure consisted of comparing the measured low shear viscosity data of a chemically well-defined fluid with the data published by the American Society of Mechanical Engineers.[10] The fluid used for

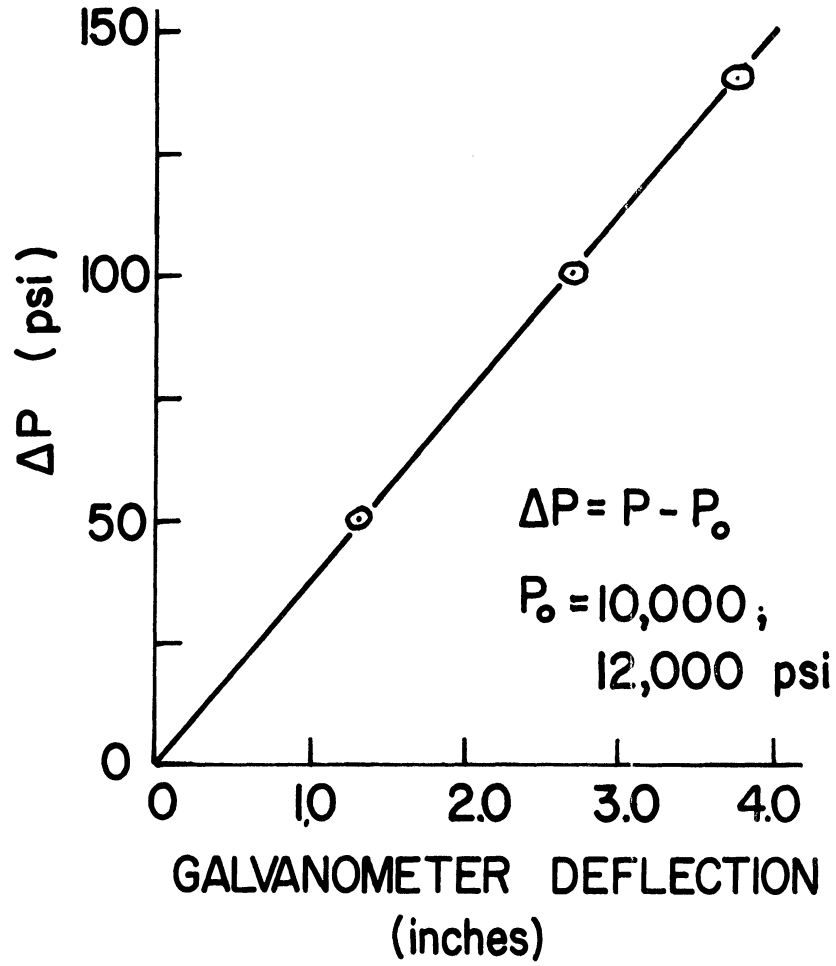

Figure 9. Typical Calibration Curve for Differential Pressure Transducers.

this purpose was Plexol 201, bis-2-ethyl hexyl sebacate, (ASME, A-1), donated by the Rohm and Haas Company. The properties of all other fluids examined are presented in Appendix A.

Figure 10 is a curve of viscosty-versus-pressure for this fluid (Fluid A) which contains both the reported ASME data and the mean value of the measured data. This figure shows that both sets of data agree favorably. Table V is a summary of the reported and measured data, the percent deviation between the two data sets, and the standard deviation for the measured data.

TABLE V

SUMMARY OF REPORTED AND MEASURED DATA FOR FLUID A
BIS 2-ETHYL HEXYL SEBACATE

Pressure (psig)	μ^* ASME Data (cps)	$\bar{\mu}$ Measured (cp)	Deviation (Percent)	Standard Deviation for $\bar{\mu}$(S)	$S/\bar{\mu}$
0	11.22	10.95	-2.40	--	--
10,000	29.0	28.8	0.69	1.24	.043
18,800	60.0	59.0	-1.67	2.14	.0357
29,500	133.	131.6	-1.04	4.0	.030
37,300	232.	235.	1.29	15.	.064
47,500	455.	455.	--	30.	.0675
58,500	880.	870.	1.14	18.2	.0210
67,500	1500.	1460.	2.66	89.8	.060
79,300	2900.	2900.	--	153.	.0527

* Data taken from Viscosity-Pressure Curve, Figure 10.

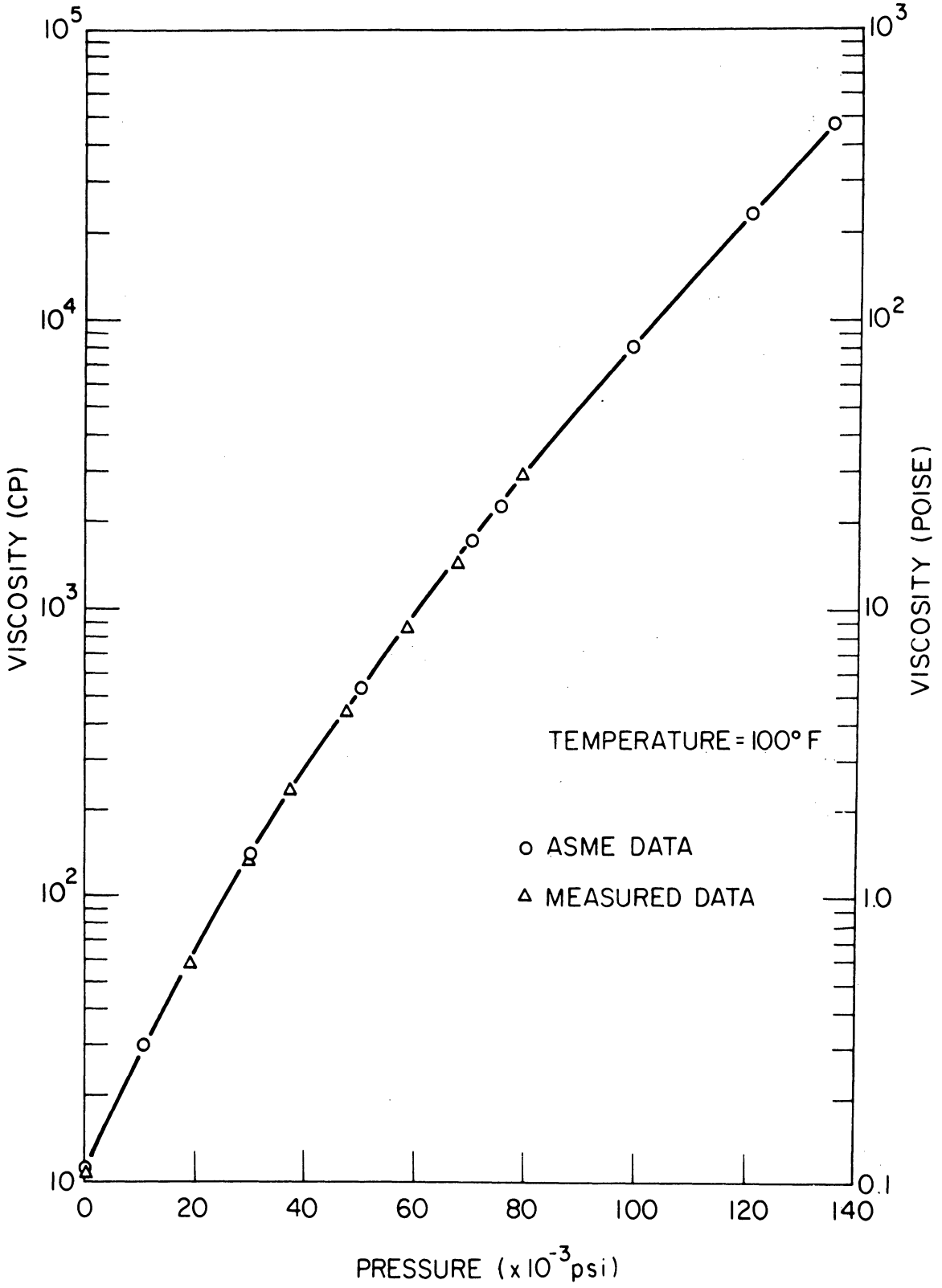

Figure 10. Comparison of Reported and Measured for Fluid A (Diester).

Figure 11 is a curve of viscosity versus shear stress for the same fluid. It shows that Fluid A is Newtonian at both atmospheric pressure and 50,000 psi for the shear stress range shown.

The data in Table V deviated from the reported values by less than 1.7 percent for all but one case. This is within the two percent accuracy estimated for the comparison data. As a result of this verification procedure, it can be concluded that the accuracy of the experimental apparatus is sufficient ($< \pm 5\%$) for the complete range pressure levels obtainable. The overall accuracy of the equipment is further discussed in the last section of this chapter.

E. Error Analysis

The major source of error which limits the accuracy of the data was the measurement of the galvanometer signals on the recording. The magnitudes of these signals were determined by using a scale, with 0.01 inch graduations, to measure the distance between the projected references and the galvanometer traces. Thus both the projection of the reference points and the measurement of the distance between the reference points and the galvanometer traces were possible sources of error. The possibility of error in the reference projection was minimized by first setting all four galvanometer traces to convenient positions and then running several inches of recording paper before the signals were produced. The maximum error in the distance measurement between the reference lines and the galvanometer traces was estimated to be less than 0.02 inch. Thus the percentage of error could be reduced by obtaining large galvanometer deflections.*

---

* The linearity of any deflection is with ± 2 percent of the reading.

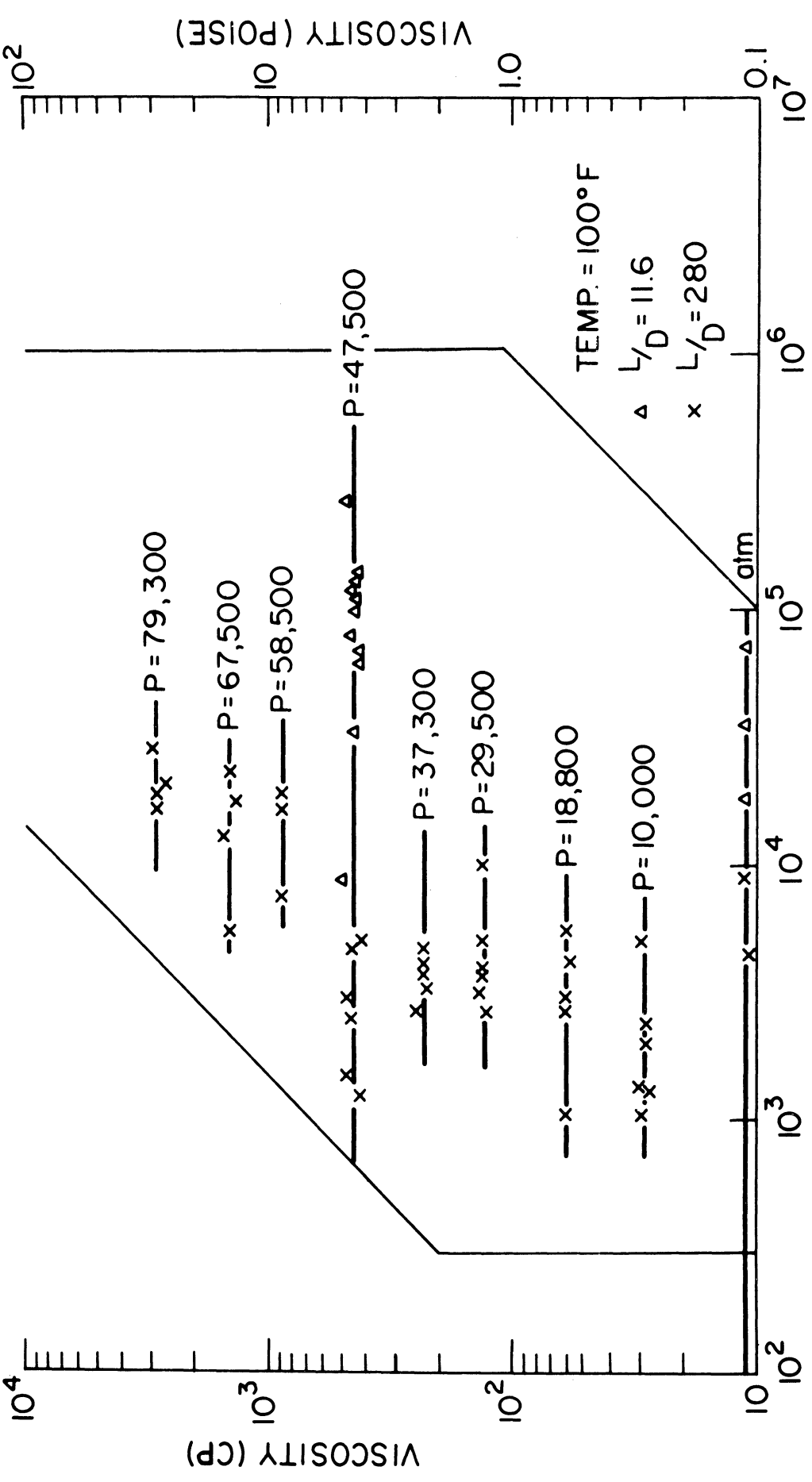

Figure 11. Flow Curve for Fluid A (Diester).

The possible calibration error is discussed in Appendix B, Section 2. This discussion shows that the error of the galvanometer signals for all four transducers was less than one percent of the phenomenon being measured. Therefore, the measurements of the galvanometer signals during data acquisition presented a much greater possibility of error than the possible error in either the transducers calibrations or the calibration constants. Hence, the following discussion only considers the measurement error of the data acquisition signals because this was the most important factor.

From the Hagen-Poiseuille equation, the viscosity, μ , of a fluid is:

$$\mu = \frac{\pi D^4 \Delta P}{128\ LQ} \qquad (24)$$

where D is the capillary diameter in inches,

L is the capillary length in inches,

ΔP is the pressure drop across the capillary in psi,

Q is the volumetric flow rate through the capillary in in^3/sec.

The length of each capillary was measured with a micrometer. The diameter to the fourth power of each capillary was determined by passing a fluid of known viscosity through the capillary and measuring the pressure drop and volumetric flow rate. The equipment used to determine the capillary diameters is described in Section C of this chapter. The test fluid temperature was controlled by a constant temperature bath and was measured by a calibrated mercury-in-glass thermometer.

Thus for each available capillary, the equation for viscosity was reduced to

$$\mu = k \frac{\Delta P}{Q} \tag{25}$$

where $$\Delta P = (K_1 \delta_1 - K_2 \delta_2) - KEC ,$$

$$Q = k_2 \delta_4 / t .$$

δ_1 and δ_2 = galvanometer displacement for the two differential pressure signals

δ_4 = galvanometer displacement for the displacement signal

t = time during which δ_4 occurred*

KEC = kinetic energy correction

The displacement signal δ_4, was only measured for discrete time increments, thus reducing the possible error of the time measurement to a negligible quantity. Since K_1 was approximately equal to K_2 and the kinetic energy correction was usually negligible, the viscosity equation reduced further to:

$$\mu \approx \frac{K(\delta_1 - \delta_2)}{\delta_4} \tag{26}$$

Figure 12 shows the maximum possible random error in the viscosity calculation as a function of the galvanometer signals. The smallest possible random error of ± 1.0 percent would be reached if the three galvanometer signals each produced their maximum displacement of five inches. For the majority of the experimental data, however, the displacement transducer signal was between 0.5 and 1.5 inches while the differential pressure signals were between 1.0 and 3.0 inches. Thus from Figure 12 it can be seen that the random error for one data point was usually between ± 2.0 percent and approximately ± 6.0 percent.

---

* Time signals were produced by the internal circuitry of the oscillographic recorder with an accuracy of approximately one percent.

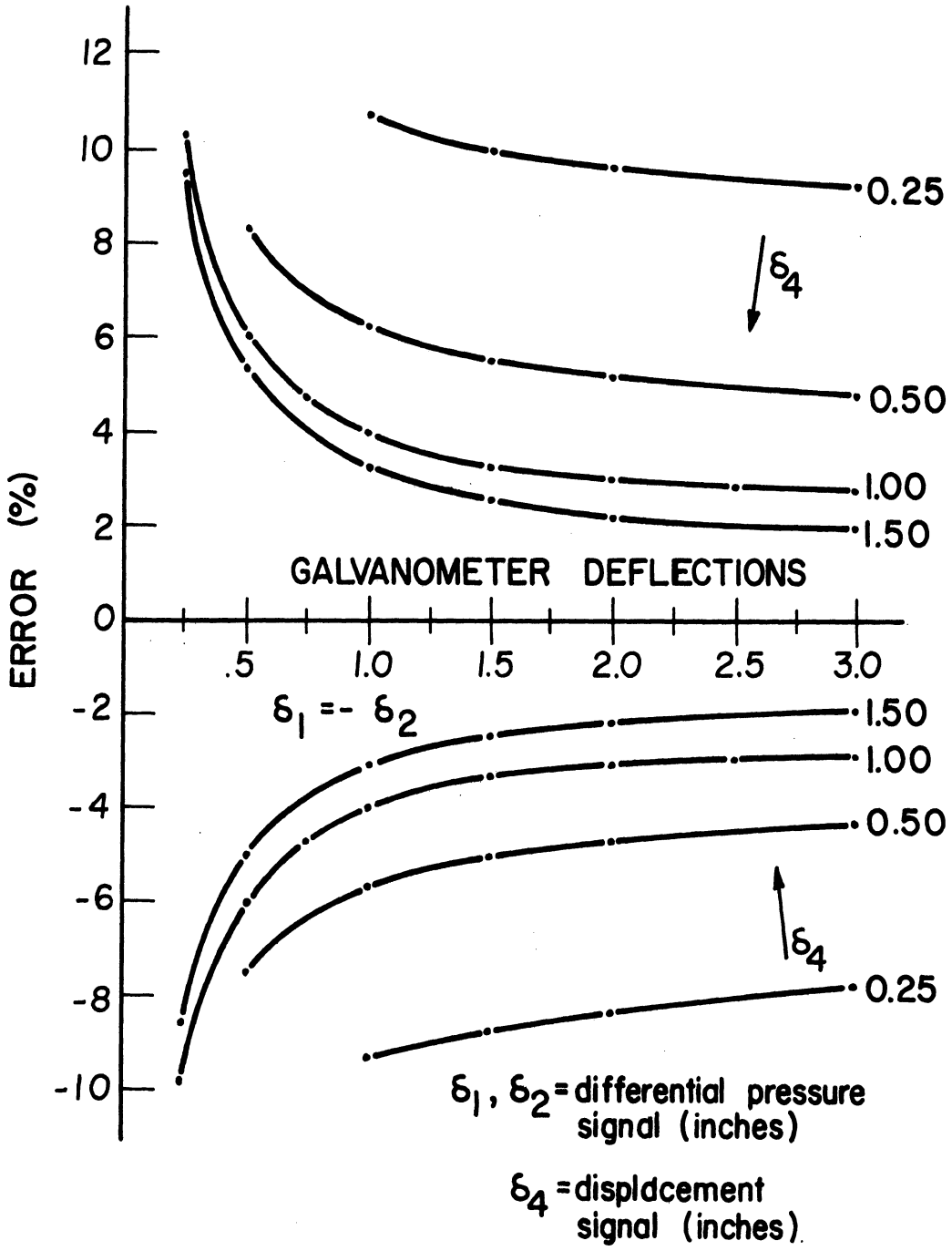

Figure 12. Possible Random Error in Viscosity Measurements.

It must be emphasized that Figure 12 shows the maximum possible error for any one data point. The probable error for each point is less than the values shown in Figure 12 because the possible errors of the three signals may tend to cancel each other. The reliability will also be increased if several data points are obtained and their mean value used. This fact is exemplified by the data for fluid A recorded in Table V. The majority of this data would have a maximum possible random error of approximately four percent if Figure 12 was used. The mean value of several data points, however, deviated from the reported values by less than 1.7 percent for all but one case. Only a few data points were taken for the mean viscosity value which deviated from the reported value by 2.66 percent.

The accuracy of pressure level data will also significantly affect accuracy of the measured viscosity data. The slope of the viscosity-pressure curve, S, (plotted on semilogarithmic paper) is:

$$S = \frac{d(\log_{10} \mu)}{dP} = \frac{1}{2.3} \quad \frac{d(\log_e \mu)}{dP}$$

$$S = \frac{1}{2.3\,\mu} \quad \frac{d\mu}{dP} \tag{27}$$

Thus the fractional change of viscosity with pressure is

$$\frac{\Delta\mu}{\mu} \approx 2.3\ S\ \Delta P \tag{28}$$

where ΔP is the possible inaccuracy of the pressure measurement. The possible error in the pressure measurement, E_p, is

$$E_p = \frac{\Delta P}{P} \times 100 \tag{29}$$

and therefore

$$\Delta P = \frac{E_p P}{100} \tag{30}$$

Thus the possible error in the viscosity measurement, E_μ , is

$$E_\mu = \frac{\Delta\mu}{\mu} 100 = 100 \times 2.3 \times S \times \Delta P \tag{31}$$

Hence, substituting Equation (30) into Equation (31) results in

$$E_\mu = 2.3 \times S \times E_p \times P \quad (\%) \tag{32}$$

The fractional change of viscosity with pressure (2.3 x S) for fluid A, for example, varies from about 1.07×10^{-4} psi^{-1} at low pressure to 0.59×10^{-4} psi^{-1} at high pressure. The maximum error in the pressure level, which is the sum of the calibration error and the galvanometer signal measurement error is approximately one percent. Therefore the resulting inaccuracy of the viscosity measurement is about 1.1 percent at 10,000 psi and 5.9 percent at 100,000 psi.

CHAPTER IV

FLUID BEHAVIOR

A. Experimental Fluids

The ten fluids investigated in this research are listed in Table VI and further characterization of the components of each fluid is shown in Appendix A. These fluids were chosen because they are well defined counterparts of some typical commercially available lubricants and this selection enables several trends and interrelations to be investigated. The list of fluids includes both a paraffinic and a naphthenic oil and these blended with two polymeric viscosity-index improvers. It also includes four synthetic fluids.

TABLE VI

EXPERIMENTAL FLUIDS

Letter	Description
A	Diester-Plexol 201 bis-2-ethyl hexyl sebacate
B	Paraffinic Base Oil R-620-12
C	B + 4% polyalkylmethacrylate (PAMA)
D	B + 8% polyalkylmethacrylate (PAMA)
E	B + 4% polyalkylstyrene (PAS)
F	Naphthenic Base Oil R-620-15
G	F + 4% polyalkylmethacrylate (PAMA)
H	Polybutene LF-5193
I	Dimethylsiloxane
J	Trifluoropropylmethylsiloxane

Some of the questions to be answered by the experimental data (and the fluids chosen to do so) are presented in the following list.*

* The answers to these questions are presented in detail in Section B of this chapter and summarized in Chapter V.

1. What is the effect of adding various amounts of a given polymer to a given base oil? (Fluids B, C, D)

2. How are the results affected when a given amount of different polymers are added to a base oil? (Fluids B, C, E)

3. How are the results for a given amount of polymer affected by the selection of the base oil? (Fluids B, C, F, G)

4. How does the behavior of some synthetic fluids differ from that of the petroleum oils? (Fluids H, I, J)

B. Experimental Results

The figures presented in the following discussion are visual aids which help in understanding the behavior of the experimental fluids and do not contain all of the data obtained. Section D of this chapter does contain a complete tabulation of the experimental data. All of these tabulated data do account for the kinetic energy of the fluid leaving the capillary while some data account for the elastic energy stored in the fluid and/or account for the effect of a non-parabolic velocity profile (i.e. the Rabinowitsch analysis). Since a parabolic velocity profile does exist for Newtonian fluids and the elastic energy is negligible, or nonexistent, the tabulated data for the Newtonian fluids (A, B, F, H, I, J) are in final form and therefore need no further interpretation. However, for the non-Newtonian fluids, the effect of a non-parabolic velocity profile must be investigated and also the magnitude of the elastic energy must be determined. These two effects are discussed later in this section.

The density of the experimental fluids at all temperatures and pressures was determined from bulk modulus correlations.[27,28] These density data were necessary in order to convert the experimental

absolute viscostiy data to kinematic viscosity necessary for the standard ASTM viscosity-temperature charts.

1. General Trends

The flow curves, the viscosity-temperature relations, and the viscosity-pressure relations for all ten fluids examined are presented in Figures 10, 11, and 13 through 38. These figures indicate the following general behavior:

(1) The flow curves show that the basic behavior of a fluid is not affected by temperature or pressure unless gelation occurs. Six of the fluids (A, B, F, H, I, J) exhibit a Newtonian behavior at all temperatures and pressures examined. The other four fluids (C, D, E, G) are non-Newtonian at all temperatures and pressures.

(2) Straight line relations are obtained on the ASTM viscosity-temperature charts for all fluids when pressure and shear stress are constant.

(3) The viscosity-pressure relations for the silicones are basically different than the viscosity-pressure relations for the other fluids examined. The viscosity-pressure curves for the silicones (Figure 38) posses inflection points while similar curves for the other fluids do not.

(4) The flow curves for the four non-Newtonian fluids show that the viscosity is constant in a low shear stress range (initial Newtonian region) and then begins to decrease with increasing shear stress. The shear stress value at which this temporary viscosity loss begins seems to be only a function of the viscosity level, and independent of the temperature. This is observed by noting that for Fluid C

the flow curve (Figure 16) for 100°F and 20,000 psig is almost superimposed on the flow curve for 210°F and 50,000 psig. This same trend is indicated by the flow curves for Fluid G (Figure 28). As the first Newtonian viscosity increases, the maximum shear stress in the first Newtonian region increases while the corresponding shear rate decreases. Thus the temporary viscosity loss seems to begin near a line of constant energy input, i.e. a line of constant shear-stress shear-rate product. No permanent viscosity loss was observed in these fluids.

These four general trends were observed after Fluids A, B, C, F, and G had been examined and this information led to the conclusion that it was not necessary to obtain flow curves over a wide shear stress range at all temperatures and pressures in order to define the behavior of the remaining fluids. Therefore, the decision was made to eliminate any further data at 300°F. Additional flow curves were only obtained at atmospheric pressure and both 100°F and 210°F as well as at some elevated pressure and 100°F. Low shear data, however, were still obtained at several pressures and temperatures of 100°F and 210°F. This reduced quantity of data still enabled the validity of the above mentioned trends to be examined for each additional fluid.

A partial summary of the experimental data is presented in Table VII which contains viscosity values as well as viscosity-temperature and viscosity-pressure coefficients at two pressures for all fluids examined.

TABLE VII

DATA SUMMARY[a]

Pressure	Viscosity, and Viscosity-Temperature Coefficient (VTC[b])						Viscosity-Pressure Coefficient (α[c])	
	Atmospheric			50,000 psi			Atmospheric	50,000 psi
Fluid	μ (cp)	ν (cs)	VTC	μ (cp)	ν (cs)	VTC	$\alpha \times 10^4$ (psi^{-1})	$\alpha \times 10^4$ (psi^{-1})
A	11.0	12.2	.740	538.	528.	.913	1.07	0.59
B	29.	34.1	.845	7400.	7650.	.965	1.31	0.92
C	65.	76.5	.823	12000.	12400.	.950	1.21	0.98
D	140.	165.	.843	45000.	46500.	.975	1.15	1.15
E	105.	124.	.876	18000.[d]	19100.[d]	--	1.39	1.15[d]
F	22.	24.3	.873	460.[e]	477.[e]	.950[e]	1.53	1.53[e]
G	60.	66.3	.837	1140.[e]	1188.[e]	.943[e]	1.49	1.49[e]
H	90.	108.	.906	112000.[d]	121000.[d]	.991[d]	2.09	1.71[d]
I	79.	82.6	.620	5100.	4480.	.794	1.15	0.81
J	100.	81.3	.833	62000.	44000.	.971	1.53	1.35

(a) $T = 100°F$, $\tau = 10^4$ dyn/cm^2

(b) $VTC = 1 - (\mu_{210}/\mu_{100})_P$

(c) $\alpha = \frac{1}{\mu} \left.\frac{\partial \mu}{\partial P}\right|_T$

(d) Press. = 40,000 psi

(e) Press. = 20,000 psi.

2. Specific Fluids

a. Diester

As mentioned previously, the diester (Fluid A) was investigated to verify the accuracy of the experimental equipment. Figures 10 and 11 contain the experimental results for this fluid which have been discussed in Chapter III.

b. Paraffinic Based Fluids

Figures 13 through 24 and 39 through 44 contain data for the paraffinic based fluids with varying amounts of two polymer additives (Fluids B through E). Gelation limited the maximum pressure to 50,000 psig for these fluids. As discussed in Chapter III, Figure 13 shows that Fluid B (Paraffinic Base Oil) is Newtonian at all temperatures and pressures examined and indicates that viscous dissipation was negligible for this fluid. The flow curves for Fluids C, D, and E (Figures 16, 19, and 22) show that these fluids are non-Newtonian at all temperatures and pressures investigated. The elastic energy stored in these fluids is negligible below a shear stress of approximately 10^5 dyn/cm^2 as indicated by the consistency of the data obtained with different capillaries. The data at atmospheric pressure and 100°F show that a small elastic energy is present in these fluids for shear stresses greater than 10^5 dyn/cm^2.

Figure 39 contains the flow curves of the four paraffinic based fluids at atmospheric pressure and temperatures of 100°F and 210°F. The flow curves are drawn through the data points which contain the elastic energy correction. The uncorrected data points are also included. The elastic energy stored in these fluids was evaluated from the data presented in this figure according to the method discussed in Chapter II.

Table VIII and Figure 40 summarize the elastic energy calculations for the four non-Newtonian fluids. Figure 40 shows that, at a temperature of 100°F and a given shear rate, the elastic energy in Fluid E is greater than the energy in Fluid C and less than the energy in Fluid D. It was not possible to evaluate the elastic energy in any of the non-Newtonian fluids at atmospheric pressure and 210°F because the lower viscosity values made it impossible to obtain the necessary high shear data in the available equipment.

Equation 23, Chapter II, and Figure 39 show that if the elastic energy stored in the fluid is not taken into account, the viscosity data will be higher than the correct value. Figure 41 contains the flow curves for Fluids B, C, D, and E, at 20,000 psig and 100°F, and shows that the high shear viscosity of these fluids does not begin to approach the viscosity of the base oil (Fluid B). This relatively small temporary viscosity loss led to some speculation that the recoverable shear strain, S_r , might be large. Considerable effort was expended, with little success, to evaluate the magnitude of the elastic energy stored in the polymer blends at elevated pressures by obtaining data with different capillaries.

With the present high pressure data on Fluid C it is not possible to evaluate the elastic energy above 10^5 dyn/cm^2 because this data was obtained with a single capillary. The high pressure data for Fluid D are also insufficient to evaluate the elastic energy because the maximum shear stress (2.8×10^5 dyn/cm^2) obtained with capillary Number 2 (L/D = 50.9) was smaller than the minimum shear stress (4.7×10^5 dyn/cm^2) obtained with capillary Number 1 (L/D = 11.6). These data, however,

TABLE VIII

ELASTIC ENERGY CALCULATION SUMMARY*

Fluid	Temperature (°F)	Pressure (psig)	Shear Stress (dyn/cm^2)	Shear Rate (sec^{-1})	Recoverable Shear Strain (in/in)
C	100.	0.	1.5×10^5	3.2×10^5	4.7
C	100.	0.	3.0×10^5	7.6×10^5	7.2
D	100.	0.	1.4×10^5	1.2×10^5	7.1
D	100.	0.	2.4×10^5	2.8×10^5	8.2
D	100.	0.	4.4×10^5	5.9×10^5	10.1
D	100.	50,000.	$\sim 3 \times 10^5$	$\sim 10^3$	$0 < S_R < 13.8$
E	100.	0.	2.6×10^5	4.2×10^5	6.5
G	100.	0.	$.94 \times 10^5$	2.1×10^5	4.6
G	100.	0.	1.5×10^5	4.1×10^5	11.8
G	100.	0.	2.5×10^5	8.0×10^5	15.5

* The values in this table were calculated from data obtained from capillaries Number 1 and 2. With these capillaries, the smallest measurable recoverable shear strain is approximately four.

were sufficiently close together to enable an estimate to be made of the possible bounds of the elastic energy correction. This was accomplished by placing a band of ± 5 percent around each data point obtained with capillaries Number 1 and 2. When a smooth curve is drawn through these data, it indicates that no elastic energy is stored in the fluid at a shear stress of approximately 3.3×10^5 dyn/cm^2 (shear rate of 10^3 sec^{-1}, viscosity of 330 poise). When separate curves are drawn, the curve through the capillary Number 2 data is below the corresponding curve through the capillary Number 1 data, thus indicating that elastic energy is stored in the fluid. When this energy is taken into account the resulting viscosity (280 poise) is 15 percent below the uncorrected value. The elastic energy in Fluid E cannot be evaluated at high pressures either because of insufficient data.* Thus it was not possible to obtain the necessary high pressure data with the existing equipment. However, the high pressure data which was obtained did show, that the elastic energy effect is not large. The atmospheric pressure data confirmed that the elastic energy correction is small for the shear stress range investigated. The corrected data in Figure 39 also show that the high shear viscosity of the polymer blends does not reach a second Newtonian value close to that of the base oil, as expected. Thus it appears that the small temporary viscosity loss at high shear stresses for the fluids examined is the actual behavior of the fluids and is not caused by an elastic energy effect. However, the recoverable shear strain is known to increase with shear stress,[20] to some maximum value, and hence the

---

* Chapter V contains further discussion of the elastic energy in these fluids subjected to high pressure.

temporary viscosity loss may increase significantly outside the experimental shear stress range obtained in this research and thus a second Newtonian region may occur in which the viscosity is significantly closer to the viscosity of the base oil than the data obtained.

The technique employed to determine whether or not any permanent viscosity loss was caused by high shear stresses applied to the fluids consisted of first obtaining the low shear viscosity data and then obtaining data at ever increasing shear stresses. After the maximum shear stress is obtained, the fluid is again passed through the capillary with a low shear stress. If the two low shear stress viscosity values agree, it is assumed that a permanent viscosity loss was not caused by the high shear stresses. The fallacy in this method is that it does not assure that the permanent viscosity loss is negligible because only the fluid near the capillary wall is actually subjected to the high shear stress and therefore permanent viscosity loss only occurs in a small percentage of the fluid. When the fluid is repassed through the capillary, the probability will be very small that the "ruptured" fluid will again be near the capillary wall. Thus a permanent viscosity loss may not be detected by this technique when subsequent low shear data are obtained.

The Rabinowitsch analysis for Fluids C, D, and E showed that the effect of non-parabolic velocity profiles increased the shear rate at the wall by less than five percent in all cases. Therefore, the resulting reduction in viscosity was also less than five percent. Since in many data sets it was impossible to account for the elastic energy stored in the fluid, the Rabinowitsch analysis could not be used because these data must be corrected for the elastic energy stored in the fluid

before the true shear stress can be evaluated, and hence the true shear rate determined.

Contant pressure data for Fluid B yield straight line relationships on an ASTM viscosity-temperature chart, Figure 14. The slopes of these lines decrease with increasing pressure. However, the percentage change in viscosity, for a given temperature increase, actually increases with increasing pressure. Constant pressure and constant shear stress data for Fluids C, D, and E also yield straight line relationships on an ASTM viscosity-temperature chart (Figures 17, 20 and 23). The slope of any viscosity-temperature line for Fluid C is less than the slope of the corresponding line for Fluid B and greater than the corresponding slope in Fluid D. This trend was expected because the viscosity of polymer blends is known to decrease less with increasing temperature than the viscosity of the base oil. This viscosity-temperature curves at 10,000 psig for the paraffinic based fluids (Figure 42) and the viscosity-pressure curves for these fluids (Figure 43) at 100°F indicate that the four percent styrene (Fluid E) has both a steeper viscosity-temperature slope and a higher viscosity-pressure coefficient than the four percent methacrylate (Fluid C). Figure 44 shows the effect of polymer in the paraffinic base oil as a function of pressure.

The viscosity-pressure curves for the paraffinic based fluids partially answer the first question presented in Section A of this chapter: what is the effect of adding various amounts of a given polymer to a given base oil? Figure 43 shows that the slope of the viscosity-pressure curve for Fluid B decreases with increasing pressure. The same trend is true for Fluid C except that the viscosity-pressure curve tends

to become straight near 50,000 psi. The corresponding curve for Fluid D has a constant slope throughout the pressure range examined. Thus while the slopes of the viscosity-pressure curves decrease with increasing polymer content at atmospheric pressure the opposite is true at 50,000 psi. This trend can readily be seen by studying the viscosity-pressure coefficients for these fluids presented in Table VII.

Figure 44 also helps to explain the effect of various amounts of polyalkylmethacrylate (PAMA) in the paraffinic base oil. This figure shows that viscosity of the blend increases with increasing polymer content as expected, but it also shows that eight percent PAMA has more of an effect at 50,000 psi than it does at lower pressures.

c. Naphthenic Based Fluids

The data for the naphthenic based fluids (Fluids F and G) indicate a behavior similar to the corresponding paraffinic based fluids (Fluids B and C), as anticipated. The flow curves for the naphthenic base oil (Figure 25) show that this fluid is also Newtonian at all temperatures and pressures examined and indicates that viscous heating appears to be negligible below a shear-rate shear-stress product 10^{10} dyn/cm^2 sec. The flow curves for Fluid G (Figure 28) indicate that this fluid is non-Newtonian at all temperatures and pressures investigated. The elastic energy stored in Fluid G appears to be negligible below 10^5 dyn/cm^2 at elevated pressures. Figure 45 contains the flow curves of these two fluids at atmospheric pressure and temperatures of 100°F and 210°F. As in Figure 39, the flow curve is drawn through the data points which contain the elastic energy correction and the uncorrected data points are included for completeness. The values of the recoverable

shear strain obtained from these atmospheric data are presented in Table VIII. These data indicate that, for a constant shear rate, four percent polyalkylmethacrylate has a larger elastic energy when blended with the naphthenic base oil (Fluid G) than when blended with the paraffinic base oil (Fluid C).

As with the paraffinic based fluids, the high pressure data for Fluid G were not sufficient to evaluate the elastic energy. The general comments regarding the elastic energy in Fluids C, D, and E also seem to be applicable to Fluid G. These comments are:

1. the high pressure data indicate that the elastic energy is not large;

2. the atmospheric pressure data confirmed that the elastic energy correction is small for the experimental shear stress range; and

3. it appears that the small temporary viscosity loss observed at high shear stresses is the actual behavior of the fluids and is not caused by an elastic energy effect.

The third comment must be qualified by noting that the recoverable shear strain increases with shear stress,[20] to some maximum value, and hence the temporary viscosity loss may increase significantly outside the experimental shear stress range obtained in this research and thus a second Newtonian region may occur in which the viscosity is significantly closer to the viscosity of the base oil than the data obtained.

The Rabinowitsch analysis for Fluid G showed that the effect of non-parabolic velocity profiles increased the shear rate at the wall by less than 10 percent for the high shear data at atmospheric pressure and a temperature of 100°F. For all other data sets the resulting increase in the shear rate was negligible or it was not possible to apply the Rabinowitsch analysis. As explained previously, in some data sets

it was impossible to account for the elastic energy stored in the fluid and thus the true shear rate could not be determined.

Straight line relations are obtained on ASTM viscosity-temperature charts when constant pressure data are plotted for Fluid F and when constant pressure and constant shear stress data are plotted for Fluid G. The slope of any constant pressure line for the polymer blend (Fluid G) is less than the slope of the corresponding line for the base oil (Fluid F), as expected.

Figures 46 and 47 contain data comparing the naphthenic based fluids with some of the other fluids examined. Figure 46 contains the viscosity-temperature relations at atmospheric pressure for the six petroleum oils examined and shows that at 100°F, (1) the viscosity of the naphthenic based fluids is less than that of the paraffinic based fluids and (2) the viscosity of the naphthenic based fluids decreases more with increasing temperature than the viscosity of the corresponding paraffinic based fluids.

Table VII shows that the viscosity-pressure coefficients for the naphthenic based fluids are greater than those for all other fluids examined except the polybutene. Figure 47 contains the viscosity-pressure data for five of the petroleum oils as well as the diester and the polybutene.

d. Polybutene

Figure 31 is the flow curve for the polybutene which shows that this fluid also has a Newtonian behavior at all temperatures and pressures investigated. The viscosity-temperature and the viscosity-pressure relations are presented in Figures 32 and 33. Table VII shows that the

viscosity of this fluid changes more with temperature and pressure than the viscosity of the other nine fluids investigated. Thus the viscosity of 1.2×10^5 cp. at 39300 psig and 100°F was the largest value obtained in this research (cf. Figure 47).

e. Siloxane Fluids

The flow curves for the siloxane fluids (Figures 34 and 36) indicate a small temporary viscosity loss (~11 percent for Fluid I and ~15 percent Fluid J). As mentioned previously, the viscosity-pressure relations for these fluids are basically different than the viscosity-pressure relations of the other fluids examined. The viscosity-pressure curves for the silicones (Figure 38) possess inflection points while similar curves for the other fluids do not. This behavior was also observed by Bridgman[11] on dimenthylsiloxane fluids. Figure 35 and 37 contain the viscosity-temperature data for these fluids. The dimethylsiloxane examined has the least change in viscosity with temperature of the ten fluids examined.

C. Correlation

1. Techniques

The experimental data obtained covered a wide shear stress range at various pressures and temperatures. The effect of these three variables upon viscosity is very desirable, but it also presents a problem in presenting the experimental results in a convenient form. Therefore, a literature survey was made to determine whether or not any satisfactory data correlation and presentation techniques were readily available. The techniques surveyed included analytical and graphical

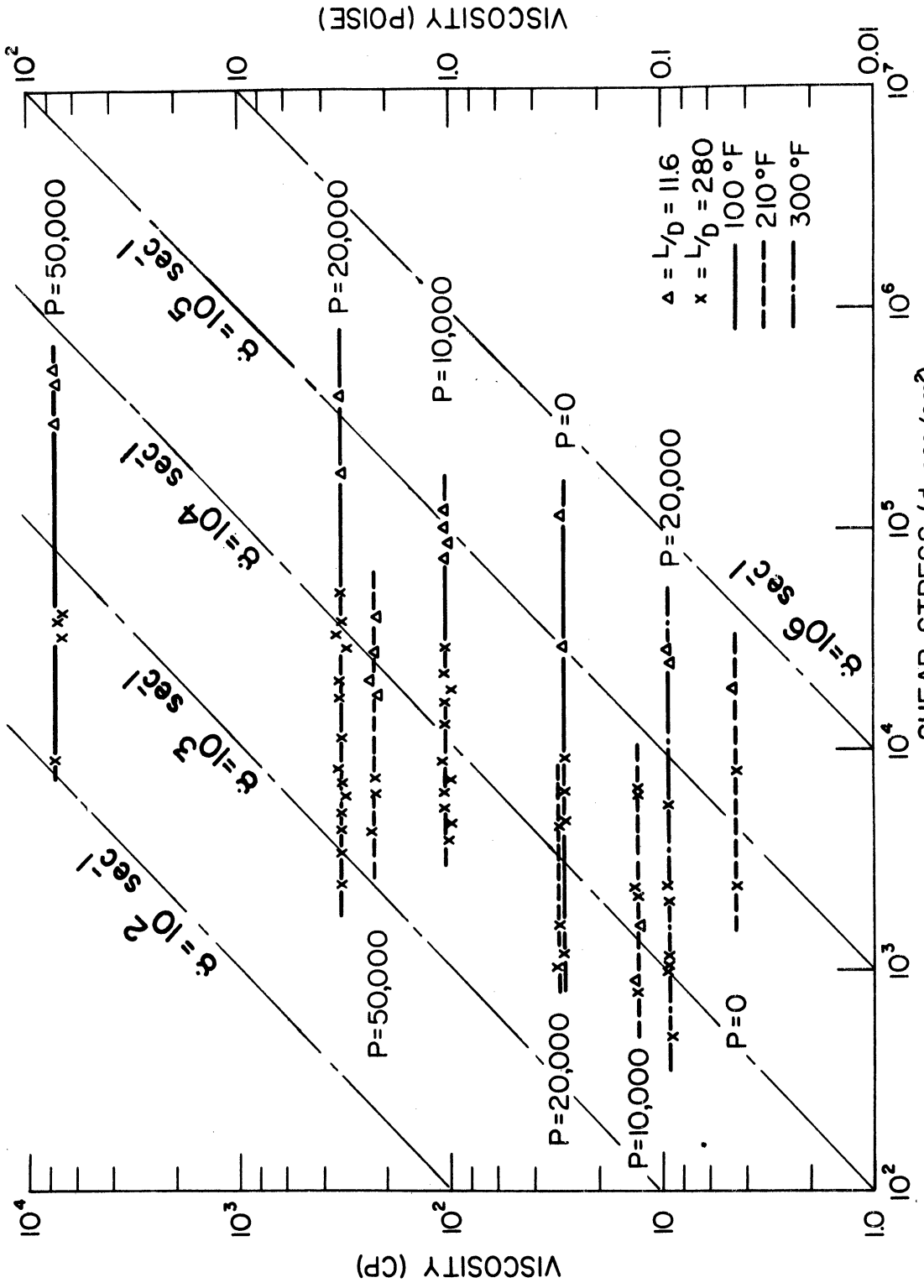

Figure 13. Flow Curves for Fluid B.

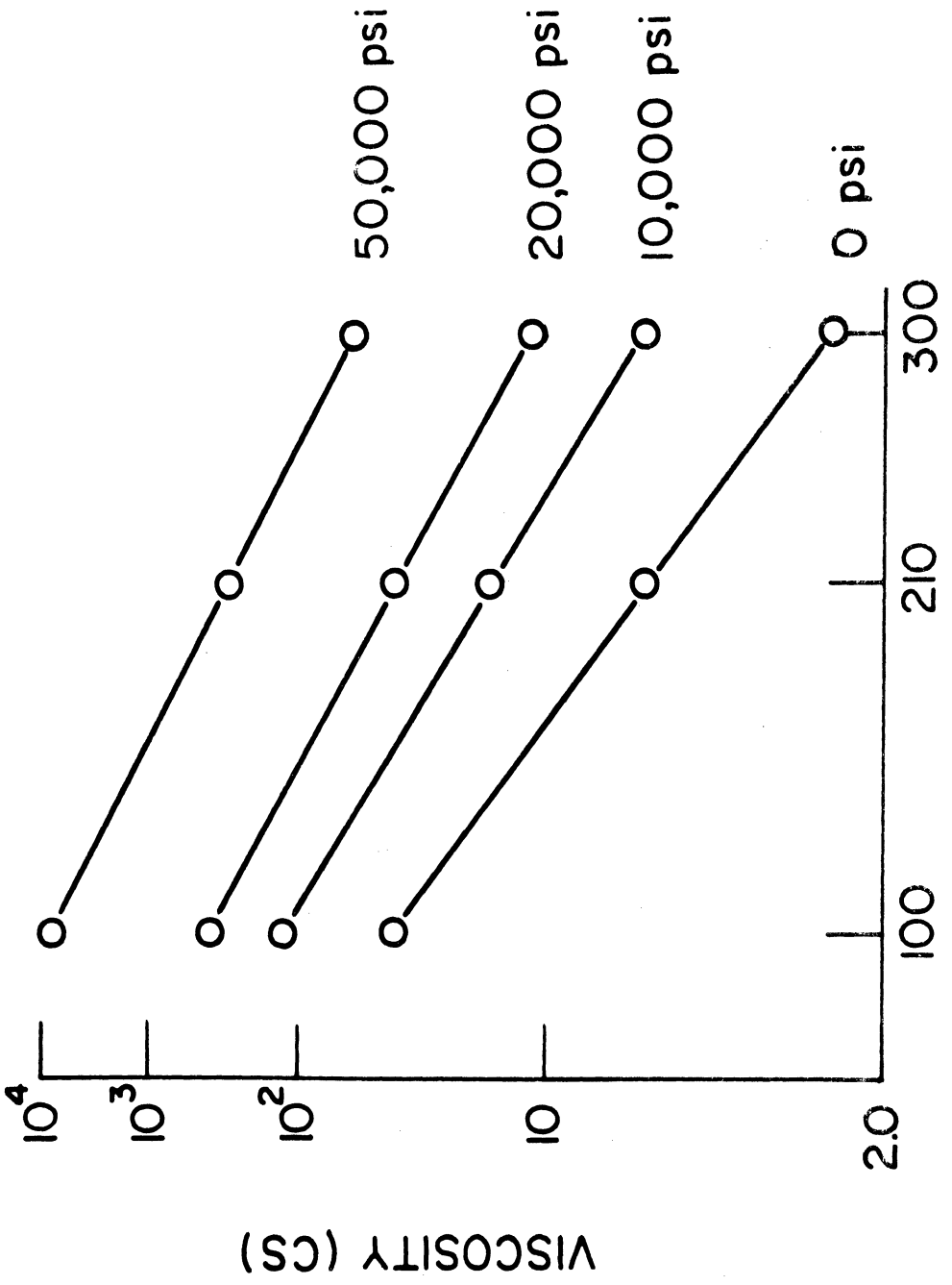

Figure 14. Viscosity-Temperature Relation for Fluid B.

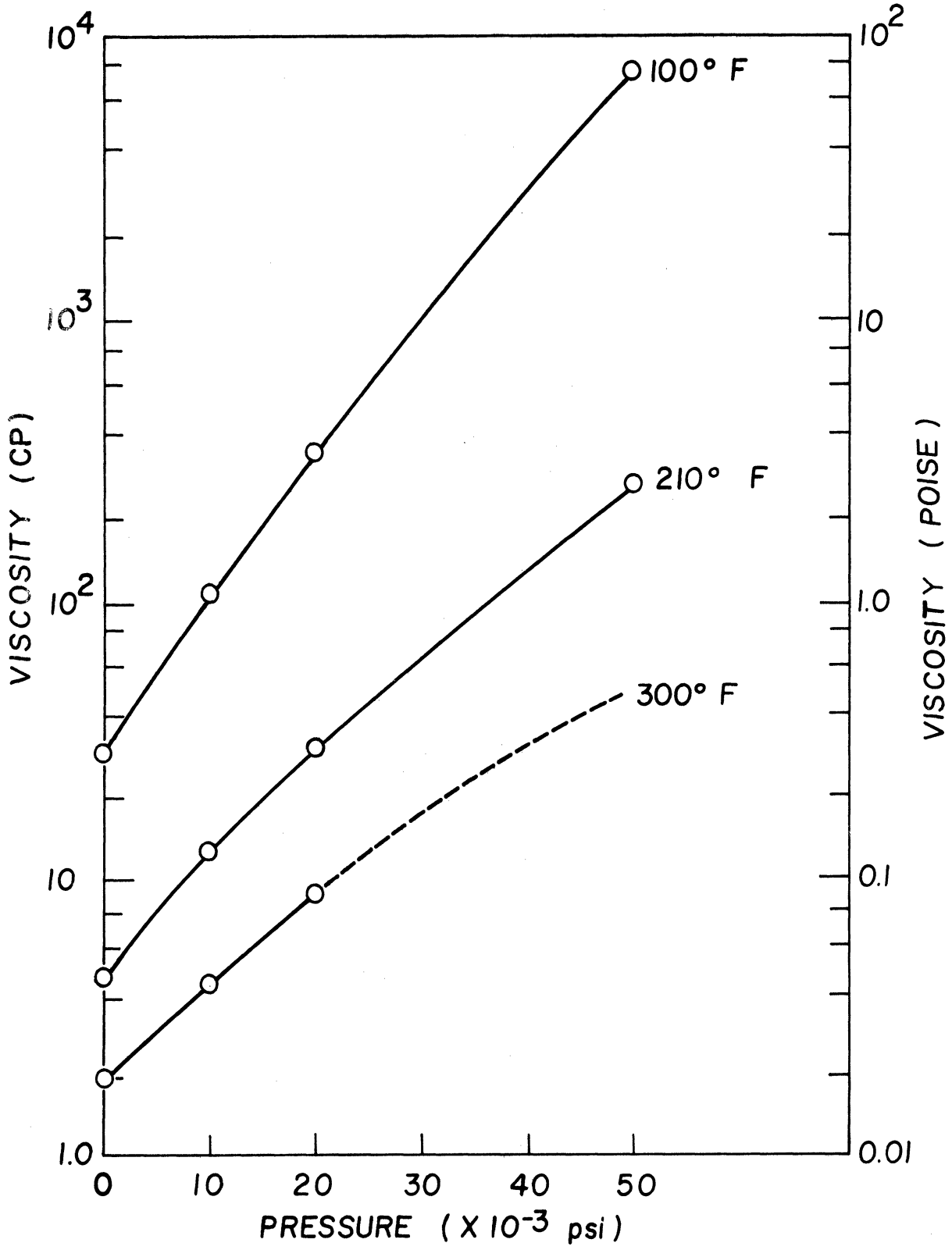

Figure 15. Viscosity-Pressure Relation for Fluid B.

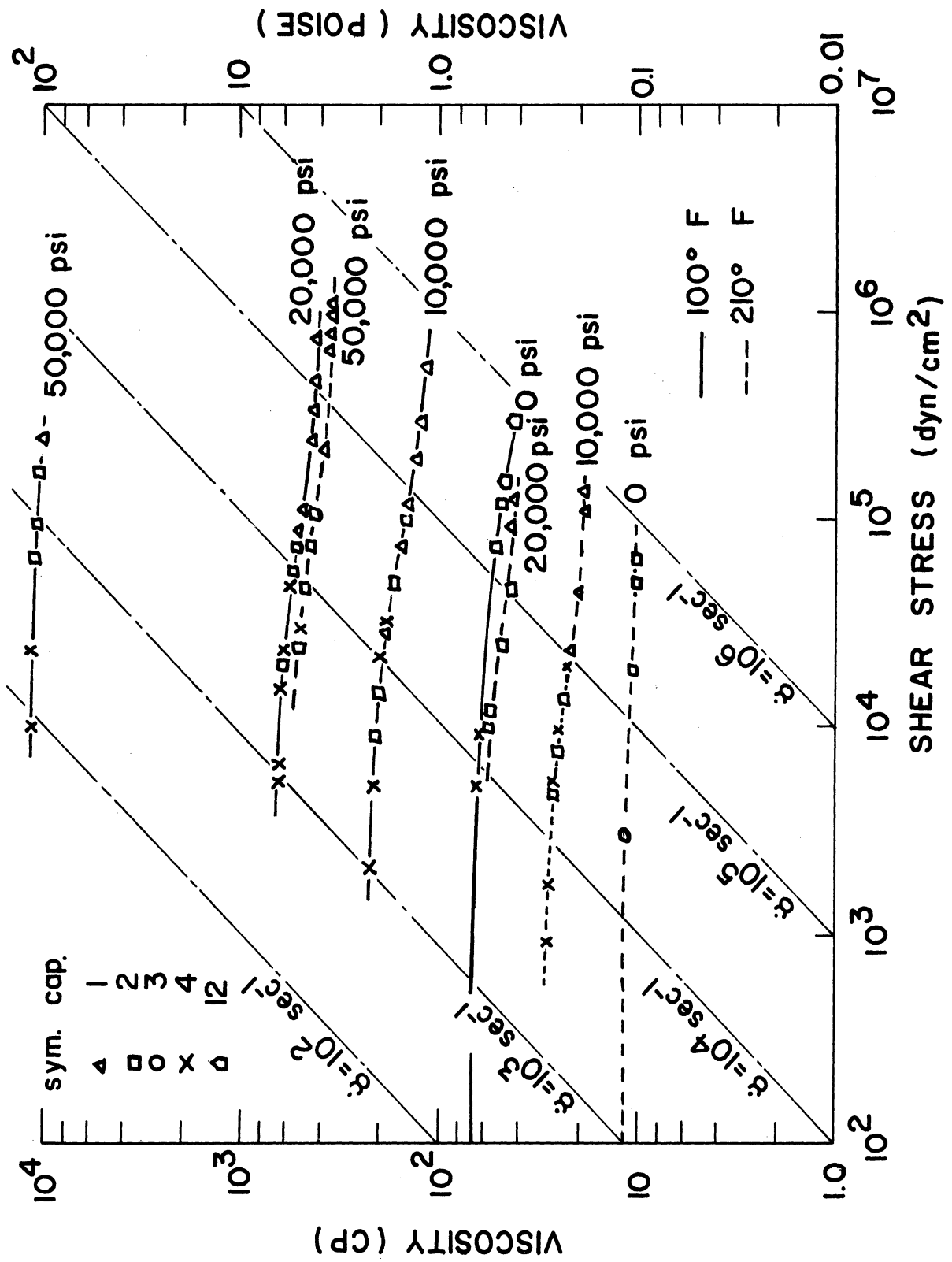

Figure 16. Flow Curves for Fluid C.

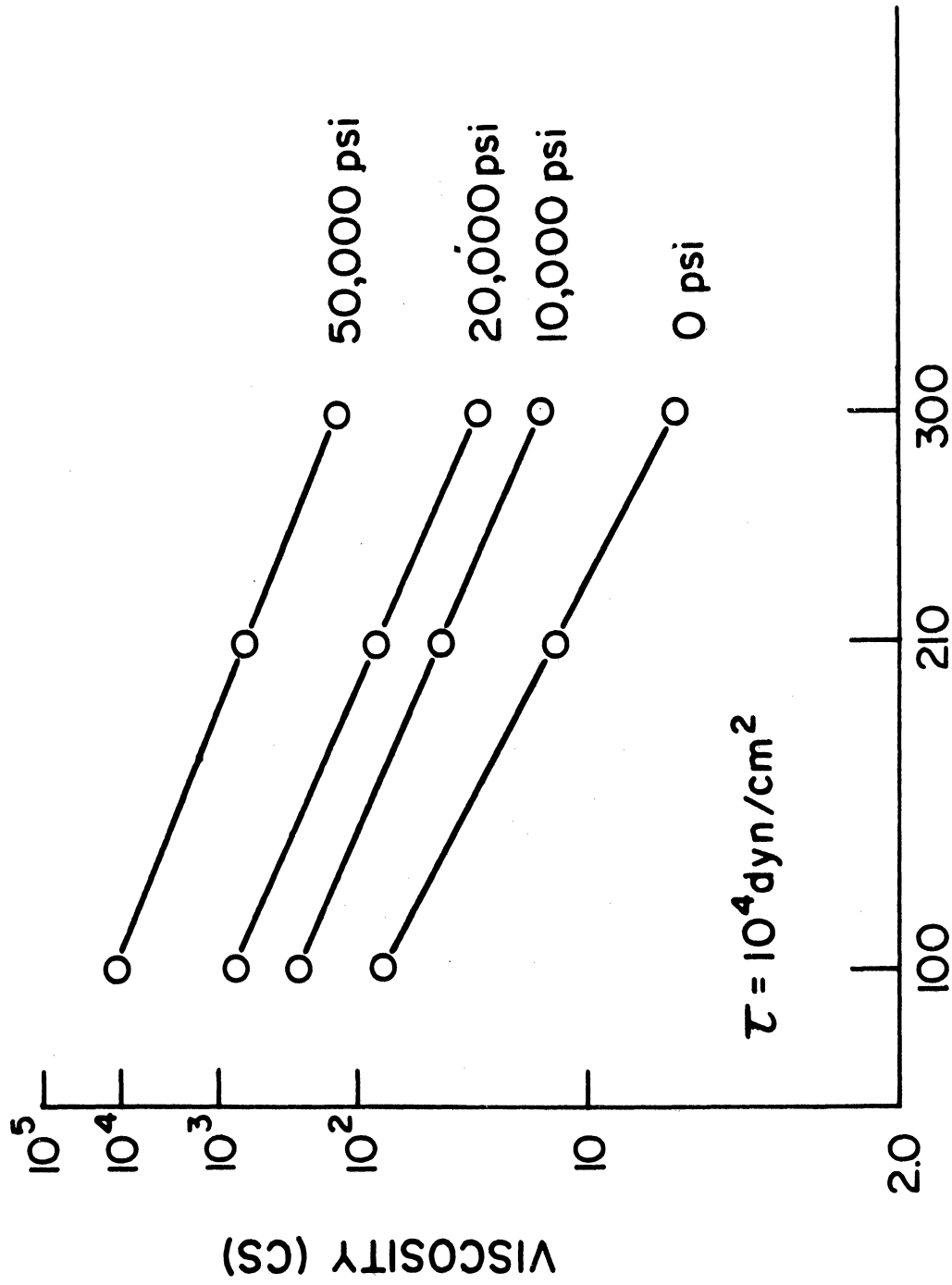

Figure 17. Viscosity-Temperature Relation for Fluid C.

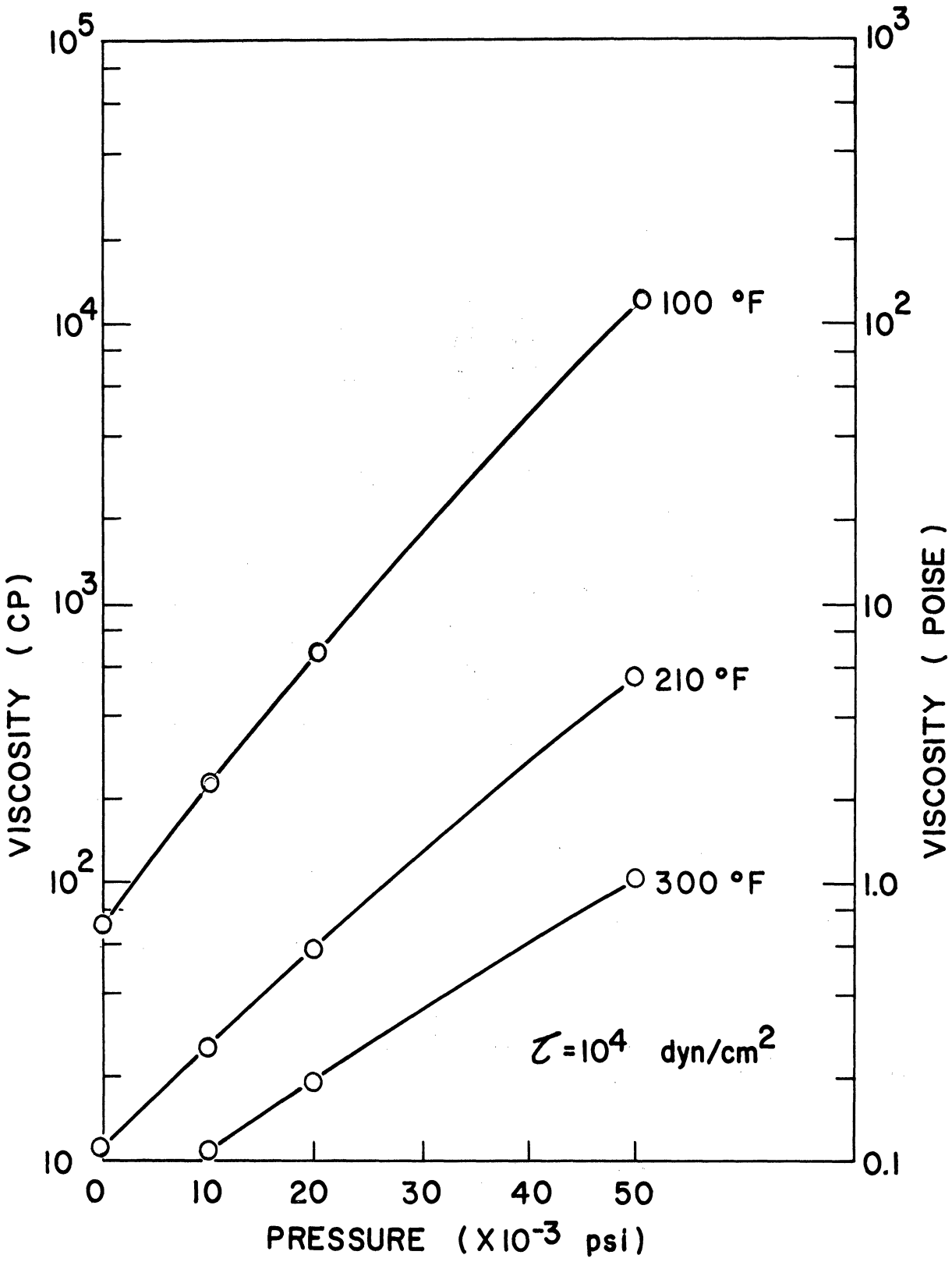

Figure 18. Viscosity-Pressure Relation for Fluid C.

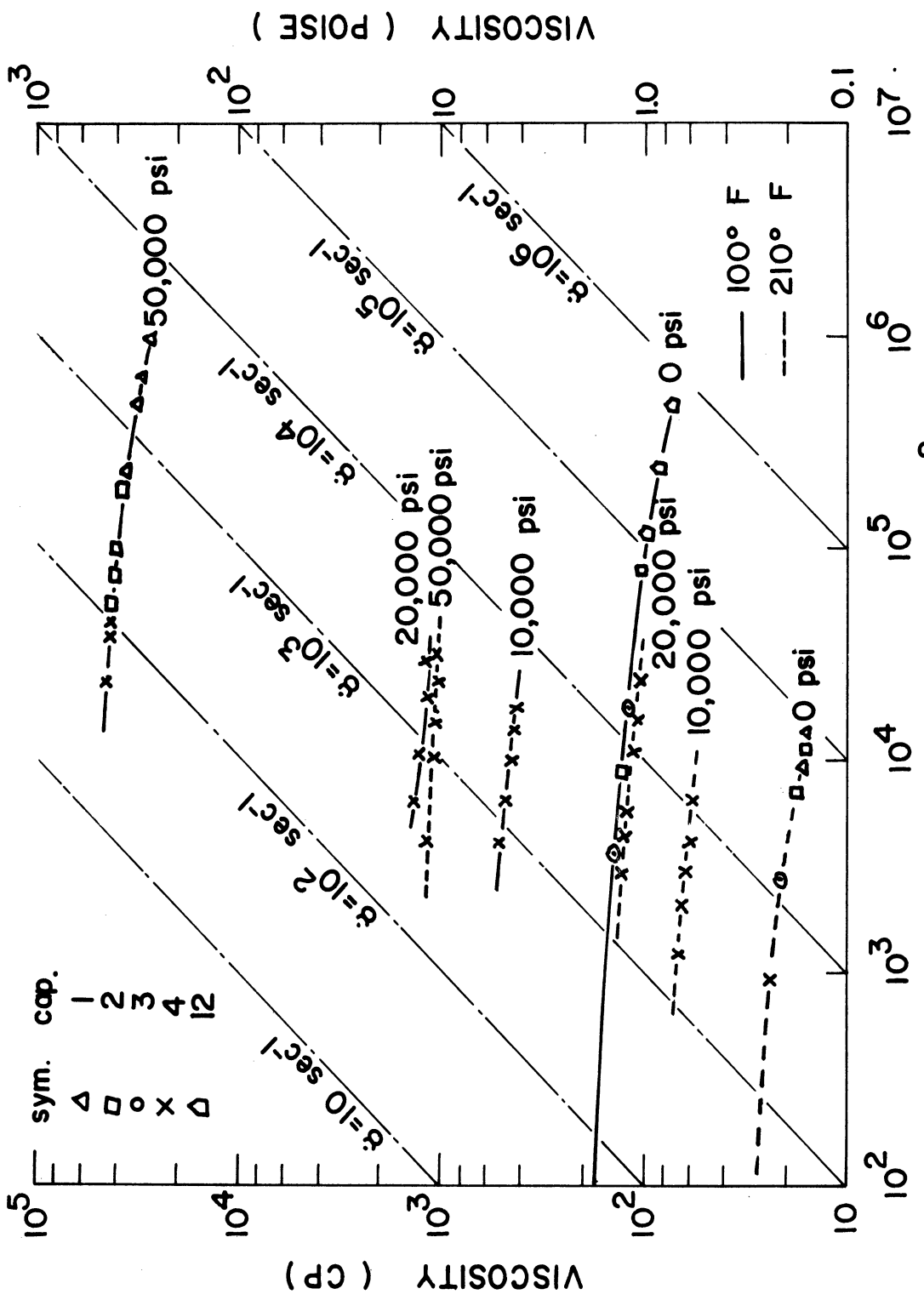

Figure 19. Flow Curves for Fluid D.

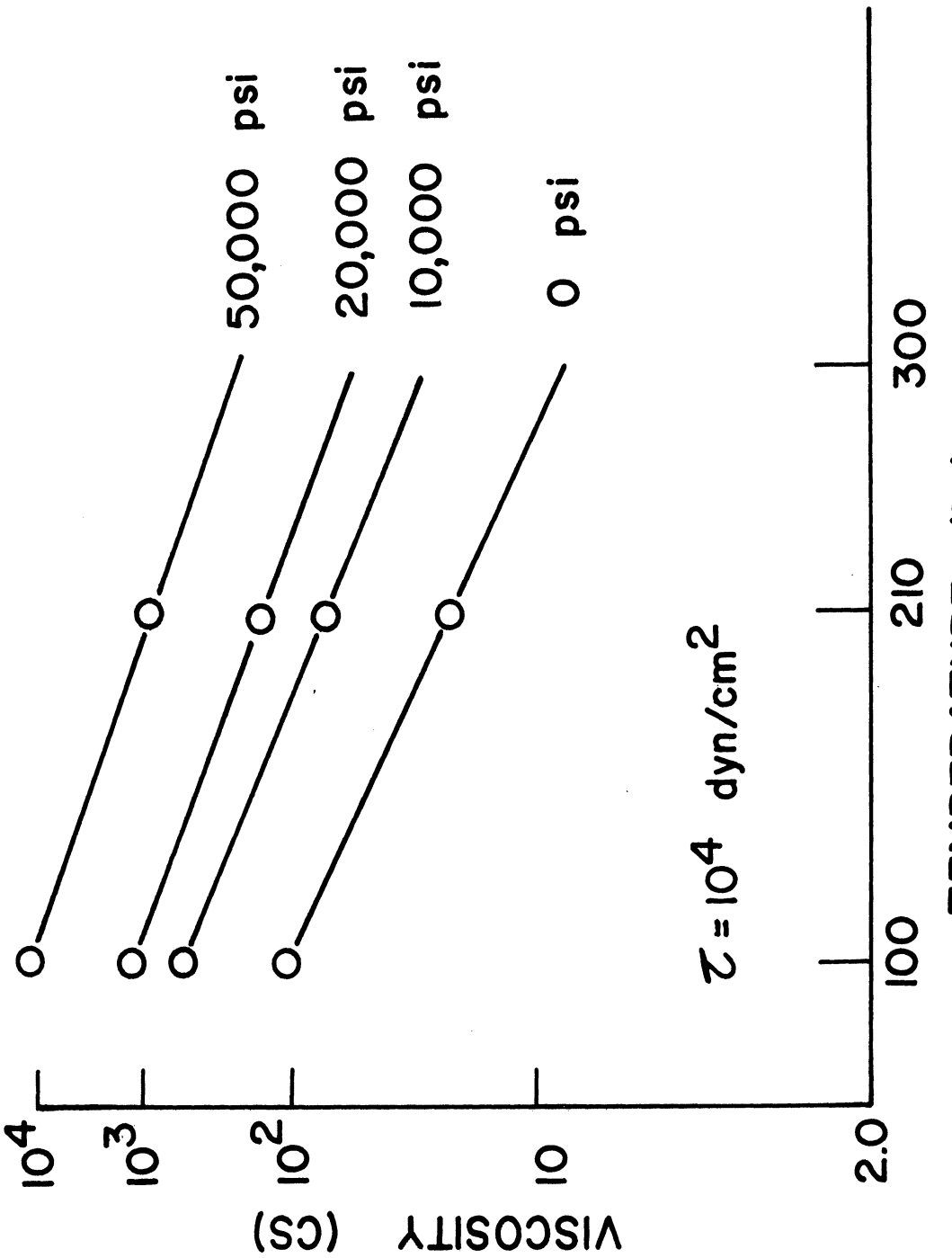

Figure 20. Viscosity-Temperature Relation for Fluid D.

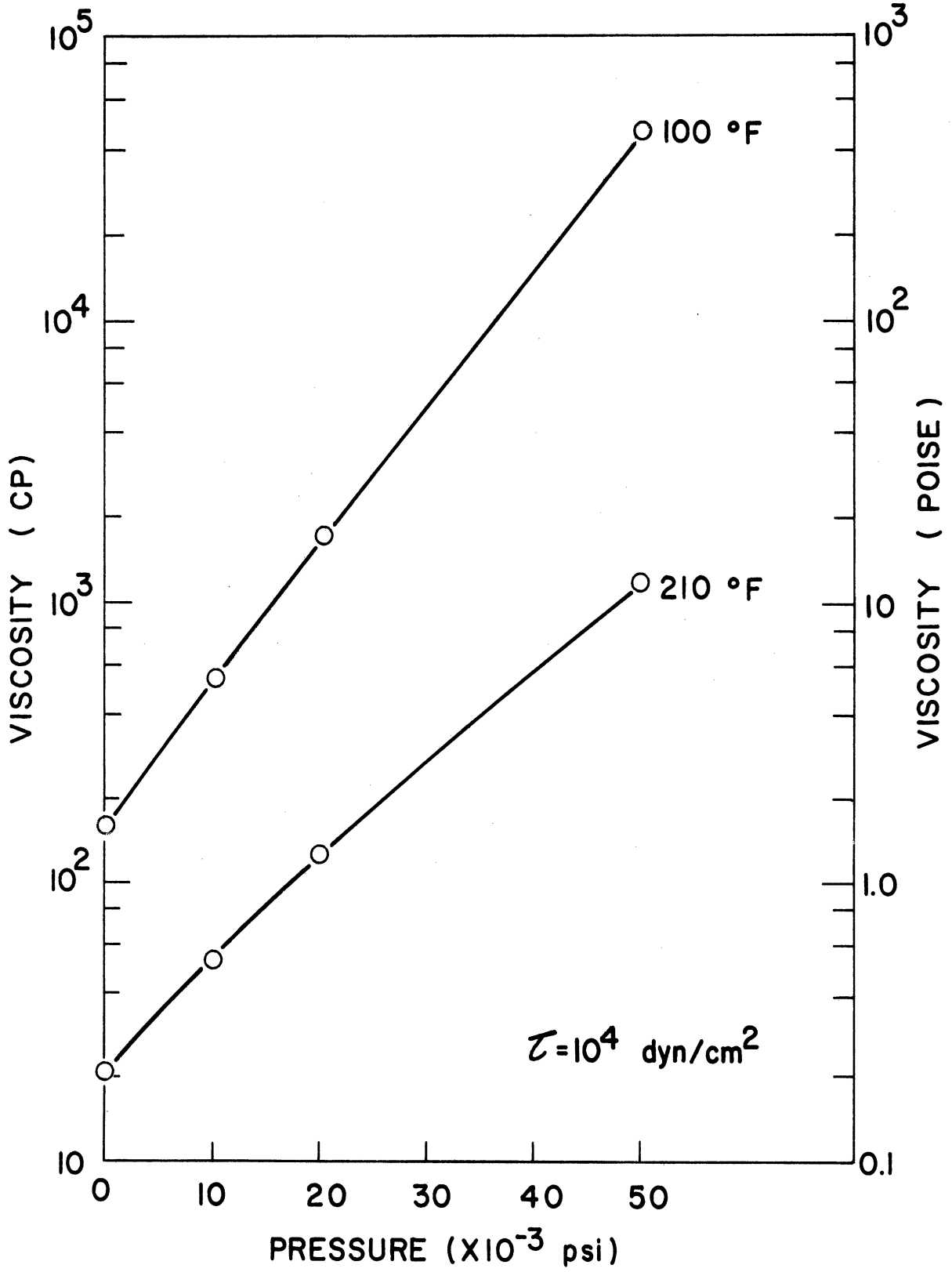

Figure 21. Viscosity-Pressure Relation for Fluid D.

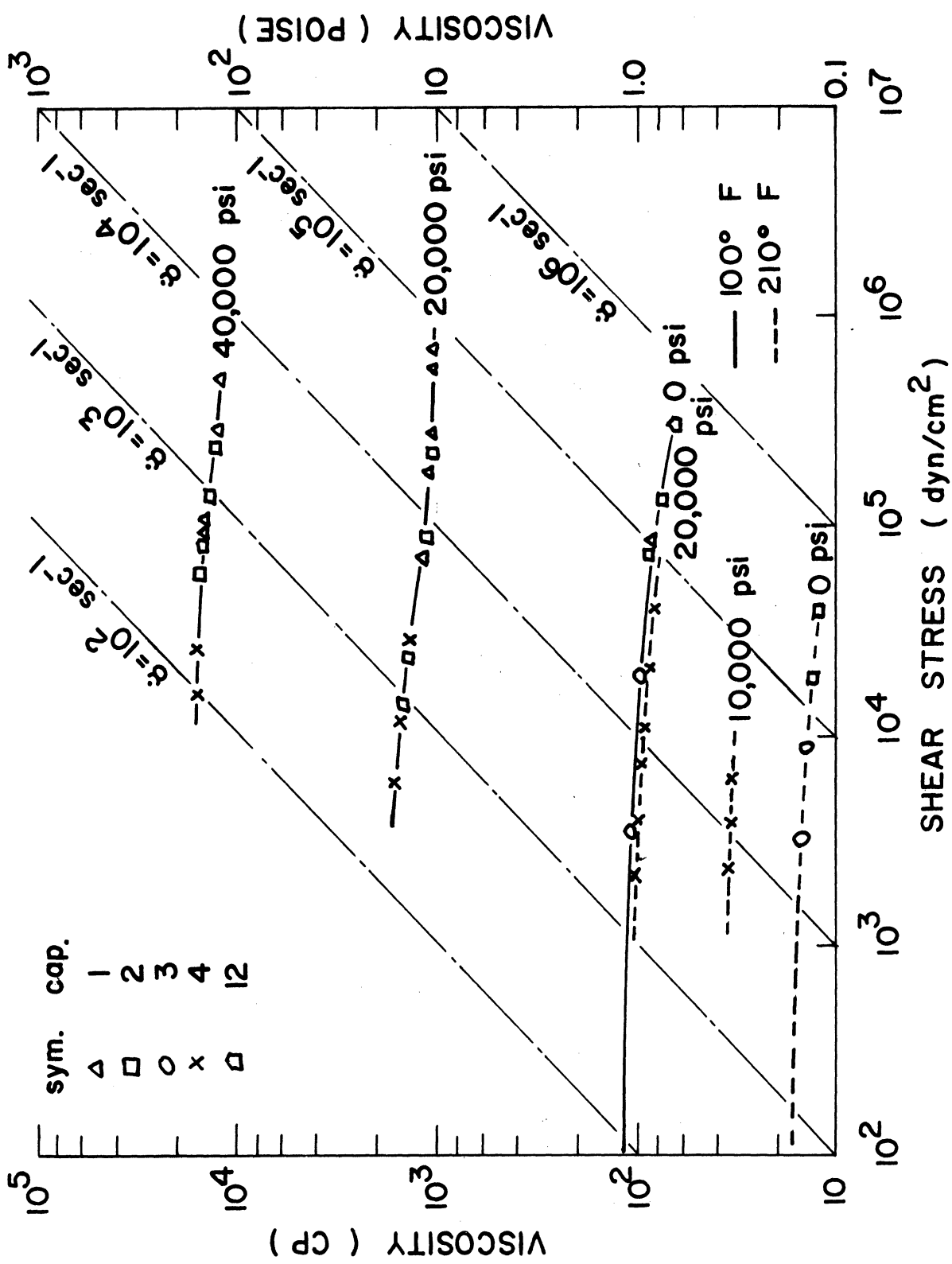

Figure 22. Flow Curves for Fluid E.

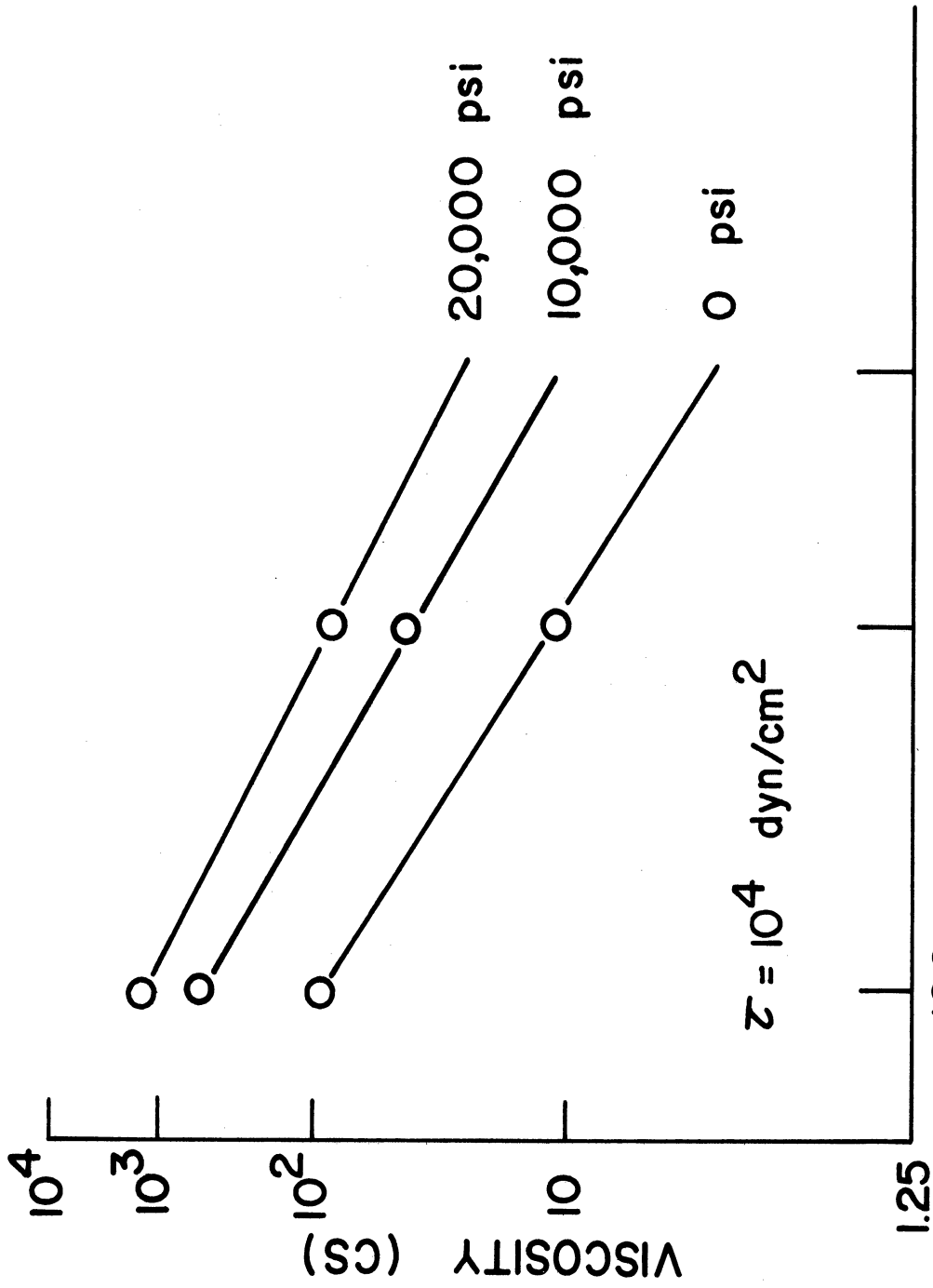

Figure 23. Viscosity-Temperature Relation for Fluid E.

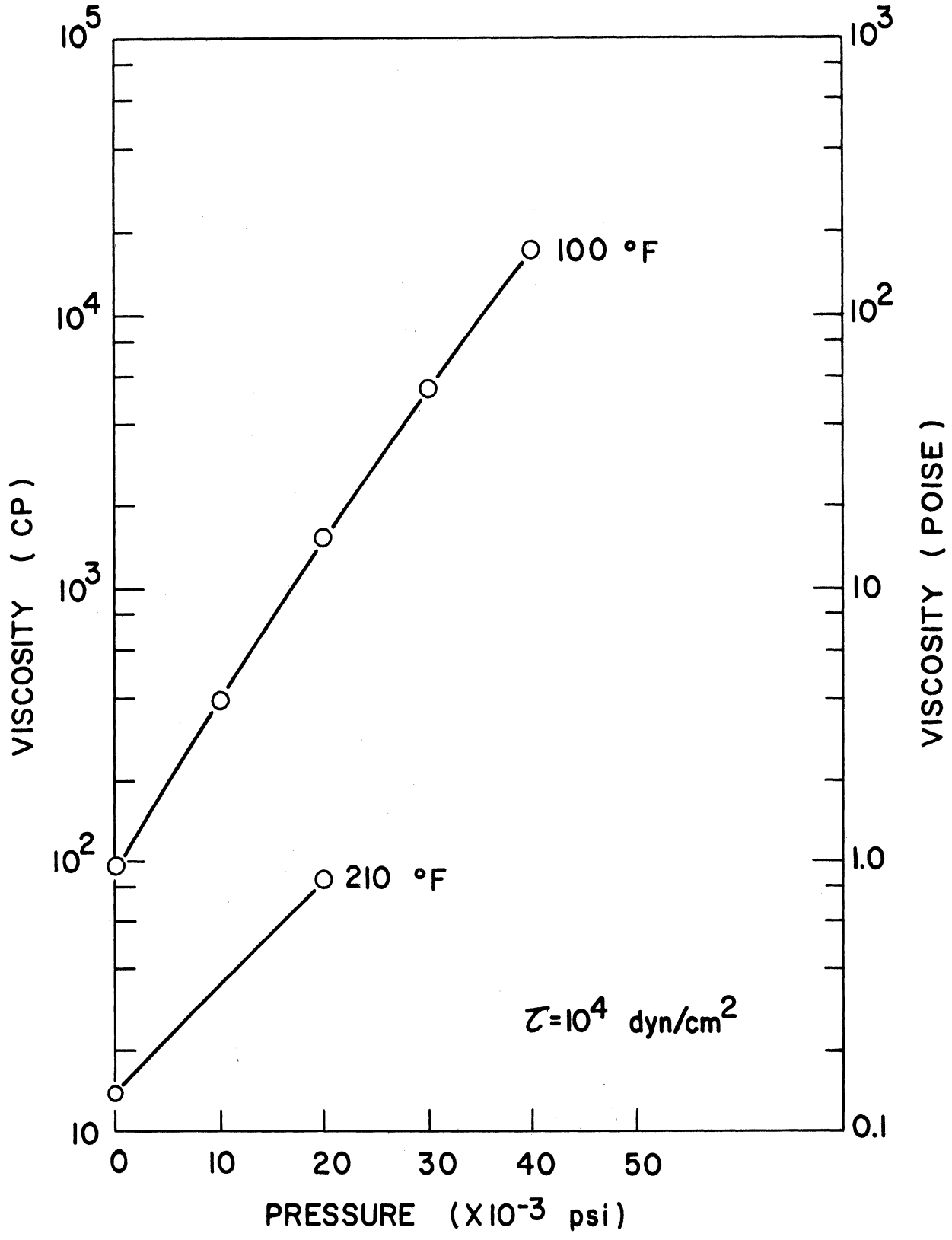

Figure 24. Viscosity-Pressure Relation for Fluid E.

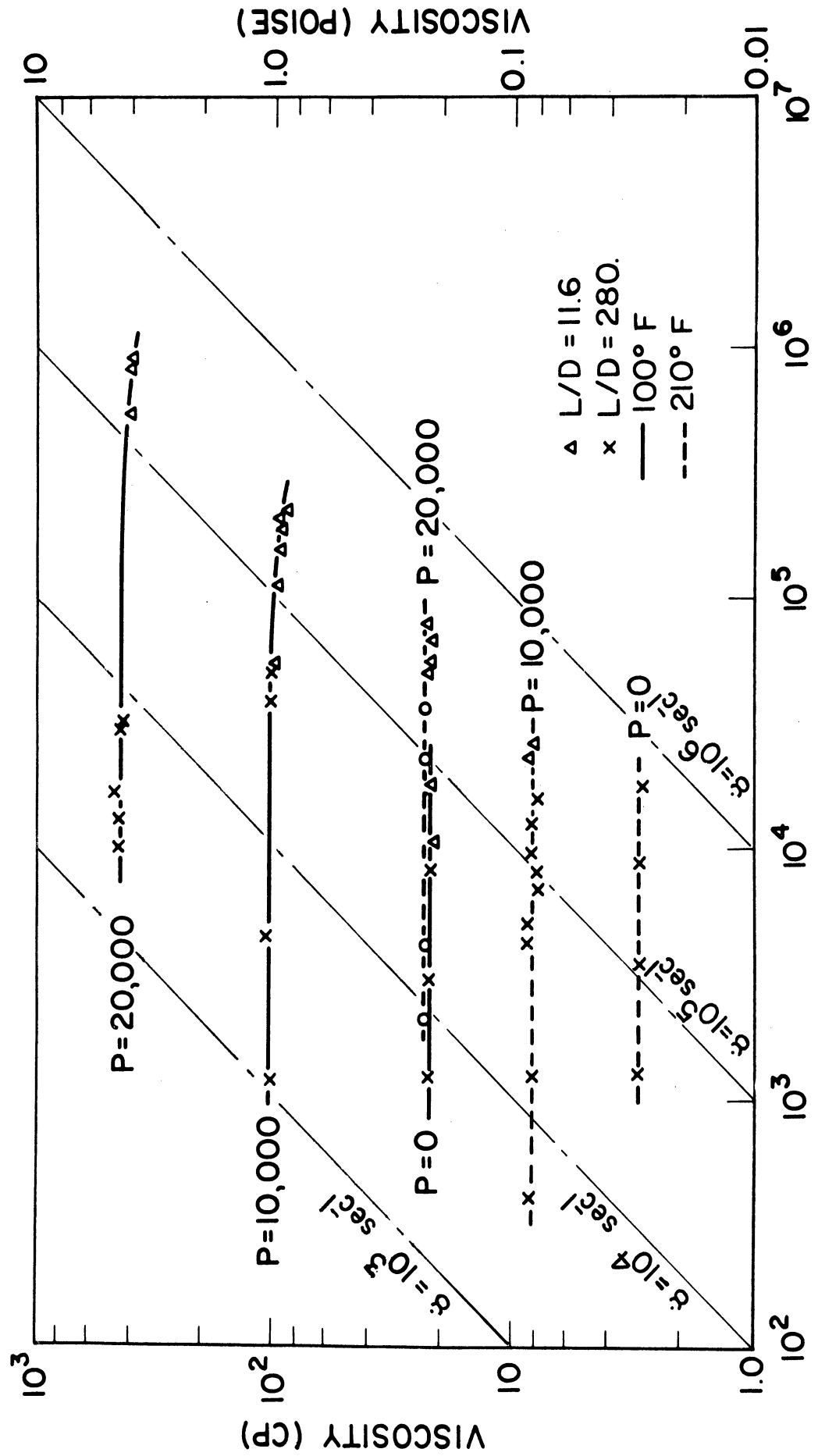

Figure 25. Flow Curves for Fluid F.

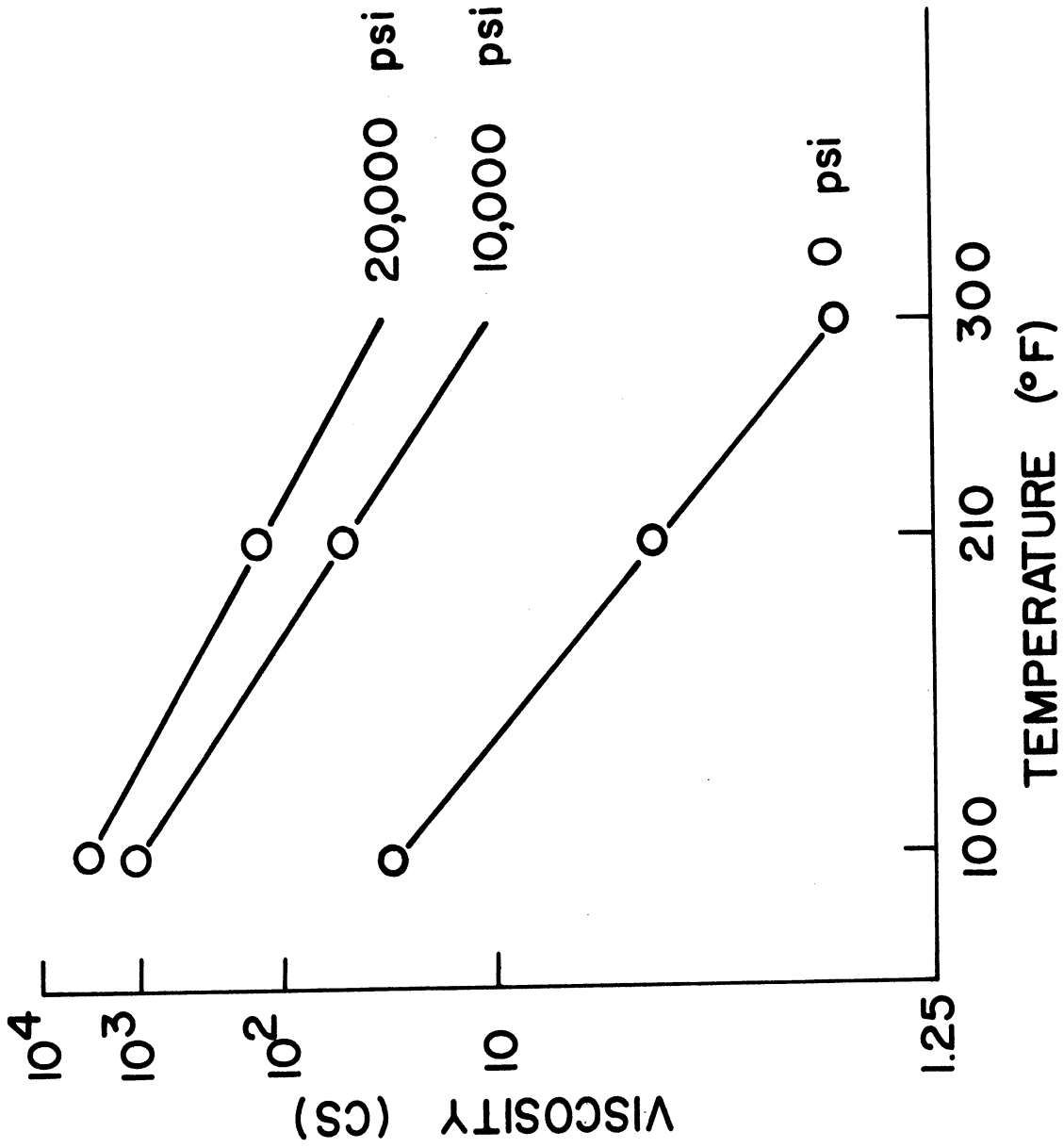

Figure 26. Viscosity-Temperature Relation for Fluid F.

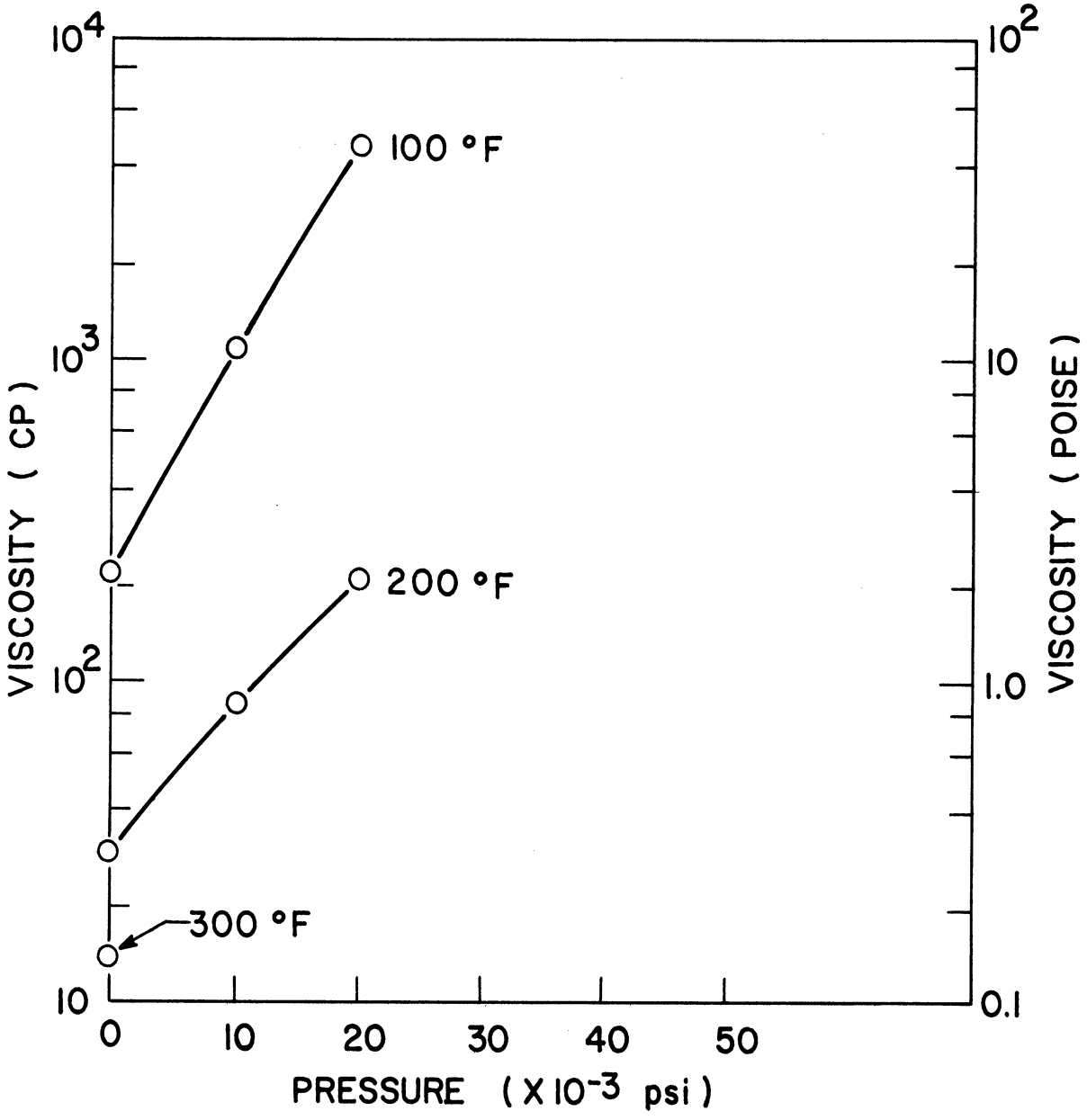

Figure 27. Viscosity-Pressure Relation for Fluid F.

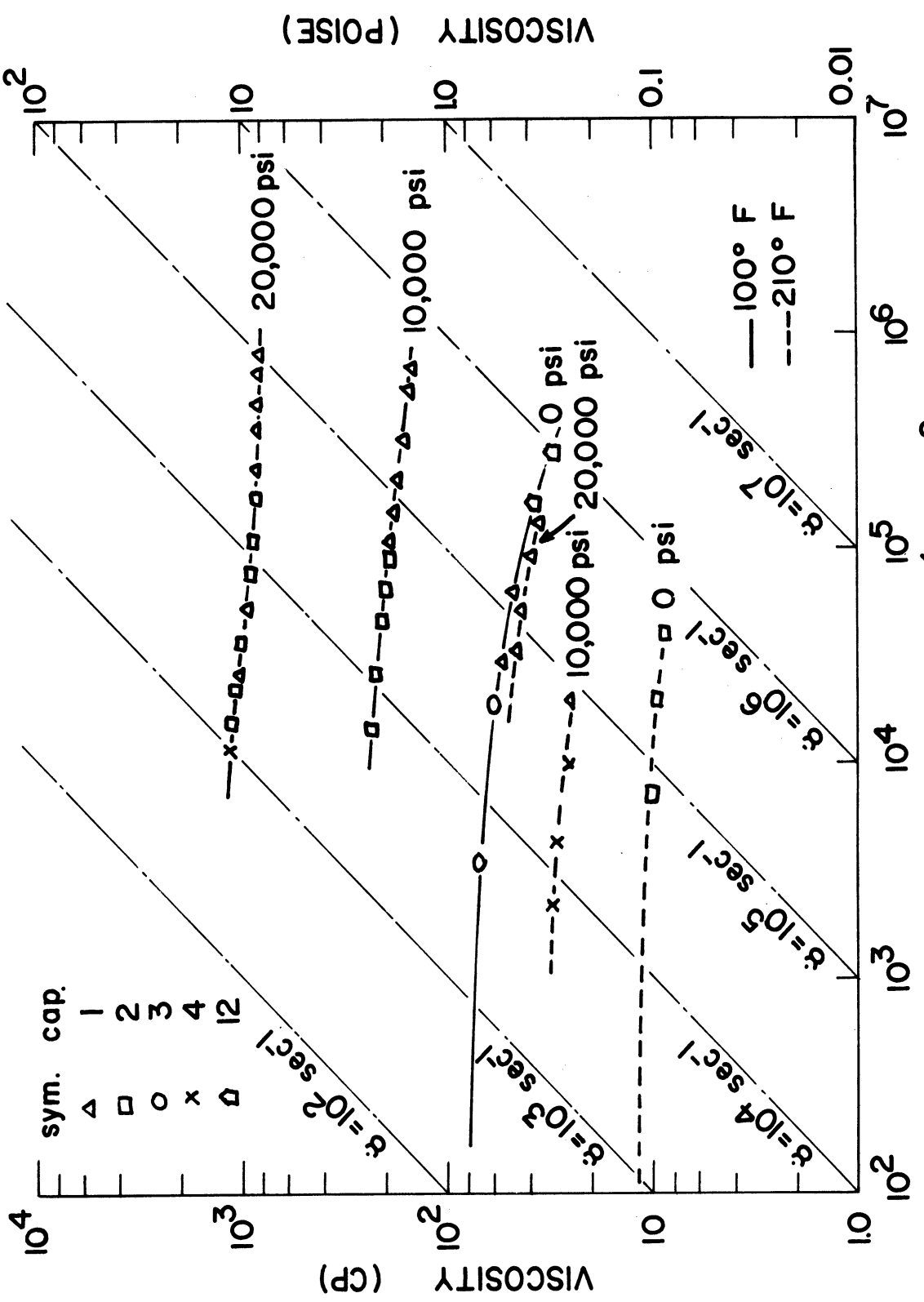

Figure 28. Flow Curves for Fluid G.

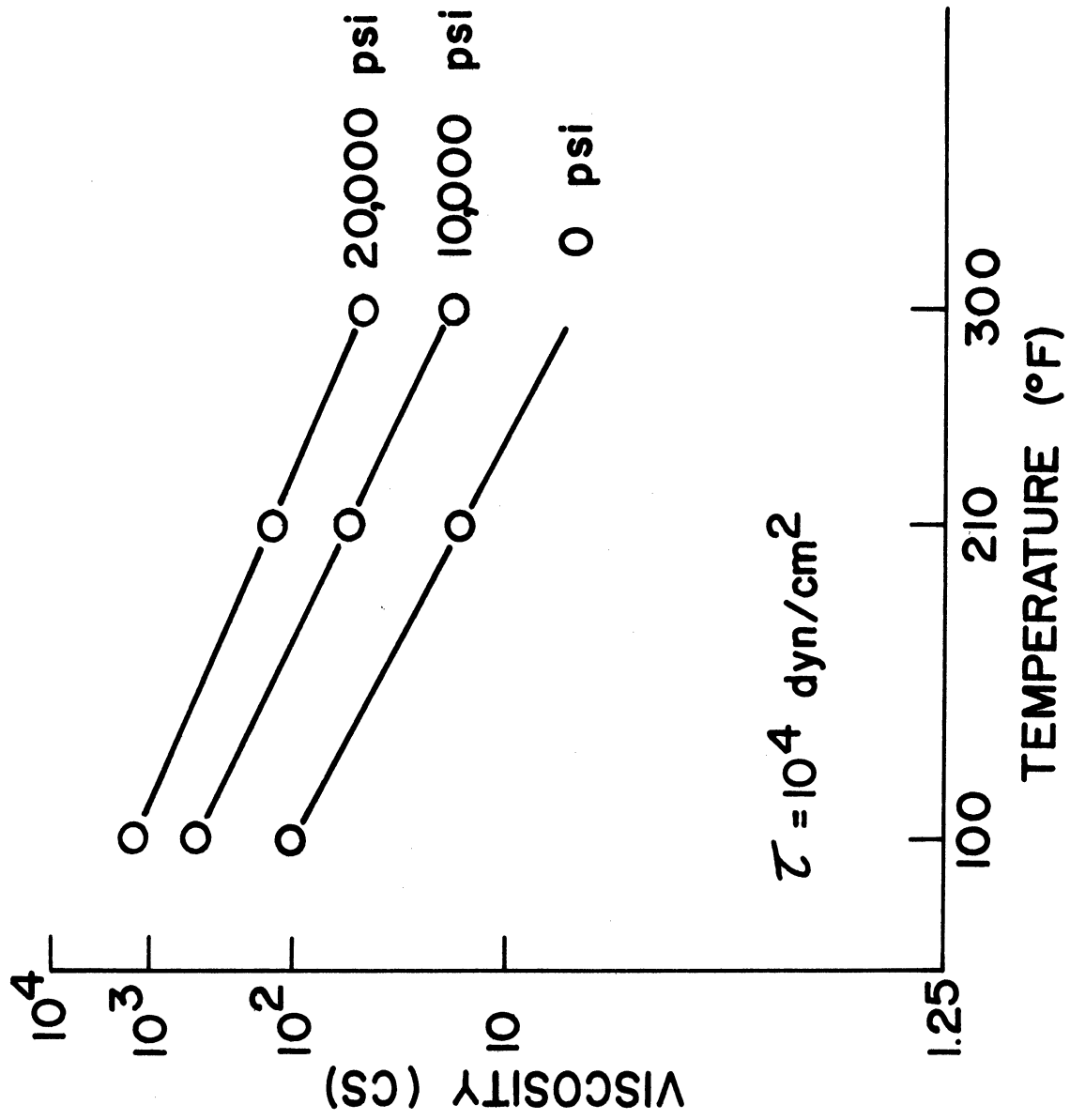

Figure 29. Viscosity-Temperature Relation for Fluid F.

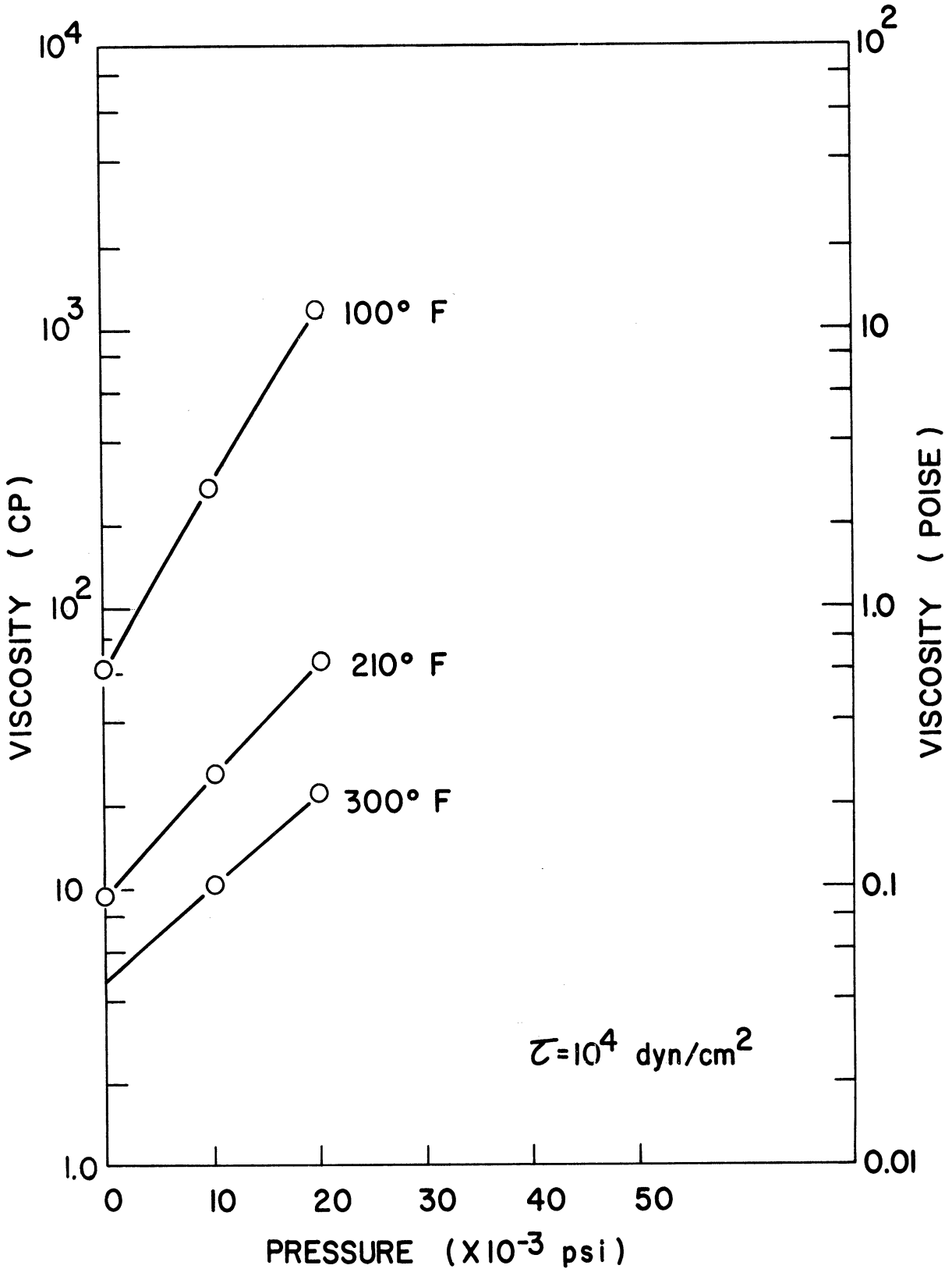

Figure 30. Viscosity-Pressure Relation for Fluid G.

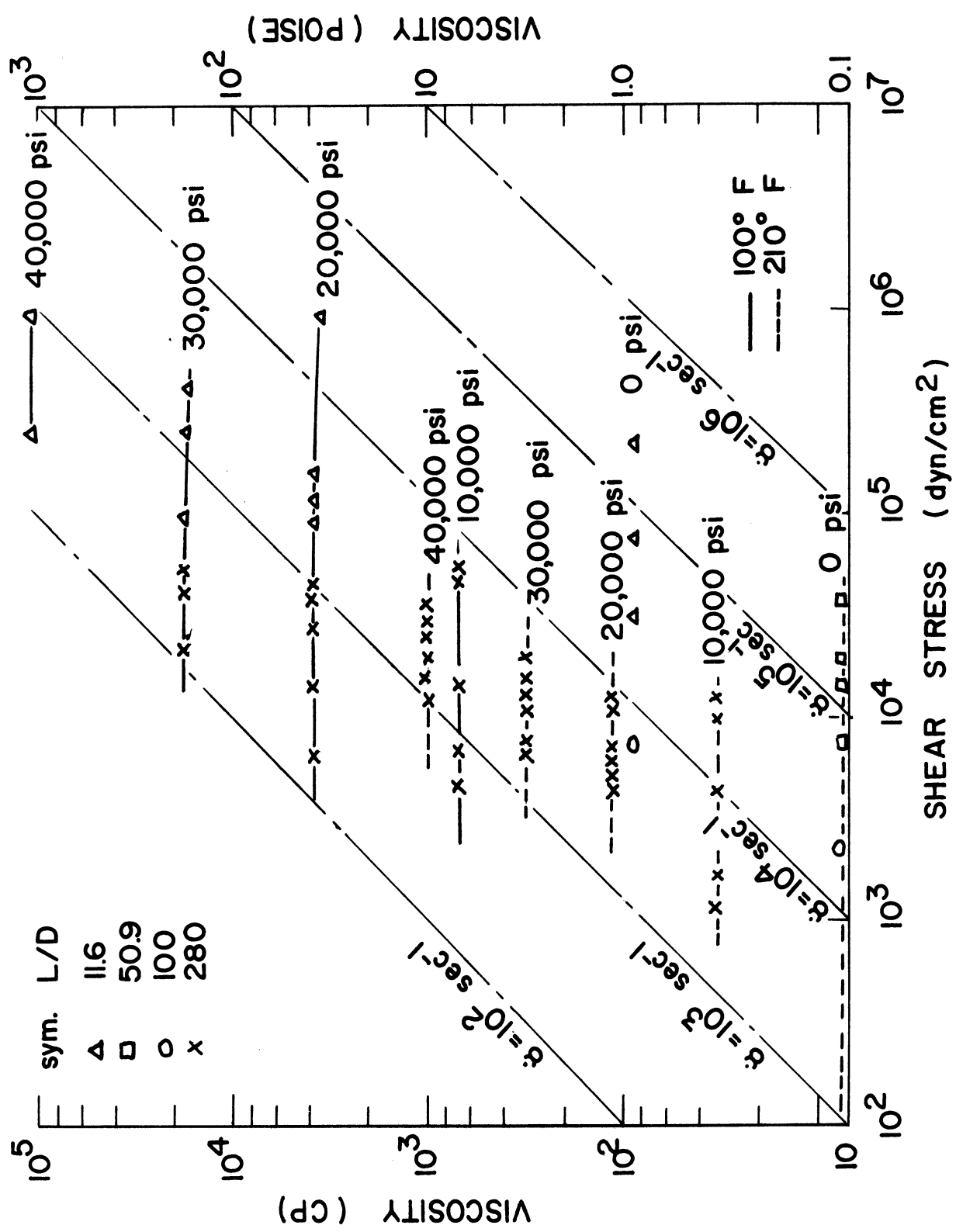

Figure 31. Flow Curves for Fluid H.

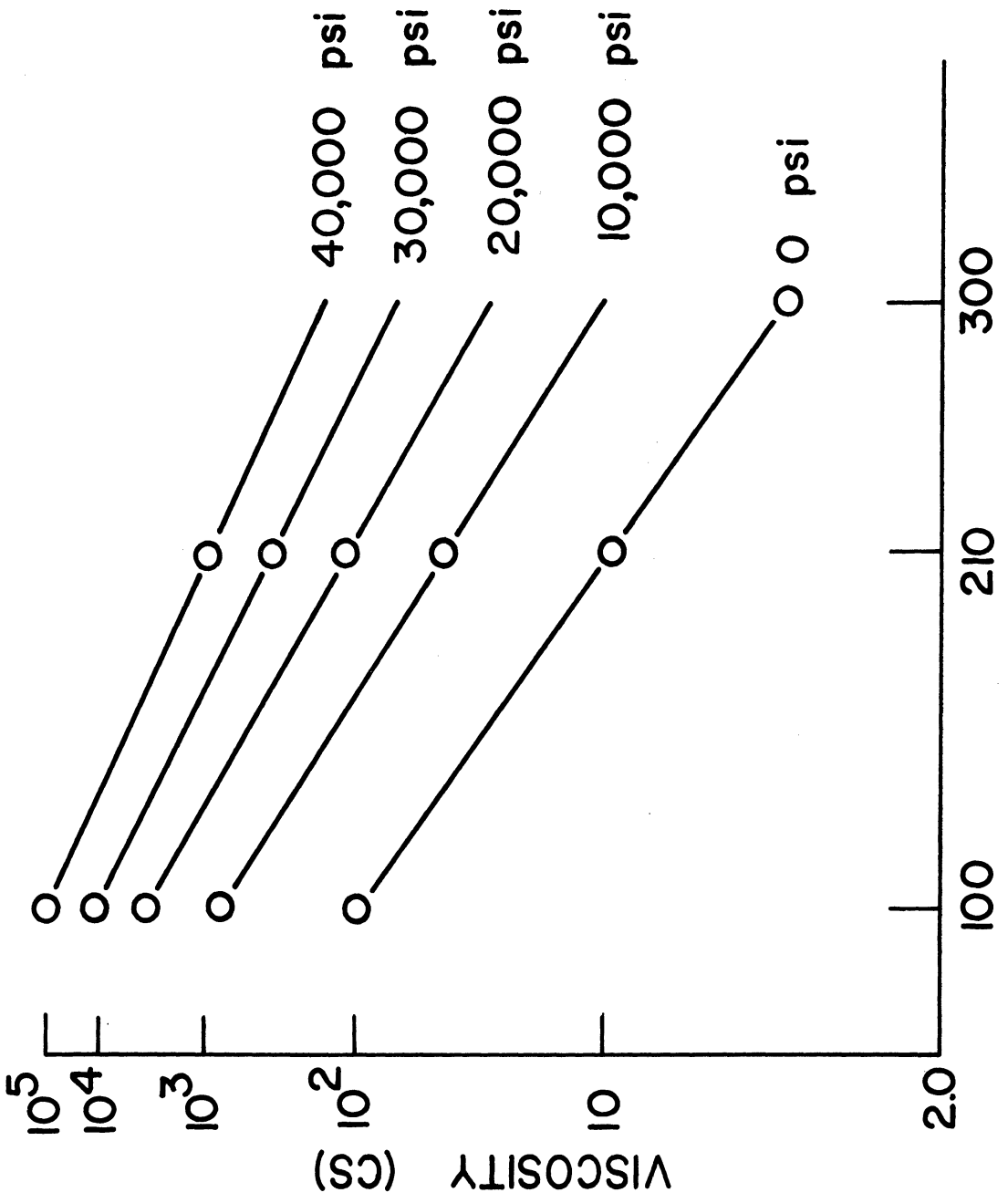

Figure 32. Viscosity-Temperature Relation of Fluid H.

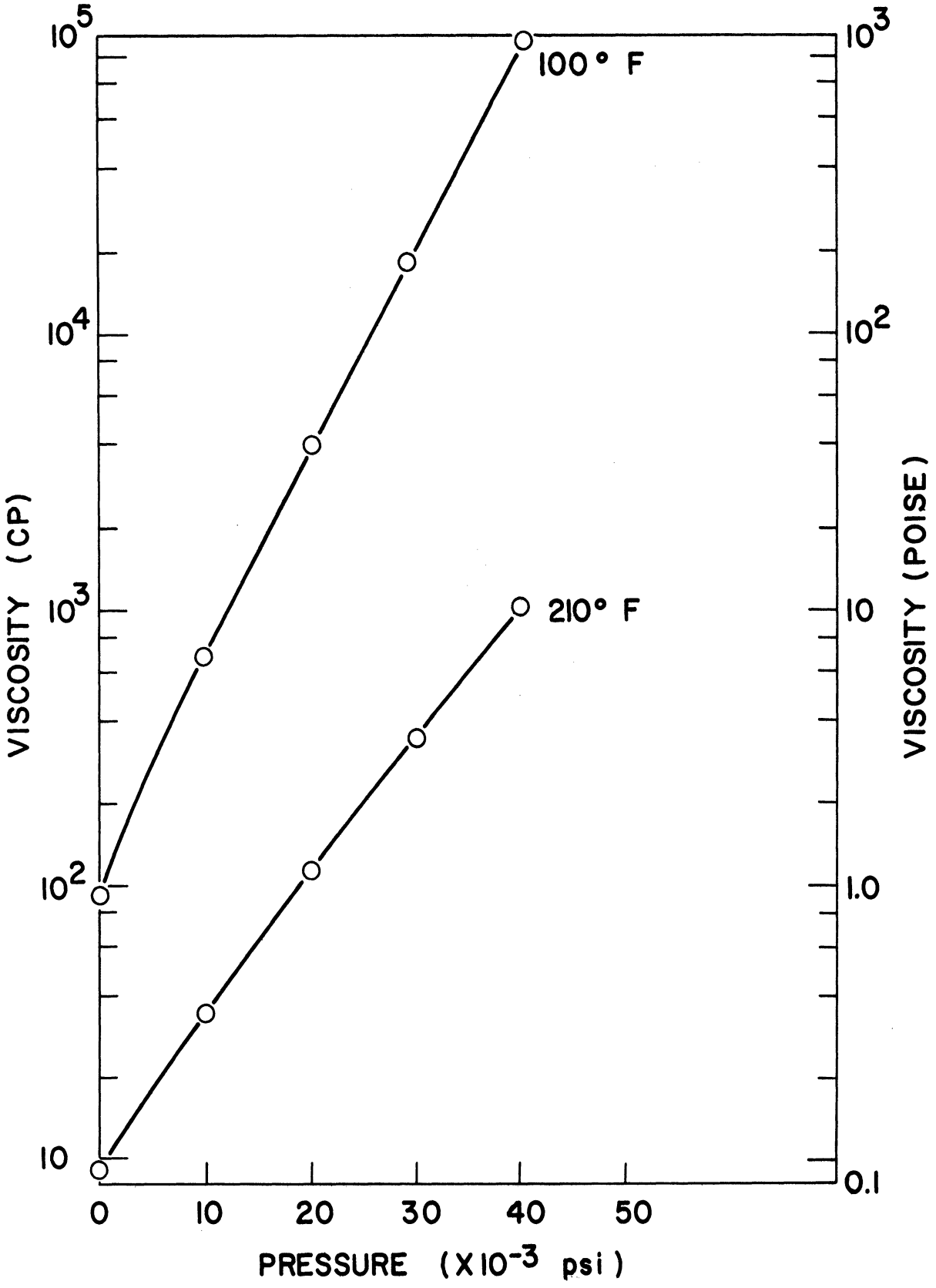

Figure 33. Viscosity-Pressure Relation for Fluid H.

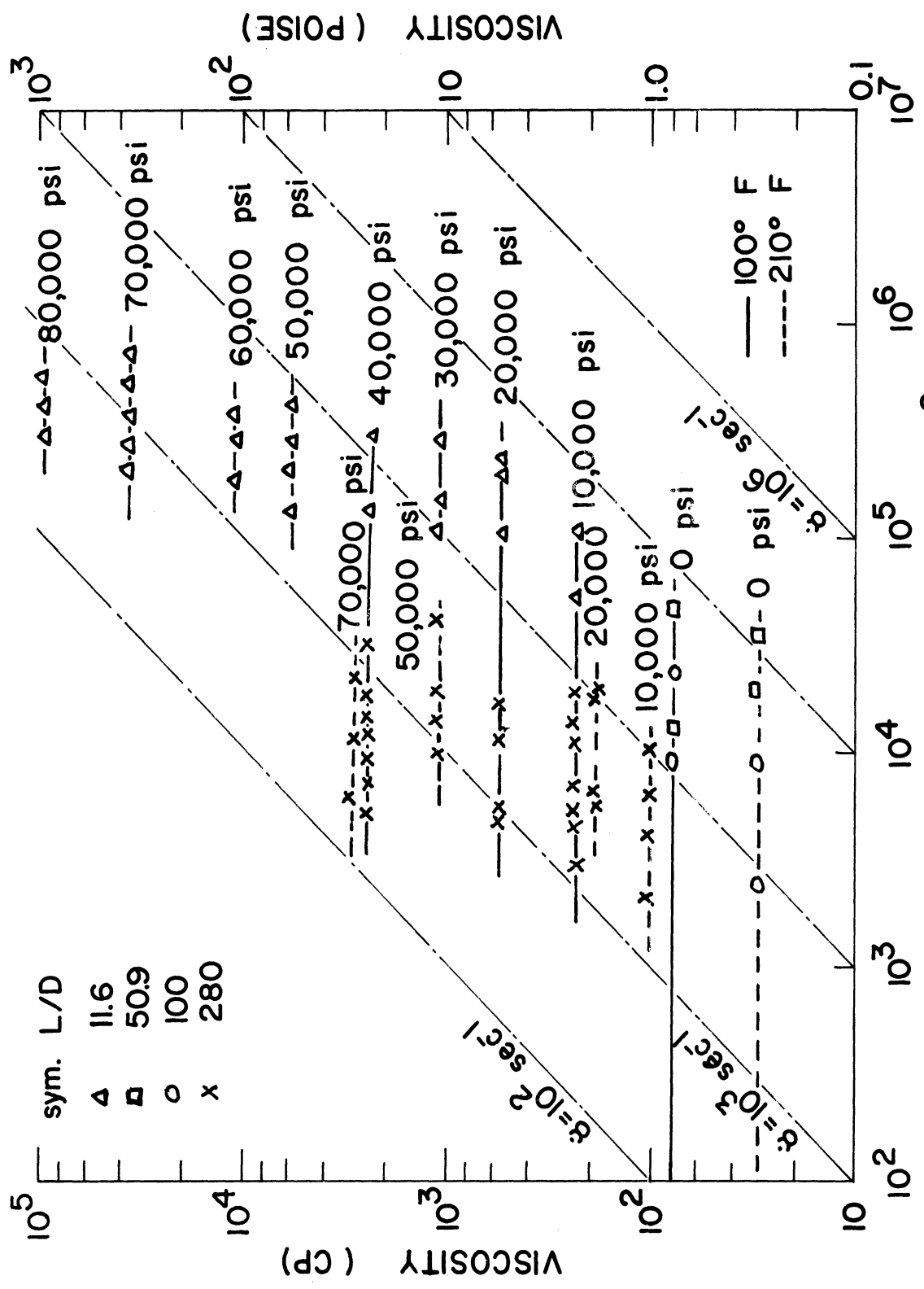

Figure 34. Flow Curves for Fluid I.

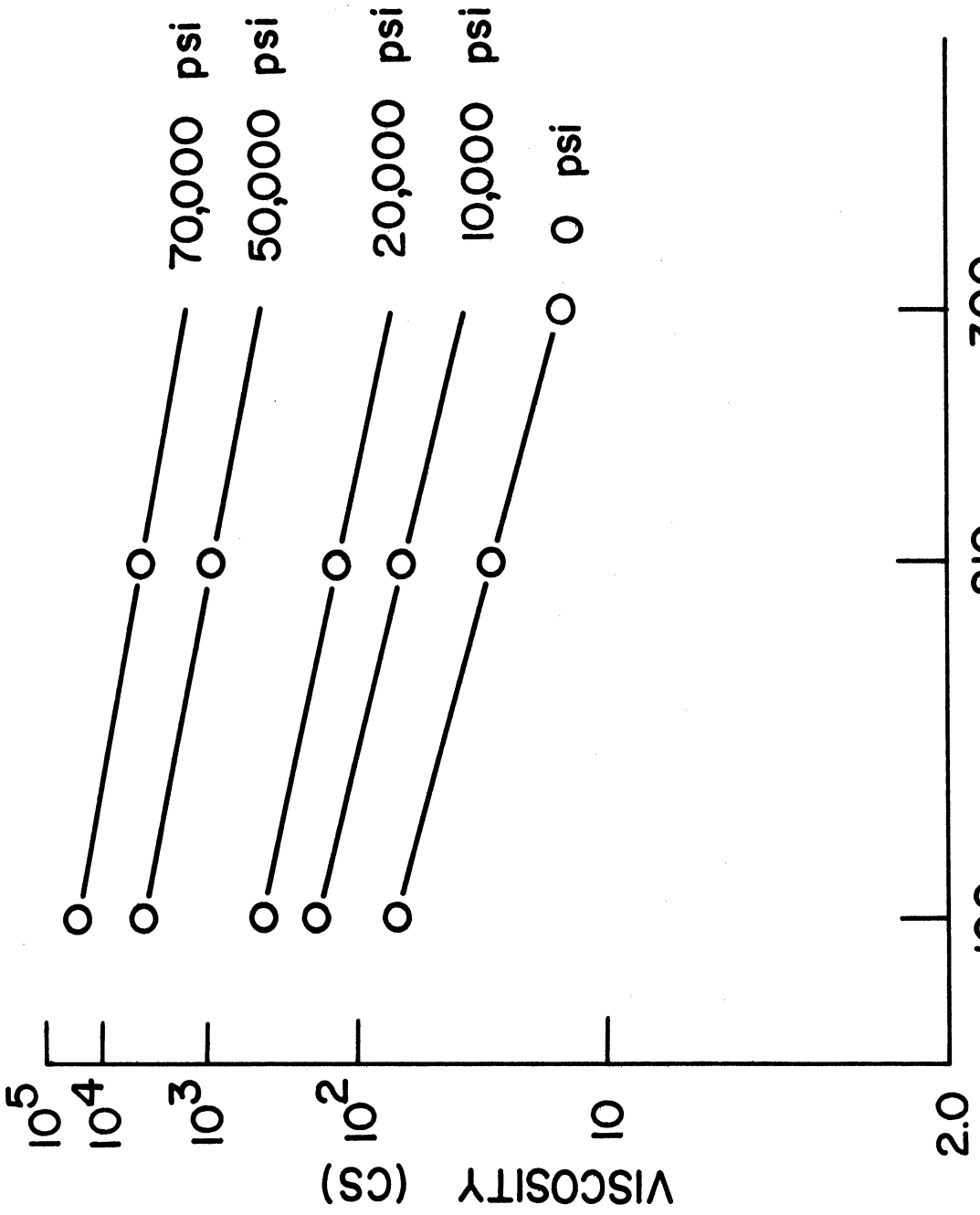

Figure 35. Viscosity-Temperature Relation for Fluid I.

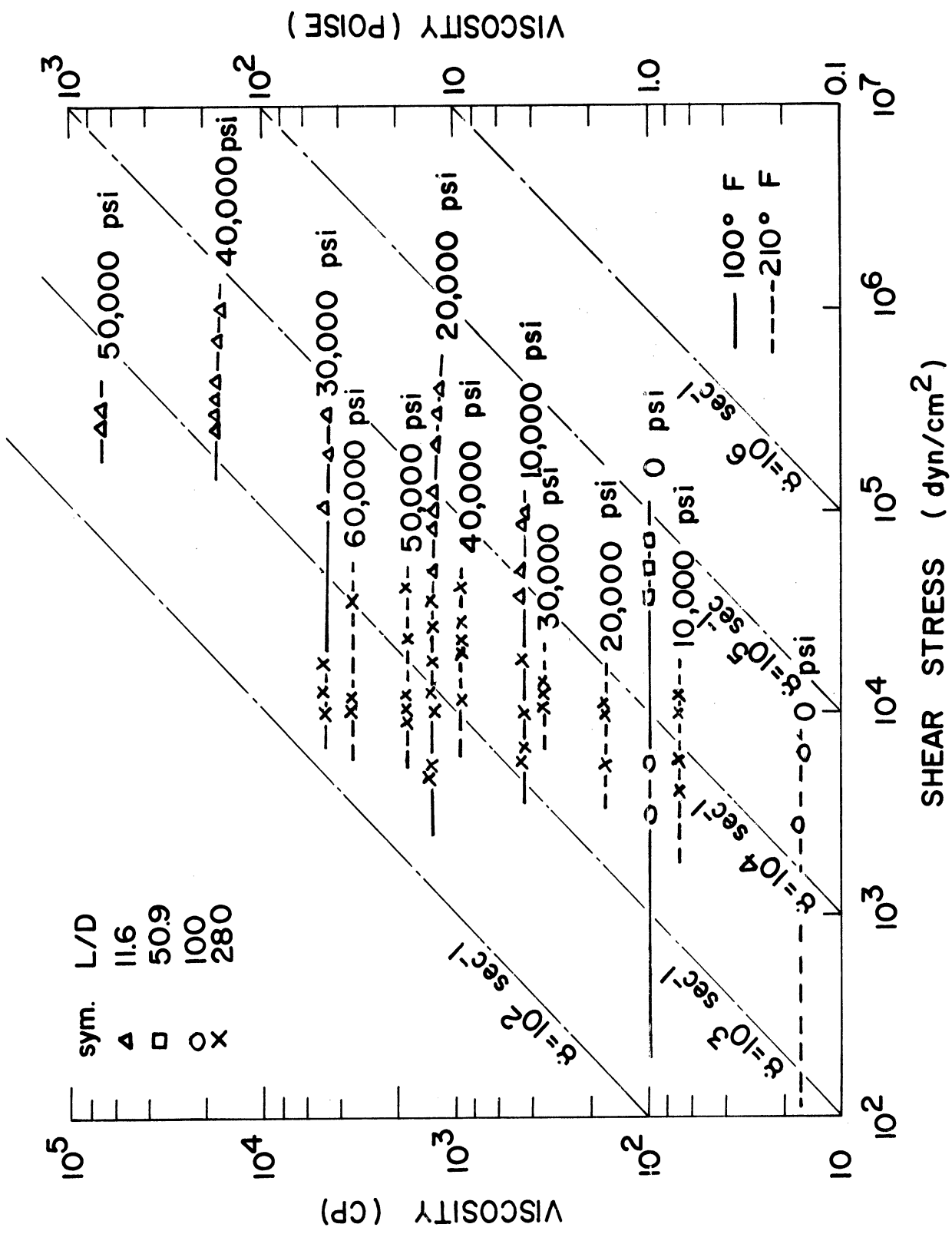

Figure 36. Flow Curves for Fluid J.

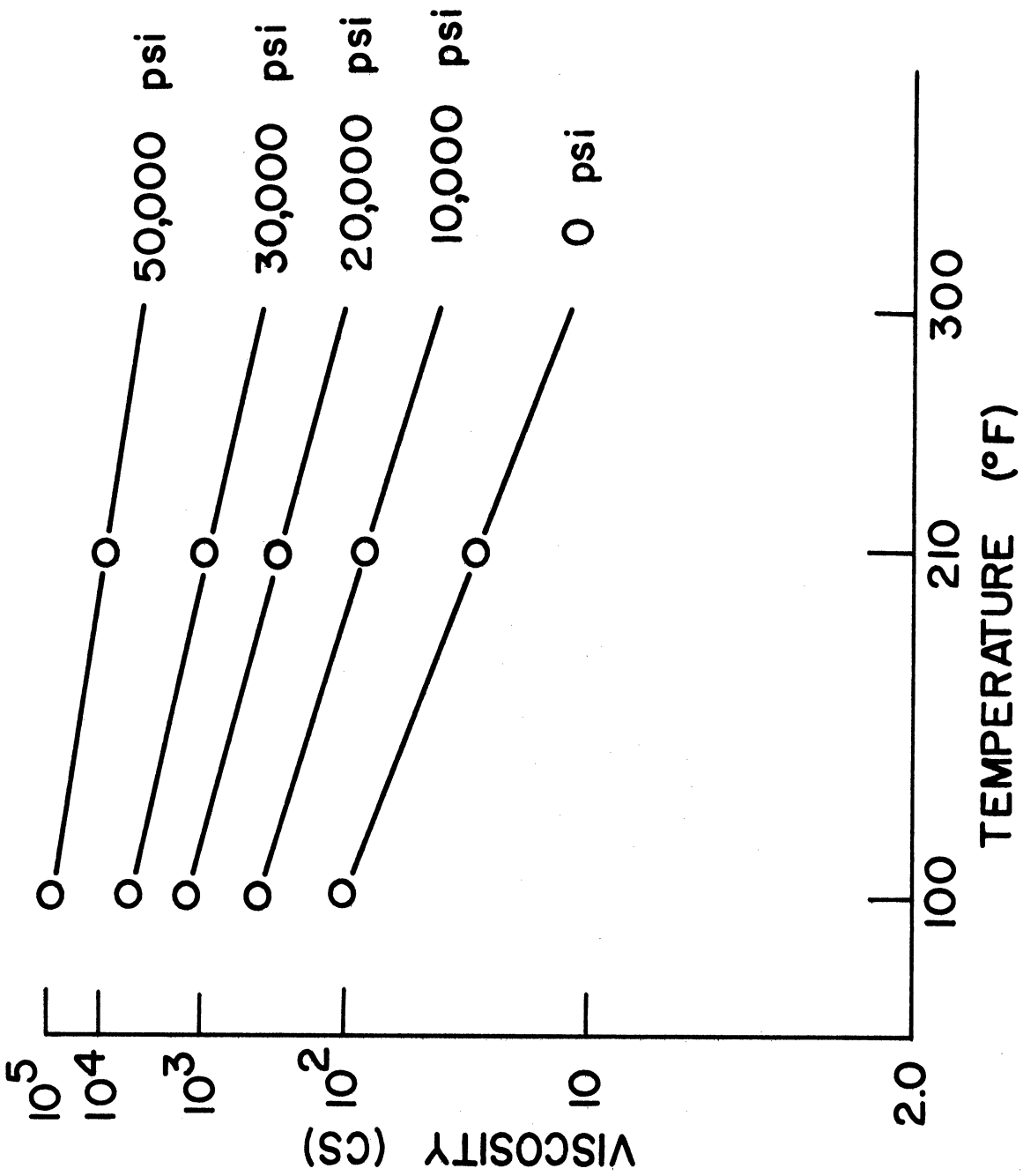

Figure 37. Viscosity-Temperature Relation for Fluid J.

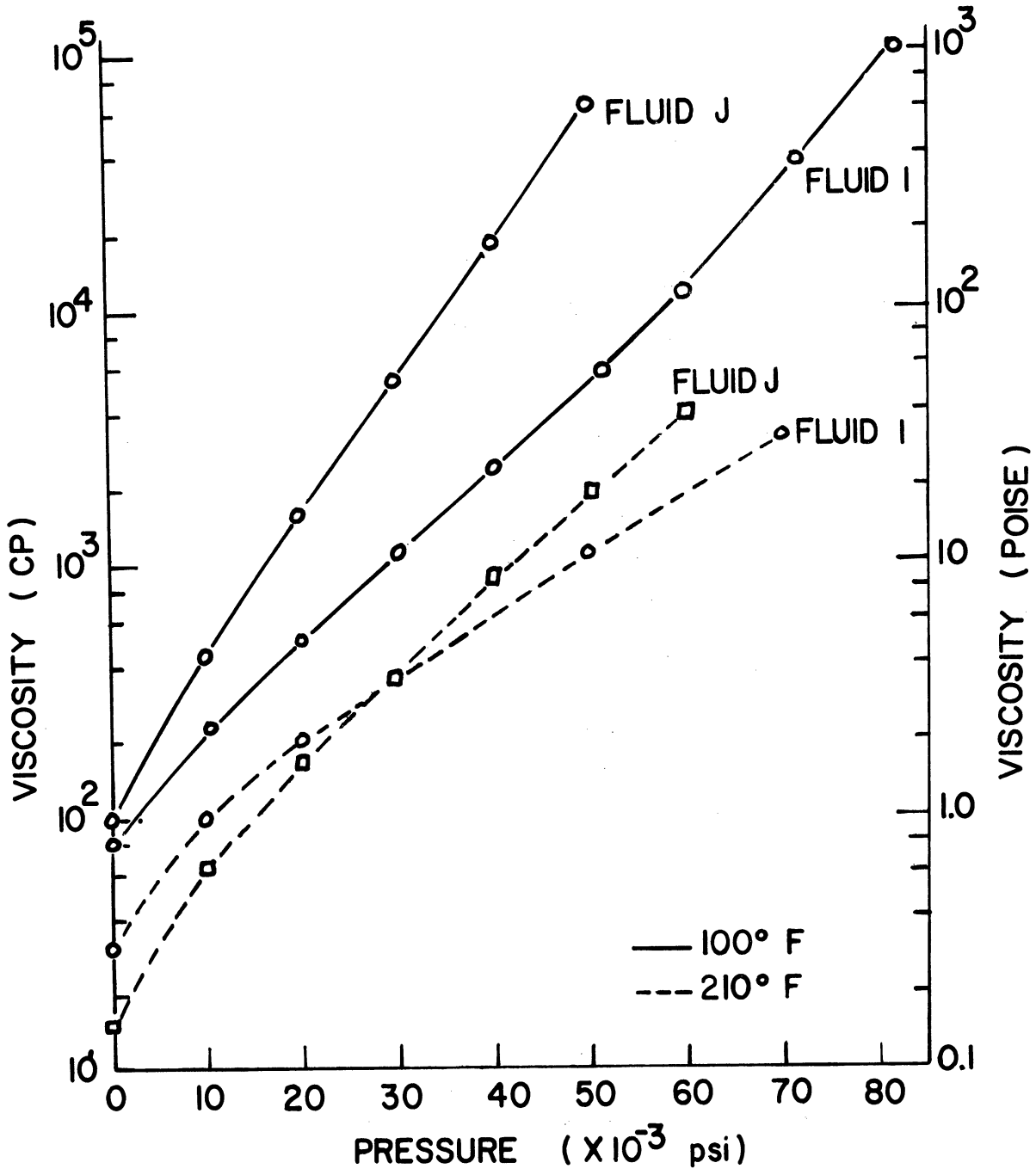

Figure 38. Viscosity-Pressure Relations for Fluids I and J.

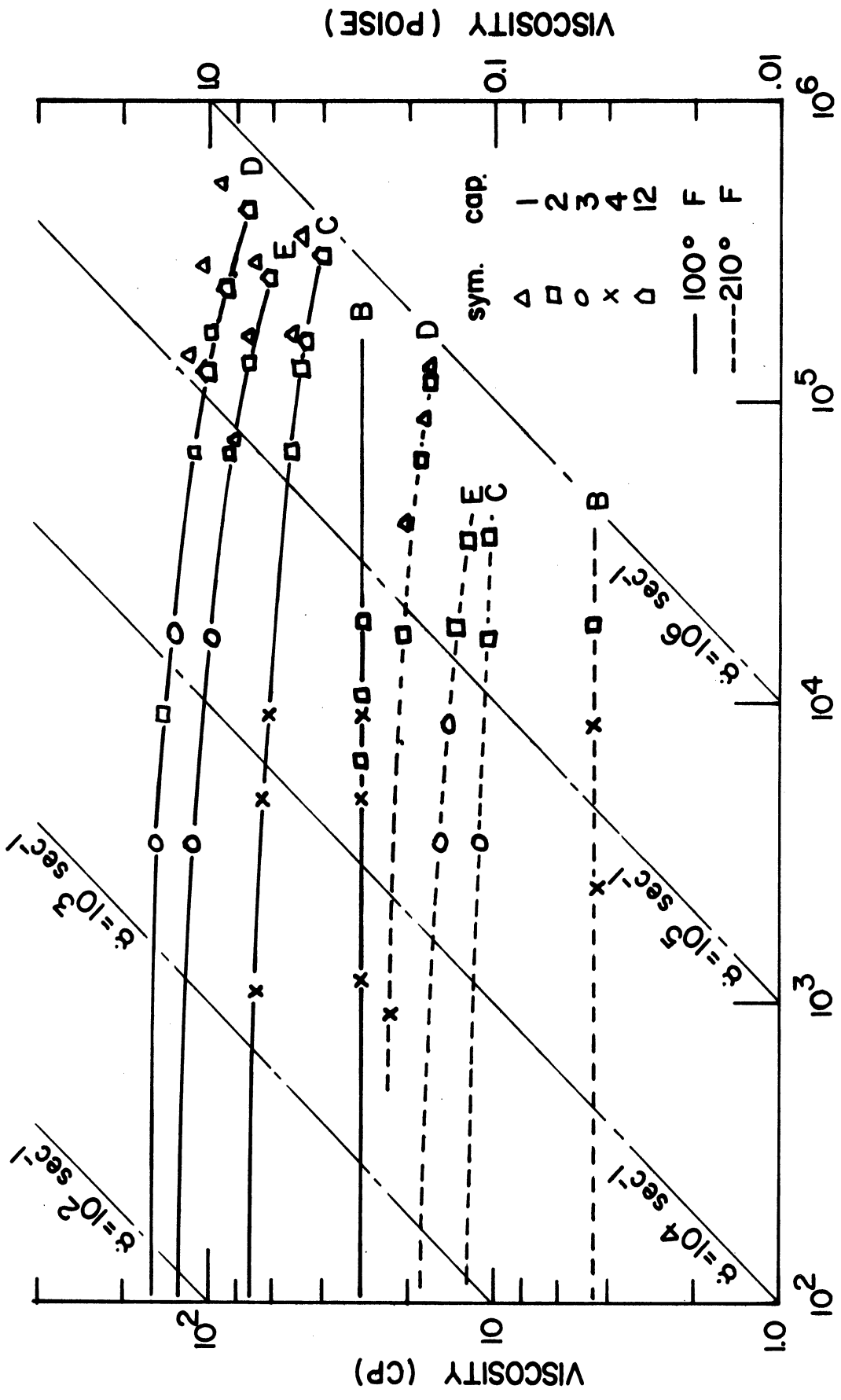

Figure 39. Flow Curves for Paraffinic Based Fluids at Atmospheric Pressure.

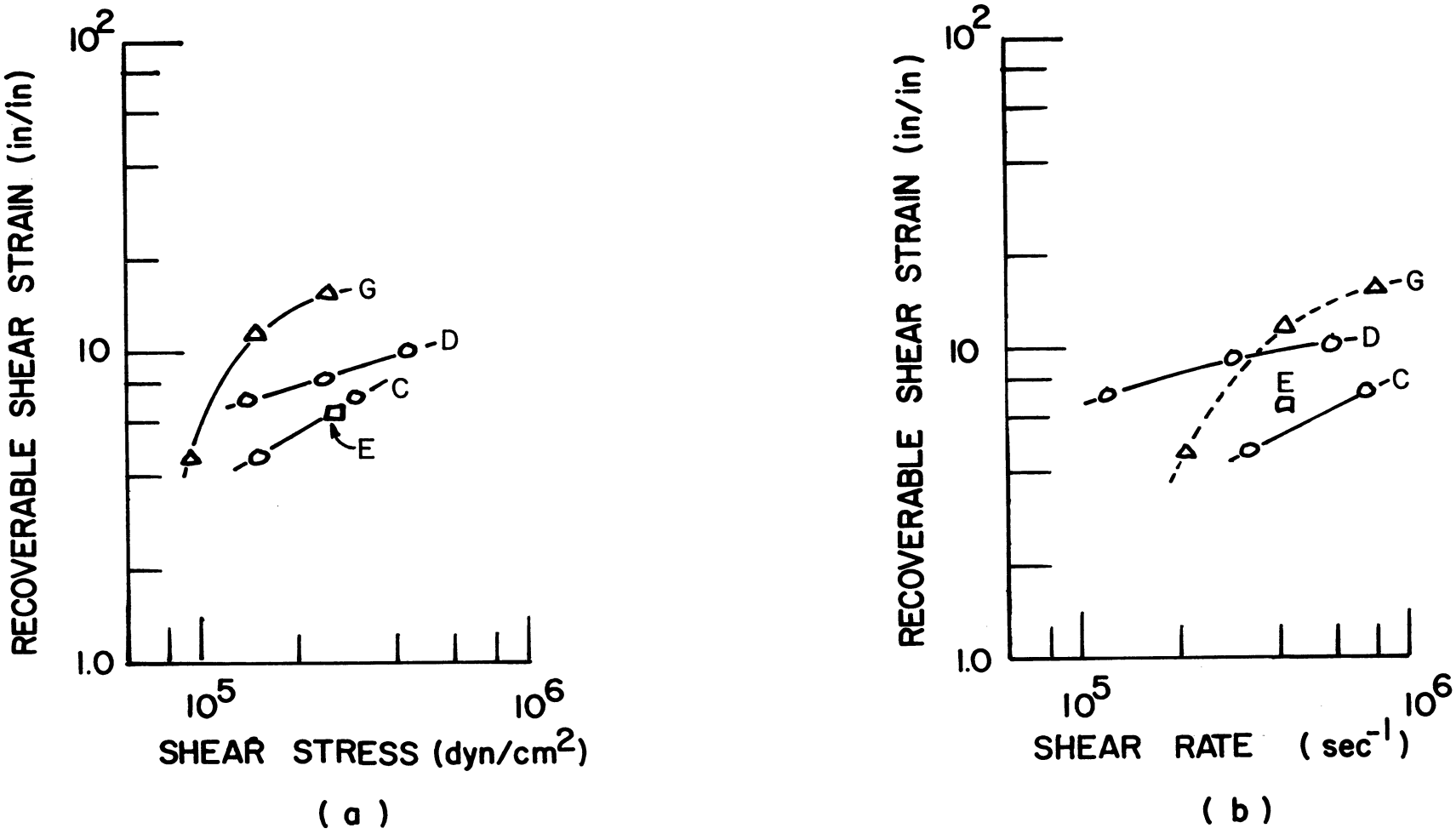

Figure 40. Recoverable Shear Strain in Petroleum Oils.

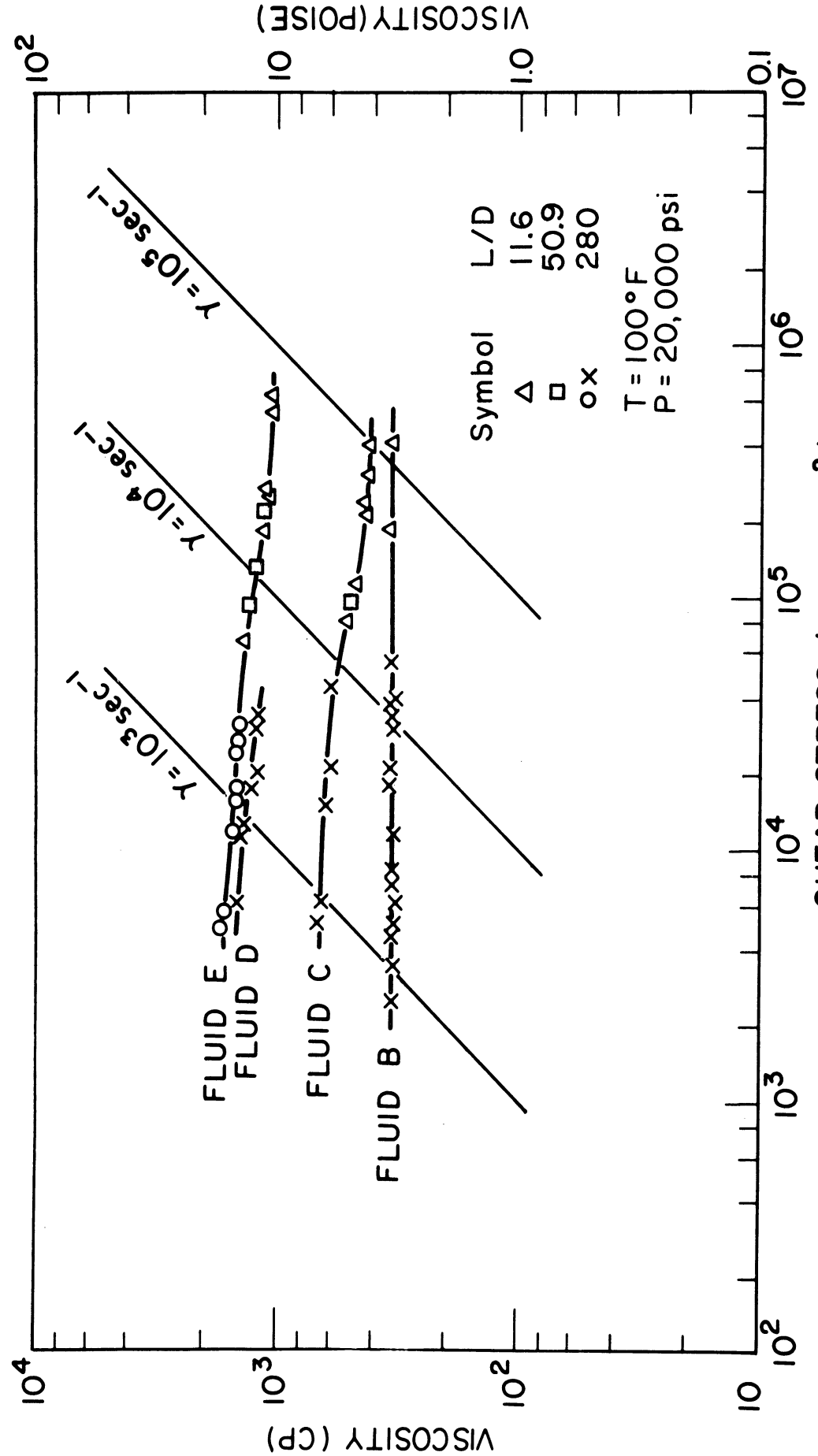

Figure 41. Flow Curves for Paraffinic Based Fluids at 20,000 psig.

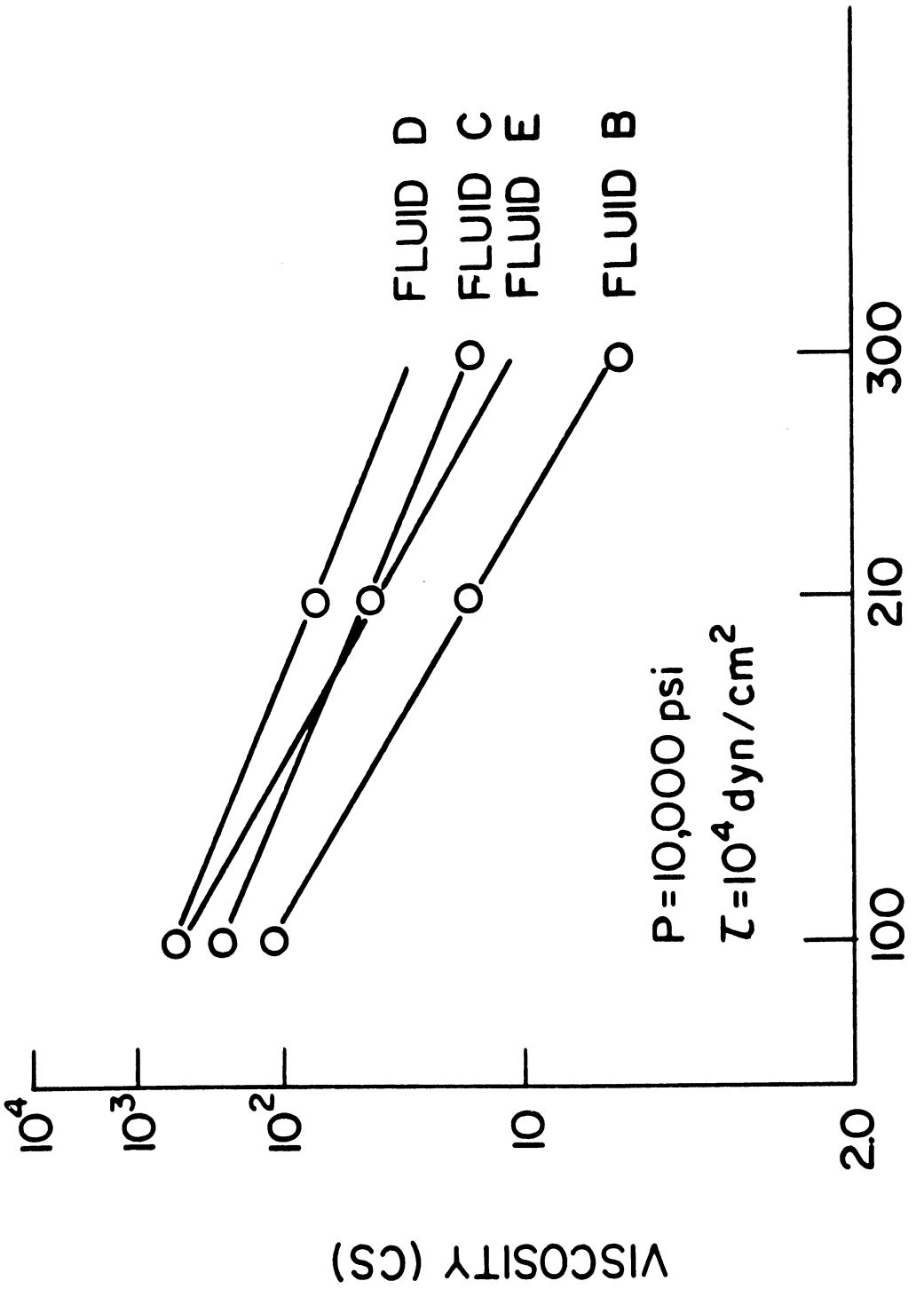

Figure 42. Viscosity-Temperature Relations for the Paraffinic Based Fluids at 10,000 psig.

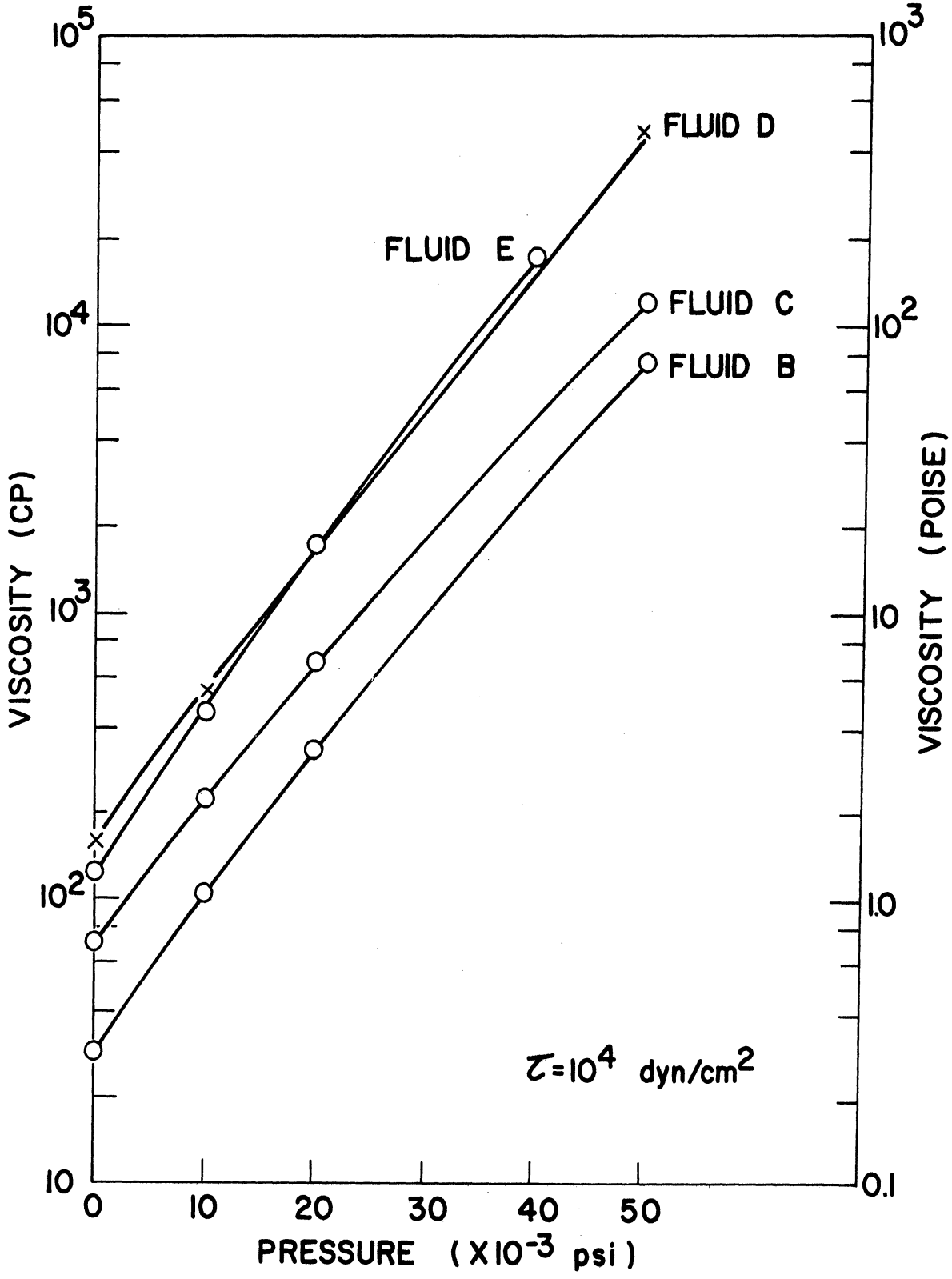

Figure 43. Viscosity-Pressure Relations for the Paraffinic Based Fluids at 100°F.

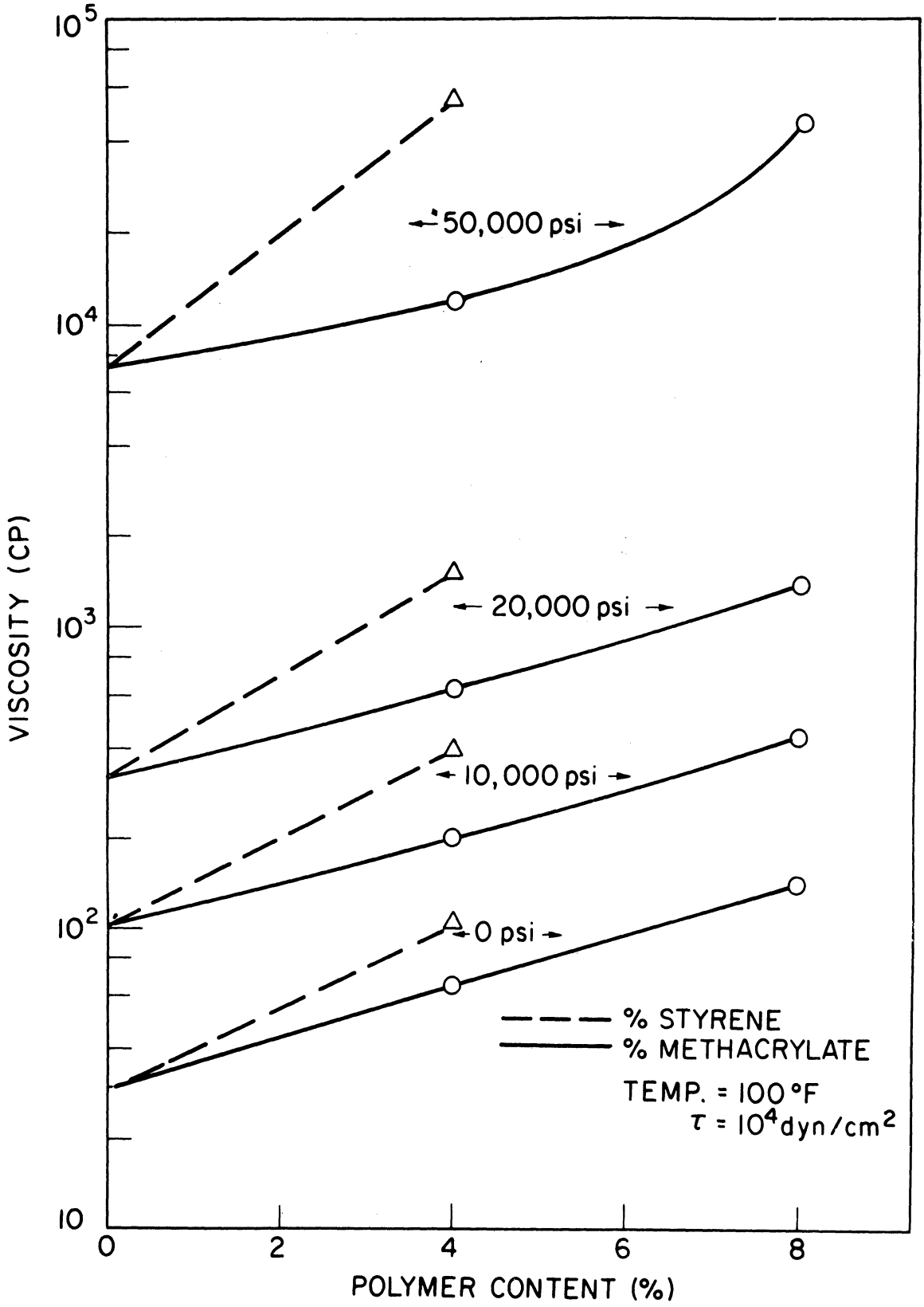

Figure 44. Effect of Polymer in Parraffinic Base Oil.

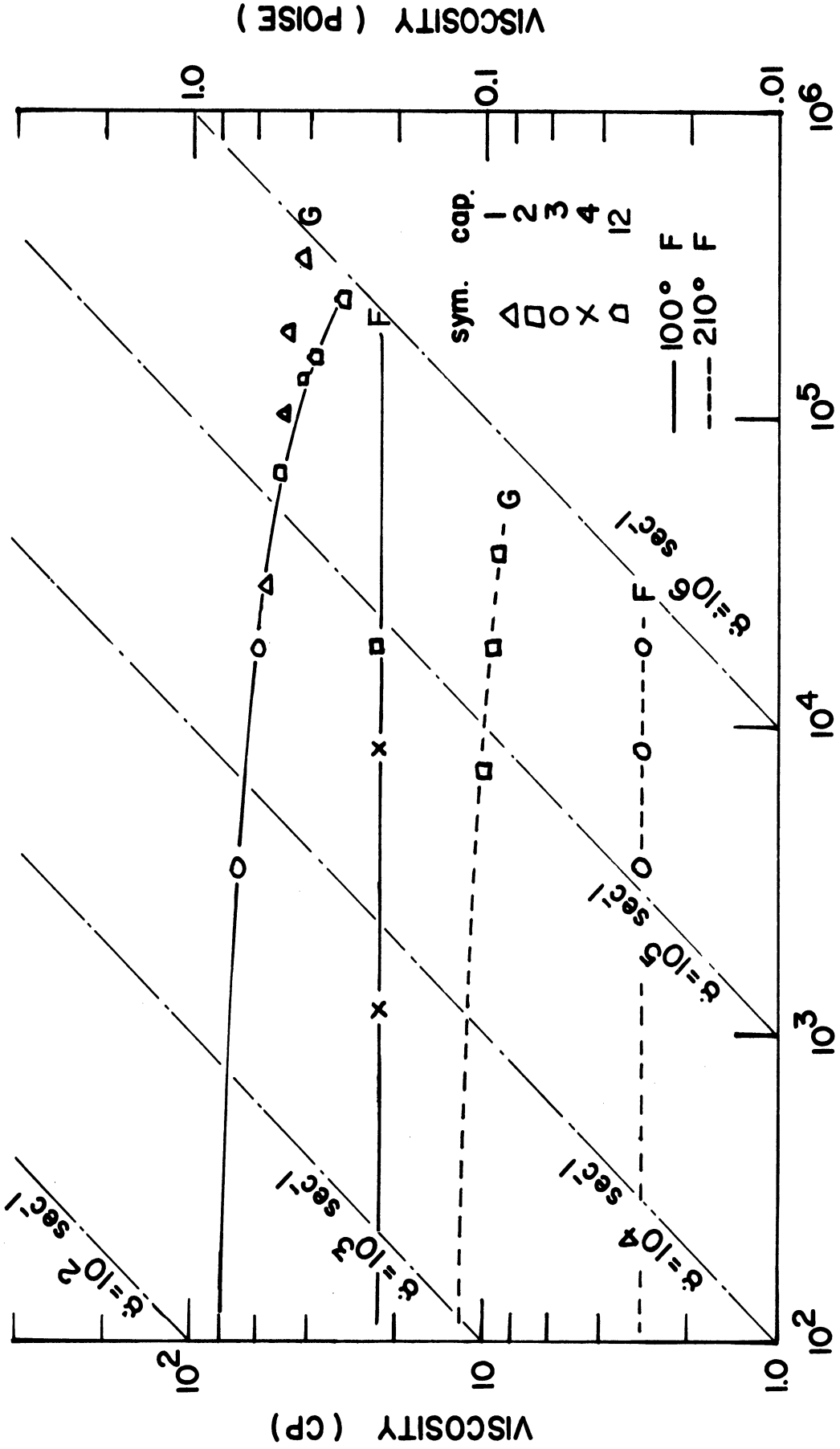

Figure 45. Flow Curves for Naphthenic Based Fluids at Atmospheric Pressure.

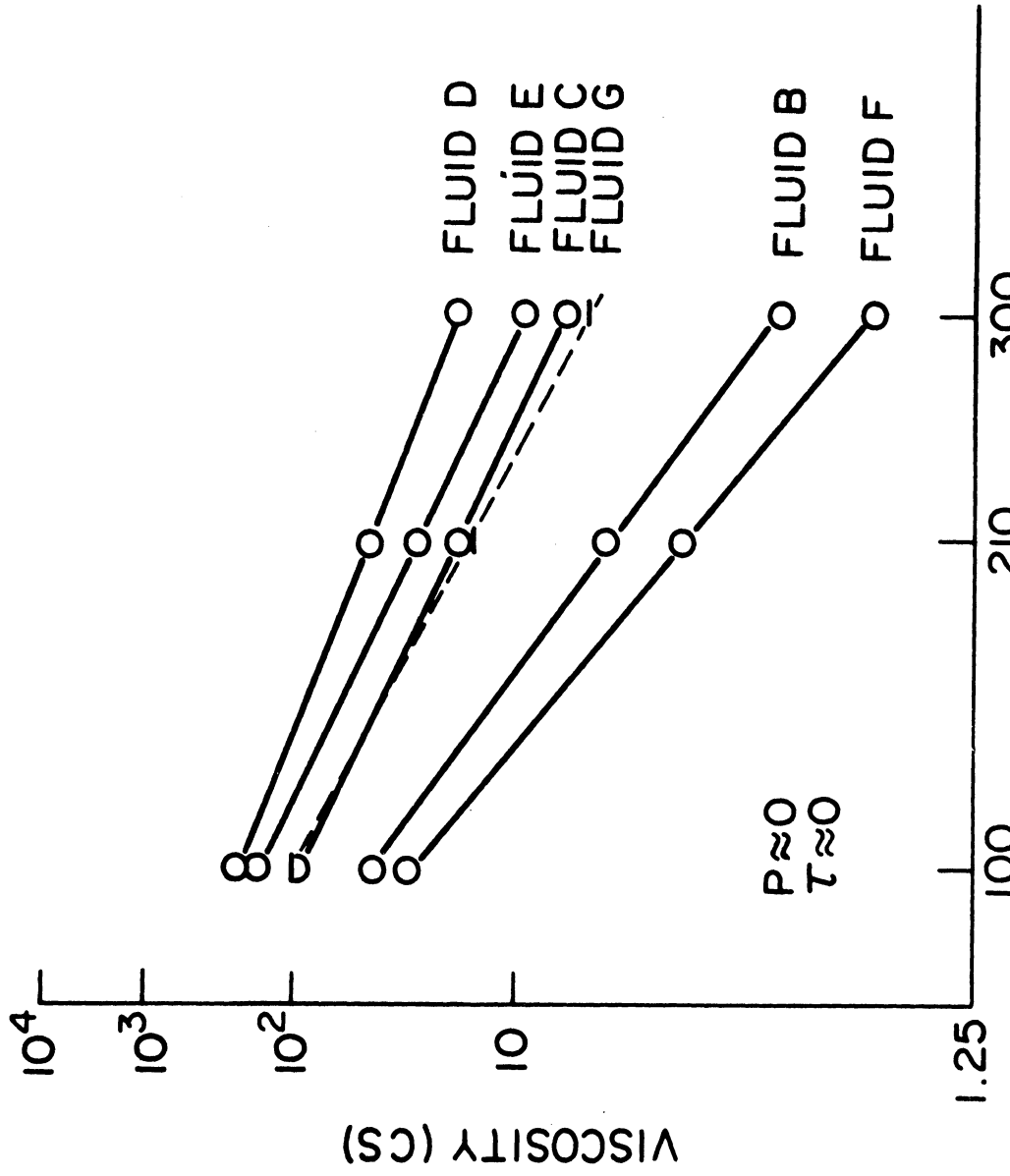

Figure 46. Viscosity-Temperature Relations for Petroleum Oils.

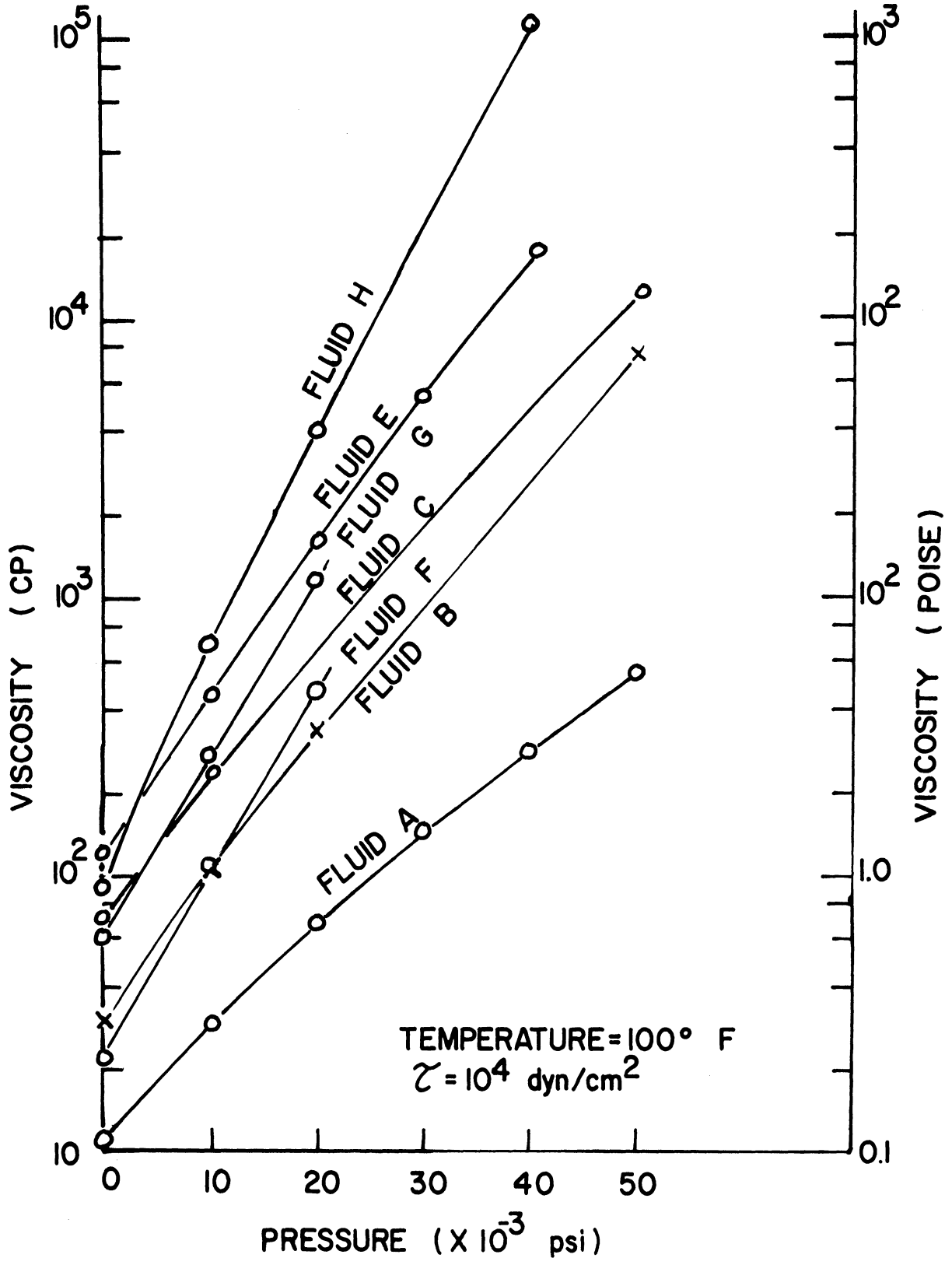

Figure 47. Viscosity-Pressure Relations for Fluids A,B,C,E,F,G,H.

methods for both Newtonian and non-Newtonian fluids (References 29-38). Of these several techniques, only the four to be discussed were investigated because they were considered to be the most promising and useful.

Graphical presentation of the data for the six Newtonian fluids was considered sufficient since these data are independent of shear stress. The most informative presentation of these data are lines of constant temperature on viscosity-pressure curves. Flow curves and lines of constant pressure on viscosity-temperature curves are also presented for completeness.

The analytical method investigated for Newtonian fluids was the following equation presented by Appeldoorn.[29]

$$\log \mu/\mu_o = a \log (T/T_o) + bP + cP \log (T/T_o) \qquad (33)$$

or

$$\mu/\mu_o = (T/T_o)^{a+cP}\, 10^{bP} \qquad (34)$$

where μ is the dynamic viscosity, T and P are the temperature and pressure, respectively, and the subscript o refers to reference values. These equations are only valid for fluids which have a constant slope on viscosity-pressure curves. Thus these equations cannot be used for the diester, the paraffinic base oil, the polybutene, or the silicones. They are valid, however, for the naphthenic based fluids as well as the paraffinic base oil blended with eight percent polyalkylmethacrylate.

This technique was successful for Appeldoorn because his data were limited to pressures below 15,000 psig. Since the viscosity-pressure relations for the data obtained in this research can also be approximated by straight lines at low pressures, this technique should also be applicable

in this narrow pressure range. The method was not employed, however, because the majority of the data was outside the limited pressure range in which satisfactory correlations could be obtained.

Graphical techniques for the presentation of non-Newtonian data are not very useful if quantitative information is desired. But the carpet plots presented in Figure 48 can be helpful in qualitatively understanding the fluid behavior.

One advantage of the analytical techniques in general is that they readily permit viscosity values to be predicted outside the limits of experimental data thus allowing the range of variables to be expanded. A disadvantage of these techniques for non-Newtonian fluids, however, is that the fluid behavior is generalized in such a manner that physical interpretation of the data is not possible as when the flow curves, the viscosity-temperature relations, and the viscosity pressure curves are used. Another possible difficulty is that the final equation may require a large number of data sets to evaluate all necessary constants and hence the value of the correlation is limited.

The two analytical techniques for non-Newtonian fluids which seemed to be the most promising were reported by Wright[30] and Philipoff.[14] The first method reduces the viscosity-shear stress data (at a given temperature and pressure) to a straight line by plotting the energy dissipated by the fluid (shear-stress shear-rate product) against a flow function. The second method is more general because it considers all three variables: temperature, pressure, and shear rate.

The technique presented by Wright[30] is valid for fluids whose flow curves are characterized by the existence of initial and ultimate

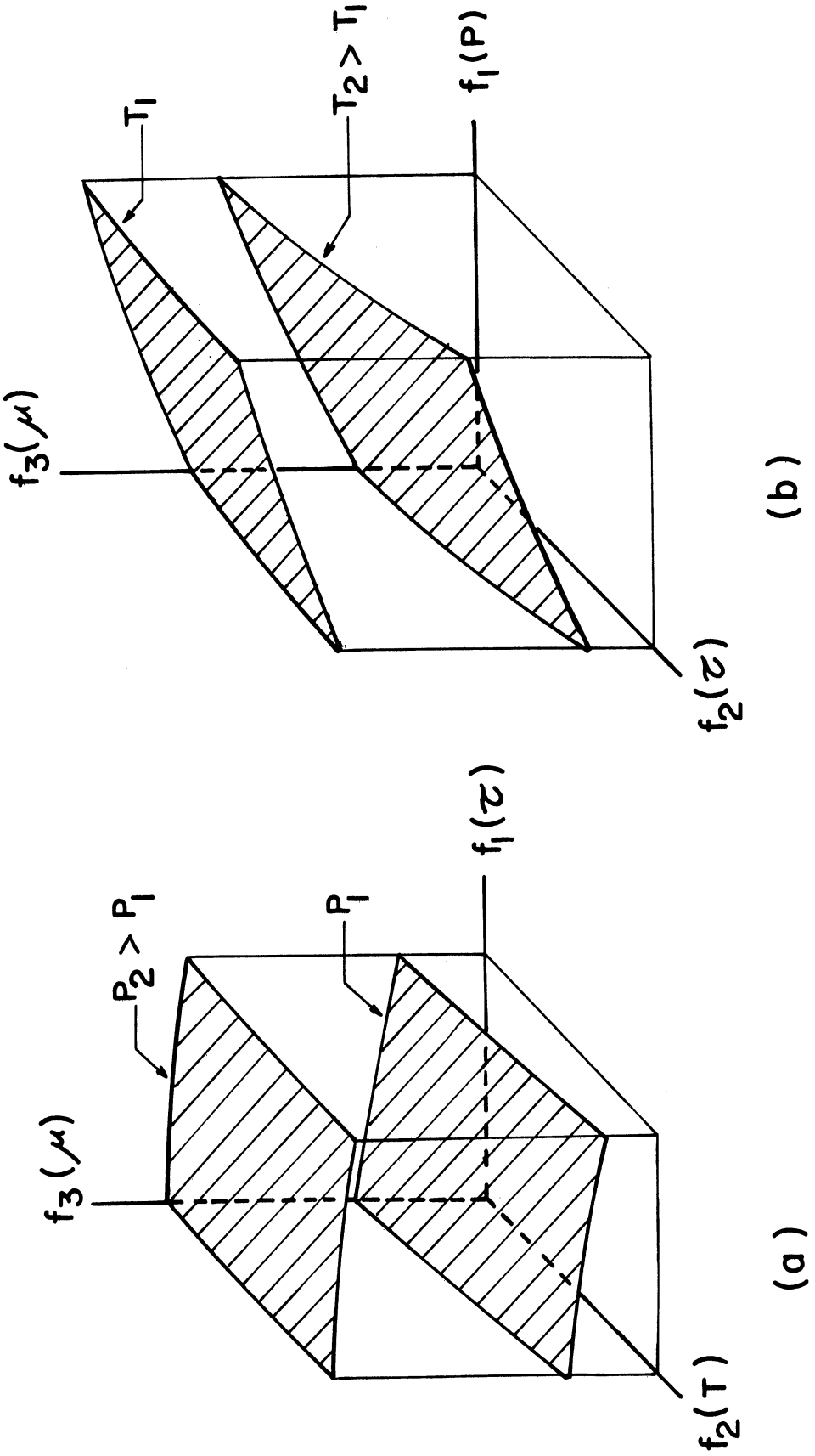

Figure 48. Graphical Presentation of Viscosity Data for Non-Newtonian Fluids.

Newtonian flow regions. It is postulated that the logaithm of the viscosity has a normal distribution between the limits of the first and second Newtonian regions when referred to the logarithm of the rate of energy input. Thus for a given temperature and pressure the flow data can be expressed as a straight line relationship (Figure 49). Even though the data for the non-Newtonian fluids examined are not complete enough to assure the existence of an ultimate Newtonian region, this method was investigated in detail because of the possibility that it could be expanded to include the effects of temperature and pressure.

This technique was employed by assuming that the viscosity of the fluid in the initial Newtonian region was equal to that of the data point with the lowest shear stress (point 1 on Figure 49). Similarly, the viscosity of the fluid in the ultimate Newtonian region was assumed to be equal to that of the data point with the largest shear stress (point 2 on Figure 49). The flow function which is plotted against the rate of energy dissipation is defined as

$$\phi = \frac{\log(\mu) - \log(\mu_2)}{\log(\mu_1) - \log(\mu_2)} \tag{35}$$

or

$$\mu = \mu_2(\mu_1/\mu_2)^{\phi} \tag{36}$$

where μ is the absolute viscosity and the subscripts 1 and 2 refer to initial and ultimate Newtonian regions, respectively. A computer program was written which, at each temperature and pressure, calculated and printed the values of the slope and intercept of the line in Figure 49. The viscosity was then calculated from the measured energy input and this value was printed along with the corresponding temperature, pressure,

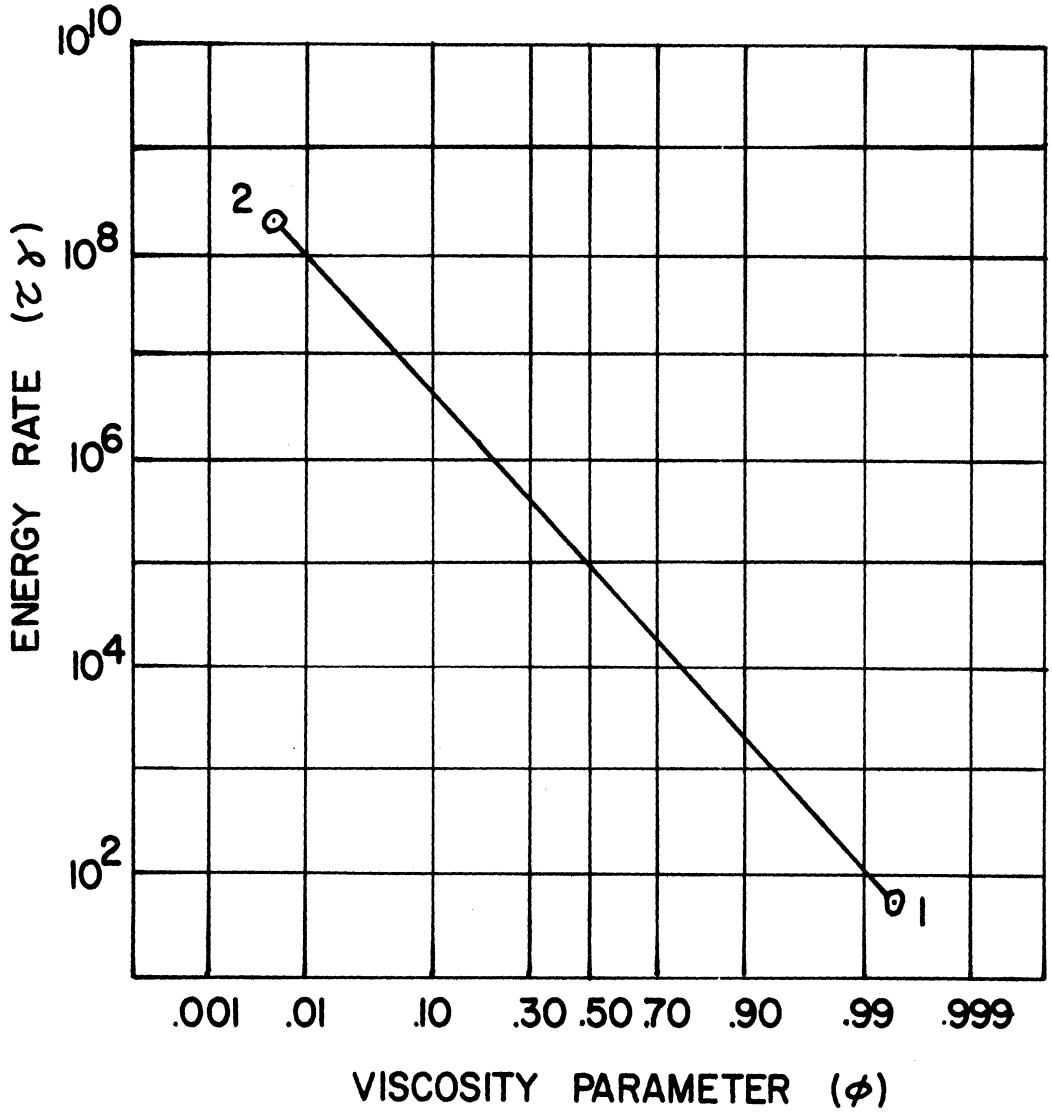

Figure 49. Generalized Non-Newtonian Flow Data.

shear stress, energy, flow function, measured viscosity, and the percent deviation between the two viscosity values. The results obtained from this method and the reduced variables technique are discussed later.

Ferry[31] described a reduced variables technique for correlating viscosity-temperature-shear rate data. This method resulted in a straight line relationship when the logarithm of the reduced viscosity was plotted against the logarithm of the reduced shear rate. The equations used for obtaining the reduced variables are:

$$\mu_{red} = \mu_{T,\gamma} \, (\bar{\mu} / \mu_{T,o}) \tag{37}$$

$$\gamma_{red} = a_T \, \gamma \tag{38}$$

and

$$a_T = (\mu_{T,o}/\bar{\mu}) \, \frac{T_o \rho_o}{T \rho} \tag{39}$$

where μ_{red} = reduced viscosity,

$\mu_{T,\gamma}$ = viscosity at T and γ,

$\mu_{T,o}$ = viscosity at T and γ,

$\bar{\mu}$ = viscosity at T_o and low γ,

γ_{red} = reduced shear rate,

γ = measured shear rate,

a_T = shear rate scale factor,

T = absolute temperature,

ρ = density,

and the single subscript o refers to the reference values.

Philippoff[14] expanded Ferry's reduced variable technique to include the influence of pressure. One difficulty immediately encountered was that the scale factor a_T requires viscosity values obtained at low

shear rates. Since Philippoff's equipment was not capable of producing the necessary low shear rates, he had to obtain these data by other methods. Ordinary capillary viscometers were used at atmospheric pressure and different temperatures. But he could not obtain low shear rate data at different pressures. This difficulty was circumvented by noting that for his data the relative viscosity* of the polymer blend is nearly constant with pressure. That is, the polymer blend has the same viscosity-pressure slope as the base oil at low shear rates.** Thus knowing the behavior of the base oil under pressure, the low shear viscosity of the blend at the given temperature and pressure $(\mu_{T,P,o})$ could be calculated. Hence Philippoff's equation for the shear rate scale factor, a_{TP}, was

$$a_{TP} = \left(\frac{T_o \rho_o}{T \rho} \frac{\mu_{T,o,o}}{\bar{\mu}}\right)_{\text{Blend}} \left(\frac{\mu_{T_o,P,o}}{\bar{\mu}}\right)_{\text{Base Oil}} \tag{40}$$

$$\gamma_{red} = a_{TP}\, \gamma \tag{41}$$

$$\mu_{red} = \mu_{T,P,\gamma} \left(\frac{\mu_{T,P,o}}{\bar{\mu}}\right)_{\text{Base Oil}} \tag{42}$$

The definitions of terms in the above equations are identical to those in Equations (37), (38), and (39) except for the addition of the subscript P for pressure.

Since the experimental apparatus used in this research enabled the low shear viscosity to be measured, it was not necessary to use the method presented by Philippoff and the following equations were used:

---

* Relative viscosity is defined as the ratio of the viscosity of the blend to the viscosity of the base oil.

** Table VII shows that this relation is not true for the petroleum oils used in the research.

$$a_{TP} = \frac{T_o \rho_o}{T\rho} \frac{\mu_{T,P,o}}{\bar{\mu}} \tag{43}$$

$$\gamma_{red} = a_{T,P}\, \gamma \tag{44}$$

$$\mu_{red} = \mu_{T,P,\gamma} \frac{\mu_{T,P,o}}{\bar{\mu}} \tag{45}$$

where all terms are identical to those in Equations (40), (41), and (42).

A computer program was also written for this method which was very similar to the one written to apply the generalized non-Newtonian technique. At each temperature and pressure, the shear rate scale factor was calculated and printed as well as the slope and intercept of the straight line. The measured shear rate was then used to calculate a viscosity and this value was printed along with the corresponding temperature, pressure, shear stress, measured viscosity, and the percent deviation between the two viscosity values.

2. Results

These two analytical techniques employed for the non-Newtonian fluids both reduced the viscosity-shear stress data to straight line relationships for a given temperature and pressure. Therefore the slopes of the resulting straight lines and their intercepts with the ordinate had to be determined for each temperature and pressure. The reduced variables technique also required that a scale factor be evaluated as a function of temperature and pressure. This latter method also required that all data be represented by a single line. Therefore, the slope and intercept had to be constant for all temperatures and pressures.

The objective of the correlation for the generalized non-Newtonian technique was to obtain equations for both the slope and the

intercept which were explicit functions of temperature and pressure. The objectives of the reduced variables technique were (1) to determine whether or not a single curve could represent all the experimental data, and (2) to obtain an expression for the shear rate scale factor which was an explicit function of temperature and pressure. If the objectives for either correlation could be accomplished, it would then be possible to predict viscosity values under a wide range of conditions and possibly the results could be extended to include the effect of polymer content.

The first step in each of these correlation methods consisted of applying the technique to the data and determining whether or not the methods were satisfactory at each temperature and pressure. If the methods did give satisfactory results, the next step could be taken to determine the necessary explicit functions, if possible.

Both the generalized non-Newtonian method and the reduced variables technique produced satisfactory results at any given temperature and pressure as the error between the calculated and measured viscosity values was in general less than ten percent. The results for Fluid C, for example, showed that the slope of the straight line in the generalized non-Newtonian technique decreased with increasing temperature and pressure, while the intercept increased with pressure up to 20,000 psig. The intercept for 50,000 psig, however, was less than that for 10,000 psig. Both the intercept and the slope in the reduced variables technique behaved in a similar manner.

As a result the intercept in the generalized non-Newtonian technique could not be evaluated by a linear equation. It could be described by a higher degree polynomial but this is unsatisfactory because

of the increased number of data sets required to evaluate the necessary constants. Since the slope and the intercept in the reduced variables technique varied with temperature and pressure, the experimental data could not be represented by a single curve.

In summary, both of the analytical correlation techniques investigated for the non-Newtonian fluids produced satisfactory results at each temperature and pressure. The generalized non-Newtonian technique was developed for atmospheric pressure data and it was also shown to be applicable to high pressure viscosity data, but it could not be generalized to include the effects of temperature and pressure. Philippoff[14] has previously shown that the reduced variables technique was capable of correlating viscosity data at pressures up to 15,000 psig for certain fluids, but this method could not be successfully applied to the data obtained in this research.

D. Tabulated Data

As mentioned previously, all of the tabulated data account for the kinetic energy of the fluid leaving the capillary, while some data account for the elastic energy stored in the fluid and/or the effect of a non-parabolic velocity profile. The capillary number listed with each data set can be used to determine whether or not the elastic energy has been evaluated. These capillary numbers contain one, two, or three digits. The one digit numbers (one through four) refer to the stainless steel capillaries designed for this research. The three digit numbers refer to the standard glass capillaries used to obtain the low-shear, atmospheric pressure data. The data sets with the one or the three digit

capillary numbers do not account for the elastic energy in the fluid. Only the data sets with two digit capillary numbers account for this energy. The two digit number is formed by using the numbers of the two stainless steel capillaries employed. For example, a data set with a capillary number of 12 means that the elastic energy was evaluated by using data obtained from capillaries 1 and 2. Where necessary, some of the tabulated data sets for the non-Newtonian fluids contain two viscosity values. The first value, in parentheses, is the final value which does account for all necessary effects, including a non-parabolic velocity profile. The second value accounts for the kinetic and elastic energies where necessary but does not account for the non-parabolic velocity profile. The shear rates in these data sets correspond to the second viscosity value.

FLUID A

TEMP. (DEG. F)	PRESS. (PSIG)	DENSITY (GM/CC)	VISCOSITY (POISE)	SHEAR STRESS (DYN/SQ.CM.)	SHEAR RATE (SEC-1)	CAPILLARY NUMBER
100	0	.903	.110	0	0	100
100	0	.903	.106	3440	32453	3
100	0	.903	.110	9050	82273	2
100	0	.903	.110	18100	164545	2
100	0	.903	.109	36200	332110	2
100	0	.903	.110	72000	654545	2
100	10040	.940	.298	1037	3480	4
100	10040	.940	.280	1281	4575	4
100	10040	.940	.298	1329	4460	4
100	10040	.940	.285	2055	7211	4
100	9999	.940	.285	2388	8379	4
100	10040	.940	.302	5020	16623	4
100	18770	.964	.609	1041	1709	4
100	18770	.964	.614	2661	4334	4
100	18830	.964	.554	2895	5226	4
100	18830	.964	.593	2963	4997	4
100	18830	.964	.578	4097	7088	4
100	18830	.964	.592	4638	7834	4
100	29530	.989	1.260	2678	2125	4
100	29590	.989	1.320	2740	2076	4
100	29590	.989	1.370	3346	2442	4
100	29590	.989	1.330	3610	2714	4
100	29590	.989	1.340	3865	2884	4
100	29650	.989	1.300	3866	2974	4
100	29530	.989	1.260	4597	3648	4
100	29590	.989	1.330	4599	3458	4
100	29530	.989	1.300	5044	3880	4
100	29590	.989	1.350	5166	3827	4
100	29590	.989	1.310	9927	7578	4
100	37460	1.030	2.420	2653	1096	4
100	37160	1.030	2.180	3319	1522	4
100	37310	1.030	2.490	3795	1524	4
100	37310	1.030	2.260	4007	1773	4
100	37610	1.030	2.290	4173	1822	4
100	37460	1.030	2.480	4400	1774	4
100	37460	1.030	2.230	4633	2078	4
100	37460	1.030	2.530	4739	1873	4
100	37310	1.030	2.290	4762	2079	4
100	47360	1.200	4.330	1233	285	4
100	47360	1.200	4.840	1543	319	4

FLUID A

TEMP. (DEG. F)	PRESS. (PSIG)	DENSITY (GM/CC)	VISCOSITY (POISE)	SHEAR STRESS (DYN/SQ.CM.)	SHEAR RATE (SEC-1)	CAPILLARY NUMBER
100	47510	1.200	4.630	2484	537	4
100	47510	1.200	4.740	3028	639	4
100	47360	1.200	5.000	3098	620	4
100	47510	1.200	4.470	4657	1042	4
100	47510	1.200	4.200	5310	1264	4
100	47590	1.200	4.880	8780	1799	1
100	47590	1.200	4.300	33260	7735	1
100	47590	1.200	4.130	63880	15467	1
100	47590	1.200	4.340	68850	15864	1
100	47590	1.200	4.540	80490	17729	1
100	47590	1.200	4.350	98240	22584	1
100	47590	1.200	4.470	119900	26823	1
100	47590	1.200	4.430	124800	28172	1
100	47290	1.200	4.360	131600	30183	1
100	47590	1.200	4.140	141100	34082	1
100	47590	1.200	4.340	142800	32903	1
100	49280	1.200	5.220	169500	32471	1
100	48430	1.200	4.730	274300	57992	1
100	58350	1.370	8.910	7611	854	4
100	58670	1.370	8.840	16390	1854	4
100	58510	1.370	8.500	16600	1953	4
100	58350	1.370	8.770	17980	2050	4
100	58510	1.370	8.450	19240	2277	4
100	67700	1.500	14.000	5575	398	4
100	67540	1.500	15.600	13300	853	4
100	67540	1.500	13.700	18380	1342	4
100	67700	1.500	14.100	23470	1665	4
100	79780	1.650	29.400	17450	594	4
100	78670	1.650	28.900	19420	672	4
100	79460	1.650	27.200	21220	780	4
100	78980	1.650	30.800	29110	945	4

FLUID B

TEMP. (DEG. F)	PRESS. (PSIG)	DENSITY (GM/CC)	VISCOSITY (POISE)	SHEAR STRESS (DYN/SQ.CM.)	SHEAR RATE (SEC-1)	CAPILLARY NUMBER
100	0	.849	.292	0	0	200
210	0	.809	.045	0	0	100
300	0	.777	.019	0	0	150
100	0	.849	.295	1204	4081	4
100	0	.849	.290	4816	16607	4
100	0	.849	.286	9030	31573	4
100	0	.849	.295	10860	36814	2
100	0	.849	.286	18100	63287	2
100	0	.849	.272	29500	108456	1
100	9945	.882	1.020	4436	4349	4
100	9945	.882	1.020	5537	5428	4
100	9979	.882	1.100	8434	7667	4
100	9945	.882	1.150	16680	14504	4
100	9911	.882	1.110	18570	16730	4
100	9911	.882	1.120	24070	21491	4
100	10140	.882	1.070	74230	69374	1
100	10180	.882	1.040	87450	84087	1
100	10020	.882	1.040	103200	99231	1
100	10060	.882	1.040	124400	119615	1
100	20070	.908	3.350	2604	777	4
100	19940	.908	3.290	6174	1877	4
100	20070	.908	3.280	7202	2196	4
100	19500	.908	3.350	18150	5418	4
100	19440	.908	3.360	31150	9271	4
100	19440	.908	3.410	33400	9795	4
100	19380	.908	3.400	47640	14012	4
100	19380	.908	3.350	49600	14806	4
100	19440	.908	3.440	188900	54913	1
100	19630	.908	3.330	426700	128138	1
100	49080	.961	72.700	39530	544	4
100	48770	.961	72.000	44970	625	4
100	50530	.961	76.200	306800	4026	4
100	49900	.961	73.500	475200	6465	1
100	50220	.961	76.500	521200	6813	1
100	49900	.961	77.200	525600	6808	1
210	0	.809	.044	2408	55229	4
210	0	.809	.046	8240	179913	4
210	0	.809	.047	18100	381053	2
210	10270	.849	.134	866	6463	1
210	10160	.849	.128	1699	13273	1

FLUID B

TEMP. (DEG. F)	PRESS. (PSIG)	DENSITY (GM/CC)	VISCOSITY (POISE)	SHEAR STRESS (DYN/SQ.CM.)	SHEAR RATE (SEC-1)	CAPILLARY NUMBER
210	10250	.849	.130	2194	16877	4
210	10330	.849	.135	2400	17778	4
210	10370	.849	.124	6309	50879	4
210	10370	.849	.124	6734	54306	4
210	20260	.878	.325	1104	3397	4
210	20190	.878	.299	1650	5518	4
210	20260	.878	.290	5665	19534	4
210	49420	.935	2.400	4499	1875	4
210	49420	.935	2.380	6784	2850	4
210	48940	.935	2.360	7302	3094	4
210	48960	.935	2.450	29450	12020	1
210	49280	.935	2.300	40700	17696	1
300	10180	.825	.043	1191	27698	4
300	10180	.825	.044	1430	32500	4
300	10220	.825	.046	1506	32739	4
300	10180	.825	.046	3316	72087	4
300	19630	.857	.088	513	5830	4
300	19630	.857	.091	1211	13308	4
300	19690	.857	.088	2818	32023	4
300	19750	.857	.086	5160	60000	4
300	20130	.857	.089	24380	273933	1
300	20130	.857	.090	31580	350889	1

FLUID C

TEMP. (DEG. F)	PRESS. (PSIG)	DENSITY (GM/CC)	VISCOSITY (POISE)	SHEAR STRESS (DYN/SQ.CM.)	SHEAR RATE (SEC-1)	CAPILLARY NUMBER
100	0	.849	.720	0	0	200
100	0	.849	.414	303000	731884	12
100	0	.849	.688	1204	1750	4
100	0	.849	.651	4816	7398	4
100	0	.849	.633	9030	14265	4
100	0	.849	.515	68000	132039	2
100	0	.849	.485	132000	272165	2
100	0	.849	.469	152000	324094	12
100	0	.849	.518	167500	323359	1
100	0	.849	.479	353000	736952	1
100	10290	.882	2.200	2014	915	4
100	10610	.882	1.360	557000	409559	1
100	10210	.882	2.140	5364	2507	4
100	10280	.882	2.140	8963	4188	2
100	10280	.882	2.120	11250	5307	2
100	9902	.882	1.980	14200	7172	4
100	10280	.882	2.110	15540	7365	2
100	10130	.882	1.800	17940	9967	1
100	9936	.882	2.000	21880	10940	4
100	10280	.882	1.950	24420	12523	2
100	10130	.882	1.810	29940	16541	1
100	9902	.882	1.950	32460	16646	4
100	10280	.882	1.820	32920	18088	2
100	9760	.882	1.900	43360	22821	4
100	10280	.882	1.830	44220	24164	2
100	10470	.882	1.840	65000	35326	2
100	10210	.882	1.740	71200	40920	1
100	10430	.882	1.780	73110	41073	2
100	10510	.882	1.820	84420	46385	2
100	10510	.882	1.810	91450	50525	2
100	10510	.882	1.750	113500	64857	2
100	10290	.882	1.510	117900	78079	1
100	10170	.882	1.400	195600	139714	1
100	10250	.882	1.320	272100	206136	1
100	19950	.908	6.230	15530	2493	4
100	20070	.908	4.370	712700	163089	1
100	19740	.908	6.400	20420	3191	2
100	20140	.908	5.980	23210	3881	4
100	19800	.908	5.410	50820	9394	2
100	19860	.908	5.370	72360	13475	2

FLUID C

TEMP. (DEG. F)	PRESS. (PSIG)	DENSITY (GM/CC)	VISCOSITY (POISE)	SHEAR STRESS (DYN/SQ.CM.)	SHEAR RATE (SEC-1)	CAPILLARY NUMBER
100	19630	.908	5.180	84600	16332	1
100	19760	.908	4.750	116300	24484	1
100	19880	.908	4.280	223300	52173	1
100	19880	.908	4.180	414700	99211	1
100	49740	.961	123	13400	109	4
100	47400	.961	105	231300	2199	2
100	49900	.961	120	26360	220	4
100	47870	.961	119	55680	468	2
100	47720	.961	109	61100	563	2
100	47870	.961	109	95890	884	2
100	47720	.961	110	170300	1554	2
100	47560	.961	109	197000	1812	2
100	47560	.961	106	226000	2124	2
100	49420	.961	106	328600	3109	1
100	49260	.961	100	840200	8394	1
210	0	.809	.125	0	0	150
210	0	.809	.111	3440	30991	3
210	0	.809	.105	16200	154286	2
210	0	.809	.110	44600	405455	2
210	0	.809	.111	57600	518919	2
210	10650	.849	.309	929	3006	4
210	10250	.849	.171	120300	703509	1
210	9945	.849	.296	1900	6419	4
210	10240	.849	.287	4345	15139	2
210	9945	.849	.289	4876	16872	4
210	10200	.849	.275	6910	25127	2
210	9877	.849	.249	7804	31341	4
210	10160	.849	.272	8042	29566	2
210	10220	.849	.264	8990	34053	2
210	9945	.849	.235	9329	39698	4
210	10240	.849	.261	10160	38927	2
210	10160	.849	.248	12580	50726	2
210	10330	.849	.251	15690	62510	1
210	10410	.849	.238	18780	78908	4
210	10090	.849	.249	22750	91365	1
210	10370	.849	.219	41550	189726	1
210	10290	.849	.181	109100	602762	1
210	22370	.878	.758	1255	1656	4
210	19940	.878	.445	215500	493258	1
210	22370	.878	.747	4037	5404	4

FLUID C

TEMP. (DEG. F)	PRESS. (PSIG)	DENSITY (GM/CC)	VISCOSITY (POISE)	SHEAR STRESS (DYN/SQ.CM.)	SHEAR RATE (SEC-1)	CAPILLARY NUMBER
210	19800	.878	.610	9468	15521	2
210	19740	.878	.589	12340	20951	2
210	19770	.878	.565	14360	25416	2
210	19740	.878	.545	17150	31468	2
210	19710	.878	.507	24600	48521	2
210	19680	.878	.466	39790	85386	2
210	19750	.878	.463	93250	201404	1
210	19750	.878	.443	128800	290745	1
210	19940	.878	.451	167100	370510	1
210	50840	.935	5.320	24260	4560	2
210	51330	.935	3.870	1039000	268475	1
210	51660	.935	5.770	24480	4243	4
210	51820	.935	5.450	28060	5149	4
210	50840	.935	5.140	28600	5564	2
210	50840	.935	5.160	35600	6899	2
210	50840	.935	5.020	42340	8434	2
210	51000	.935	4.820	54570	11322	2
210	50840	.935	4.790	67160	14021	2
210	50840	.935	4.720	107200	22712	2
210	50690	.935	4.030	195100	48412	1
210	51010	.935	3.960	629100	158864	1
210	50530	.935	3.950	925400	234278	1
300	10970	.825	.145	356	2455	4
300	11610	.825	.100	37770	377700	4
300	11250	.825	.144	1103	7660	4
300	11210	.825	.128	3167	24742	4
300	11130	.825	.111	12190	109820	4
300	10690	.825	.106	19590	184811	4
300	11590	.825	.102	30000	294118	4
300	19500	.857	.245	1910	7796	4
300	20000	.857	.190	15570	81947	4
300	19750	.857	.188	23560	125319	4
300	19750	.857	.195	29380	150667	4
300	19750	.857	.187	34350	183690	4
300	50530	.917	1.280	5889	4601	4
300	50370	.917	.925	56340	60908	4
300	49100	.917	1.260	6048	4800	4
300	50210	.917	1.100	19700	17909	4
300	50370	.917	1.100	40920	37200	4
300	50580	.917	1.000	47040	47040	4

FLUID C

TEMP. (DEG. F)	PRESS. (PSIG)	DENSITY (GM/CC)	VISCOSITY (POISE)	SHEAR STRESS (DYN/SQ.CM.)	SHEAR RATE (SEC-1)	CAPILLARY NUMBER
300	59450	.949	2.200	4973	2260	4
300	59850	.949	2.160	24340	11269	4
300	59930	.949	1.990	9872	4961	4
300	59610	.949	1.950	15650	8026	4
300	0	.777	.055	0	0	100

FLUID D

TEMP. (DEG. F)	PRESS. (PSIG)	DENSITY (GM/CC)	VISCOSITY (POISE)	SHEAR STRESS (DYN/SQ.CM.)	SHEAR RATE (SEC-1)	CAPILLARY NUMBER
100	0	.849	1.570	0	0	300
100	0	.849	.746	438000	587131	12
100	0	.849	1.540	3440	2234	3
100	0	.849	1.490	9050	6074	2
100	0	.849	1.320	17200	13030	3
100	0	.849	1.140	68800	60351	2
100	0	.849	1.010	126000	124752	12
100	0	.849	.883	240000	271801	12
100	0	.849	1.180	145000	122881	1
100	0	.849	.985	170000	172589	2
100	0	.849	1.040	283000	272115	1
100	0	.849	.909	534000	587459	1
100	10100	.882	5.580	3860	692	4
100	10140	.882	3.880	18570	4786	4
100	10180	.882	4.920	5910	1201	4
100	10140	.882	4.420	9873	2234	4
100	10140	.882	4.230	12500	2955	4
100	10140	.882	4.250	13420	3158	4
100	10140	.882	4.250	14110	3320	4
100	10100	.882	3.920	16460	4199	4
100	19750	.908	14.530	6204	427	4
100	19500	.908	12.290	32520	2646	4
100	19640	.908	13.670	11650	852	4
100	19500	.908	12.900	17850	1384	4
100	19500	.908	12.600	19060	1513	4
100	51320	.961	448	22700	51	4
100	51160	.961	269	1040000	3866	1
100	51010	.961	414	37100	90	4
100	51010	.961	414	43900	106	4
100	51000	.961	424	49240	116	2
100	50850	.961	401	75085	187	2
100	51000	.961	415	98870	238	2
100	51000	.961	424	110400	260	2
100	50610	.961	386	188400	488	2
100	50650	.961	332	285600	860	2
100	51480	.961	308	477900	1553	1
100	51240	.961	300	641500	2138	1
100	51480	.961	275	722300	2627	1
100	51160	.961	271	983500	3629	1
210	0	.809	.296	0	0	150

FLUID D

TEMP. (DEG. F)	PRESS. (PSIG)	DENSITY (GM/CC)	VISCOSITY (POISE)	SHEAR STRESS (DYN/SC.CM.)	SHEAR RATE (SEC-1)	CAPILLARY NUMBER
210	0	.809	.171	130000	760234	1
210	0	.809	.232	903	3892	4
210	0	.809	.216	3439	15921	3
210	0	.809	.212	16900	79717	2
210	0	.809	.208	38800	186538	1
210	0	.809	.182	63700	350000	2
210	0	.809	.179	88400	493855	1
210	0	.809	.172	118900	691279	2
210	10160	.849	.692	2106	3043	4
210	10060	.849	.565	7070	12513	4
210	10180	.849	.646	2721	4212	4
210	10120	.849	.632	4100	6487	4
210	10120	.849	.589	6400	10866	4
210	19870	.878	1.530	2777	1815	4
210	19570	.878	1.120	31930	28509	4
210	19810	.878	1.470	3986	2712	4
210	19810	.878	1.440	5647	3922	4
210	19720	.878	1.240	10750	8669	4
210	19660	.878	1.210	14500	11983	4
210	19530	.878	1.120	25600	22857	4
210	50060	.935	12.600	4790	380	4
210	50060	.935	9.830	37000	3764	4
210	50060	.935	11.000	10630	966	4
210	50060	.935	10.900	15600	1431	4
210	50060	.935	10.800	23360	2163	4
210	50060	.935	10.300	27900	2709	4
300	0	.777	.122	0	0	150

FLUID E

TEMP. (DEG. F)	PRESS. (PSIG)	DENSITY (GM/CC)	VISCOSITY (POISE)	SHEAR STRESS (DYN/SC.CM.)	SHEAR RATE (SEC-1)	CAPILLARY NUMBER
100	0	.849	1.240	0	0	300
100	0	.849	.616	259000	420455	12
100	0	.849	1.160	3440	2966	3
100	0	.849	.975	17200	17641	3
100	0	.849	.868	68500	78917	2
100	0	.849	.825	73750	89394	1
100	0	.849	.734	135000	183924	2
100	0	.849	.729	147500	202332	1
100	0	.849	.701	295000	420827	1
100	10090	.882	4.570	3650	799	4
100	9911	.882	3.690	35970	9748	4
100	10170	.882	4.440	4213	949	4
100	10170	.882	4.420	5405	1223	4
100	10130	.882	4.120	6823	1656	4
100	10170	.882	3.990	9781	2451	4
100	9945	.882	3.830	13080	3415	4
100	9945	.882	3.740	26160	6995	4
100	19880	.908	17.200	5044	293	4
100	20190	.908	10.300	650000	63107	1
100	19820	.908	16.600	5840	352	4
100	19820	.908	16.900	6438	381	4
100	19190	.908	15.000	12080	805	4
100	19770	.908	14.900	15080	1012	2
100	19570	.908	14.700	16550	1126	4
100	19630	.908	14.500	17120	1181	4
100	19800	.908	15.300	22500	1471	2
100	19820	.908	15.000	25100	1673	4
100	19880	.908	14.100	32600	2312	4
100	19740	.908	13.800	33880	2455	2
100	19620	.908	13.300	54270	4080	2
100	19750	.908	13.400	68210	5090	1
100	19650	.908	12.300	83740	6808	2
100	19620	.908	12.200	90420	7411	2
100	19620	.908	12.000	115700	9642	2
100	19630	.908	11.200	187200	16714	1
100	20080	.908	10.300	201800	19592	2
100	20170	.908	10.300	241800	23476	2
100	19750	.908	10.900	274200	25156	1
100	20000	.908	10.300	547700	53175	1
100	29400	.925	54.000	29780	551	2

FLUID E

TEMP. (DEG. F)	PRESS. (PSIG)	DENSITY (GM/CC)	VISCOSITY (POISE)	SHEAR STRESS (DYN/SQ.CM.)	SHEAR RATE (SEC-1)	CAPILLARY NUMBER
100	29590	.925	36.000	592000	16444	1
100	29400	.925	49.000	37210	759	2
100	29340	.925	45.600	71610	1570	2
100	29280	.925	43.300	94750	2188	2
100	29280	.925	40.100	103400	2579	2
100	29590	.925	44.400	107200	2414	1
100	29660	.925	40.300	123100	3055	1
100	29590	.925	37.100	168900	4553	1
100	29030	.925	33.500	240200	7170	2
100	29530	.925	34.400	318200	9250	1
100	29590	.925	35.700	534800	14980	1
100	39240	.943	174	15550	90	4
100	39590	.943	122	470400	3872	1
100	39240	.943	174	23910	137	4
100	39860	.943	178	57580	324	2
100	39860	.943	160	75750	474	2
100	39860	.943	161	87380	543	2
100	39740	.943	154	89550	581	1
100	39710	.943	156	105700	679	2
100	39740	.943	153	106200	694	1
100	39860	.943	143	157900	1107	2
100	39710	.943	128	218800	1716	2
100	39740	.943	120	255700	2136	1
100	39560	.943	113	278900	2459	2
100	39740	.943	116	297200	2562	1
100	50530	.961	516	105400	204	1
100	50370	.961	372	617300	1659	1
100	50370	.961	446	142500	320	1
100	49980	.961	463	143400	310	2
100	49900	.961	400	243800	610	2
100	50370	.961	389	480000	1234	1
210	0	.809	.180	0	0	150
210	0	.809	.124	36200	291935	?
210	0	.809	.153	3440	22484	3
210	0	.809	.141	18100	128369	2
210	10410	.849	.478	2309	4831	4
210	10550	.849	.414	7590	18333	4
210	10410	.849	.452	3604	7973	4
210	10410	.849	.448	5840	13036	4
210	20200	.878	1.130	2033	1799	4

FLUID E

TEMP.	PRESS.	DENSITY	VISCOSITY	SHEAR STRESS	SHEAR RATE	CAPILLARY NUMBER
(DEG. F)	(PSIG)	(GM/CC)	(POISE)	(DYN/SQ.CM.)	(SEC-1)	
210	20390	.878	.850	34860	41012	4
210	19820	.878	1.110	3641	3280	4
210	20130	.878	.991	7217	7283	4
210	20130	.878	.904	10620	11748	4
210	20130	.878	.868	11490	13237	4
210	20070	.878	.861	19920	23136	4
300	0	.777	.073	0	0	150

FLUID F

TEMP. (DEG. F)	PRESS. (PSIG)	DENSITY (GM/CC)	VISCOSITY (POISE)	SHEAR STRESS (DYN/SQ.CM.)	SHEAR RATE (SEC-1)	CAPILLARY NUMBER
100	0	.904	.217	0	0	200
210	0	.866	.032	0	0	100
300	0	.835	.014	0	0	150
100	0	.904	.229	1204	5258	4
100	0	.904	.229	8428	36803	4
100	0	.904	.238	18100	76050	2
100	10400	.936	.990	1192	1204	4
100	10440	.936	1.100	4289	3899	4
100	10730	.936	1.060	39570	37330	4
100	10730	.936	1.040	50940	48981	4
100	10240	.936	1.040	51970	49971	1
100	10320	.936	.990	11210	11323	1
100	10400	.936	.940	18820	20021	1
100	10520	.936	.950	20190	21253	1
100	20140	.960	4.640	10300	2220	4
100	20140	.960	4.680	29940	6397	4
100	19950	.960	4.490	35300	7862	4
100	20140	.960	4.310	42740	9916	1
100	19890	.960	4.280	569100	132967	1
100	20390	.960	4.080	867600	212647	1
100	19700	.960	3.920	877600	223878	1
210	0	.866	.029	3440	120280	3
210	0	.866	.029	8600	299652	3
210	0	.866	.028	17200	616487	3
210	10180	.905	.088	511	5807	4
210	11330	.905	.084	1212	14429	4
210	10140	.905	.090	4060	45111	4
210	10140	.905	.081	7982	98543	4
210	10300	.905	.085	9784	115106	4
210	10140	.905	.085	12360	145412	4
210	9949	.905	.082	15200	185366	4
210	10410	.905	.089	22620	254157	1
210	10370	.905	.087	25250	290230	1
210	20130	.933	.229	2090	9127	4
210	20060	.933	.213	5295	24859	4
210	20250	.933	.236	22310	94534	4
210	20260	.933	.223	32410	145336	1
210	19810	.933	.224	36520	163036	4
210	20230	.933	.224	55800	249107	1
210	20260	.933	.220	69660	316636	1

FLUID G

TEMP. (DEG. F)	PRESS. (PSIG)	DENSITY (GM/CC)	VISCOSITY (POISE)	SHEAR STRESS (DYN/SQ.CM.)	SHEAR RATE (SEC-1)	CAPILLARY NUMBER
100	0	.904	.798	0	0	300
100	0	.904 (.340)	.372	153000	411290	12
100	0	.904	.706	3440	4873	3
100	0	.904	.604	18100	29967	3
100	0	.904	.570	29000	50877	1
100	0	.904	.512	66800	130469	2
100	0	.904	.423	133000	314421	2
100	0	.904 (.281)	.308	246000	798701	12
100	0	.904	.493	102800	208519	1
100	0	.904	.467	192000	411135	1
100	0	.904	.410	328000	800000	1
100	10230	.936	2.740	9612	3508	2
100	10970	.936	1.620	633400	390988	1
100	10610	.936	2.760	12290	4453	4
100	10200	.936	2.480	15930	6423	2
100	10500	.936	2.750	16300	5927	4
100	10560	.936	2.770	24540	8859	4
100	10230	.936	2.340	24820	10607	2
100	10310	.936	2.050	43080	21015	2
100	10010	.936	2.170	47240	21770	1
100	10350	.936	2.020	58230	28827	2
100	10240	.936	1.980	61780	31202	2
100	10350	.936	2.020	65580	32465	2
100	10130	.936	2.030	66470	32744	1
100	10390	.936	2.010	92240	45891	2
100	10090	.936	2.020	105700	52327	1
100	10010	.936	1.840	143700	78098	1
100	10290	.936	1.850	194000	104865	1
100	10650	.936	1.740	301700	173391	1
100	10650	.936	1.730	514400	297341	1
100	20010	.960	11.600	12400	1069	4
100	19450	.960	7.610	929800	122181	1
100	19680	.960	11.150	14840	1331	2
100	20200	.960	10.500	16810	1601	4
100	20140	.960	10.500	23620	2250	1
100	19680	.960	10.500	23660	2253	2
100	19680	.960	9.840	34120	3467	2
100	19620	.960	9.250	40260	4352	2
100	19560	.960	8.790	67840	7718	2
100	19560	.960	8.900	75210	8451	2

FLUID G

TEMP. (DEG. F)	PRESS. (PSIG)	DENSITY (GM/CC)	VISCOSITY (POISE)	SHEAR STRESS (DYN/SQ.CM.)	SHEAR RATE (SEC-1)	CAPILLARY NUMBER
100	19530	.960	8.600	90460	10519	2
100	19440	.960	8.540	121600	14239	2
100	19440	.960	8.010	172600	21548	2
100	19340	.960	7.890	186400	23625	2
100	19880	.960	8.620	230500	26740	1
100	19880	.960	8.260	346200	41913	1
100	19570	.960	8.730	475500	54467	1
100	19570	.960	8.000	621200	77650	1
210	0	.866	.122	0	0	150
210	0	.866	.092	36000	392585	2
210	0	.866	.101	7200	71287	2
210	0	.866	.095	18100	189727	2
210	9950	.905	.282	4350	15426	2
210	10090	.960	.261	18440	70651	1
210	10250	.905	.300	4613	15377	4
210	9961	.905	.248	6962	28073	2
210	9945	.905	.239	9270	38787	2
210	10250	.905	.263	9943	37806	4
210	9945	.905	.236	11010	46653	2
210	10250	.905	.264	11060	41894	4
210	10370	.960	.267	13170	49326	4
210	10090	.960	.249	9228	37060	1
210	19620	.933	.685	5367	7835	2
210	19820	.933	.388	152100	392010	1
210	19620	.933	.636	9157	14398	2
210	20010	.933	.648	12460	19228	4
210	19650	.933	.590	12650	21441	2
210	19820	.933	.635	14810	23323	1
210	19620	.933	.547	19250	35192	2
210	19620	.933	.509	22760	44715	2
210	19680	.933	.481	30080	62536	2
210	19940	.933	.503	36960	73479	1
210	19880	.933	.484	49080	101405	1
210	19880	.933	.402	89730	223209	1
300	9970	.881	.131	517	3947	4
300	20390	.913	.242	15170	62686	4
300	9936	.881	.134	1007	7515	4
300	10050	.881	.127	2199	17315	4
300	10410	.881	.103	6317	61330	4
300	10410	.881	.103	7016	68117	4

FLUID G

TEMP. (DEG. F)	PRESS. (PSIG)	DENSITY (GM/CC)	VISCOSITY (POISE)	SHEAR STRESS (DYN/SQ.CM.)	SHEAR RATE (SEC-1)	CAPILLARY NUMBER
300	10410	.881	.100	16210	162100	4
300	20200	.913	.296	1907	6443	4
300	20390	.913	.296	3032	10243	4
300	0	.835	.053	0	0	150

FLUID H

TEMP. (DEG. F)	PRESS. (PSIG)	DENSITY (GM/CC)	VISCOSITY (POISE)	SHEAR STRESS (DYN/SQ.CM.)	SHEAR RATE (SEC-1)	CAPILLARY NUMBER
100	0	.836	.907	0	0	300
210	0	.796	.084	0	0	100
300	0	.736	.031	0	0	150
100	0	.836	.881	6880	7809	3
100	0	.836	.890	73750	82865	1
100	0	.836	.905	205000	226519	1
100	10220	.869	7.250	4449	614	4
100	10260	.869	6.900	6454	935	4
100	10300	.869	6.680	13650	2043	4
100	10220	.869	6.640	45830	6902	4
100	10220	.869	6.710	46290	6899	4
100	10260	.869	7.040	49000	6960	4
100	19690	.894	37.400	6725	180	4
100	19630	.894	39.900	15060	377	4
100	19500	.894	37.600	27130	722	4
100	19500	.894	39.000	35500	910	4
100	19380	.894	38.700	43070	1113	4
100	19870	.894	38.300	95000	2480	1
100	19870	.894	39.000	114800	2944	1
100	19870	.894	38.900	138000	3548	1
100	19870	.894	38.600	174400	4518	1
100	19570	.894	34.900	816100	23384	1
100	29470	.911	182	20090	111	4
100	29240	.911	188	38000	202	4
100	29280	.911	191	39210	206	4
100	29780	.911	196	51690	263	4
102	29910	.911	190	100000	526	1
102	29840	.911	181	250000	1378	1
102	29840	.911	174	340000	1954	1
102	29590	.911	160	930700	5824	1
100	39740	.930	1142	288100	252	1
100	38810	.930	1163	957000	823	1
100	39430	.930	1058	1017000	961	1
210	0	.796	.087	3340	38391	3
210	0	.796	.082	7240	88293	2
210	0	.796	.089	18100	203371	2
210	0	.796	.088	36200	411364	2
210	10220	.837	.339	4975	14676	4
210	10140	.837	.341	9843	28865	4
210	10140	.837	.333	11960	35916	4

FLUID H

TEMP. (DEG. F)	PRESS. (PSIG)	DENSITY (GM/CC)	VISCOSITY (POISE)	SHEAR STRESS (DYN/SQ.CM.)	SHEAR RATE (SEC-1)	CAPILLARY NUMBER
210	19870	.853	1.200	4170	3475	4
210	19940	.853	1.200	5178	4315	4
210	19870	.853	1.230	6490	5276	4
210	19870	.853	1.150	7459	6486	4
210	19870	.853	1.170	13160	11248	4
210	19870	.853	1.100	14700	13364	4
210	29530	.876	3.380	6295	1862	4
210	29590	.876	3.400	7505	2207	4
210	29470	.876	3.260	113600	34847	4
210	29470	.876	3.340	125300	37515	4
210	29470	.876	3.300	145800	44182	4
210	29400	.876	3.260	165400	50736	4
210	39270	.900	9.800	12800	1306	4
210	39350	.900	10.000	14700	1470	4
210	39270	.900	9.900	18060	1824	4
210	39430	.900	10.500	23800	2267	4
210	39430	.900	10.500	26360	2510	4
210	39430	.900	10.400	28620	2752	4
210	39430	.900	10.600	31800	3000	4

FLUID I

TEMP. (DEG. F)	PRESS. (PSIG)	DENSITY (GM/CC)	VISCOSITY (POISE)	SHEAR STRESS (DYN/SQ.CM.)	SHEAR RATE (SEC-1)	CAPILLARY NUMBER
100	0	.957	.792	0	0	100
210	0	.906	.306	0	0	200
300	0	.864	.157	0	0	150
100	0	.957	.832	6880	8269	3
100	0	.957	.814	14480	17789	2
100	0	.957	.800	43400	54250	2
100	0	.957	.837	49600	59259	2
100	10430	1.020	2.570	3056	1189	4
100	10390	1.020	2.520	4662	1850	4
100	10390	1.020	2.600	5704	2194	4
100	10300	1.020	2.520	7305	2899	4
100	10260	1.020	2.510	15480	6167	4
100	10220	1.020	2.380	16750	7038	4
100	10350	1.020	2.480	52130	21020	1
100	10350	1.020	2.370	96860	40869	1
100	10350	1.020	2.380	106500	44748	1
100	10350	1.020	2.280	118500	51974	1
100	20220	1.050	5.590	4005	716	4
100	20220	1.050	5.360	4365	814	4
100	20220	1.050	5.550	5330	960	4
100	20160	1.050	5.340	11240	2105	4
100	20090	1.050	5.410	15840	2928	4
100	20090	1.050	5.130	121300	23645	1
100	20090	1.050	5.180	20140	3888	1
100	20090	1.050	5.320	21890	4115	1
100	30370	1.080	12.000	114000	9500	1
100	30400	1.080	11.600	163500	14095	1
100	30240	1.080	10.600	281400	26547	1
100	30370	1.080	11.200	300100	26795	1
100	40420	1.110	26.400	5127	194	4
100	40420	1.110	25.500	9865	387	4
100	40420	1.110	25.800	12700	492	4
100	40420	1.110	26.200	16370	625	4
100	40590	1.110	26.200	27560	1052	4
100	40130	1.110	25.200	147200	5841	1
100	40130	1.110	23.500	152500	6489	1
100	40130	1.110	23.400	320000	13675	1
100	51350	1.140	58.300	166600	2858	1
100	51510	1.140	61.300	215900	3522	1
100	51350	1.140	59.000	265500	4500	1

FLUID I

TEMP. (DEG. F)	PRESS. (PSIG)	DENSITY (GM/CC)	VISCOSITY (POISE)	SHEAR STRESS (DYN/SQ.CM.)	SHEAR RATE (SEC-1)	CAPILLARY NUMBER
100	51350	1.140	57.200	314900	5505	1
100	59970	1.160	124	170900	1380	1
100	59810	1.160	112	271300	2429	1
100	59730	1.160	108	361600	3348	1
100	59650	1.160	116	369600	3197	1
100	71370	1.180	371	206100	556	1
100	71370	1.180	368	259800	705	1
100	71200	1.180	375	520800	1389	1
100	71370	1.180	365	705000	1929	1
100	81430	1.200	992	298200	301	1
100	81270	1.200	949	380200	401	1
100	81430	1.200	965	418900	434	1
210	0	.906	.312	18100	58013	2
210	0	.906	.288	36200	125694	2
210	0	.906	.312	54000	173077	2
210	10430	.976	1.020	2238	2194	4
210	10470	.976	1.080	4004	3707	4
210	10470	.976	1.050	4435	4224	4
210	10470	.976	1.000	5169	5169	4
210	10550	.976	.980	10670	10888	4
210	10510	.976	.940	14320	15234	4
210	20290	1.020	2.130	3992	1874	4
210	20290	1.020	2.090	6105	2921	4
210	20290	1.020	2.000	17190	8595	4
210	20290	1.020	1.950	17600	9026	4
210	20350	1.020	1.870	19580	10471	4
210	51350	1.110	11.600	10070	868	4
210	51350	1.110	11.600	15350	1323	4
210	51350	1.110	11.700	18220	1557	4
210	51190	1.110	11.600	37510	3234	4
210	51190	1.110	11.800	38730	3282	4
210	51350	1.110	12.100	40190	3321	4
210	71600	1.160	33.400	6909	207	4
210	71430	1.160	32.400	11770	363	4
210	71430	1.160	30.700	12460	406	4
210	71430	1.160	32.500	21110	650	4

FLUID J

TEMP. (DEG. F)	PRESS. (PSIG)	DENSITY (GM/CC)	VISCOSITY (POISE)	SHEAR STRESS (DYN/SQ.CM.)	SHEAR RATE (SEC-1)	CAPILLARY NUMBER
100	0	1.230	.950	0	0	300
210	0	1.170	.169	0	0	150
100	0	1.230	.968	3440	3554	3
100	0	1.230	.998	8600	8617	3
100	0	1.230	1.040	36200	34808	2
100	0	1.230	1.060	5400	5094	2
100	0	1.230	1.020	71800	70392	2
100	10360	1.290	4.460	5870	1316	4
100	10340	1.290	4.370	6600	1510	4
100	10160	1.290	4.290	9604	2239	4
100	10160	1.290	4.220	9844	2333	4
100	10320	1.290	4.100	9952	2427	4
100	9962	1.290	4.100	13730	3349	4
100	10120	1.290	4.270	19020	4454	4
100	10430	1.290	4.630	38560	8328	1
100	10470	1.290	4.510	53360	11831	1
100	10470	1.290	4.430	86300	19481	1
100	10470	1.290	4.220	100500	23815	1
100	20080	1.330	16.500	4524	274	4
100	20080	1.330	16.700	5700	341	4
100	20170	1.330	16.400	27350	1668	4
100	20210	1.330	17.200	36760	2137	4
100	20220	1.330	15.200	54750	3602	1
100	20280	1.330	16.000	86800	5425	1
100	20220	1.330	15.400	117100	7604	1
100	19710	1.330	15.400	152000	9870	1
100	20410	1.330	14.500	253900	17510	1
100	20380	1.330	14.400	316500	21979	1
100	20350	1.330	14.100	400000	28369	1
100	30010	1.360	53.800	10170	189	4
100	30070	1.360	52.600	13540	257	4
100	29940	1.360	51.700	17080	330	4
100	29940	1.360	52.600	18770	357	4
100	30560	1.360	55.700	116000	2083	1
100	30500	1.360	50.400	153900	3054	1
100	30460	1.360	49.300	242000	4909	1
100	30430	1.360	52.800	354800	6720	1
100	40290	1.380	182	314300	1727	1
100	40130	1.380	182	364900	2005	1
100	40210	1.380	178	39600	222	1

FLUID J

TEMP. (DEG. F)	PRESS. (PSIG)	DENSITY (GM/CC)	VISCOSITY (POISE)	SHEAR STRESS (DYN/SQ.CM.)	SHEAR RATE (SEC-1)	CAPILLARY NUMBER
100	40290	1.380	180	442600	2459	1
100	40290	1.380	184	722300	3926	1
100	40130	1.380	176	107700	612	1
100	51190	1.410	720	267700	372	1
100	51350	1.410	722	310400	430	1
210	0	1.170	.173	3440	19884	3
210	0	1.170	.157	8600	54777	3
210	10390	1.260	.686	4075	5940	4
210	10350	1.260	.691	6040	8741	4
210	10430	1.260	.675	10020	14844	4
210	10430	1.260	.648	13100	20216	4
210	20730	1.290	1.840	4066	2210	4
210	20480	1.290	1.690	5866	3471	4
210	20800	1.290	1.720	12730	7401	4
210	20730	1.290	1.750	12900	7371	4
210	30240	1.320	3.560	9806	2754	4
210	30240	1.320	3.650	13250	3630	4
210	30270	1.320	3.640	15240	4187	4
210	40260	1.360	8.900	21940	2465	4
210	40260	1.360	8.820	22200	2517	4
210	40780	1.360	8.890	26100	2936	4
210	40940	1.360	8.860	29820	3366	4
210	40780	1.360	8.730	31070	3559	4
210	51350	1.390	18.200	11840	651	4
210	51350	1.390	18.100	12100	669	4
210	51680	1.390	18.100	14520	802	4
210	51510	1.390	19.000	24840	1307	4
210	51510	1.390	19.000	32740	1723	4
210	62120	1.410	37.000	11000	297	4
210	62120	1.410	38.100	12030	316	4
210	62120	1.410	36.900	27340	741	4

CHAPTER V

CONCLUSIONS AND RECOMMENDATIONS

The conclusions and recommendations are presented in two sections. The first section considers the experimental equipment while the second considers fluid behavior. Both of these sections summarize the discussion in previous chapters and then recommendations are made concerning future work.

A. Experimental Equipment

A unique two-way high pressure capillary viscometer was proven to produce accurate viscosity measurements at pressures from 10,000 to 80,000 psig, temperatures from 100 to 300°F, and over a shear stress range from 300 to 1.2×10^6 dynes/cm^2. The system accuracy was verified by comparing measured low shear viscosity-pressure data with previously reported data on a chemically well defined fluid (bis-2-ethyl hexyl sebacate). The two sets of viscosity data differed by less than 2 percent. As a result of this research, a useful system has been developed which can measure viscosities from 1.0 to 100,000 centipoise.

The equipment is designed for a maximum pressure of 100,000 psi and is presently capable of producing viscosity measurements at this pressure provided the viscosity is less than 100,000 centipoise at this pressure and room temperature. Higher viscosities could be measured if the system is modified such that shear rates less than 100 sec^{-1} could be measured. The minimum measurable shear rate could be reduced if the period of steady flow through the capillary could be increased by increasing the duration of constant pressure in the low pressure hydraulic

system. In order to achieve long constant pressure periods (greater than thirty seconds) in the hydraulic system, some mechanical system should replace the present hand-actuated pumps.

The temperature of the experimental fluid in the capillary section can presently be varied from approximately -50 to 450°F. The temperature of the fluid in the high pressure reservoirs, however, cannot be adequately controlled at this time. This inability led to premature gelation of the petroleum oils examined. As a result, the maximum pressure was limited to 50,000 psig for the paraffinic based fluids and to 20,000 psig for the naphthenic based fluids. Since gelation occurs when some constituents in the fluid solidify at certain combinations of temperature and pressure, it can be prevented by controlling the temperature of the experimental fluid outside the constant temperature bath. An attempt was made to prevent gelation by heating the appropriate sections with electrical heaters. This effort was unsuccessful because of inadequate instrumentation. An automatic temperature sensing and control system could be designed which would solve the gelation problem.

Considerable effort was expended in an unsuccessful attempt to evaluate the elastic energy stored in the petroleum oils at elevated pressures. The two major reasons for the inability to obtain the necessary data were (1) equipment limitations and (2) the small magnitude of the elastic energy.* In order to evaluate the elastic energy (recoverable shear strain) it is necessary to obtain constant shear rate viscosity data from capillaries with different length-to-diameter ratios.

---

* The existing system is capable of measuring large elastic energies, $S_r > 5.0$, at elevated pressures.

Even though constant shear rate data are required, the experimental shear stress range for each capillary is the limiting factor. Thus the maximum shear stress obtainable for the longer of the two capillaries must be increased, and similarly, the minimum shear stress obtainable for the shorter capillary must be decreased. The corrected shear stress at the capillary wall, τ_{corr}, as defined by Equation (14) in Chapter II is

$$\tau_{corr} = \frac{\Delta P - KEC}{4\ L/D} \qquad (14)$$

where ΔP is the measured pressure differential across the capillary, KEC is the kinetic energy correction, and L/D is the capillary length-to-diameter ratio. Since the maximum ΔP is used when the maximum shear stress is sought, the only way to increase the shear stress is to use a capillary with a smaller length-to-diameter ratio. Thus the maximum shear stress for the longer of the two capillaries can only be increased by using a capillary with a smaller length-to-diameter ratio than the one previously employed. The minimum measurable shear stress for the shorter capillary can be decreased by either decreasing the minimum measurable pressure differential or by increasing the capillary length-to-diameter ratio. This latter suggestion is not desireable because it is advantageous to use capillaries with as large a difference in their length-to-diameter ratios as possible. Thus decreasing the minimum measurable shear stress is the best method. This decrease can be achieved if the sensitivity of the differential pressure measurements is increased by increasing the amplifier gain settings or by increasing the differential pressure transducer excitation voltages from six to

twelve, or even twenty-four, volts. Therefore, by using capillaries with length-to-diameter ratios of 25 and 11, instead of the ratios of 50 and 11 used in this work, and by also increasing the sensitivity of the differential pressure measurements, it should be possible to evaluate the recoverable shear strain at elevated pressures in the fluids examined.

The noise level in the differential pressure transducers was acceptable but could possibly have been reduced further. The following three measures may or may not accomplish the desired results:

1. twist all pairs of wires where possible,
2. obtain a better ground,
3. ground cable shields, avoiding ground loops.

This first item may reduce the noise level because twisting pairs of wires tends to cancel the induced voltages. The existing common electrical ground in the laboratory is sufficient from a safety viewpoint, but inadequate for noise suppression. Therefore, a ground point as close as possible to the equipment should reduce the noise level by significantly reducing the path resistance from the equipment to ground. All the transducer cables are shielded but the shields are not grounded. Grounding the shields should also reduce the noise level, <u>if done properly</u>. The major difficulty in achieving noise reduction via this method is the very high probability of ground-loops which may <u>increase</u> the noise level. The major objective in grounding the complete system is to start from a common ground and work radially outward.

B. Fluid Behavior

The viscosity of ten well defined fluids was measured in a capillary-type viscometer at pressures up to 80,000 psig, temperatures of 100, 210, and 300°F and shear stresses from 300 to 1.2×10^6 dynes/cm^2. In addition to the fluid used to verify the accuracy of the system, the nine additional fluids were: (1) a paraffinic base oil (A), (2) A plus four percent polyalkylmethacrylate (5.6×10^5 weight average molecular weight), (3) A plus eight percent polyalkylmethacrylate, (4) A plus four percent polytertiarybutylstyrene (3.9×10^5 weight average molecular weight), (5) Naphthenic base oil (B), (6) B plus four percent polyalkylmethacrylate, (7) polybutene (409 Number average molecular weight), (8) dimethylsiloxane (82.6 cp. at 100°F), and (9) trifluoropropylmethylsiloxane (81.3 cs. at 100°F). Data correlation and presentation techniques were also investigated in order to facilitate comprehension of the significant trends and interrelations among the fluids examined.

The experimental data indicate the following general trends:

1. The flow curves show that the basic behavior of a fluid is not affected by temperature or pressure unless gelation occurs. Six of the fluids exhibit a Newtonian behavior at all temperatures and pressures examined. The other four fluids are non-Newtonian at all temperatures and pressures.

2. Straight line relations are obtained on the ASTM viscosity-temperature charts for all fluids when pressure and shear stress are constant.

3. The viscosity-pressure relations for the silicones are basically different than the viscosity-pressure relations of the other fluids examined. The viscosity-pressure curves for the silicones possess inflection points while similar curves for the other fluids do not.

4. The flow curves for the non-Newtonian fluids show that the viscosity is constant in a low shear stress range (initial Newtonian region) and then begins to decrease with increasing shear stress. The shear stress value at which this temporary viscosity loss begins seems to be independent of pressure and temperature. This temporary viscosity loss also seems to begin near a line of constant energy input, i.e. a line of constant shear-stress shear-rate product. No permanent viscosity loss was observed in these fluids.

The various amounts of polyalkylmethacrylate (PAMA) added to the paraffinic base oil resulted in the following effects being observed.

1. The slopes of the viscosity-pressure curves (or viscosity-pressure coefficient*, α) decreased with polymer content at atmospheric pressure while they increased with polymer content at 50,000 psig. Thus the viscosity-pressure curves approached straight lines with increasing polymer content.

2. The viscosity of the polymer blends decreased less with increasing temperature than the viscosity of the base oil.

3. The elastic energy stored in the fluids at high shear stress increased with polymer content. A measure of the elastic energy is the recoverable shear strain which was negligible, or nonexistent,

---

* $\alpha \equiv \frac{1}{\mu} \left.\frac{\partial \mu}{\partial P}\right|_T$

for the base oils at atmospheric pressure, 100°F, and the shear stress range examined. For the same temperature and pressure, the recoverable shear strain was also negligible for the polymer blends at shear stresses less than 10^5 dynes/cm^2. However, the recoverable shear strain was measurable in the polymer blends for higher shear stresses. The four percent PAMA blend had a recoverable shear strain of 7.2 at a shear stress of 3.0×10^5 dynes/cm^2 and a shear rate of 7.6×10^5 sec^{-1}, while the corresponding value for the eight percent PAMA blend was 10.1 at a shear stress of 4.4×10^5 dynes/cm^2 and a shear rate of 5.9×10^5 sec^{-1}. It is not possible to evaluate the recoverable shear strain at elevated pressures with the existing data. But these high pressure data do indicate that the recoverable shear strain is negligible (i.e. $S_r < 4$) at shear stresses less than 10^5 dynes/cm^2.

4. Some of the constituents in these paraffinic based fluids solidified at room temperature and pressures above 50,000 psig and thus gelation prevented viscosity measurements above this pressure.

The following differences were noted between the data for the paraffinic base oil blended with four percent polyalkylmethacrylate (PAMA) and the data for the same base oil blended with four percent polyalkylstyrene (PAS).

1. The slopes of the viscosity-temperature and the viscosity-pressure curves for the four percent PAS blend are greater than the corresponding slopes for the four percent PAMA blend.

2. The recoverable shear strain is 6.5 for both the PAS and the PAMA blends at atmospheric pressure, 100°F and a shear stress of 2.6×10^5 dynes/cm^2.

3. Gelation also occurred in these fluids at room temperature and pressures above 50,000 psig thus limiting the viscosity measurements to pressures of 50,000 psig or lower.

A comparison of the data for the paraffinic and naphthenic base oils and the data for these oils blended with four percent polyalkylmethacrylate (PAMA) indicates the following trends.

1. Gelation of the naphthenic based fluids occurs at pressures greater than 20,000 psig at room temperature while gelation does not occur in the paraffinic based fluids at room temperature until the pressure exceeds 50,000 psig.

2. At atmospheric pressure, the viscosity of the naphthenic based fluids is less than the viscosity of the corresponding paraffinic based fluids and the viscosity of the former also decreases more with temperature than the corresponding paraffinic based fluids.

3. The viscosity-pressure coefficients for the naphthenic based fluids are greater than their paraffinic based counterparts.

4. The recoverable shear strain is greater for the naphthenic blend (15.5 at a shear stress of 2.5×10^5 dynes/cm^2) than for the paraffinic blend (7.2 at 3.0×10^5 dynes/cm^2).

The experimental data for the four synthetic fluids indicate the following behavior.

1. Gelation did not occur in any of these fluids and therefore the maximum pressure at which viscosity measurements were made was limited by the smallest measurable shear rate.

2. The diester (bis-2-ethyl hexyl sebacate) has the lowest viscosity-pressure coefficient of the ten fluids examined while the polybutene has the largest viscosity-pressure coefficient.

3. The polybutene also has the largest viscosity-temperature coefficient*, VTC, of the ten fluids and therefore has the largest change in viscosity with temperature.

4. The dimethylsiloxane has the smallest viscosity-temperature coefficient and hence the smallest change in viscosity with temperature.

5. The viscosity-pressure curves for the two siloxane fluids are basically different than similar curves for the other eight fluids because the curves for these two fluids possess inflection points while similar curves for the other eight fluids do not.

The viscosity data for the Newtonian fluids can be adequately presented by constant temperature lines on viscosity-pressure curves. The viscosity data for the non-Newtonian fluids cannot be adequately presented on a single curve.

The analytical correlation methods surveyed for Newtonian fluids were unsatisfactory because they were either difficult to employ or were only applicable to relatively low pressure data. The generalized non-Newtonian technique as presented by Wright[30] was shown to be applicable to high pressure viscosity data but it could not be generalized to include the effects of temperature and pressure. The reduced variables technique presented by Philippoff[14] could not be successfully applied to the data obtained in this research.

The high pressure data for the petroleum oil-polymer blends examined indicate that the temporary viscosity loss is not large for the shear stress range investigated. The polymers used in this research were in the relatively low to medium molecular weight range. Therefore,

---

* $VTC \equiv (1 - \mu_{210}/\mu_{100})_P$

if subsequent data prove that the elastic energy is not large at shear stresses outside the range examined, there is a possibility that it may be more desirable to use a larger quantity of low molecular weight polymer to obtain a given low shear reference viscosity than to use a smaller quantity of high molecular weight polymer.

APPENDIX A

FLUID DESCRIPTIONS

The following table summarizes the experimental fluids used in this research. The remaining pages in this appendix contain the descriptive data supplied with the fluids.

EXPERIMENTAL FLUIDS

Letter	Description
A	Diester-Plexol 201 bis-2-ethyl hexyl sebacate
B	Paraffinic Base Oil R-620-12
C	B + 4% polyalkylmethacrylate
D	B + 8% polyalkylmethacrylate
E	B + 4% polyalkylstyrene
F	Naphthenic Base Oil R-620-15
G	F + 4% polyalkylmethacrylate
H	Polybutene LF-5193
I	Dimethylsiloxane
J	Trifluoropropylmethylsiloxane

FLUID CHARACTERIZATION

Symbol: A

Type: bis-2-ethyl hexyl sebacate

Source: Rohm and Haas Company

Property	
Viscosity at 210°F, cs	3.32
Viscosity at 100°F, cs	12.75
Viscosity at -65°F, cs	7988
Viscosity Index (ASTM D-974)	150
Neutralization Number (ASTM D-974)	0.02
Cloud Point (ASTM D-2500)°F	below -65

Symbol: B and F

Types: Paraffinic (B) and Naphthenic (F) Base Oils

Source: Sun Oil Company

Fluid	B	F
Viscosity at 100°F (cs)	33.33	24.06
Viscosity at 210°F(cs)	5.336	3.728
SUS/100	156.2	115.2
SUS/210	43.74	38.59
Viscosity Index (ASTM D-2270)	102	-13
Flash Point (°F)	410	315
Fire Point (°F)	470	365
Pour Point (°F)	5	-45
Refractive Index	1.4754	1.5085
Density at 68°F (gm/cc)	.8596	.9157
Molecular Weight [1]	401	305
Percentage of Carbon atoms in aromatic rings[2]	4.0	21.5
Percentage of Carbon atoms in naphthenic rings[2]	28.0	36.0
Percentage of Carbon atoms in paraffinic rings[2]	68.0	42.5
Percentage of Carbon atoms in aromatic rings[3]	4.0	20.3
Percentage of Carbon atoms in naphthenic rings[3]	27.4	34.5
Percentage of Carbon atoms in paraffinic rings[3]	68.8	45.2
Average number of aromatic rings per molecule[3]	0.20	0.77
Average number of naphthenic rings per molecule[3]	1.59	1.74
Average number of total rings per molecule[3]	1.79	2.51

[1] Calculated from viscosity data using the method of A. E. Hirschler, J. Inst. Petroleum, 32, 133-61, 1946.

[2] Obtained using the Viscosity-Gravity Constant and the Refractivity Intercept using the method of S.S. Kurtz, Jr., R.W.King, W.J. Stout, and D.J. Gilbert, from a paper, "Relationship between Carbon Type Composition Viscosity-Gravity Constant and Refractivity Intercept", presented before the Petroleum Div., ACS, Sept., 1955.

3 Calculated using the n-d-M method of structural group analysis of of mineral oil fractions of Van Nes and Van Westen, "Aspects of the Constitution of Mineral Oils", Elsevier Publishing Co., Inc. 1951.

Symbol: (None; used as additive in C, D, G)

Type: Polyalkylmethacrylate

Source: Rohm and Haas Company

The polymer had a viscosity average molecular weight of 560,000 and was in solution with a paraffinic hydrocarbon very similar to fluid B in this investigation. The solution contained 36.1 percent polymer and had a viscosity of 796 cs at 210°F. The percent additive reported in Table III (i.e. 4 or 8%) was the percent polymer in the final solution.

Symbol: (None; used as additive in E)

Type: Polytertiarybutylstyrene

Source: Dow Chemical Company

The polymer had a weight average molecular weight of 375,000 as determined by an ultracentrifuge method. The polymer was supplied in solution with a paraffinic hydrocarbon similar to Fluid B. The solution contained 25% polymer. Fluid E contained 4% polytertiarybutylstyrene polymer.

Symbol: H

Type: Polybutene

Source: American Oil Company

Figure A1 shows the molecular weight distribution of this fluid as determined by a gel-permeation chromatograph.

Viscosity:	0°F, cs/SSU	18836/86740
	100°F, cs/SSU	109/505
	210°F, cs/SSU	10.6/61.6
Viscosity Index (ASTM D-2270)		87
Flash Point, COC, °F		300
Unsaturation by Hydrogenation, %		91
Density at 25°C, gm/cc.		0.8443
Molecular Weight (No. average).		409

Symbol: I and J

Types: Dimethylsiloxane (I) and Trifluoropropylmethylsiloxane (J)

Source: Dow Corning Corporation

Fluid		I	J
Viscosity:	100°F, cs	82.6	81.3
	210°F, cs	33.1	14.3
Flash Point, °F		575	500
Freeze Point, °F		-67	-55
Density at 25°C, gm/cc		0.968	1.23
Molecular Weight		7000	4000

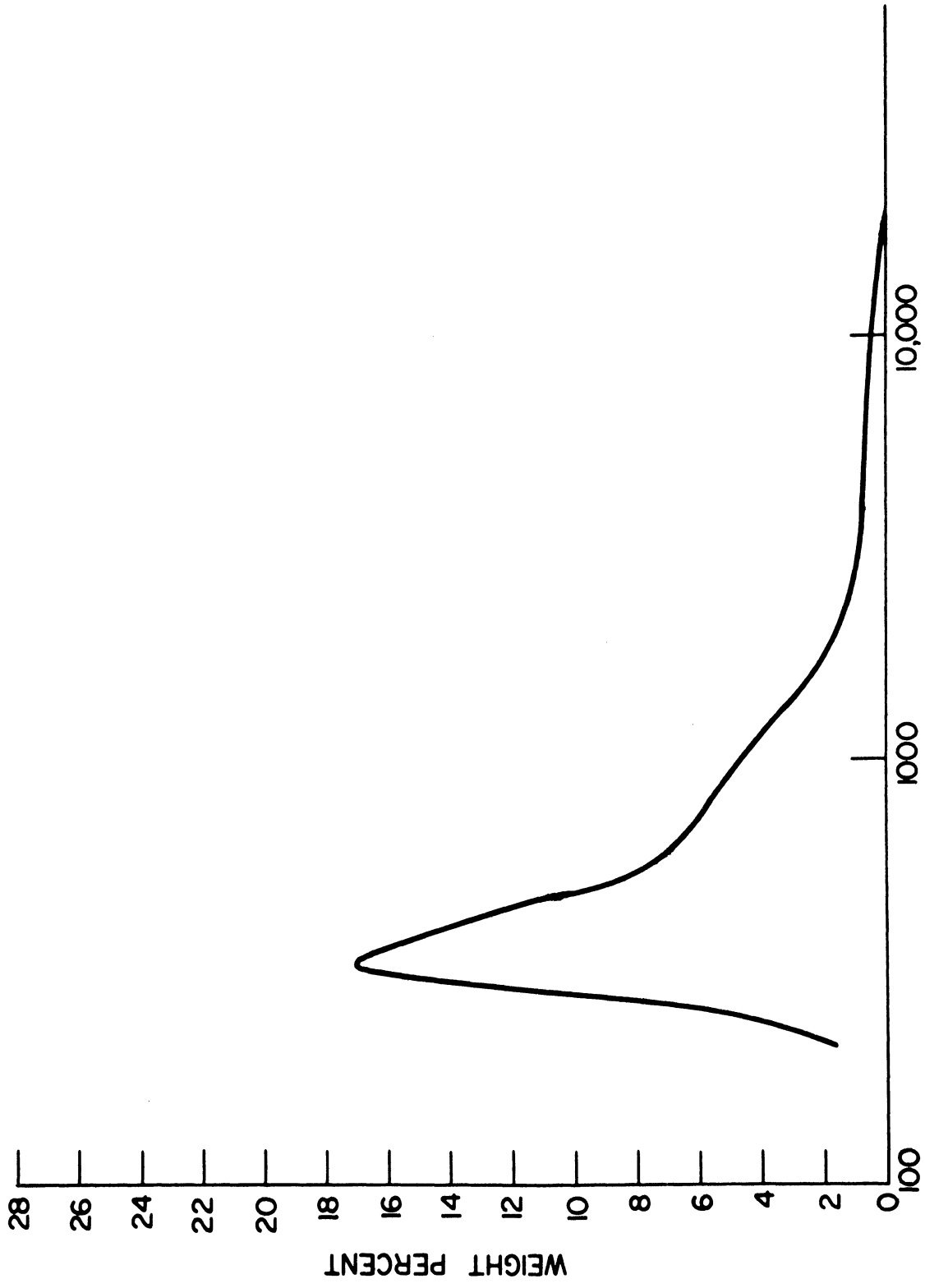

Figure A1. Molecular Weight Distribution for Fluid H.

APPENDIX B

EXPERIMENTAL EQUIPMENT

B.1 Operating Procedure

The following list briefly outlines the steps necessary to operate the high pressure viscometer and associated electronics used in this research. Explanations of the steps follow when necessary.

Operating Procedure Check List

I. Clean and Fill Viscometer Test Section and Reservoirs

II. Calibration

A. Pressure Level Transducer (at atmospheric pressure)

1. Excite transducer and turn on galvanometer No. 3.
2. Null output signal by balancing wheatstone bridge circuit.
3. Select sensitivity and calibration switch positions.
4. Record zero position.
5. Push red calibration button and record calibration signal (Table B3).

B. Differential Pressure Transducers (at each elevated pressure level)

1. Excite transducers and null output signals by balancing wheatstone bridge circuits.
2. Select sensitivity and calibration switch positions.
3. Turn on galvanometers No. 1 and No. 2.
4. Record zero position.
5. Push red calibration buttons and record calibration signal (Table B2).

C. Displacement Transducer

Step II A. automatically calibrates this transducer.

III. Data Acquisition

A. Obtaining Pressure Level

1. Turn off galvanometers No. 1 and No. 2 and battary excitation switches for the differential pressure transducers.

2. Increase static pressure to desired level with by-pass level open.

B. Viscosity Data

1. Set visicorder timing switch to desired position and select visicorder paper speed.

2. Set displacement transducer sensitivity switch (SS4) to desired position and set galvanometer No. 4 signal at a convenient position by adjusting micrometer head.

3. Close by-pass valve.

4. Excite differential pressure transducer No. 1 and null output as before.

5. Repeat step 4 for pressure transducer No. 2.

6. Turn on visicorder paper drive.

7. Record zero position of pressure transducer No. 3 by temporarily pushing the black zero button.

8. Move traversing piston.

C. Reset procedure

1. Turn off paper drive and galvanometers No. 1 and No. 2.

2. Open by-pass valve until the deviation amplifiers are almost saturated.

3. Reposition galvanometer No. 4 (displacement signal).

4. Repeat steps B3 through B8.

The preceeding list shows that there are only two basic steps in using the existing electronic control box. The first step is calibration of the transducers and the second is adjustment of the transducer outputs at elevated pressures to obtain data.

Calibration is accomplished in two parts. The first part calibrates the pressure level transducer as well as the displacement transducer and the second part calibrates the differential pressure transducers. The first part, which determines the voltage of the battery used to excite both the pressure level transducer (No. 3) and the displacement transducer, is accomplished by nulling the output signal from the pressure level transducer at atmospheric pressure. Next the sensitivity and calibration switches (SS3 and CS3) are set at the desired positions. Finally the zero position and calibration signal are recorded. These latter signals are obtained by pushing the red calibration button for pressure transducer No. 3. The second part of the calibration procedure determines the coefficients for the differential pressure transducers which are a function of the amplifier gain settings and the excitation battery voltages. This calibration procedure is identical to that for the calibration of the pressure level transducer except that it should be followed at each pressure level to insure that the gain of the amplifiers has not changed with time.

The positions of the sensitivity switches, (SS1 and SS3), the positions calibration switches, (CS1 and CS3), and the calibration signals (deflections of galvanometers No. 1, 2 and 3) are used as input data to the data reduction computer program (See appendix C1).

The data reduction computer program is written such that there is no need to calibrate any of the pressure transducers at more than one position of the sensitivity switch. The program only needs the displacement transducer excitation voltage and output signal in order to calculate the translating piston displacement. Since the voltage of the battery

which excites both the pressure level transducer and the displacement transducer is determined in the pressure level calibration, there is no need to calibrate the displacement transducer.

Once the calibration data has been obtained, the collection of viscosity data can begin. It is important to turn off galvanometers No. 1 and No. 2 before the pressure level is increased because of their extreme sensitivity. Permanent damage to the galvanometers may result if this step is omitted. The excitation voltage to pressure transducers No. 1 and No. 2 should also be removed before the pressure level is increased, otherwise the amplifiers will become saturated.

The pressure level should be set at a value slightly less than desired because the pressure will increase when the by-pass valve is closed. The rest of the operating procedure is straight-forward and only one step requires additional comments. The translating piston is moved in step B8. This motion should be made in such a manner that the pressure drop (galvanometer signals No. 1 and No. 2) across the capillary remain constant. Care must be exercised not to saturate the deviation amplifiers when a large pressure drop is sought.

B.2 Instrumentation

B.2.a Measurement Error

The error analysis section, (Chapter III, Section E), discussed the major possible error in the measurement of the galvanometer signals. In this section other less important error sources are discussed as well as the accuracy of the pressure transducer calibration data and the accuracy of the calibration constants.

The measurement of the transducer signals were made from the edges of the galvanometer traces. This method eliminated the necessity of accurately locating the center of the 0.050 inch wide trace. Other possible errors inherent in this method were (1) measurements made from opposite edges of the galvanometer trace, and (2) measurements made from the wrong reference line. These minor errors were obviously eliminated by exercising sufficient care.

The position of the reference lines for the differential pressure signals could be affected by variations in the amplifier characteristics. The amplifier gain and zero drift were the two characteristics which had to be closely watched. The gain was checked by recalibrating the amplifier signals after every series of runs at a given pressure level. The zero drift was minimized by allowing at least one hour warm up time and only using short time intervals for data collection.

The following discussion of the equivalent pressure values for the calibration resistors assumes that the pressures produced by the Ruska Model 2400 dead weight gage were exact. This assumption is acceptable because, as mentioned in Chapter III, the possible error in the pressure, approximately 0.2 psi, could not be accurately detected by the existing instrumentation at normal gain settings.

With the above assumption, the equivalent pressure values for the calibration resistors were evaluated and recorded in Table B2 of the next section. The accuracy of these values only depended upon the accuracy of the galvanometer displacement measurement. From Figure B1 it is seen that the equivalent pressure, P_{eq} , is:

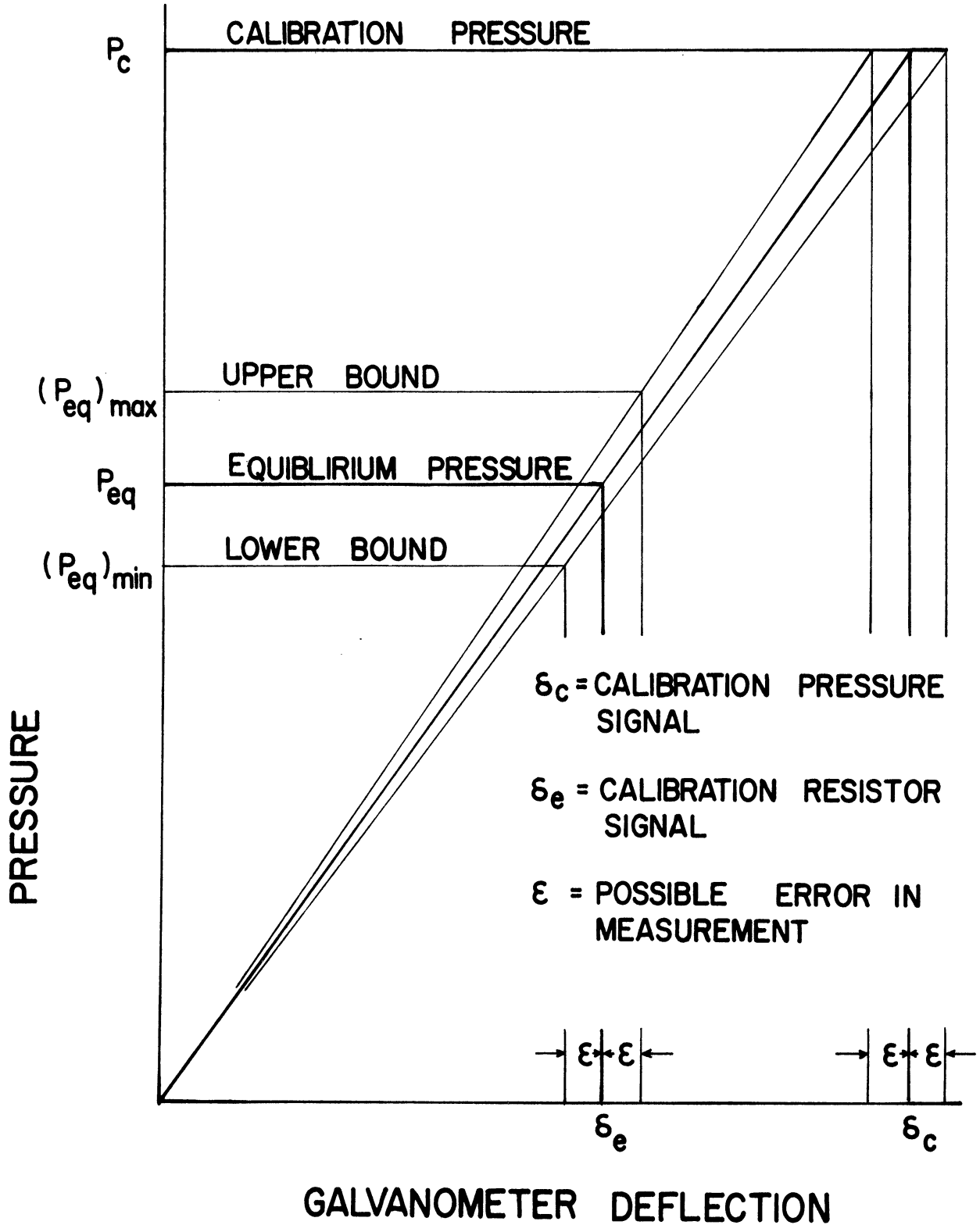

Figure B1. Typical Pressure Transducer Calibration Curve.

$$P_{eq} = P_c \frac{(\delta_e)}{(\delta_c)} \quad ,$$

$$(P_{eq})_{max} = P_c \frac{(\delta_e+\epsilon)}{(\delta_c-\epsilon)} \quad ,$$

and

$$(P_{eq})_{min} = P_c \frac{(\delta_e-\epsilon)}{(\delta_c+\epsilon)} \quad ,$$

where $(P_{eq})_{max}$ = upper bound of P_{eq} ,

$(P_{eq})_{min}$ = lower bound of P_{eq} ,

P_c = calibration pressure, (psi),

δ_c = galvanometer signal produced by P_c , (inches),

δ_e = galvanometer signal produced by the calibration resistor, (inches), and

ϵ = possible error in any displacement measurement, (inches).

Thus it can be shown that the true equivalent pressure is less than

$$100 \frac{\epsilon[1 + \delta_e/\delta_c]}{(\delta_e/\delta_c)(1 - \epsilon/\delta_c)} \quad \%$$

above P_{eq} and less than

$$100 \frac{\epsilon[1 + \delta_e/\delta_c]}{(\delta_e/\delta_c)(1 + \epsilon/\delta_c)} \quad \%$$

below P_{eq}. Table B1 shows that the possible error in the equivalent pressure values for all pressure transducers is less than one percent.

It should be noted that the estimated possible error of the displacement measurements was 0.01 inch instead of the 0.02 inch value mentioned previously. The reason for the increased accuracy is that ϵ = 0.02 inch is a maximum estimated value for normal data acquisition. For the calibration measurements however, the reference points were constantly checked, thus eliminating one possible source of error.

TABLE B1

PRESSURE TRANSDUCER CALIBRATION DATA

Pressure Transducer	No. 1	No. 2	No. 3
Transducer Function	Differential Pressure		Pressure Level
Sensitivity Switch Position Calibration Switch Position	4 3	4 3	4 5
Calibration Resistor* (ohms) Calibration Pressure, P_c (psi)	20 M 150.0**	20 M 150.0**	75 K 12,000
Calibration Pressure Signal, δ_c (inch) Calibration Resistor Signal, δ_e (inch)	3.72 1.33	3.98 1.51	3.50 3.37
Estimated Possible Error, (inch) Possible Error in δ_e Measurement (%)	0.01 ± 0.75	0.01 ± 0.66	0.01 ± 0.296
Equivalent Pressure, P_{eq} (psi) Upper Bound, $(P_{eq})_{max}$ (psi)	53.6 54.1	56.9 57.4	11,500. 11,600.***
Lower Bound, $(P_{eq})_{min}$ (psi) Possible Equivalent Pressure Error (5)	53.1 ± 0.93	56.4 ± 0.88	11,500.*** ± 0.43

* Resistors most frequently used for calibration

** The reference pressure level was 10,030 psi and the calibration pressure difference was obtained by increasing the pressure level to 10,180 psi.

*** This transducer is not linear over the complete calibration range. Therefore derived equations are not correct, but they do give an adequate approximation of the error bounds.

Now that the error in the equivalent pressures has been evaluated, the accuracy of the calibration constants can be determined. For the three pressure transducers, these three constants converted the galvanometer deflections to voltages, which were then used with the manufacturers calibration data to obtain the desired information. In the case of the displacement transducer, the calibration constant was used to convert the galvanometer displacement directly to the displacement of the translating piston.

For the three pressure transducers, the accuracy of this method was checked by using the galvanometer deflections, obtained from the calibration pressure signals, as computer input data. The calculated values were then compared with the values of the calibration pressure. In all cases, the error in the calculated values was within the measurement error of the galvanometer calibration signals.

Since this checking procedure verified the accuracy of calibration constants, it was assumed that for the three pressure transducers the accuracy of the galvanometer signals were equal to the accuracy of the equivalent pressure values.

These calibrations constants for the differential pressure transducers were a function of the excitation voltage, amplifier gain, and attenuation resistor magnitude. Therefore, these constants were recalculated frequently. The constant for the pressure level transducer was only a function of the excitation voltage and attenuation resistor. Therefore, only the excitation voltage had to be determined. This was accomplished using the calibration resistor signal. This method of determine the excitation voltage was verified by a vacuum tube voltmeter which was calibrated with a standard cell.

The calibration constant for the displacement transducer was only a function of the excitation voltage and attenuation resistor. Since the same battery was used to excite both the pressure level transducer and the displacement transducer, it was not necessary to recalculate this constant. This method was verified by comparing the calculated displacements with the known displacement of the micrometer head. The calculated values were within the possible error of the calibration signal measurements. Thus for the displacement transducer, the accuracy of the galvanometer signal was equal to the accuracy of the excitation voltage calculation.

B.2.b Transducer Details and Calibration Data

i. Pressure Transducers

The three strain gage pressure transducers were manufactured by the Advanced Technology Division of American-Standard. The following four pages contain a technical data sheet for a typical transducer and the manufacturer's calibration data for the three transducers.

As mentioned in Chapter III, Section C, the two goals of the calibration procedure were (1) to check the accuracy of the manufacturer's data where possible and (2) to determine equivalent pressures for the calibration resistors. The pressure source was a Ruska Model 2400 dead weight gage which has an upper limit of 12140 psi. A Heise bourdon tube gauge was used to extend the calibration range of the pressure level transducer because it was not accurate enough to calibrate the differential pressure transducers.

34 -114

PERFORMANCE

BRIDGE	Four active arms
COMBINED NON-LINEARITY AND HYSTERESIS	Less than 1.0% of full scale by best straight line drawn through calibration curve
REPEATABILITY	Within 0.1% of F.S.
RESOLUTION	Infinite
ACCELERATION EFFECT	Less than 0.1% of F.S. per "G", all planes
VIBRATION EFFECT	Insensitive from 50 to 2000 cps to 100 "G", 3 planes
TEMPERATURE RANGE	— 65° to 300°F. uncooled; 2000°F. (gases) cooled
ZERO PRESSURE OUTPUT	Less than ± 2% of F.S.
THREAD TEMPERATURE	300°F. maximum
THERMAL ZERO SHIFT (0° to 200°F.)	Less than 0.02% F.S./°F. change
THERMAL SENSITIVITY SHIFT (0° to 200°F.)	Less than 0.02% F.S./°F. change

RESONANT FREQUENCY	Approx. 45,000 cps
PRESSURE LIMIT	150% F.S. for static pressures Full scale for dynamic pressures
NEGATIVE PRESSURE	Usable to full vacuum
BURST PRESSURE	Above 200% F.S.
EXCITATION	Recommended 10 volts DC or AC Maximum 17 volts DC or AC
COOLING AIR	2 cfm at 15 to 20 psig clean, dry air
MATERIAL	347 stainless steel diaphragm and 17-4 PH stainless steel body
— 34 BRIDGE	Uncompensated. Maximum voltage output
— 35 BRIDGE	Voltage compensated. Single shunt calibration resistor: 280,700 ohms, 10% F.S. 112,200 ohms, 25% F.S. 56,000 ohms, 50% F.S.
— 36 BRIDGE	Voltage compensated. Bridge input symmetrical. External calibration resistor values not specified.

ORDERING

CATALOG NUMBER SELECTION TABLE

BASIC MODEL NO.	TYPE COOLING ORDER NO.	MAXIMUM PRESSURE (psig) ORDER NO.	BRIDGE			MOUNTING THREADS			DIAPHRAGM ORDER NO.
			ORDER NO.	IMPEDANCE INPUT AS SHOWN OUTPUT ± 10%	F.S. OUTPUT AT 10 V. EXCITATION (MV)	ORDER NO.	DESCRIPTION	MOUNTING TORQUE (FT.-LB.)	
114	— 1 air-cooled or — 3 uncooled	20,000 30,000 50,000 60,000	— 34 — 35 — 36	350 ± 10% 350 ± 2% 350 ± 2%	32 minimum 30 ± 2% 30 ± 2%	— 13	1-1/16-16 UN-2A	42	— 61 (347 SS welded)
	— 3 uncooled	100,000							

114 — 3 — 50,000 — 34 — 13 — 61

EXAMPLE ORDER NUMBER AS SELECTED FROM TABLE

EXAMPLE AS WRITTEN: 114-3-50,000-34-13-61

It is requested that the full six-part catalog number be used when ordering

PIN IDENTIFICATION

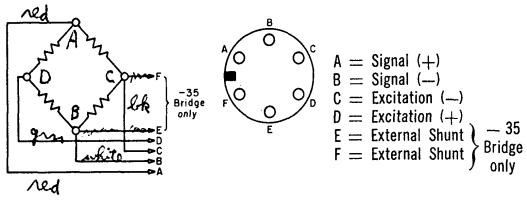

ACCESSORY EQUIPMENT

CABLES (12 FT.) AND CONNECTORS

BRIDGE TYPE	CABLE NUMBER		CONNECTOR NUMBER
	COOLED	UNCOOLED	
— 34	192-2	191-2	51009-2
— 35	192-1	191-1	51009-1
— 36	192-2	191-2	51009-2

AMERICAN-Standard
ADVANCED TECHNOLOGY DIVISION
MONROVIA INSTRUMENTS DEPARTMENT
1401 SO. SHAMROCK AVENUE
MONROVIA, CALIFORNIA
Phone (213) 359-9317

AMERICAN-Standard

ADVANCED TECHNOLOGY DIVISION
MONROVIA INSTRUMENT DEPARTMENT
1401 SOUTH SHAMROCK AVENUE • MONROVIA, CALIFORNIA 91016
AREA CODE 213 359-9317

CALIBRATION RECORD

#1

Model No.:	114-1-100,000-34-13-61	Serial No.:	8458
Sensitivity:	8.159 MV/V	Excitation:	10V AC/DC
Input Resistance:	349.0	Pressure Range:	0-100,000 PSI
Mounting Torque:	42 Ft. Lbs.	Coolant Inlet Pressure:	20 PSIG Flowing

Non-Linearity and Hysteresis Combined B. S. L.: .76 % F.S.

Input PSI %Rated Pressure	Output in %	
	Increasing	Decreasing
0%	0	-.07
10%	8.80	8.48
20%	18.85	18.55
40%	39.12	38.70
60%	59.37	59.16
80%	79.87	79.79
100%	99.95	---

PIN IDENTIFICATION

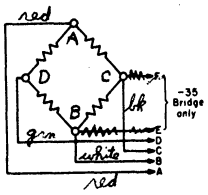

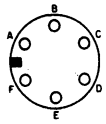

A = Signal (+)
B = Signal (—)
C = Excitation (—)
D = Excitation (+)
E = External Shunt } — 35 Bridge only
F = External Shunt }

Calibrated by: Little & Zeeve
Inspected by: RMC 5
Date: 3-23-66

AMERICAN-Standard

ADVANCED TECHNOLOGY DIVISION
MONROVIA INSTRUMENT DEPARTMENT
1401 SOUTH SHAMROCK AVENUE • MONROVIA, CALIFORNIA 91016
AREA CODE 213 359-9317

CALIBRATION RECORD

#2

Model No.:	114-1-100,00-34-13-61	Serial No.:	8481
Sensitivity:	8.080 MV/V	Excitation:	10V AC/DC
Input Resistance:	350.1	Pressure Range:	0-100,000 PSI
Mounting Torque:	42 Ft. Lbs.	Coolant Inlet Pressure:	20 PSIG Flowing

Non-Linearity and Hysteresis Combined B. S. L.: .49 % F.S.

Input PSI %Rated Pressure	Output in %	
	Increasing	Decreasing
0%	0	-.10
10%	9.53	9.15
20%	19.20	19.13
40%	39.03	39.24
60%	59.15	59.49
80%	79.14	79.72
100%	100.02	---

PIN IDENTIFICATION

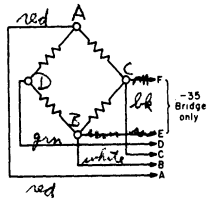

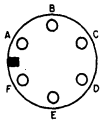

A = Signal (+)
B = Signal (–)
C = Excitation (–)
D = Excitation (+)
E = External Shunt } – 35 Bridge only
F = External Shunt }

Calibrated by: Davenport & Little
Inspected by: RMC 5
Date: 4-1-66

AMERICAN-Standard
ADVANCED TECHNOLOGY LABORATORIES DIVISION
DATA INSTRUMENT DEPARTMENT
369 WHISMAN ROAD • MOUNTAIN VIEW, CALIFORNIA
SUNNYVALE PLANT
PHONE: 415 968-4461 TWX: 408 737-9963

CALIBRATION RECORD

#3

Model No.:	114-1-100,000-34-13-61	**Serial No.:**	7627
Sensitivity:	9.240 MV/V	**Excitation:**	10V
Input Resistance:	351.8 ohms	**Pressure Range:**	100,000 PSIG
Mounting Torque:	42 ft. lbs.	**Coolant Inlet Pressure:**	20 PSIG

Non-Linearity and Hysteresis Combined B. S. L.: 1.02 **% F.S.**

Input PSI %Rated Pressure	Output in %	
	Increasing	Decreasing
0%	0	-.03
10%	11.94	11.41
20%	22.05	21.44
40%	41.90	41.55
60%	61.40	61.30
80%	80.60	80.40
100%	100.00	-

PIN IDENTIFICATION

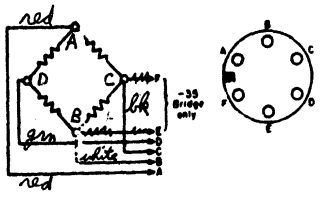

A = Signal (+)
B = Signal (−)
C = Excitation (−)
D = Excitation (+)
E = External Shunt
F = External Shunt
} − 35 Bridge only

Calibrated by: Nicolai & Little

Inspected by: [signature]

Date: May 24, 1965

The differential pressure transducers, No. 1 and No. 2, were each calibrated at five different pressure levels, 3030, 4930, 5030, 10030, and 12030 psi. Table B2 contains a summary of the calibration data. Figure 9, Chapter III, shows that the assumption of a constant slope for the pressure-output curve between 10,000 and 12,000 psi is correct.

TABLE B2

DIFFERENTIAL PRESSURE TRANSDUCER CALIBRATION SUMMARY

Transducer No. 1 Calibration Switch Position (CS1)	1	2	3	4	5	6
Calibration Resistor	80M	40M	20M	10M	5M	2.5M
Pressure level (psi)	Equivalent Pressure Difference (psi)					
3030	15.75	31.5	62.4			
4930	14.75	29.25	58.5			
5030	14.50	29.2	58.3	115.	225.	463.
10030	13.2	26.5	53.6	106.	218.	432.
12030	13.2	26.5	53.5			
Transducer No. 2 Calibration Switch Position (CS1)	1	2	3	4	5	6
Calibration Resistor	80M	40M	20M	10M	5M	2.5M
Pressure level (psi)	Equivalent Pressure Difference (psi)					
3030	15.75	31.75	64.75			
4930	14.75	29.75	60.3			
5030	14.7	29.75	60.0	120.	248.	496.
10030	14.4	28.8	56.9	114.	222.	443.
12030	14.4	28.8	56.8			

Table B3 contains a summary of the calibration data for the pressure level transducer while Figure B2 contains the pressure versus galvanometer deflection curve for the maximum instrumentation sensitivity (SS3 = 4). Figure B3 contains the pressure versus galvanometer deflection curves for all four instrumentation sensitivities.

TABLE B3

PRESSURE LEVEL TRANSDUCER CALIBRATION SUMMARY

Calibration Switch Position (CS3)	1	2	3	4	5	6
Calibration Resistor	1M	301K	150K	100K	75K	30.1K
Equivalent Pressure (psi)	750	2800	5630	8500	11500	

ii. Displacement Transducers

The two displacement transducers were manufactured by the Sanborn Division of the Hewlett-Packard Company. Calibration was achieved by plotting the galvanometer deflection versus core deflection. Figures B4 is a typical calibration curve. This figure shows that the output signal becomes non-linear for large core displacements. The problems associated with non-linearity were avoided by only operating in the linear range.

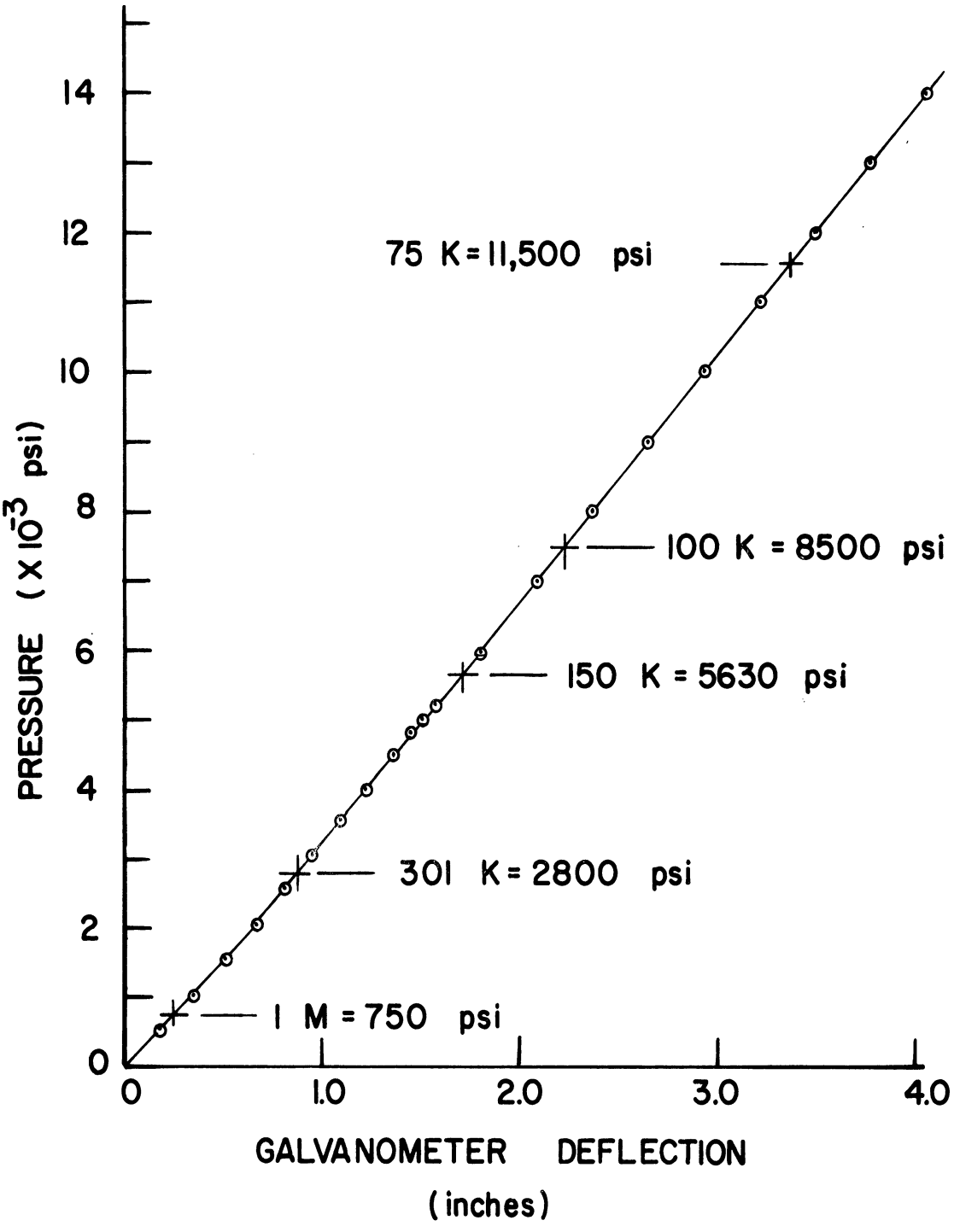

Figure B2. Pressure Level Transducer Calibration Curve.

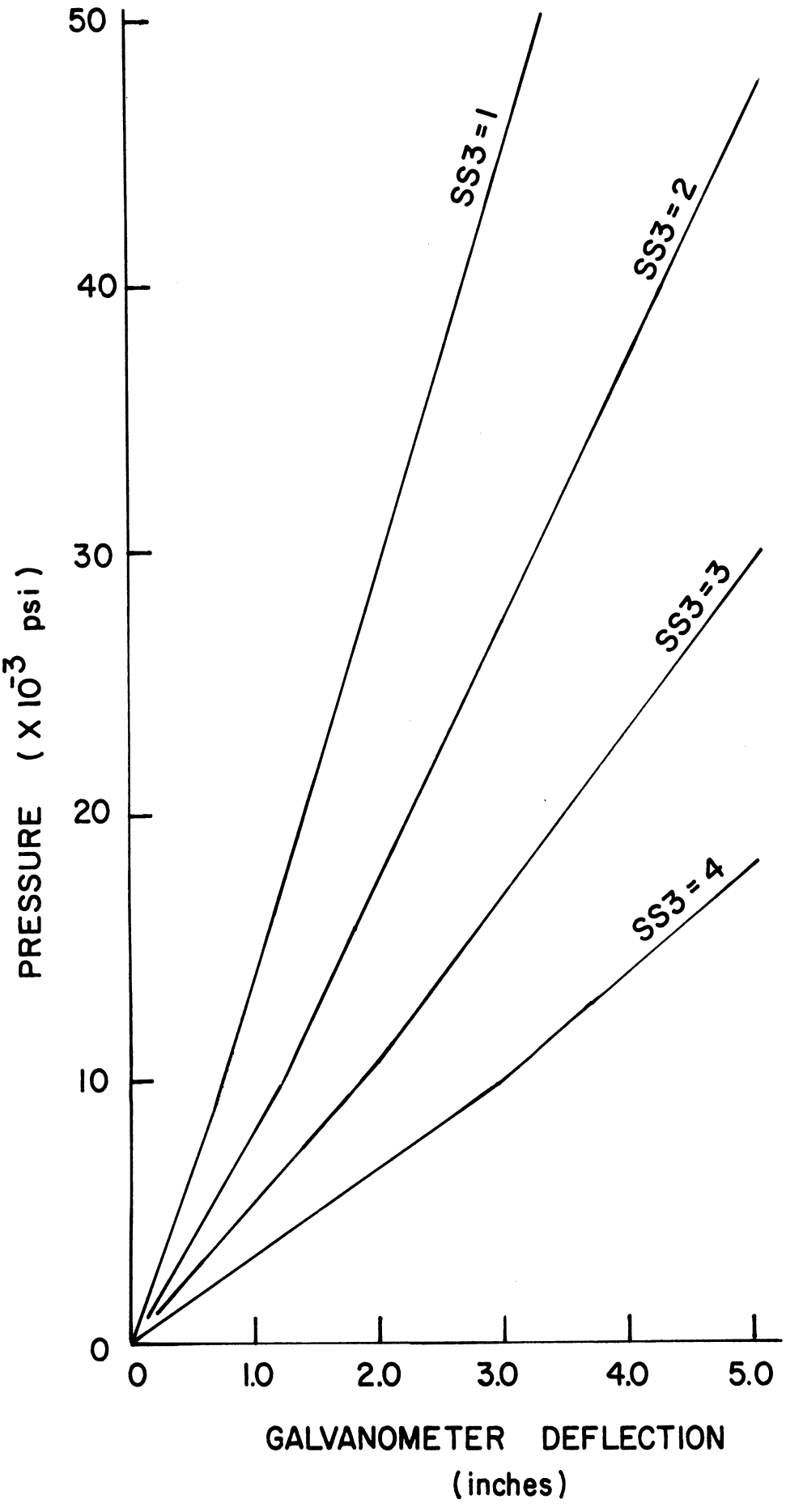

Figure B3. Pressure Level Transducer Output Signal Curve.

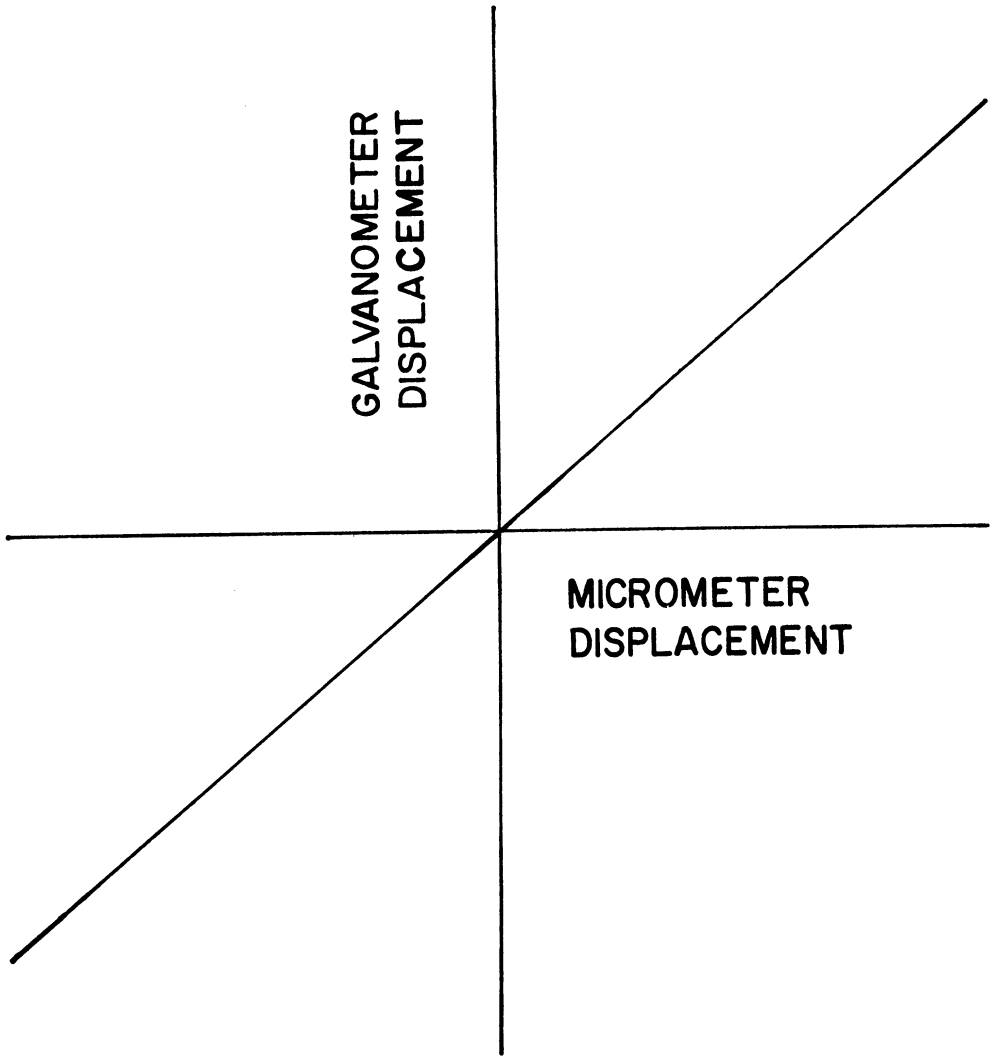

Figure B4. Typical Displacement Transducer Calibration Curve.

B.2.c Electronic Circuits

This section contains schematic circuit diagrams for the instrumentation control box and equivalent circuits for all transducers. The following is a list of figures presented in this section.

LIST OF FIGURES IN SECTION B.2.b

Figure B5 shows the general block diagram for the instrumentation. The transducer connectors are not numbered, but all connectors on the control box and visicorder are numbered. Figure B5 should be

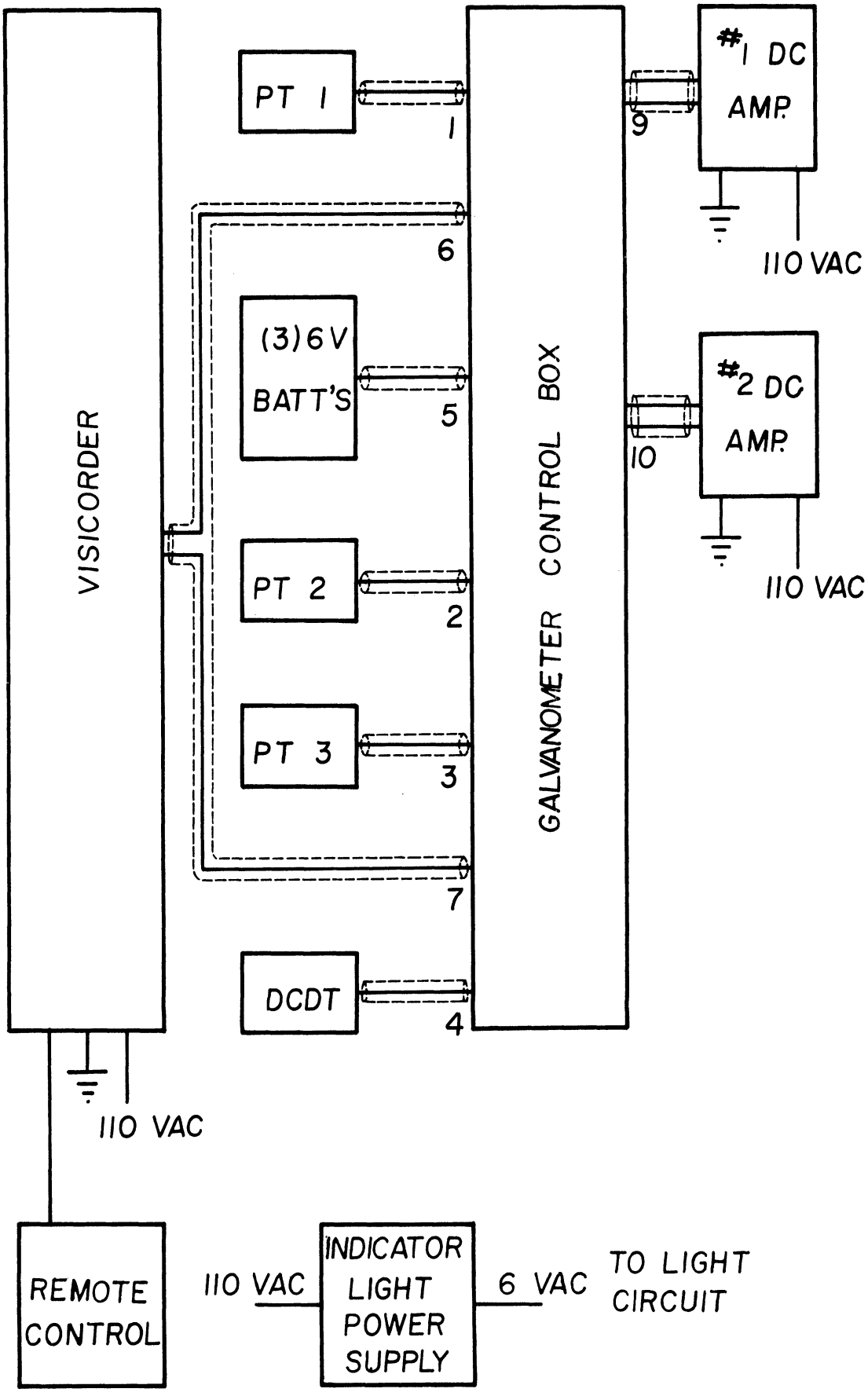

Figure B5. Instrumentation Block Diagram.

referred to when studying figures B6 through B12 in detail because the control box connector numbers are consistent in all figures.

Figure B6 is a photograph of the control panel and shows the position of all control knobs, switches, and lights. Tables B2 and B3 summarize the values of resistors and their corresponding equivalent pressure signals for the two calibration switches CS1 and CS3.

Figures B7, B8, and B9 are self explanatory and require no further comments. Figures B10 and B11 are the schematic diagrams for the differential pressure transducer circuits in the instrumentation control box. These circuits have been divided into two figures for clarity. When studying these figures, it should be kept in mind that the circuits for both differential pressure transducers are identical, but physically and electrically isolated. Figure B10 contains the portion of the circuits from the transducer cable connections (No. 1 and No.2) to the DC amplifier input connectors (No. 9 and No. 10). The balance potentiometers, excitation voltage connector (No. 5) and the calibration resistors are also included. Figure B11 contains the portion of the circuits from the DC amplifier output signals (connectors No. 9 and No. 10) to the visicorder connector (No. 6). The attenuation resistors and filter capacitors are also included.

Figures B10, B11, and B12 all contain indicator light circuits. A single transformer provides the six volt AC source. The red lights indicate when the excitation voltage is applied to each transducer. The white warning lights indicate when the galvanometers are activated.

Figure B12 contains the complete circuits for both the pressure level transducer and the displacement transducer.

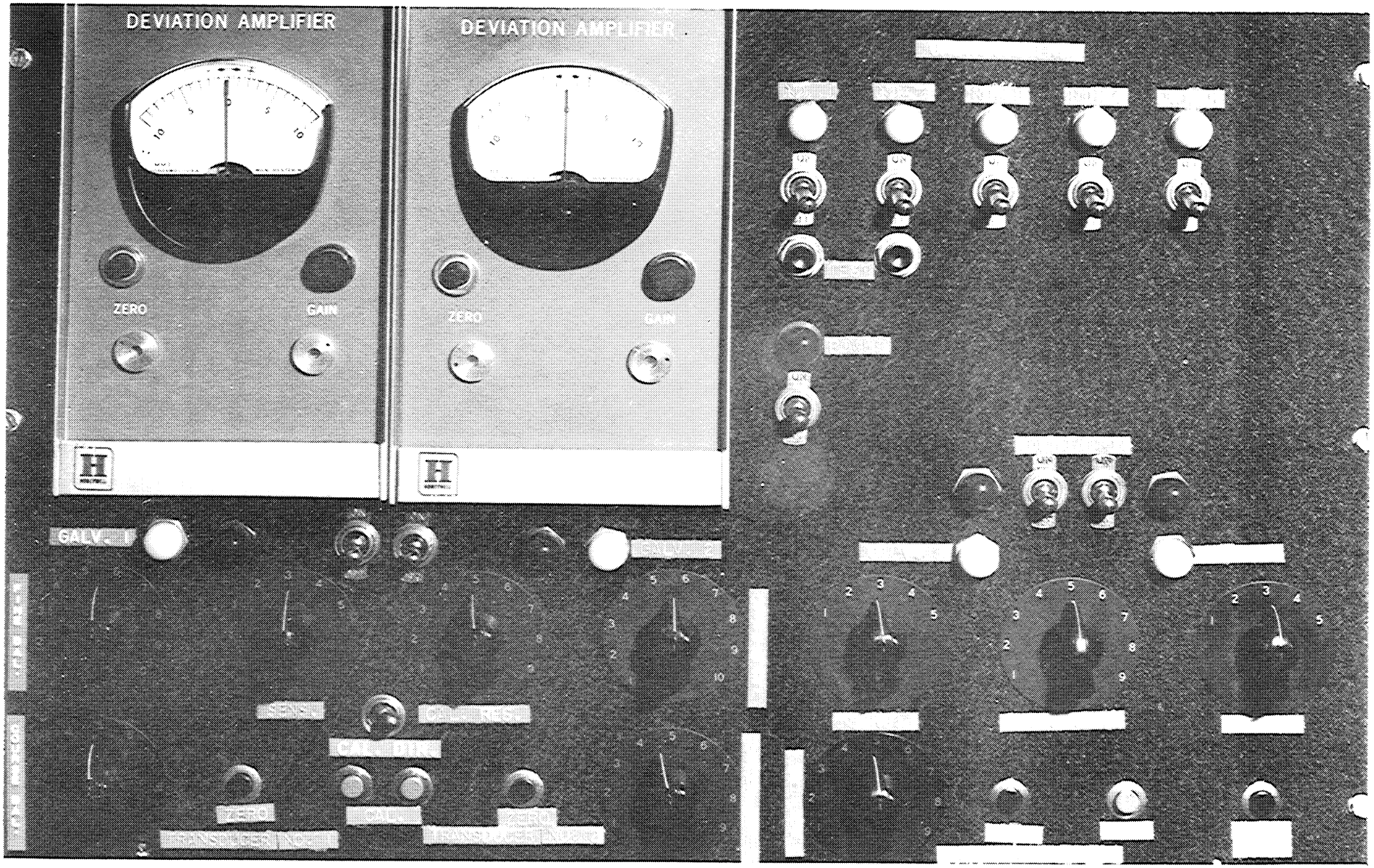

Figure B6. Instrumentation Control Box Panel.

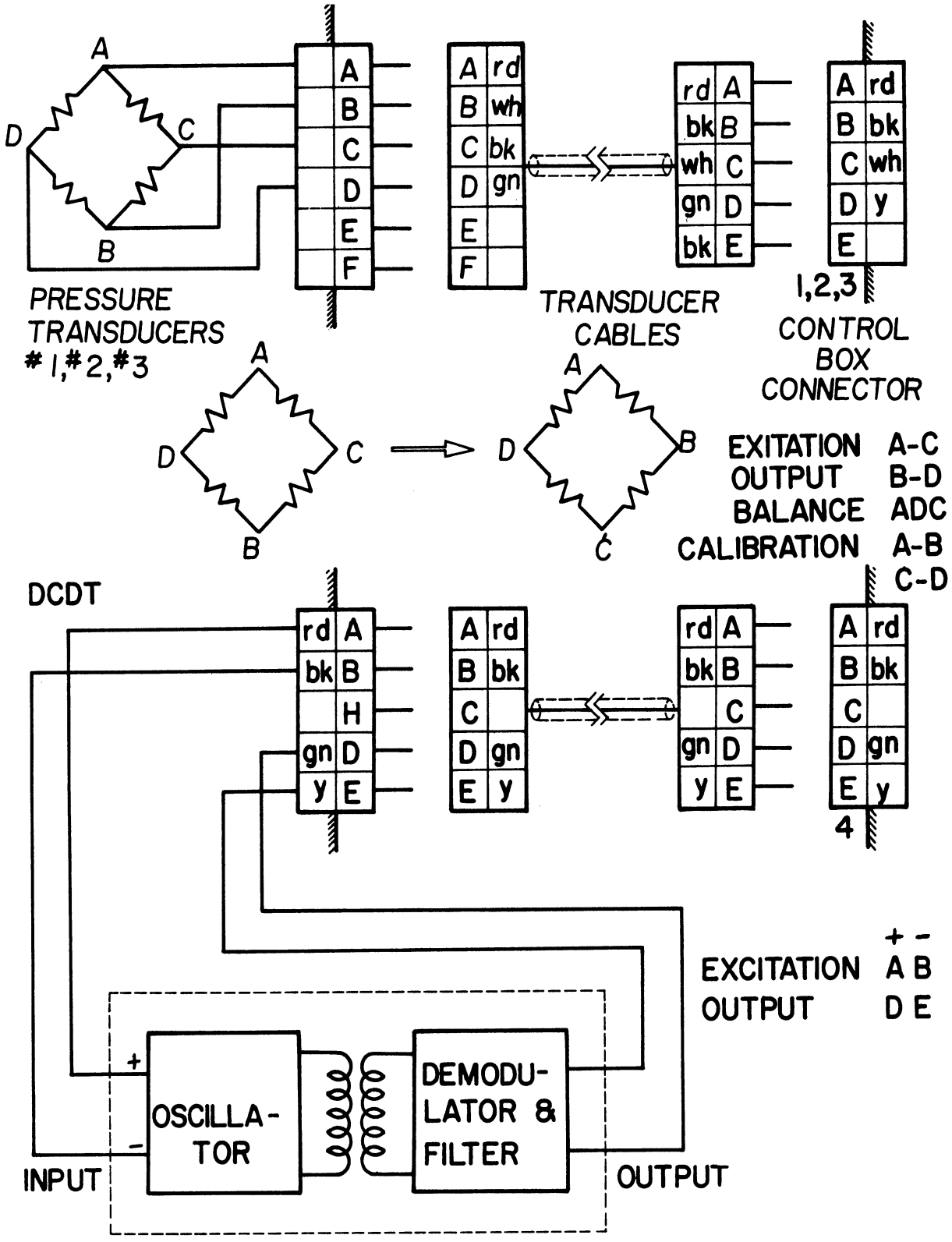

Figure B7. Transducer Cables - Schematic Diagrams.

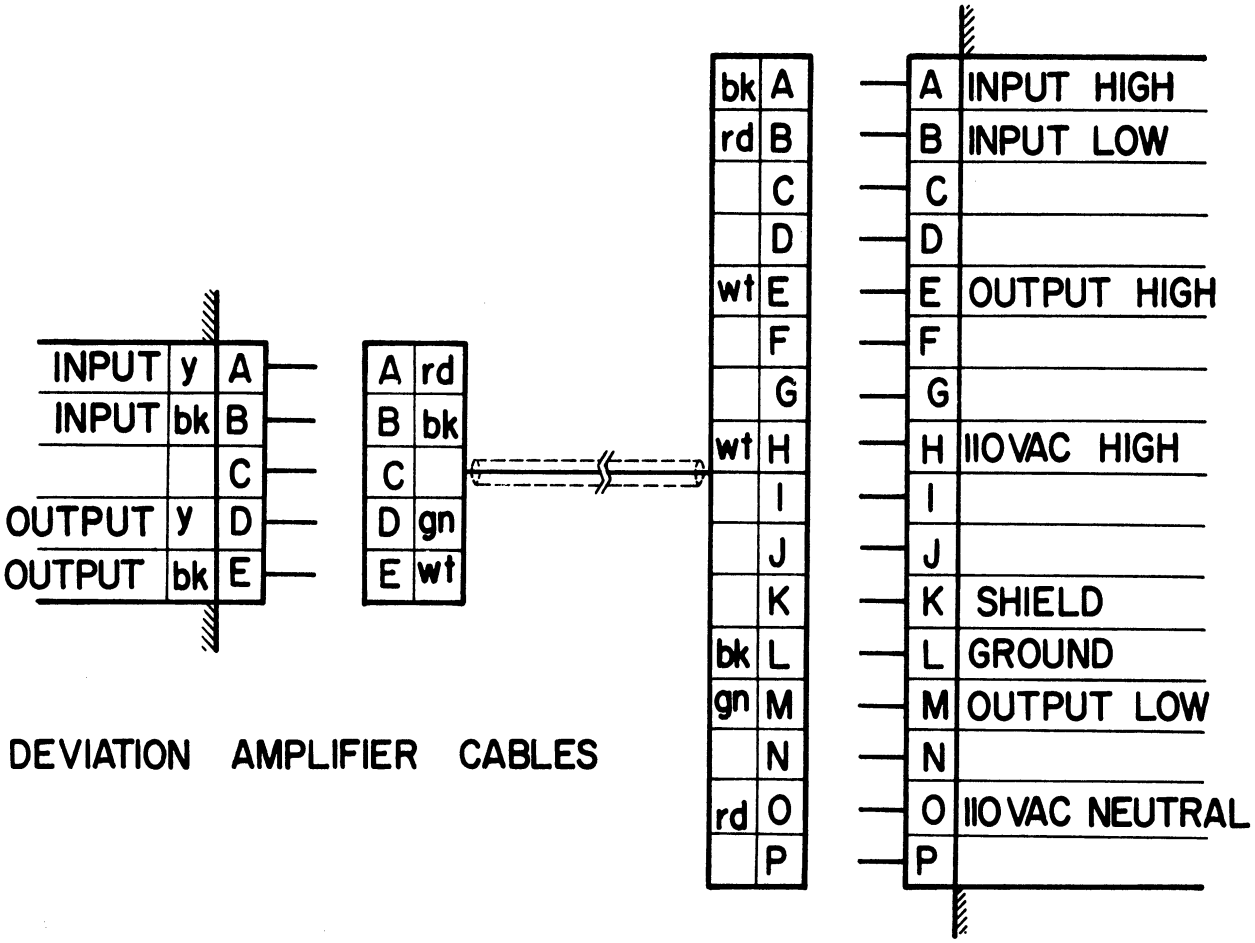

Figure B8. Deviation Amplier Cables - Schematic Diagrams.

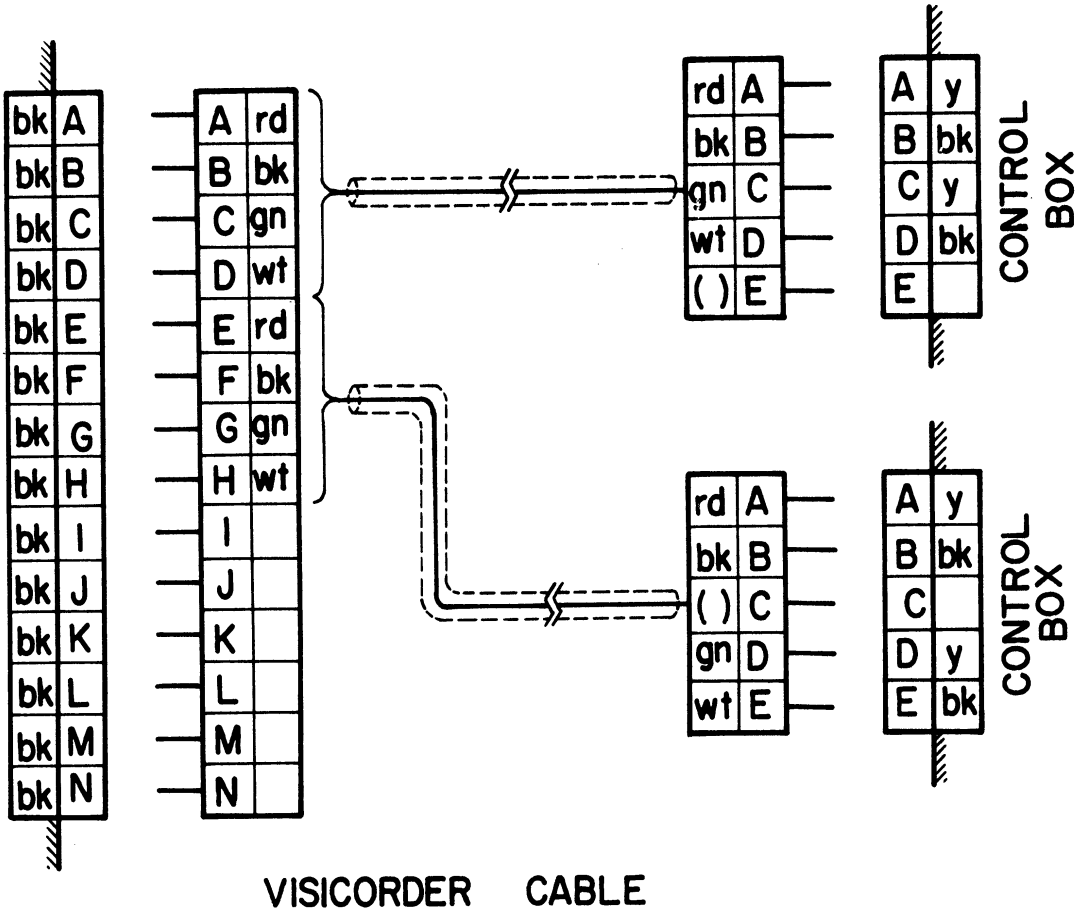

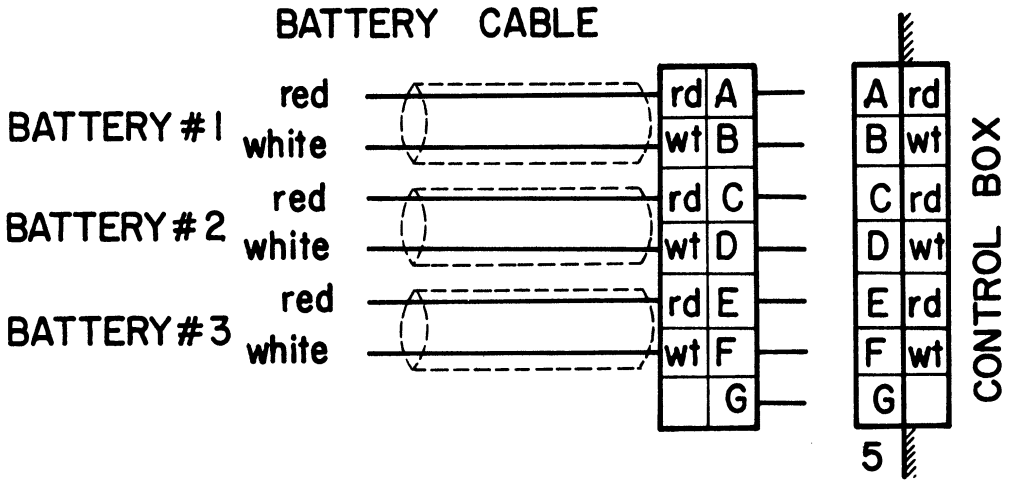

Figure B9. Visicorder and Battery Cables - Schematic Diagrams.

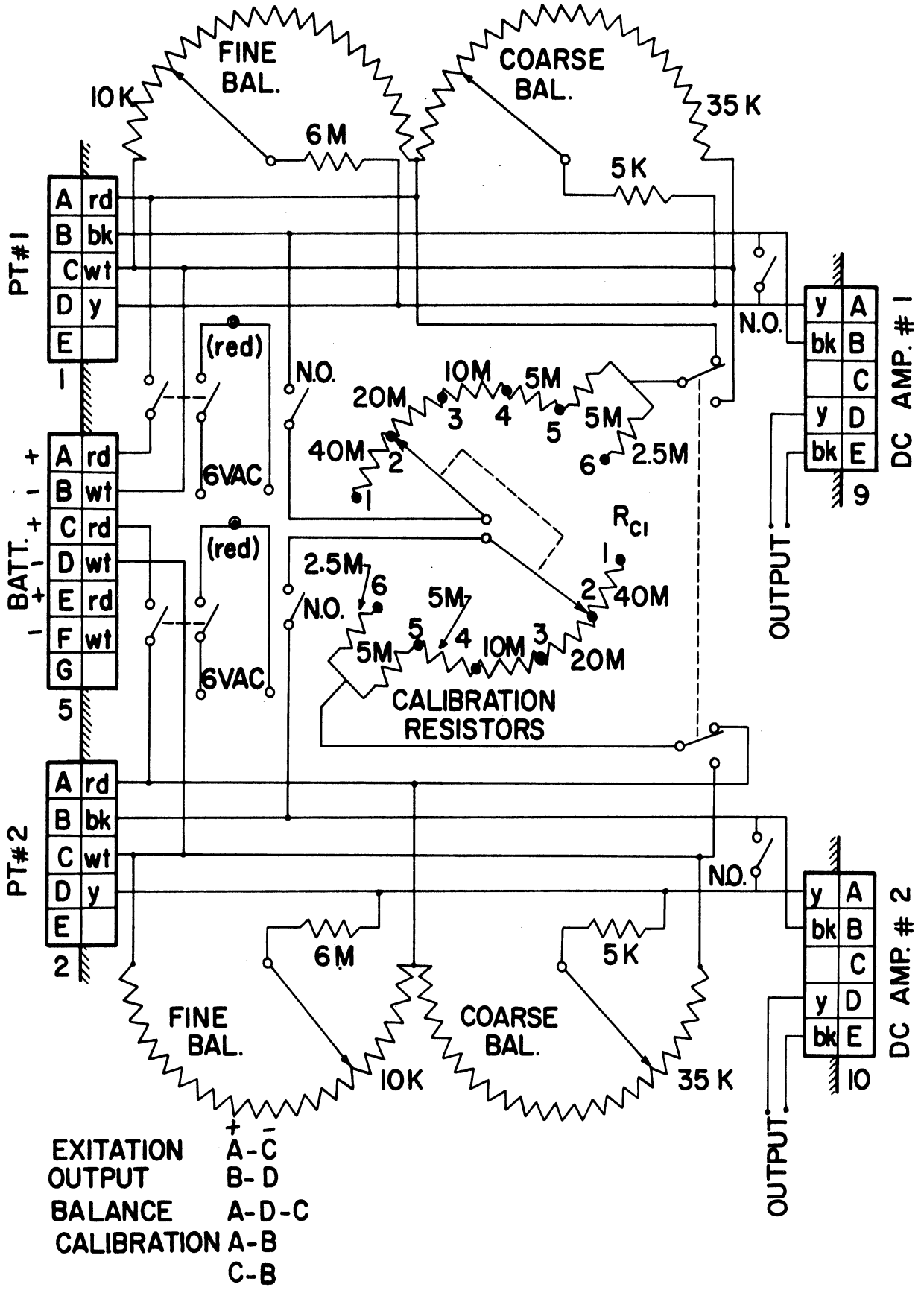

Figure B10. Control Box Schematic - Differential Pressure Transducer Circuits.

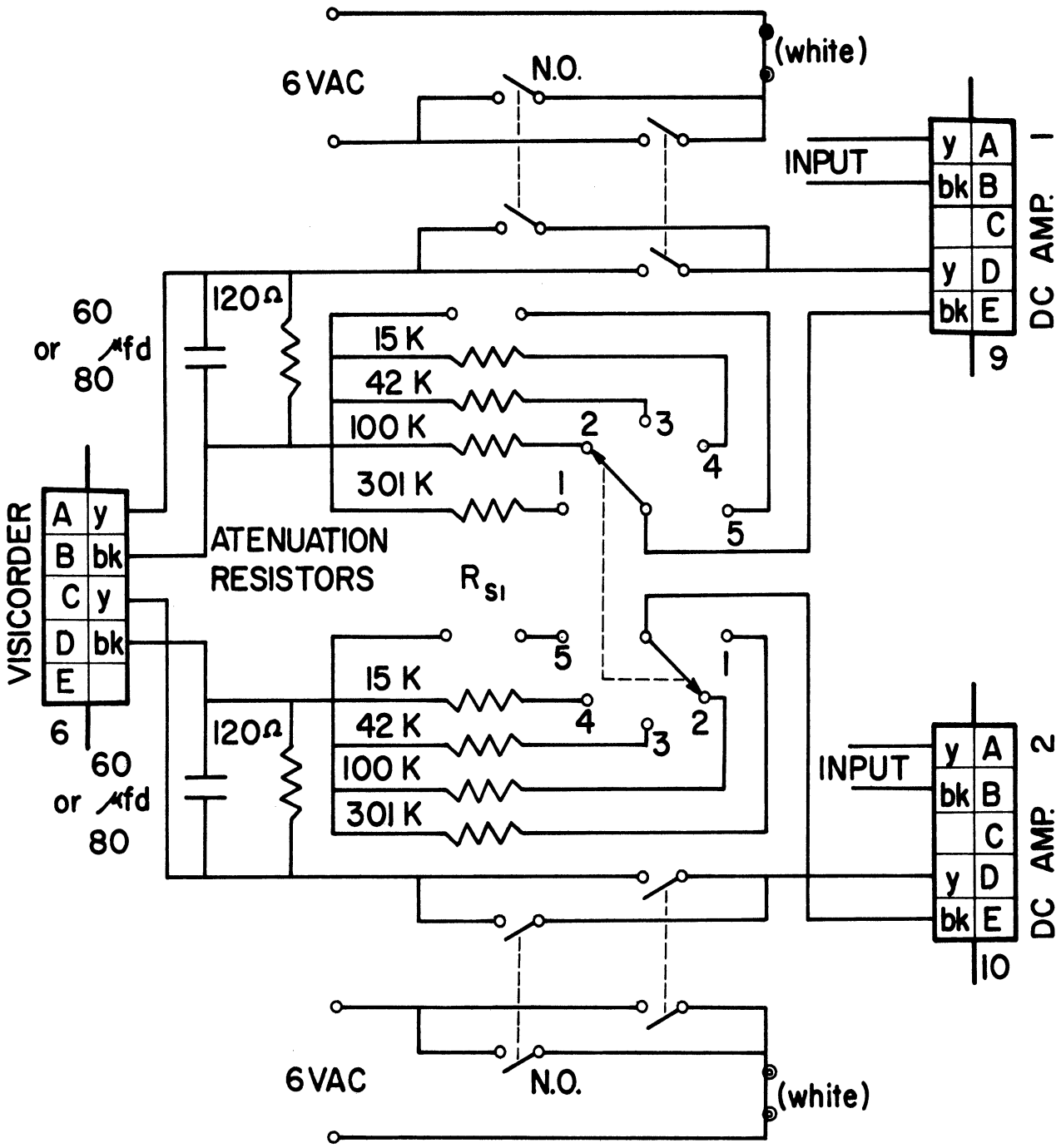

Figure B11. Control Box Schematic -
Differential Pressure Transducer Circuits.

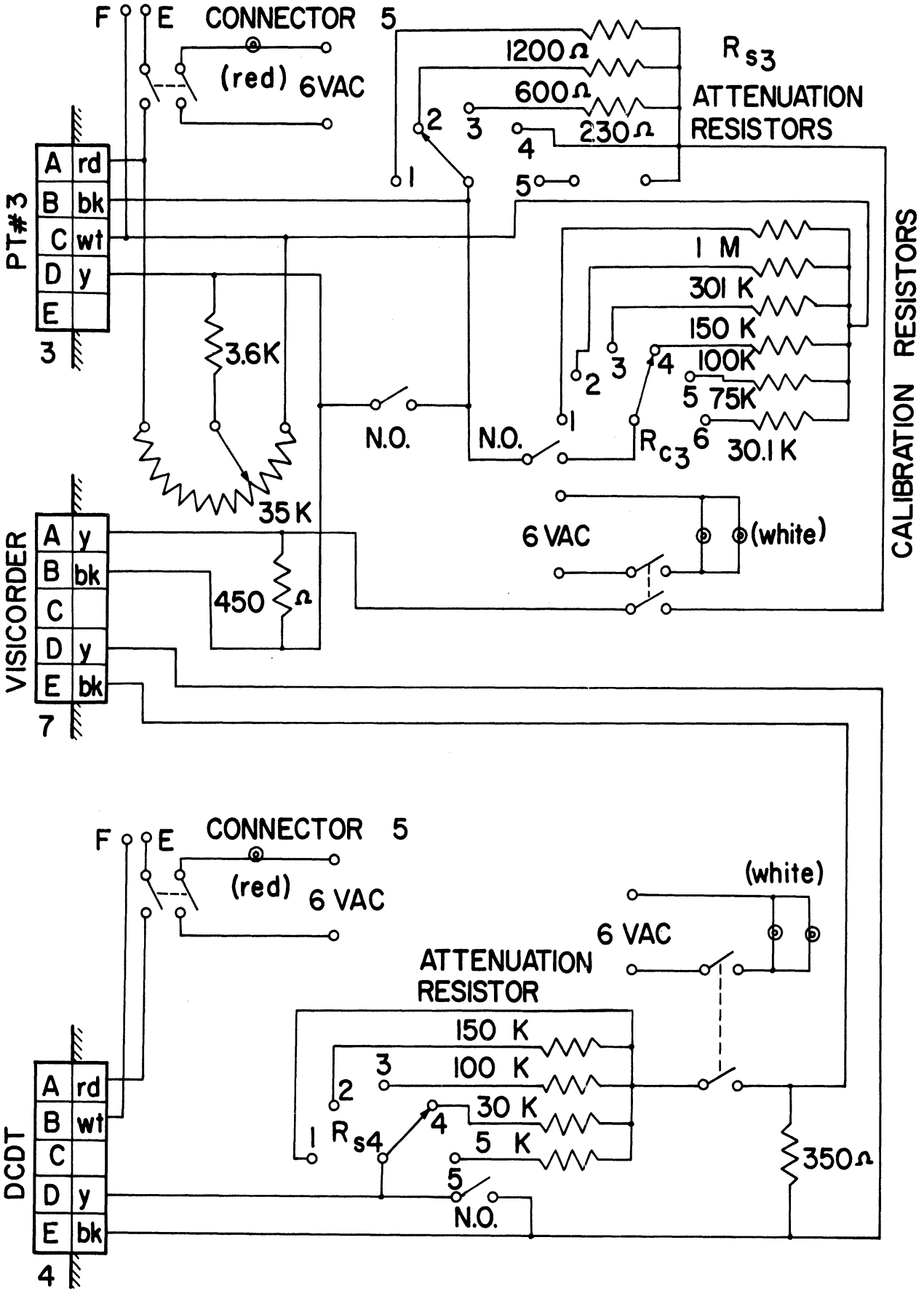

Figure B12. Control Box Schematic - Pressure Level and Displacement Transducer Circuits.

Figures B13, B14, and B15 are the equivalent circuits for the transducers. For the differential pressure transducers, the relation between the transducer output, (% of total), ΔE_o and the galvanometer deflection δ is:

$$\Delta E_o = \frac{\delta}{K}\left\{\left[R_a + 18.2\left(\frac{R_a}{120} + 1\right)\right]\left(\frac{1}{12 s_v} + \frac{1}{S_i}\right) 10^3 + \left(\frac{R_{s1}}{120} + 1\right)\frac{1}{s_v}\right\}$$

where $K = f(V, R_a, R_i, G)$ (determined from calibration data)

V = excitation voltage

R_a = attenuation resistor

R_i = amplifier input impedance

G = amplifier gain

S_v = galvanometer voltage sensitivity (in/mv)

S_i = galvanometer current sensitivity (in/μa)

For this circuit,

$$S_i = (.125)\ 12000/12028.6 = .124703 \text{ (in/mv)}$$

and

$$S_v = \frac{(4.37)\ 12000.\ (28.6 + 136)}{12000\ (28.6 + 119.6 + 18.2) + 28.6\ (18.2 + 119.6)} = 4.070098 \text{ (in/μa)}$$

The relation between the transducer output E03 and the galvanometer deflection δ for the pressure level transducer can be reduced to

$$E03 = 100\ K_3\ \delta/(9.24\ V)\ \%$$

where $K_3 = f(R_a)$ (determined from calibration data)

R_a = attenuation resistor

V = excitation voltage (volts)

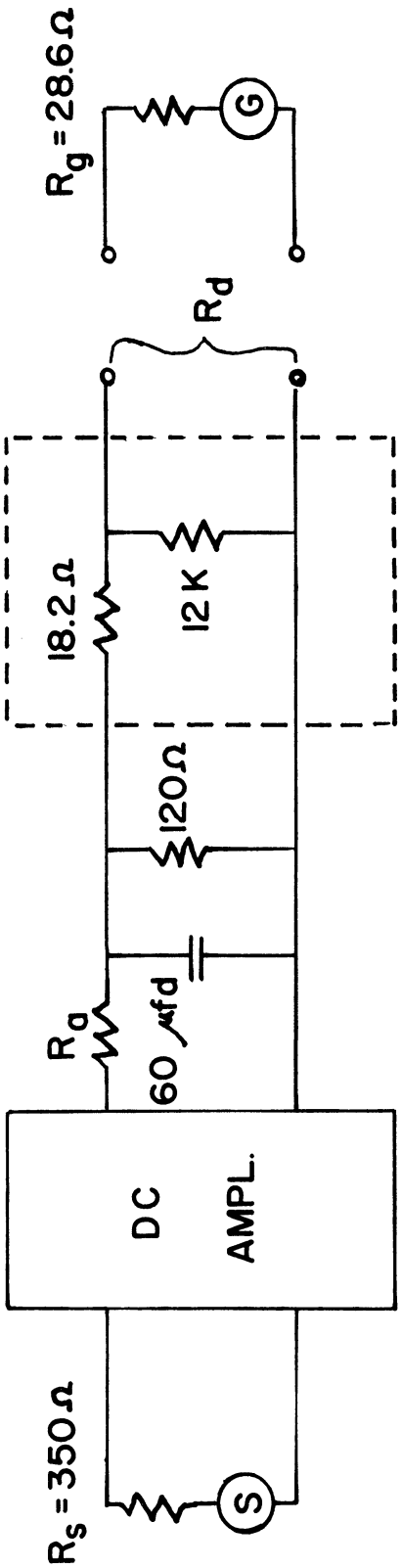

Figure B13. Equivalent Circuit for Differential Pressure Transducers.

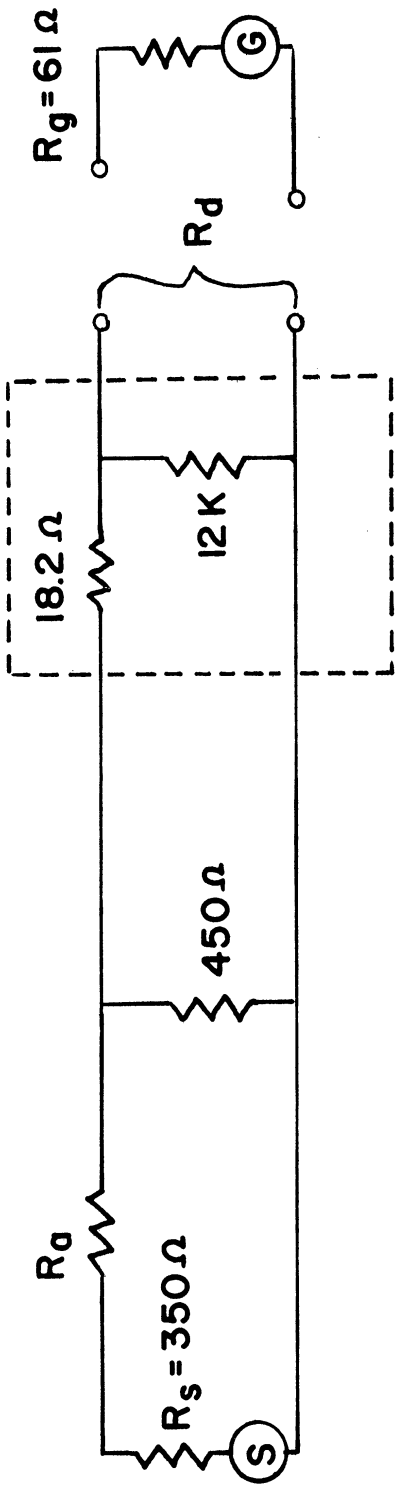

Figure B14. Equivalent Circuit for Pressure Level Transducer.

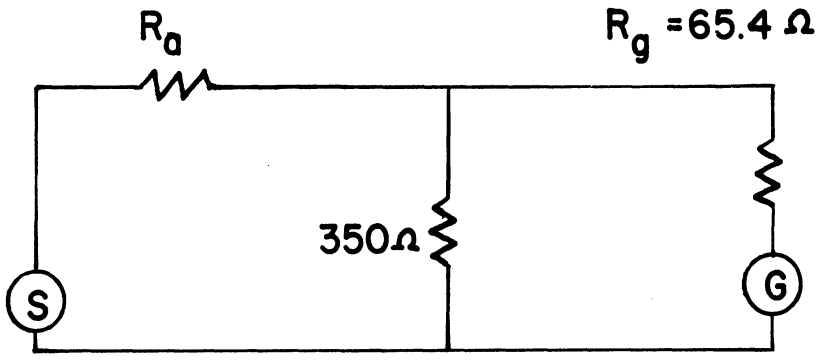

Figure B15. Equivalent Circuit for Displacement Transducer.

For the displacement transducer, the relation between the core displacement and the galvanometer deflection is:

$$d = K_4 \, V \, \delta$$

where: d = core displacement (inches)

$K_4 = f(R_a)$ (determined from calibration data)

R_a = attenuation resistor

V = excitation voltage (volts)

δ = galvanometer deflection (inches)

B.2.d. Visicorder Oscillograph

A Honeywell visicorder oscillograph Model 906C was used to simultaneously record the signals from all for transducers. This model can record up to 14 channels of data at frequencies from DC up to 5000 cps. It contains a high-pressure mercury vapor light source, mirror galvanometers, timing light, an optical system and a paper transport system. Table B4 contains a summary of the galvanometer data.

TABLE B.4

GALVANOMETER INFORMATION

Channel*	1	2	3	4
Galvanometer	M40-120A	M40-120A	M40-350A	M100-350
Nominal Undamped Natural Freq. (cps)	40	40	40	100
Flat Frequency Response (cps)	0-24	0-24	0-24	0-60
Required External Damping Resistance (ohms)	120	120	350	350
Nominal Coil Resistance (ohms)	28.6	28.6	61.0	65.4
Current Sensitivity (in/μa)	.125	.125	.243	.158
Voltage Sensitivity (in/mv)	4.37	4.37	4.00	2.41

* Channel Transducer

1 differential pressure
2 differential pressure
3 pressure level
4 displacement

APPENDIX C

DATA REDUCTION COMPUTER PROGRAM

C.1 Program Objectives

This program was written to convert the raw experimental data to useful quantities such as test fluid pressure, pressure difference across the capillary, shear stress, shear rate, kinetic energy correction, Reynolds number, entrance length, and finally the viscosity.

C.2 Program Description and Equations

The first data card read into the computer was a remark card which could contain any comment punched between columns 1 and 72, inclusive. This had to be the first data card and no additional comment cards were allowed. The second data card contained the capillary dimensions and transducer calibration data in the following manner.

D = .xxxx, L = x.xxxx, CALI(0) = x,x,x,x, CALF(0) = x.xx,x.xx,x.xx*

where D and L were the capillary diameter and length respectively. The first two quantities in the CALI vector were the integers SS1 and CS1 which were the sensitivity and calibration switch positions for the differential pressure transducers. The third and fourth quantities in the CALI vector were the integers SS3 and CS3 which were the sensitivity and calibration switch positions for the pressure level transducer. The quantities in the CALF vector were the floating point numbers DEL1, DEL2, and DEL3 which were the calibration signals from the three pressure transducers. The computer used this information to calculate the transducer excitation voltage V3 and the coefficients K1 and K2.

The next data card was repeated for each data run until new calibration data was to be read.

DATAI(0) = x,x,x, DATAF(0) = x.xx,x.xx,x.xx,x.xx,x.xx, -1.0* RUN NUMBER

The variables in the DATAI vector were the integers SS1, SS3, and SS4, the sensitivity switch position for the displacement transducer. The variables in the DATAF vector were the floating point numbers DEL1, DEL2, DEL3, DEL4, TIME and CALDAT. The first four elements were the galvanometer deflections which represented the output signal of the various transducers. The fifth element, TIME, was the time interval in seconds, during which the displacement transducer signal, DEL4, was obtained. The last element in the DATAF vector, CALDAT, was a dummy variable which signaled whether or not the next data card contained calibration data. If new calibration was to be read, this variable was set equal to 1.0, otherwise it could be omitted from the list, or could contain any number less than zero. The fluid density RHO was also included in this list if the assumption of RHO = 50 lbm/ft^3 was not sufficient. The last item on this card, RUN NUMBER, was any desired identification in columns 61 and 72, inclusive.

After the calibration data had been used to calculate the necessary coefficients and the experimental data had been read, the computer calculated the desired quantities.

First the pressure level, P3 , was calculated.

$$P3 = \text{PRESS.}(V3) \qquad \text{(psi)}$$

The internal function PRESS used three variables to determine the

percent output of the pressure level transducer, EO3.

$$EO3 = 100 * K3(SS3) * DEL3/(9.24 * V3) \qquad (\%)$$

This value was used with appropriate constants given by the manufacturer's calibration data to determine the pressure level, P3 .

$$P3 = PI3 + DPDE3 * (EO3 - EI3) \qquad (psi)$$

The displacement of the translating piston, DISPL , was

$$DISPL = SENS4(SS4) * V3 * DEL4 \qquad (in)$$

The flow rate through the capillary was

$$Q = PI * .49 * .49/4. * DISPL/TIME \qquad (in^3/sec)$$

The average velocity in the capillary, V , was

$$V = Q/(PI * D * D/4.) \qquad (in/sec)$$

The kinetic energy correction, KEC , was

$$KEC = RHO * V * V/(32.2 * 144. * 144.) \qquad (psi)$$

As mentioned previously, the program assumed a density RHO of 50 lbm/ft^3 unless RHO was included in the input data.

Next the pressure drop across the capillary was calculated. The pressure levle determined the slope of the Pressure-Output curves for the differential pressure transducers. The output of each transducer, DE1 and DE2, was then calculated and finally the corrected pressure drop across the capillary, DELTAP.

$$DELTAP = .ABS.\ (DPDE1 * DE1 - DPDE2 * DE2) - KEC \qquad (psi)$$

The pressure drop and capillary geometry were then used to determine the shear stress at the capillary wall.

$$TAU = DELTAP/(4. * L/D) \qquad (psi)$$

$$TAUDYN = 68950. * TAU \qquad (dyn/cm^2)$$

The Newtonian shear rate, or apparent shear rate, at the capillary wall was

$$NSRATE = 32. * Q/(PI * D.P.3) \qquad (sec^{-1})$$

Thus the apparent viscosity was

$$VISC = TAU/NSRATE \qquad (Lbf.sec/in^2)$$

$$VISCP = 68950. * VISC \qquad (poise)$$

The Reynolds number was

$$REYN = RHO * V * D/VISC$$

The Boussenesq relation was used to determine the ratio of entrance length--to capillary length.

$$LEOL = .065 * REYN * D/L$$

Then the results were printed. Finally, the next data card was read and the necessary calculations repeated.

C.3 MAD Symbol Definitions

Symbol	Definition
CALDAT	Dummy variable = 1.0 if next data card contains calibration data. Otherwise, it can be omitted.
CALF	Vector containing the floating point calibration data DEL1, DEL2, DEL3.
CALI	Vector containing the integer calibration data SS1, CS1, SS3, CS3.
CS1	Position of calibration switch No. 1, input data.
CS3	Position of calibration switch No. 3, input data.
DATAF	Vector containing the floating point input data DEL1, DEL2, DEL3, DEL4, TIME, CALDAT.
DATAI	Vector containing the integer input data SS1, SS3, SS4.
DE1	Output of Pressure Transducer No. 1 (%)
DE2	Output of Pressure Transducer No. 2 (%)
DEL1	Deflection of Galvanometer No. 1, Pressure Transducer No. 1 output signal. input data (in)
DEL2	Deflection of Galvanometer No. 2, Pressure Transducer No. 2 output signal. input data (in)
DEL3	Deflection of Galvanometer No. 3, Pressure Transducer No. 3 output signal. input data (in)
DEL4	Deflection of Galvanometer No. 4, Displacement Transducer output signal. input data (in)
DELPC1	Vector containing calibration data for Pressure Transducer No. 1.
DELPC2	Vector containing calibration data for Pressure Transducer No. 2.
DELTAP	Pressure drop across capillary. (psi)
DISPL	Displacement of transversing piston (inches)
DPDE1	Slope of Pressure-Output curve for pressure transducer No. 1 (psi/%)

Symbol	Definition
DPDE2	Slope of Pressure-Output curve for pressure transducer No. 2 (psi/%)
DPDE3	Slope of pressure-output curve for pressure transducer No. 3 (psi/%)
D	Capillary diameter, input data (inches)
E3C	Vector containing calibration data for pressure transducer No. 3
EI3	Output of pressure transducer No. 3 corresponding to pressure values on manufacturer's calibration data (%)
EO3	Calculated output of pressure transducer No. 3 (%)
HEAD	Vector used to contain information on remark card.
K1	Quantity used to calculate DE1
K2	Quantity used to calculate DE
K3	Vector containing coefficients for EO3 calculation.
KEC	Kinetic Energy Correction (psi)
LEOL	Ratio of entrance length-to-capillary length. (in/in)
L	Capillary Length, input data (inches)
NSRATE	Newtonian shear rate at capillary wall ($sec.^{-1}$)
P3	Pressure Level (psi)
PI3	Pressure values given on manufacturer's calibration data for pressure transducer No. 3. (psi)
PI	Program constant = 3.1415926
PUNCH	Boolean variable = 1B if punched card output is desired. input data
Q1	Integer used for list TAUSAV
Q2	Integer used for list VISAVE
Q	Volumetric flowrate ($in^3/sec.$)
REYN	Reynolds Number

Symbol	Definition
RHO	Fluid Density (lbm/ft^3)
RS1	Vector containing values of series resistors in pressure transducers No. 1 and No. 2 electrical circuit (ohms)
RUN	Vector containing identification in columns 60 through 72 inclusive
SENS4	Vector containing coefficients for displacement transducer.
SI1	Current sensitivities for galvanometers No. 1 and No. 2 (in/a)
SS1	Position of sensitivity switch No. 1, input data
SS3	Position of sensitivity switch No. 3, input data
SV1	Voltage sensitivity of galvanometers No. 1 and No.2 (in/mv)
TAUDYN	Wall shear stress (dyn/cm^2)
TAU	Wall shear stress (psi)
TAUSAV	List contain values of TAUDYN
TIME	Time obtained from visicorder trace. (Sec)
V3	Excitation voltage for pressure transducer No. 3 and displacement transducer (volts)
VISAVE	List containing values of VISCP
VISCP	Apparent viscosity (poises)
VISC	Apparent viscosity ($lbf\ sec/in^2$)
V	Average fluid velocity in capillary (in/sec)

C.4 Program Listing

```
 .....HIGH PRESSURE VISCOSITY PROGRAM .....


  REFERENCES ON
  PARAMETER PI(3.1415926),SI1(.124703), SV1(4.C70098)
  EQUIVALENCE (CALF(0),DATAF(0),DEL1),(CALF(1),DEL2),(CALF(2),
1  DEL3),(DATAF(3),DEL4),(DATAF(4),TIME),(DATAF(5),CALDAT),
1  (Q1,TAUSAV),(Q2,VISAVE),(DATAI(0),SS1),(DATAI(1),SS3),
1  (DATAI(2),SS4)
  DIMENSION CALF(2),DATAF(5),TAUSAV(300),VISAVE(300)
  INTEGER CALI(3),DATAI(2),RUN(1),Q1,Q2,SS1,SS3,SS4,CS1,CS3,HEAD(12
1 )
  BOOLEAN PUNCH

  VECTOR VALUES RS1(1)=3010CC.,100000.,4200C.,15CCC.
  VECTOR VALUES DELPC1(1)=13.2,26.5,53.2,106.,218.,432.
  VECTOR VALUES DELPC2(1)=14.4,28.8,56.6,114.,222.,443.
  VECTOR VALUES SENS4(1)=0.001398,0.03935,0.026,0.00899,0.00253,
1 C.0000581,0.CC629,0.00408,C.C0128,0.000238
  VECTOR VALUES E3C(1)=.896,3.33,6.83,1C.15,13.53,33.2
  VECTOR VALUES K3(1)=8.65,5.42,3.50,2.25

 .....INTERNAL FUNCTION, PRESSURE CALCULATION.....

  INTERNAL FUNCTION PRESS.(VV)
  E03 = 100. *K3(SS3)*DEL3/(9.24*VV)
  WHENEVER E03.GE.80.6
           EI3=80.6
           PI3=80000.
           DPDE3=20000./(10C.-80.60)
  OR WHENEVER EC3.GE.61.4
           EI3=61.4
           PI3=60000.
  DPDE3=20000./(80.60-61.4C)
  OR WHENEVER   E03.GE.41.9
           EI3=41.9
           PI3=40000.
           DPDE3=20000./(61.40-41.90)
  OR WHENEVER   E03.GE.22.C5
           EI3=22.05
           PI3=20000.
           DPDE3=20000./(41.90-22.05)
   OR WHENEVER  E03.GE.11.94
           EI3=11.94
           PI3=10000.
           DPDE3=10000./(22.C5-11.94)
  OTHERWISE
           EI3=0.0
           PI3=0.0
           DPDE3 = 10C00./11.94
  END OF CONDITIONAL
           P3=PI3+DPDE3*(EC3-EI3)
  FUNCTION RETURN P3
```

```
      END OF FUNCTION
      RHO=50.

      SETEOF.(PLOT)

      PUNCH=08
      Q1=0
      Q2=0
      READ FORMAT $12C6*$,HEAD(1)...HEAD(12)
      PRINT FORMAT $1H1,S10,12C6//*$,HEAD(1)...HEAD(12)

     .....TRANSDUCER CALIBRATION.....

     .....PRESSURE LEVEL TRANSDUCER (NO.3).....

NEWCAL  READ DATA PUNCH,D,L,CALI(0)=SS1,CS1,SS3,CS3,CALF(0)=DEL1,
             DEL2,DEL3*
      CALDAT=-1.0
      SS1=CALI(0)
      CS1=CALI(1)
      SS3=CALI(2)
      CS3=CALI(3)
      V3 = 100.*K3(SS3)*DEL3/(9.24*E3C(CS3))

     .....DIFFERENTIAL PRESSURE TRANSDUCERS(NO.1 AND 2).....

      P3=PRESS.(V3)
      DE1 = 0.001005 * DELPC1(CS1)
      DE2 = 0.000967 * DELPC2(CS1)
      K1=((RS1(SS1)+18.2*(RS1(SS1)/120.+1.))*(.08333/SV1+1./SI1)*
     1   .001 +(RS1(SS1)/120.+1.)/SV1) * DEL1/DE1
      K2 = K1 * DE1/DEL1 * DEL2/DE2
      PRINT FORMAT ONE.SS3,CS3,DEL3,V3,SS1,CS1,DEL1,DEL2,K1,K2,P3,L,D,L/D,
     1  RHO

     .....VISCOSITY CALCULATIONS.....

NEWDAT  LOOK AT FORMAT $S60,2C6*$,RUN(0),RUN(1)
      READ DATA DATAI(0)=SS1,SS3,SS4,   DATAF(0)=DEL1,DEL2,DEL3,
     1                                  DEL4,TIME,CALDAT*   RUN NO.
      SS4 = DATAI(2)
      P3=PRESS.(V3)
      WHENEVER P3.GE.80000.
               DPDE1=20000./(99.95-79.87)
               DPDE2=20000./(100.02-79.14)
      OR WHENEVER   P3.GE.60000.
               DPDE1=20000./(79.87-59.37)
               DPDE2=20000./(79.14-59.15)
      OR WHENEVER   P3.GE.40000.
               DPDE1=20000./(59.37-39.12)
               DPDE2=20000./(59.15-39.03)
      OR WHENEVER   P3.GE.20000.
               DPDE1=20000./(39.12-18.85)
               DPDE2=20000./(39.03-19.20)
      OR WHENEVER   P3.GE.9700.
               DPDE1=10000./(18.85-8.80)
               DPDE2=10000./(19.20-9.53)
      OR WHENEVER P3 .GE. 4900. .AND. P3 .LE. 5100.
               DPDE1=1.1*10000./(18.85-8.80)
               DPDE2=1.032*10000./(19.20-9.53)
```

```
  OTHERWISE
           PRINT COMMENT $ DIFFERENTIAL PRESSURE TRANSDUCERS AR
 1 E NOT CALIBRATED AT THIS LEVEL$
           PRINT RESULTS P3
           TRANSFER TO NEWCAT
  END OF CONDITIONAL
  DISPL = SENS4(SS4)*V3*DEL4
  Q=PI*.49*.49/4.*DISPL/TIME
  NSRATE = 32.*Q/(PI*D.P.3)
  V=Q/(PI*D*D/4.)
  KEC=RHO*V*V/(32.2*144.*144.)
  DE1=1.0/K1*((RS1(SS1)+18.2*(RS1(SS1)/120.+1.))*(.08333/SV1+
 1 1./SI1))*.001+(RS1(SS1)/120.+1.)/SV1)*DEL1
  DE2=1.0/K2*((RS1(SS1)+18.2*(RS1(SS1)/120.+1.))*(.08333/SV1+
 1 1./SI1)*.001+(RS1(SS1)/120.+1.)/SV1)*DEL2
  DELTAP = .ABS.(DPDE1*DE1 - DPDE2*DE2)-KEC
  TAU=DELTAP/(4.*L/D)
  TAUDYN=68950.*TAU

  SET LIST TO TAUSAV,300
  SAVE DATA TAUDYN

  VISC=TAU/NSRATE
  VISCP=68950.*VISC

  SET LIST TO VISAVE,300
  SAVE DATA VISCP

  REYN=RHO*V*D/(VISC*32.2*144.*144.)
  LEOL=.065*REYN*D/L
  PRINT FORMAT TWO,RUN(0),RUN(1),SS1,SS3,SS4,DATAF(0)...DATAF(3),TIME,
 1   P3,VISCP,TAUDYN,NSRATE,DELTAP,KEC,VISC,TAU,REYN,LEOL
  WHENEVER PUNCH,PUNCH FORMAT THREE,RUN(0),RUN(1),VISCP,TAUDYN,
 1                                  NSRATE
  WHENEVER CALCAT.G.0.0,TRANSFER TO NEWCAL
  TRANSFER TO NEWDAT
PLOT
  PRINT COMMENT $1$
  EXECUTE SETPLT.(1,TAUSAV(1),VISAVE(1),C1,$*$,33,ORD)
  PRINT COMMENT $                TAU IN DYNES/(CM).P.2$
  EXECUTE SYSTEM.
  VECTOR VALUES ORD=$                    VISCOSITY IN POISE*$
  VECTOR VALUES ONE=$S36,H*CALIBRATION DATA*//S5,H*SS3*S2,H*CS3*S2,
 1   H*DEL3*S4,H*V3*S3,H*SS1*S2,H*CS1*S2,H*DEL1*S2,H*DEL2*S4,
 1   H*K1*S7 ,H*K2*S8 ,H*P3*/S5,I2,S3,I2,S2,F5.2,S1,F6.3,S2,
 1   I2,S3,I2,S2,F5.2,S1,F5.2,   E9.3 ,   E9.3 ,   E10.4///S36,
 1   H*VISCOSITY DATA*//S12,H*L =*F6.3,S8,H*D =*,F5.3,S8,H*L/D =
 1 *F6.1,S8,H*RHO =*F6.1////*$
  VECTOR VALUES TWO=$S5,2C6,S3,H*SS1*S3,H*SS3*S3,H*SS4*S3,H*DEL1*S3,
 1   H*DEL2*S3,H*DEL3*S3,H*DEL4*S3,H*TIME*/S20,I2,S4,I2,S4,I2,
 1   S3,F5.2,S2,F5.2,S2,F5.2,S2,F5.2,S2,F6.2//S24,H*P3*,S9,
 1   H*VISCP*,S6,H*TAUDYN*,S6,H*NSRATE*,S6,H*DELTAP*/S19,
 1   5(E10.4,S2)//S23,H*KEC*,S9,H*VISC*,S8,H*TAU*,S9,H*REYN*,
 1   S8.H*LE/L*/S19,5(E10.4,S2)////*$
  VECTOR VALUES THREE=$2C6,3(S2,E10.4)*$
  END OF PROGRAM
```

C.5 Typical Input-Output

DATA REDUCTION PROGRAM-INPUT DATA

Card
No.

1 ANY COMMENTS BETWEEN COLUMNS 1 AND 72 INCLUSIVE

---

2 PUNCH=1B.RHO=___.___,D=.____,L=.____,CALI(0)=_____,_____,_____,_____
(SS1) (CS1) (SS3) (CS3)

CALF(0)=____.____,____.____,____.____ *
(DEL1) (DEL2) (DEL3)

---

3 DATAI(0)=_____,_____,_____,DATAF(0)=____.____,____.____,____.____,____.____,____.____
(SS1) (SS3) (SS4) (DEL1) (DEL2) (DEL3) (DEL4) (TIMF)

,_____ *
CALDAT=1.0 if next card is new calibration data, otherwise omit.

_____
(Col. 60-72 inclusive)

COMMENTS:

Card #1: must be the first data card, no additional comment cards are allowed. This card is printed before any calculations are made.

Card #2: if the previous card #3 contains CALDAT=1.0, only the CALI and CALF vectors need to be punched if other quantities are unchanged.

Card #3: CALDAT=1.0 is included only when new calibration data are to be used. Then card #2 must be the next data card. Columns 61 to 72 inclusive can contain any comment. When CALDAT is omitted the next data card is also #3.

If decimal points are omitted, the quantity is an integer.

An * cannot be preceded by a comma.

SEPT. 18, 1967, FLUID A, CAPILLARY NO. 4, 100 F

CALIBRATION DATA

SS3	CS3	DEL3	V3	SS1	CS1	DEL1	DEL2	K1	K2	P3
4	5	3.43	6.173	4	3	4.30	4.35	.137E+05	.135E+05	.1157E+05

VISCOSITY DATA

L = 2.933 D = .010 L/D = 280.0 RHO = 58.6

A4.10.1

SS1	SS3	SS4	DEL1	DEL2	DEL3	DEL4	TIME
4	4	10	-.79	.65	2.97	.59	.40

P3	VISCP	TAUDYN	NSRATE	DELTAP
.9812E+04	.3099E+00	.1122E+04	.3622E+04	.1823E+02

KEC	VISC	TAU	REYN	LE/L
.1973E-02	.4494E-05	.1628E-01	.9700E+00	.2252E-03

A4.10.2

SS1	SS3	SS4	DEL1	DEL2	DEL3	DEL4	TIME
4	4	9	-1.51	1.24	2.95	.61	1.10

P3	VISCP	TAUDYN	NSRATE	DELTAP
.9746E+04	.2926E+00	.2143E+04	.7323E+04	.3481E+02

KEC	VISC	TAU	REYN	LE/L
.8069E-02	.4244E-05	.3108E-01	.2077E+01	.4821E-03

A4.10.3

SS1	SS3	SS4	DEL1	DEL2	DEL3	DEL4	TIME
4	4	9	-2.36	2.83	3.00	.65	.60

P3	VISCP	TAUDYN	NSRATE	DELTAP
.9911E+04	.2840E+00	.4063E+04	.1431E+05	.6599E+02

KEC	VISC	TAU	REYN	LE/L
.3079E-01	.4119E-05	.5892E-01	.4181E+01	.9706E-03

BIBLIOGRAPHY

1. Bowden, F. P., and Tabor, D. The Friction and Lubrication of Solids, Vol. II, Oxford University Press, 1964.

2. Bisson, E. E., and Anderson, W. J. Advanced Bearing Technology, NASA SP-38, 1964.

3. Crook, A. W. "The Lubrication of Rollers," Part I, Philosophical Transactions of the Royal Society, 250A, (1958), 387-409. Part II and III Philosophical Transactions of the Royal Society, 254A, (1961), 223-258. Part IV, Philosophical Transactions of the Royal Society, 255A, (1963), 281-312.

4. Dowson, D., Higginson, G. R., and Whitaker, A. V. "Elastohydrodynamic Lubrication: A Survey of Isothermal Solutions," Journal Mech. Engr. Science, 4, (1962), pp. 121-26.

5. Fein, R. S. "Effects of Lubricants on Transition Temperatures," American Society of Lubrication Engineers Preprint No. 64-LC-7, 1964.

6. Tabor, D., and Winer, W. O. "Silicone Fluids--Their Action as Boundary Lubricants," ASLE Trans., 8, (1965), 69-77.

7. Orcutt, F. K. "Experimental Study of Elastohydrodynamic Lubrication," ASLE Trans., 8, Oct. 1965, 381.

8. Dowson, D. "Elastohydrodynamic Lubrication: An Introduction and a Review of Theoretical Studies," Institution of Mechanical Engineers, Proceedings, 80, (1965-66), Part 3B, 7-16.

9. Barus, C. Proceedings of the American Academy of Arts and Sciences, 19 (1891-92), 13-19.

10. ASME, Pressure-Viscosity Report, I, II, A report prepared by the ASME Research Committee on Lubrication, N. Y., ASME, 1953.

11. Hersey, M. D., and Hopkins, R. F. "Viscosity of Lubricants Under Pressure," ASME, N. Y., 1954.

12. Hersey, M. D. Theory and Research in Lubrication, New York: Wiley and Sons, Inc. 1966.

13. Bridgman, P. W. "Viscosities to 30,000 kg/cm^2," Proceedings of the American Academy of Arts and Sciences, 77, (1949), 117-128.

14. Philippoff, W. "Viscoelasticity of Polymer Solutions at High Pressures and Ultrasonic Frequencies," Journal of Applied Physics, 34, No. 5, June 1963.

15. National Aeronautics and Space Administration, Lubrication, Corrosion and Wear, A continuing bibliography, NASA SP-7020, Washington D.C., June 1965.

16. Bell, J. C., Kannel, J. W., and Allen, C. M. "The Rheological Behavior of the Lubricant in the Contact Zone of a Rolling Contact System," ASLE-ASME Lubrication Conference, Rochester, N.Y., Oct. 1963, paper no. 63-Lul-8.

17. Hersey, M. D., and Snyder, G. H. S. "High-Pressure Capillary Flow," Journal of Rheology, 3, No. 3, (1932), 298-317.

18. Norton, A. E., Knott, M. J. and Muenger, J. R. "Flow Properties of Lubricants Under High Pressure," ASME Trans., 63, No. 7, (1941), 631-643.

19. Van Wazer, J. R., et al. Viscosity and Flow Measurement, Interscience Publishers, New York, 1963.

20. Philippoff, W., and Gaskins, F. H. "The Capillary Experiment in Rheology," Trans. Society of Rheology, II, (1958), 263-284.

21. Bird, R. B., et al. Transport Phenomena, New York: Wiley and Sons, Inc., 1960.

22. Philippoff, W., Gaskins, F. H., and Brodnyan, J. G. J. Appl. Physics, 28, (1957), 1118.

23. Rabinowitsch, B. "Uber die Viskositat and Elastisitat von Solen," Z. Physikal Chem., Abt. A. Bd. 145, Heft 1, 1929.

24. Gerrard, J. E., and Philippoff, W. "Viscous Heating and Capillary Flow," 4th Int'l Congress of Rheology, 1963, paper No. 51.

25. Gerrard, J. E., Steidler, F. E., and Appeldoorn, J. K. "Viscous Heating in Capillaries: The Adiabatic Case," ACS Petroleum Division Meeting, Chicago, Ill., Sept. 1964.

26. Gerrard, J. E., Steidler, F. E., and Appeldoorn, J. K. "Viscous Heating in Capillaries: The Isothermal-Wall Case," ACS Petroleum Division Meeting, Atlantic City, N.J., Sept. 1965.

27. Wright, W. A. "Prediction of Bulk Moduli and PVT Data for Petroleum Oils," 22nd ASLE Annual Meeting, Toronto, May 1967, Reprint No. 67AM-7B-1.

28. Tichy, J. A., and Winer, W. O. "A correlation of Bulk Moduli and PVT Data for Silicone Fluids at Pressures up to 500,000 psig," to be presented at the ASLE Annual Meeting, Cleveland, May, 1968.

29. Appeldoorn, J. K. "A Simplified Viscosity-Pressure-Temperature Equation," SAE Int'l meeting, Montreal, Canada, June 1963, paper No. 709A.

30. Wright, W. A., and Crouse, W. W. Jr. "A New Concept in Generalizing Non-Newtonian Fluid Flow Data," ASLE-ASME Lubrication Conference, Washington D.C., Oct. 1964, reprint No. 64-LC-11.

31. Ferry, J. D. Viscoelastic Properties of Polymers, New York: Wiley and Sons, Inc., 1961.

32. Boelhower, J. W. M. and Miss L. H. Toneman. "The Viscosity-Pressure Dependence of Some Organic Liquids," Proceedings of the Conference on Lubrication and Wear, London, (1957), 214-218.

33. Chu, P.S.Y., and Cameron, A. "Pressure Viscosity Characteristics of Lubricating Oils," Journal of the Institute of Petroleum, 48, No. 461, May, 1962, 147-155.

34. Du Bois, G. B., Ocvirk, F. W., and Whele, R. L. "Study of Effect of a Non-Newtonian Oil on Friction and Eccentricity Ratio of a Plain Journal Bearing," NASA TN D-427, May, 1960.

35. Horowitz, H. H. "Predicting Effects of Temperature and Shear Rate on Viscosity Index-Improved Lubricants," Ind. Eng. Chem. 50, (1958) 1089.

36. Pearsall, I. S., and Kane, J. "Viscosity and Specific Gravity of Five Hydraulic Oils," N.E.L. Fluids Report No. 83, East Kilbride, Glasgow, Sept. 1959.

37. Roelands, C. J. A., Vlugter, J. C., and Waterman, H. I. "The Viscosity-Temperature-Pressure Relationship of Lubricating Oils and Its Correlation with Chemical Constitution," ASME paper No. 62-WA-178.

38. Roelands, C. J. A., Blok, H., and Vlugter, J. C. "A New Viscosity-Temperature Criterion for Lubrication Oils," ASME paper No. 64-Lub-3.

39. Barwell, F. T. Lubrication of Bearings, London: Butterworths Scientific Publications, 1956.

40. Bridgman, P. W. "Viscosity of Liquids Under Pressure," Proceedings of the National Academy Arts and of Sciences, 11, (1925), 603-606.

41. Bridgman, P. W. "The Effect of Pressure on the Viscosity of Forty-Three Pure Liquids," Proceedings of the National Academy of Arts and Sciences, 61, (1926), 57-99.

42. Cannon, M. R. and Manning, R. E. "New High Shear Viscometers and New Vacuum Viscometers for Viscous Materials," Cannon Instrument Co., October, 1961.

43. Dowson, D., and Higginson, G. R. "The Effects of Material Properties on the Lubrication of Elastic Rollers," Journal Mechanical Engineering Science, 2, No.3, (1960), 188-194.

44. Frenkel, J. Kinetic Theory of Liquids, Oxford: Clarendon Press, 1946.

45. Goldstein, S. Modern Developments in Fluid Dynamics, I, Oxford: Clarendon Press, 1938.

46. Philippoff, W. "Viscosity Measurements on Polymer Modified Oils," ASLE Trans., 1, 1958, 82-86.

47. Pinkus, O., and Sternlicht, B. Theory of Hydrodynamic Lubrication, New York: McGraw-Hill Book Co., 1961.

48. Sargent, L. B. "Significance of Viscosity Studies of Fluid Lubricants at High Pressures," Lubrication Engineering, July-August 1955.

49. Sargent, L. B. "The Effect of Pressure and Molecular Weight Upon the Viscosity of Polybutene," Lubrication Engineering, July 1958.

50. Tzentis, L. S. "A Two-Way Capillary Viscometer," Journal of the A.I.Ch.E., 12, No. 1, January 1966, 45.

51. Wright, W. A., and Crouse, W. W. "General Relations for Polymer-Petroleum Oil Blends," I and Ec Product Research and Development, 3, No. 2, (June 1964), 153-158.